Industrialized bamboo in East Africa: Resource, production process and market entrance of a novel scrimber composite

D I S S E R T A T I O N

with the aim of achieving the degree of *Doctor rerum naturalium* at

University of Hamburg

Faculty of Mathematics, Informatics, Natural Sciences

Biology Department

submitted by

Goran Schmidt

born in Magdeburg, Germany

Hamburg 2020

Advisor and examiner

Prof. Dr. Jörg B. Ressel

Universität Hamburg
Department of Biology
Institute of Wood Science
Leuschnerstraße 91
Germany – 21031 Hamburg

Co-Examiner

Prof. Dr. Dr. Marius-Catalin Barbu

Salzburg University of Applied Sciences
Campus Kuchl
Markt 136a
Austria – 5431 Kuchl

Type:	Monography
Title:	Industrialized bamboo in East Africa: Resource, production process and market entrance of a novel scrimber composite
Author:	Goran Schmidt
Matriculation:	6052138
Page count:	235
Date of submission:	28.08.2020
Date of defense:	28.10.2020

Dedicated to my family

Acknowledgements

This thesis is a results of my studies at Universität Hamburg from 2014 to 2019. The practical works were carried out in different laboratories from 2015 to 2018. I wrote major parts of the monography while working part-time at Thünen Institute in 2019 and 2020. Looking back, this was not my wisest decision. But the experiences, lessons and impressions during this time are invaluable:

First and foremost, I want to thank my advisor **Prof. Dr. Jörg B. Ressel**. It has been an outstanding opportunity to be one of your last doctoral students. I appreciate your contributions of time, ideas, and funds but especially the trust in my abilities. Though always reminding me to "*Schreiben Sie zusammen*!", you have given me the freedom to find my own project and continue with bamboo research at the Institute of Wood Science. Until today I am not completely sure why you had asked me to become a doctoral student. I hope to investigate this last research question while having a drink after the disputation. My former lecturer **Prof. Dr. Dr. Marius C. Barbu** was so kind to take over the second examination of the thesis. I am aware of its extent and want to thank you very much for your willingness to support me on this endeavor.

I am also thankful for the positive social atmosphere in my two working groups. **Prof. Dr. Andreas Krause** as well as **Dr. Sebastian Rüter** gave me the flexibility to work on my thesis on the job. Thank you, to the whole BioHome project team for your patience and comprehension during the last phase of my thesis writing. The group has been a source of friendship, advice and inspiration to me. **Thomas Stute** and **Friederike Matthies**, two former master students (UHH), contributed on a very professional level and we became good friends after some time. My three „wise men" (Dr.) **Julius Gurr**, **Dr. Martin Nopens** and **Dr. Oliver Mertens** made the journey a very special experience. During my "biology period", **Dr. Jan-Henning Blohm** and **Dr. Verena Becker** discussed and laughed together with me. Without all of you I might have given up already. Special thanks and greetings.

The process engineering and product quality parts of this thesis is built on results of a GIZ funded Fraunhofer WKI project which, thanks to the open-minded policy of department head **Dr. Dirk Berthold**, I took part in. For all the discussions, presentations, meetings and quality assurance I am very grateful to **Mathias Belda** (WKI) and colleagues.

At Fraunhofer WKI, University Hamburg and Thünen Institute nothing works without technicians, sample preparation and handicraft labor. Thank you**, Stefanie Warsow** (TI), **Richard Deetz** (WKI), **Frank Froning** (WKI), **Johannes Beruda** (UHH), **Dörte Bielenberg** (UHH), **Tanja Potsch** (TI), **Gabriele Circelli** (TI), **Sabrina Heldner** (TI), **Jens Schröder** (TI) for your constant and accurate work. Additional thanks go to **Marie Lenz** (UHH) who worked with me on the fungal deterioration of bamboo scrimber. I very much appreciate your enthusiasm to conduct the long-lasting experiments together with Thomas and **Dr. Eckard Melcher** (TI). For the great photographic works, I would like to say thank you to **Christina Waitkus** (TI). In the parameter screening, there were major statistical problems. Thus, I consulted **Bettina Steffen** (TI) which led to the painful insight that the results would not change even when applying the ever more laborious ANOVA variants, I am thankful she shared her time with me.

Unfortunately, the private industrial project in Ethiopia suffered one tragic drawback when our dear colleague **Christopher Cleur** (†) from Ghana died suddenly in 2017. He was always a competent partner, capable to discuss business issues from the technical view. Although we had some contradictions, I am very grateful to have met him.

Thanks to the mobility grant provided by the German Wood Science Association (Bund deutscher Holzwirte e.V.), I was able to present some preliminary results from the biodegradation study at the IUFRO Div. 5 conference in June 2017 in Vancouver. This travel additionally opened the opportunity to visit the original scrimber industry plant and the first commercial bamboo plantation in Alabama. Thanks to **Walter Jarck** and my friend **Sebastian Roth** for making the trip a great experience going back to the roots of scrimber technology.

In 2015 my mother visited the wood and forestry research campus in Hamburg-Bergedorf and after hours of laboratory tours, she asked what the heck we did here the whole day. Former acting director **Dr. Johannes Welling** walked down the stairs and answered: We spend 50% of the time keeping the knowledge we have, 30% is administration and only one fifth goes to new research. The most important women in keeping this knowledge are the librarians **Astrid Stilke** and **Ulrike Reupke** (†). Thank you for your constant help.

Though English is my working language, it has been challenging to write the monography in a foreign language. Big thank you to **Vicki Marais** for reading the manuscript and helping to improve the language. But Chinese and Amharic are far beyond my capabilities. Thank you very much **Hanzhou Ye** and **Gebrewold Teklay** for supporting me with the translation of my abstract to 汉语 and አማርኛ.

Additionally, I would like to acknowledge honorary **Prof. Dr. Dr. h.c. mult. Walter Liese** who was the one awakening my passion for bamboo. I am now 34 years and though you were born 60 years earlier you impress me with an ever-curious mentality, a continuous working attitude, and your incredible vitality. Walter, you are an outstanding personality and example to me and the doors that you opened were not even visible to me a couple of years ago. Thank you.

Academically formed families provide a context leading to ten times more doctoral degrees than non-academics. Statistically, I am one out of hundred children of non-academic parents trying to pursue a doctoral degree. I bow my head with gratitude especially before my parents **Gudrun** and **Stefan**, my whole family, but also my teachers, professors, colleagues and friends for the support during the many years of schooling and university. Thank you for the understanding, love, and encouragement.

Abstract

The presented work offers a research contribution to the promotion of the bamboo processing industry in East Africa. The trade deficit in wood products is growing steadily in the region and in the case of Ethiopia exceeded EUR 100 million. A structural analysis of the bamboo processing sector showed that there are promising prospects to develop an exportable building product based on bamboo scrimber. For this purpose, the native African highland bamboo was investigated morphologically, anatomically and mechanically, an industrial production process was developed and the technical product suitability for export as decking boards was tested. The raw material investigations showed that the merchantable volume of the single culm is rather small (0.005 m³) and the upper two thirds of the culm are better suited for processing due to its comparably constant inner and outer taper. The characteristic fiber density gradients were also found in highland bamboo and the anatomy of its vascular bundles and fiber cells were described. The fiber length (1.4 mm) in node and internode was found equal, though the latter were slenderer. For processing into bamboo scrimber, the scrim strands were then examined and density (0.66 to 0.75 g/cm³), fiber content (29.83 to 38.32 %), strength (between 50 and 215 N/mm² in compression and tensile tests) and modulus of elasticity (21 kN/mm²) were determined. As a presumed weak point in the composite material, it was found that nodes halve the bending and tensile strength, while compressive strength was not affected. Silica content was relatively low (< 1.5 %) regardless of location, altitude and age and was successfully reduced by simply washing the raw scrims. In contrast to other woody species highland bamboo was found well suited for processing to scrimber. A fabrication process was configured based on existing technologies and the production parameters were determined. A pre-selection of pressing temperature (130 °C), heat treatment of the scrim strands (3 h, 160 to 180 °C), adhesive (8 – 12 %, sprayed phenol resin) and additive (2 % wax) was found to be promising. The wide variation of the results from the laboratory panels however made it necessary to investigate the effect of raw material variants and adhesive distribution. The influence of the height sections in the bamboo culm on internal bond and thickness swelling was negligible but the properties could be steered via layered adhesive concentrations. However, nearly all properties followed a strong correlation with specimen density and strongly overlapped other factors which made densification the most important influencing one. Industrially upscaled experiments have revealed additional challenges for the implementation phase: The specific pressure in the multi-daylight hot press must not exceed 7 N/mm² which is why the input moisture of the fiber must be kept below 5 %. Conversely, industrial heat treatment and adhesive application must adopt this target, i.e. at least 180 °C and not more than 10 % resin. In addition to the temperature in the treatment chamber, the packing density of the fiber bundle mats was of particular importance.

With an industrial scale decking product within reach, the regulatory situation was then analyzed in order to access markets with high purchasing power. The applicable test standards often refer to wood products but not high density bamboo, thus a separate test program was developed based on a number of European and Chinese product standards and guidelines. The decking boards were then tested in four categories (bending, surface, weathering, biodegradation) and compared with commercially available products. Both, the untreated and treated decking boards met bending requirements and outperformed the commercial product when exposed to long-term loads. Weak points of the heat treatment were the low resistance to weathering and the only moderate hardness. Furthermore, the effect of the heat treatment on the biological durability against wood-destroying fungi was investigated with monocultures and in ground contact (fungal cellar). In addition to a high abiotic mass loss, soft rot fungi

caused up to 20 % mass loss and 61 % stiffness loss in the control group. Heat treatment at 180 °C reduced the mass loss after ground contact to 5 %. The stiffness loss was still about 50 % independent of the treatment temperature. Depending on the test method, the heat treated scrimber showed a quality range from very durable to moderately durable and cannot be recommended for use class 3 and 4 (exterior). Basidiomycetes slightly degraded the heat treated bamboo scrimber and can thus be classified as very durable for use classes 1 and 2 (indoor). Permanent exposure to water or sunlight should be avoided as long as no UV resistant surface finishing was applied. Despite those imperfections, a marketable product was in sight so that economic aspects were considered. A detailed production cost model was worked out and recommendations for marketing and pricing were discussed. In the context of Chinese scrimber manufacturers and substitution products such as WPC, tropical wood or thermowood, the African bamboo scrimber cannot compete on the market because of cost advantages but must be promoted through branding and quality strategies. This work has shown that heat treated highland bamboo can be used to fabricate a scrimber construction product on an industrial scale, but not yet fully complies with current export standards. However, the remarkable value-added potential of industrial processing in Ethiopia gives reason to push the development forward and implement it with a suitable private sector partner.

Keywords: Industrialization, Bamboo, Scrimber, Ethiopia

Kurzfassung

Die vorliegende Arbeit bietet einen Forschungsbeitrag zur Förderung der bambusverarbeitenden Industrie in Ostafrika. Das äthiopische Handelsbilanzdefizit im Bereich der Holzprodukte wächst stetig und lag zuletzt über EUR 100 Millionen. Eine Strukturanalyse des bambusverarbeitenden Sektors zeigte, dass es aussichtsreich ist ein exportfähiges Bauprodukt auf Basis von Bambus Scrimber zu entwickeln. Zu diesem Zweck wurde der afrikanische Hochlandbambus morphologisch, anatomisch und mechanisch untersucht, stufenweise ein industrieller Produktionsprozess entwickelt und die technische Produkttauglichkeit für den Export als Terrassendiele geprüft. Die Rohstoffuntersuchungen ergaben, dass das Gesamtvolumen des Halmes vergleichsweise gering ist (0.005 m³) und die oberen zwei Drittel aufgrund der inneren und äußeren Form am besten für die Verarbeitung geeignet sind. Die charakteristischen exponentiellen Faserdichteverteilungen in der Halmwand wurden auch im Hochlandbambus gefunden und Anatomie der Gefäßbündel und seiner Faserzellen wurden beschrieben. So wurden Faserzellen in Nodium und Internodium mit gleicher Länge (1.4 mm) bestimmt obwohl letztere schlanker waren. Für die Verarbeitung zu Bambus Scrimber wurden anschließend die Fasermatten (*scrims*) auf Dichte (0.66 bis 0.75 g/cm³), Faseranteil (29.83 bis 38.32 %), Festigkeiten (zwischen 50 und 215 N/mm² im Druck- bzw. Zugversuch) und Steifigkeit (21 kN/mm²) hin untersucht. Als mutmaßlichen Schwachpunkt im späteren Verbundwerkstoff zeigte sich, dass Nodien die Biege- und Zugfestigkeit halbieren während Druckfestigkeit nicht beeinträchtigt wurde. Der Silikatgehalt war gering (< 1.5 %) unabhängig von Standort, Höhenabschnitt und Alter und wurde durch einfaches Waschen des Rohstoffs weiter reduziert. Im Gegensatz zu anderen verholzten Bambusarten eignet sich äthiopischer Hochlandbambus sehr gut für die Verarbeitung zu Scrimber. Auf Basis existierender Technologien wurde deshalb ein Verarbeitungsprozess konfiguriert und die Produktionsparameter ermittelt. Als aussichtsreich wurden dabei die Presstemperatur (130 °C), Hitzebehandlung der Fasermatten (3 h, 160 – 180 °C), Klebstoff (8 – 12 %, gesprühtes Phenolharz) und Additiv (2 % Wachs) bestimmt. Die starke Streuung der Ergebnisse aus den Laborplatten machte es notwendig die Auswirkung von Rohstoffvarianten und Klebstoffverteilung zu untersuchen. Obwohl der Einfluss der Höhenabschnitte im Bambushalm auf Querzugfestigkeit und Dickenquellung zu vernachlässigen war, konnten die Eigenschaften über abgestufte Klebstoffkonzentrationen kontrolliert werden. Die Verdichtung der Platte zeigt sich aber mithin als wichtigster Einflussfaktor und überlagerte alle anderen Variablen. Versuche im Industriemaßstab haben zusätzliche Herausforderungen aufgezeigt: Der spezifische Druck in der Etagenheißpresse darf 7 N/mm² nicht übersteigen, weshalb die Eingangsfeuchte der Faser unter 5 % liegen sollte (Dampfdruck). Im Umkehrschluss mussten deshalb die Ergebnisse der industriellen Hitzebehandlung und der Klebstoffauftrag kontrolliert werden. Im Industrieversuch stellte sich heraus, dass neben der Behandlungstemperatur in der Kammer vor allem die Packdichte der Fasermatten von Bedeutung ist.

Nachdem ein Terrassenprodukt im industriellen Maßstab in Reichweite war, wurde die regulatorische Situation analysiert, um Zugang zu Märkten mit hoher Kaufkraft zu erhalten. Die geltenden Prüfnormen beziehen sich oft auf Holzprodukte aber nicht auf hochverdichtete Bambuswerkstoffe, weshalb ein eigenes Testprogramm auf Basis einer Reihe von chinesischen und europäischen Produktnormen und Richtlinien entwickelt wurde. Die industriell gefertigten Platten wurden in vier Kategorien (Biegelasten, Oberfläche, Bewitterung, biologischer Abbau) getestet und mit kommerziellen Substitutionsprodukten verglichen. Die Biegeeigenschaften sowohl der unbehandelten und behandelten Terrassendielen erfüllten die

Anforderungen und waren bei Langzeitbelastung dem kommerziellen Produkt überlegen. Schwachpunkte der Hitzebehandlung sind die geringe Witterungsbeständigkeit und moderate Härte der Scrimberdiele. Des Weiteren wurde der Effekt der Hitzebehandlung auf die biologische Dauerhaftigkeit gegen holzzerstörende Pilze im Erdkontakt (Pilzkeller) und mit Basidiomyceten untersucht. Neben auffallend hohem abiotischen Abbau verursachten insbesondere Moderfäulepilze bis zu 20 % Masseverlust und 61 % Steifigkeitsverlust in der Kontrollgruppe. Während der Masseverlust nach Erdkontakt durch die Hitzebehandlung (180 °C) auf unter 5 % reduziert werden konnte, betrug der Steifigkeitsverlust unabhängig von der Behandlungstemperatur etwa 50 %. Abhängig von der Prüfmethode wies der hitzebehandelte Scrimber eine Qualitätsspanne von sehr bis mäßig dauerhaft auf und kann nicht ohne Weiteres für die Verwendung in Gebrauchsklasse 3 und 4 (Außenbereich) empfohlen werden. Die Inkubation mit Basidiomyceten verursachte nur geringfügigen Abbau weshalb alle Varianten für Gebrauchsklasse 1 und 2 (Innenraum) als sehr dauerhaft einzuordnen waren. Die Verwendung an Wasser- oder Sonnenlicht exponierten Stellen sollte für einen längeren Zeitraum unbedingt vermieden werden. Insgesamt zeigt sich dennoch, dass nach entsprechender Entwicklung einer Oberflächenveredelung ein marktfähiges Produkt in Aussicht steht. Deshalb wurde zuletzt ein weitreichendes Fertigungskostenmodell (COGM) erstellt und Empfehlungen für die Preisfindung und Vermarktung gegeben. Im Umfeld von chinesischen Scrimberherstellern und Substitutionsprodukten wie WPC, Tropenholz oder Thermoholz besteht der afrikanische Bambus Scrimber stellenweise, allerdings zeigte sich der Wettbewerb auf Kostenbasis aussichtslos und muss über Markenbildung und Qualität geführt werden. Grundsätzlich hat die Arbeit gezeigt, dass aus thermisch modifiziertem Hochlandbambus ein Bauprodukt auch für den Export auf industriellem Maßstab erzeugt werden kann, dieser die geltenden Standards aber nicht in Gänze erfüllt. Das bemerkenswerte Wertschöpfungspotenzial der industriellen Verarbeitung in Äthiopien gibt jedoch Anlass die Entwicklung voranzutreiben und mit einem geeigneten privatwirtschaftlichen Partner umzusetzen.

Schlüsselwörter*:* Industrialisierung, Bambus, Scrimber, Äthiopien

摘要

本研究可为促进东非竹加工产业发展作出研究贡献。木材产品的贸易赤字在东非地区正在稳步增长，其中，在埃塞俄比亚的贸易赤字已超过一亿欧元。通过对竹加工行业的结构分析表明，开发基于重组竹材料的可出口建材具有广阔的前景。本研究对非洲高原竹（African highland bamboo）的微观形态，解剖特性，及物理力学性能进行了分析，开发了一种工业化生产过程，并对其作为铺板（decking boards）出口产品的适用性进行了分析。通过对原料的研究表明，单根竹秆的商品材积较小，仅为 0.005 m³，而竹秆上部三分之二处的竹子由于其内外锥度比较稳定，较适于加工。并对非洲高原竹的纤维密度梯度特征及其维管束和纤维细胞的解剖结构进行了分析描述。研究表明，非洲高原竹的竹节与节间纤维长度基本一致，约为 1.4 mm，但后者的纤维更细长。并将非洲高原竹加工成重组竹，该重组竹的密度为 0.66 - 0.75 g/cm³，纤维含量为 29.83 - 38.32 %，压缩强度与拉伸强度为 50 - 215 N/mm²，刚度为 21 kN/mm²。竹节作为复合材料的一个假定弱点，可使重组竹的弯曲强度和拉伸强度减半，而对材料的抗压强度影响较小。非洲高原竹的二氧化硅含量相对较低（小于 1.5 %），且不受地理位置、海拔与竹龄的影响，通过水洗疏解后的竹束，可成功降低竹束的二氧化硅含量。研究表明，与其他木质资源相比，非洲高原竹非常适用于重组竹加工。本研究在现有的重组竹加工工艺基础上，对加工工艺进行了设计，并确定了生产工艺参数。研究表明，较优的重组竹制备工艺如下：预热压温度为 130 °C，竹束经 160 - 180 °C 热处理 3 小时，喷涂 8 - 12 %的酚醛树脂胶黏剂及 2 % 的蜡。然而，由于实验室制备的板材存在较大的结果偏差，因此有必要对原材料变化和胶黏剂分布的影响进行研究。竹秆的高度部分对重组竹的内结合强度和厚度尺寸膨胀率的影响可忽略不计，但重组竹的性能可通过分层胶黏剂的浓度来控制。然而，几乎重组竹的所有的性能都与试样的密度有很强的相关性，并且与其它影响因素有很强的重叠，这使竹材的致密化成为了影响重组竹性能最重要的影响因素。此外，工业上规模化放大实验揭示了具体实施阶段的挑战：多日光热压机的比压不能超过 7 N/mm²，这就是纤维含水率必须保持在 5 %以下的原因。相反，工业化热处理和胶黏剂的应用要求热压温度至少为 180 °C，树脂含量不超过 10%。除了处理室的温度，纤维束簇的包装密度也显得尤为重要。

在工业化规模生产的铺板产品触手可及的情况下，为了能让产品拥有市场高购买力，本研究还对监管状况（regulatory situation）进行了分析。相关测试标准通常适用于木制品，但不适用于高密度竹材。因此，我们以欧洲和中国相关产品的标准为基础，制定了一套独立的检测项目。然后对铺板的弯曲强度、表面性能、风化性能、及生物降解性能进行测试，并将其与市售产品进行比较。测试表明，未处理和处理的铺板均符合弯曲强度要求，且在长期负荷下的弯曲强度优于市售产品。热处理的弱点是抗风化能力降低，硬度仅达到中等硬度。此外，通过单菌培养及与地面接触(菌窖试验)研究了热处理对木腐菌生物耐久性的影响。在对照组中，除了较高的非生物质量损失外，软腐菌造成了高达 20 % 的质量损失及 61 % 的刚度损失。在 180 °C 下进行热处理使与地面接触后的质量损失降低到 5 %，而刚度损失仍约为 50 %，与处理温度无关。基于该试验方法，重组竹经热处理后的质量范围表现为从非常耐用到中等耐用，不建议将

其归为 3 级和 4 级（室外）使用。担子菌对热处理后的重组竹有轻微降解作用，因此可将其归为非常耐用的 1 级和 2 级（室内）使用。若产品需要长期暴露在水中或阳光下使用，则需对其进行抗紫外线等表面处理。尽管有这些不完善之处，但产品存在消费市场及消费价值，因此本研究还对产品经济方面的问题进行了考虑分析。在本研究中，我们制定了详细的生产成本模型，并为产品的市场营销与定价策略提出了建议。由于非洲重组竹的生产成本较高，无法在市场上取得竞争优势, 争但必须通过对产品的品牌和质量战略进行推广。本研究表明，热处理后的非洲高原竹可用于工业化生产规模的重组竹建材，但该产品还不能完全符合当前的出口标准。然而，埃塞俄比亚工业加工业显著的增值潜力使我们有理由继续推动产品发展，并与合适的私营部门合作伙伴一起推动实施。

关键词：工业化，竹子，重组竹，埃塞俄比亚

ማጠቃለያ

የቀረበው ሥራ በምስራቅ አፍሪካ የቀርቅሓ ማቀነባበሪያ ኢንዱስትሪን ለማስፋፋት የምርምር አስተዋፅኦ ያበረክታል ፡፡ በእንጨት ምርቶች ውስጥ ያለው የንግድ ጉድለት በምስራቅ አፍሪካ በቋሚነት እያደገ ሲሆን በኢትዮጵያ ሁኔታ ከ 100 ሚሊዮን ዩሮ ጭማሪ አሳይተዋል ፡፡ በቀርቅሃ ማቀነባበሪያ ዘርፍ ላይ የተደረገው መዋቅራዊ ትንታኔ እንደሚያሳየው በዚ ምርት ላይ የተመሠረተ ወደ ውጭ የሚላክ የግንባታ ምርት የማምረት ተስፋዎች እንዳሉም ያሳያል ፡፡ ለዚሁ ዓላማ የአፍሪቃ ተወላጅ የሆነ የደጋ ቀርቅሓ በሞርፎሎጂካሊ፣ አናቶሚካሊ እና ሜካኒካዊ በሆነ መልኩ ለማጥናት ሙከራ ተደርገዋል ፣ የኢንዱስትሪ ምርት ሂደት ተመርተዋል እና የተከኒካል ምርት ሰሌዳዎች ፈተነ ወደ ውጭ ለመላክ የቴክኒክ ምርት ተገቢነት ፈተነ ተደርገዋል፡፡ የጥሬ እቃው ምርመራዎች እንደሚያሳዩት፣ የነጠላ ጭማሬ ሽቀጣ ሽቀጥ እና የጥናት ውጤቶች እንዳመለከቱት ፣ የነጠላ ጭማሬ መጠን አነስተኛ (0.005 m³) እና የላይኛው ሁለት ሦስተኛ የሚሆኑት በአንጻራዊ ሁኔታ ቋሚ እና ከውጭ በኩል ባለው ተከላ ምክንያት ለሂደቱ የተሻሉ ናቸው። የባህሪያት ፋይበር መጠነኛ ቀስቶች በደለል የደጋ ቀርቅሃ ተገኝተዋል እናም የቫስኩላር እጢዎች እና ፋይበር ሴሎች የሰውነት አካል ተገልጻል፡፡ በመስቀለኛ አንጓ እና በውስጥ መስመር ያለው የፋይበር ርዝመት (1.4 ሚሜ) እኩል ሆኖ ተገኝቷል ፣ ምንም እንኳን የኋለኛው ኣነስተኛ ቢሆኑም፡፡ ወደ የቀርቅሃ ብስባሽ ሂደት ለማስኬድ የብልሹዎቹ ፈተኖች ተመርጠዋል እና መጠናቸው (0.66 እስከ 0.75 g/cm³) ፣ የፋይበር ይዘት (ከ 29.83 እስከ 38.32 %) ፣ ጥንካሬ (ከ 50 እስከ 215 N/mm² መካከል በማነፃፀር እና በተንጣለለ ትንንሽ ሙከራዎች) እና ግትርነት (21 kN/mm²) ተወስነዋል ፡፡ በተቀናበረው ቁሳቁስ ውስጥ እንደታሰበው ደካማ እንደመሆኑ መጠን የአንጓዎች መታጠፍ እና የከባድ ጥንካሬን ግማሽ እንደሚቀንስ ተገምቷል ፡፡ የሲሊኮን ይዘት ምንም እንኳን አከባቢ ፣ ከፍታ እና ዕድሜ ምንም ይሁን ምን የሲሊኮን ይዘት በአንፃራዊነት ዝቅተኛ የነበረ ቢሆንም (< 1.5 %) እና ዝቅተኛ ጥሬ እቃዎችን በማጠብ በተሳካ ሁኔታ ቀንሷል። ከሌላው የዕንጨት ዝርያዎች በተቃራኒ የቀርቅሓ ቅርጻ ቅርጾችን ለማሰራጨት በጣም ተስማሚ ሆኖ ተገኝቷል። በነባር ቴክኖሎጂዎች ላይ የተመሠረተ የማምረት ሂደት የተዋቀረ እና የምርት ልኬቶች ተወስነዋል። የቅድመ ግፊት (130 ዲግሪ ሴንቲ ግሬድ) ፣ የፍተሻውን የሙቀቶች አያያዝ (3 ሰ ፣ ከ 160 እስከ 180 ዲግሪ ሴንቲ ግሬድ) ፣ ማጣበቂያ (8 – 12 % ፣ የተረጨ phenol resin) እና ተጨማሪ (2 % ሰም) ተገኝቷል ፣ይህም ተስፋ ሰጭ ሁነዋል ፡፡ ከላቦራቶሪ ፓነሎች የተገኘው ውጤት ሰፊ ልዩነት ግን የጥሬ ዕቃዎች ልዩነቶች እና ማጣበቂያ ስርጭት ውጤትን ለመመርመር አስፈላጊ ሆነዋል፡፡ በቀርቅሓው ውስጥ የከፍታ ክፍሎቹ ተፅእኖ በውስጣዊ ትስስር ጥንካሬ እና ውፍረት እብጠት ላይ ግድየለሽ ነበር፣ ነገር ግን ንብረቶቹ በተጣበቁ ማጣበቂያዎች አማካኝነት ሊመሩ ይችላሉ ፡፡ ሆኖም ግን ሁሉም ንብረቶች ማለት ይቻላል በቁመት እና በጥልቀት ጥንካሬ ላይ ጠንካራ ትስስር ተከትለው እጅግ በጣም አስፈላጊ በሆነው ተፅእኖ ላይ ለውጥ የሚያመጣባቸውን ሌሎች ምክንያቶች በጥብቅ ደርሰዋል ፡፡ በኢንዱስትሪ ደረጃ የተደረጉ ሙከራዎች ለአፈፃፀም ደረጃ ተጨማሪ ተፈታታኝ ሁኔታዎችን ገልጠዋል-በብዝሃ ቀን ሙቅ ማተሚያ ውስጥ ያለው ልዩ ግፊት ከ 7 N/mm² መብለጥ የለበትም ለዚህም ነው የፋይሉ ግብዓት እርጥበት ከ 5 % በታች መሆን ያለበት። በተቃራኒው ፣ የኢንዱስትሪ ሙቀት ሕክምና እና ተጣጣፊ ትግበራ ይህንን ግብ ማውጣት አለበት ፣ ማለትም ቢያንስ ከ 180 ዲግሪ ሴንቲግሬድ እና ከ 10% ያልበለጠ ነው። በሕክምናው ክፍል ውስጥ ካለው የሙቀት መጠን በተጨማሪ ፋይበር ጥቅልል መጠቅለያዎች መጠቅለያ ልዩ ጠቀሜታ ነበረው ፡፡

በከፍተኛ የኢንዱስትርያል ምርቶች ገበያዎችን ለመድረስ የኢንዱስትሪ ሚዛን ምርቱ በሚተገበርበት ጊዜ የቁጥጥር ሁኔታ ለማብራራት ተሞክረዋል፡፡ የነበሩ የሙከራ ደረጃዎች ብዙውን ጊዜ የሚያመለክቱት ከእንጨት የተሰሩ ምርቶችን ነው ፣ ነገር ግን ለከፍተኛ እፍግታ የሆነ ቀርቅሓ አያመላክቲም፣ ስለሆነም በበርካታ የአውሮፓ እና የቻይና የምርት ደረጃዎች እና መመሪያዎች ላይ በመመርኮዝ የተለየ የሙከራ መርሃ ግብር ተዘጋጅቷል። ከዚያ የምርት ሰሌዳዎቹ በአራት ምድቦች (በማጠፍ ፣ በወለል ፣ በአየር ሁኔታ ፣ ብባዮኮሳሽ) እና በንግድ ከሚገኙ ምርቶች ጋር በማነነፃፀር ሙኮራ ተደርገዋል ፡፡ ሁለቱም ያልታከሙት እና ህክምና ያልተደረገላቸው የምርት ሰሌዳዎች የመገጣጠሚያ መስፈርቶችን ያሟሉ እና ለረጅም ጊዜ ጭነቶች በተጋለጡበት ጊዜ የንግድ ምርቱን በተሻለ ሁኔታ አሟልተዋል ፡፡ የሙቀት ሕክምናው ደካማው ጎን ለአየር ሁኔታ ዝቅተኛ መቋቋም እና ብቸኛው መካከለኛ ጥንካሬ በመሆኑ ነው ፡፡ በተጨማሪም ፣ ሙቀቱ በእንጨት የሚያበላሹ ፈንገሶችን ለመቋቋም ባዮሎጂያዊ ጥንካሬው ላይ የሚያሳድረው ተጽዕኖ በባህላዊ እና በመሬት ውስጥ (የፈንገስ ሴል) ለማሳየት ተሞክረዋል ፡፡ ከፍተኛ ጉዳት ከሚያስከትለው የጅምላ ጉዳት በተጨማሪ ለስላሳ የበሰለ ፈንገሶች እስከ 20% የሚደርሱ የክብደት ማጣት እና በመቆጣጠሪያው ቡድን ውስጥ የ 61 % ቅጥነት ማጣት አስከትሏል ፡፡ በ 180 ዲግሪ ሴንቲግሬድ የሙቀት ሕክምና ከመሬት ጋር ንክኪ ከተደረገ በኋላ የክብደት ብክለቱን 5 % ቀንሷል ፡፡ የቅጥነት ማጣት አሁንም ቢሆን ከህክምናው የሙቀት መጠን 50 % ያህል ነበር ፡፡ በሙከራው ዘዴ ላይ በመመርኮዝ ፣ በሙቀት ማከሚያው የተፈጠረው ሙቀትን በጣም ዘላቂ እስከ መካከለኛ ዘላቂ የሚደርስ እና ለክፍል 3 እና 4 (በውጫዊ) እንዲጠቀሙ አይመከርም ፡፡ ባሲድዮማይስተስ (Basidiomycetes) በሙቀት አማቂ የቀርቅሓ ሙቀትን በትንሹ በመቀነሱ ለአጠቃቀም ለ 1 እና 2 ክፍል (ለቤት ውስጥ) ለመጠቀም በጣም ዘላቂ እንደሆነ ሊመደብ ይችላል ፡፡ የአልትራቫዮሌት(UV Light) መቋቋም የሚችል ወለል ማድረቂያ እስካልተተገበረ ድረስ የውሃ ወይም የፀሐይ ብርሃን ቋሚ መጋለጥ መወገድ

አለበት። እነዚያ ፍጽምና የጎደላቸው ቢሆኑም ኢኮኖሚያዊ ገጽታዎች ከግምት ውስጥ እንዲገቡ አንድ የገበያ ምርት የታየ ነበር ፡፡ ዝርዝር የምርት ወጪ ሞዴል ተሠርቶ ለገበያ እና ለዋጋ አወጣጥ ምክሮች ለማስቀመት ተሞክረዋል፡፡ ከቻይና የሽርክ አምራቾች እና እንደ WPC ፣ ሞቃታማ እንጨት(thermowood) ያሉ የመተካት ምርቶች አውድ ውስጥ የአፍሪካ የቀርቅሓ ንድፍ አውጭ በዋጋ ሊተመን በሚችልበት ገበያ ላይ መወዳደር አልቻለም፣ ነገር ግን በብራንድ እና በጥራት ስልቶች መበረታታት አለባቸው ፡፡ ይህ ሥራ በሙቀት የተሞላው የቀርቅሓ ሙቀት አማቂ የግንባታ ስራን በኢንዱስትሪ ደረጃ ለመንደፍ ሊያገለግል የሚችል ቢሆንም አሁን ካለው የወጪ ንግድ መስፈርቶች ጋር ሙሉ በሙሉ የማይስማማ መሆኑን አሳይቷል ፡፡ ሆኖም በኢትዮጵያ ያለው የኢንዱስትሪ ምርት አስደናቂ ጠቀሜታ እና የልማት እድገቱን ወደፊት ለመግፋት እና ተስማሚ የሆነ የበኩሉ ዘርፍ ለመተግበር የሚያስችል ምክንያት ይሆናል ፡፡

ቁልፍ ቃል: በኢንዱስትሪ ልማት ፣ በቀርከሃ ፣ እንደገና የተፈጠረ የቀርከሃ ፣ ኢትዮጵያ

Abbreviations

Anova	Analysis of variance
B	Bottom culm height portion
bh	Breast height
BR	Brown rot
BS	Bamboo scrimber
COV	Coefficient of variation
D	Outer diameter
DC	Durability class
EMC	Equilibrium moisture content
EN	European norm
FDI	Foreign direct investment
GDP	Gross domestic product
h	Culm height
HDAT	Hot dry air treatment
HDF	High density fiberboard
IB	Internal bond
ISO	International standard organization
LEG	Liquid extrusion glueing
LVL	Laminated Veneer Lumber
m	Mass
M	Middle culm height portion
MC	Moisture content
MDF	Medium density fiberboard
ML	Mass loss
MOE	Modulus of elasticity
MOR	Modulus of rupture
OSB	Oriented strand board
PB	Particleboard
PF	Phenol formaldehyde
PLC	Private limited company
PRC	People's Republic of China
RH	Relative humidity
SR	Soft rot
SSA	Sub-Saharan Africa
T	Temperature
t	Time
T	Top culm height portion
TS	Thickness Swelling
UC	Use class
UF	Urea formaldehyde
WA	Water absorption
WBP	Wood-based panel
WPC	Wood Plastic Composites
WR	White rot
wt	Wall thickness
yr	Year

Content

Acknowledgements IV
Abstract VI
Abbreviations XIV
Content XV
1 | Introduction 18
1.1 ETHIOPIA 19
1.2 PROBLEM AND OBJECTIVE 21
1.3 PROJECT CONTEXT 22
1.4 STRUCTURE 23
2 | State of the art 24
2.1 ECONOMY OF RENEWABLE BUILDING MATERIALS 25
2.1.1 Importing wood products 26
2.1.2 Untapping the Ethiopian bamboo potential 28
2.1.3 Value web and product space analysis 31
2.2 WOOD AND BAMBOO BASED ENGINEERED PANEL PRODUCTS 37
2.2.1 Fibers 38
2.2.2 Particles 39
2.2.3 Strands 40
2.2.4 Fiber bundles 42
2.2.5 Veneers 48
2.2.6 Slats, strips and slivers 50
2.3 BAMBOO SCRIMBER 53
2.3.1 Defibration 53
2.3.2 Heat treatment 56
2.3.3 Resin systems 58
2.3.4 Mat formation 60
2.3.5 Consolidation 61
2.3.6 Applications 63
3 | Raw material study 66
3.1 INTRODUCTION 67
3.1.1 Culm biomass and volume 67
3.1.2 Anatomy 69
3.1.3 Raw material quality risks 71
3.2 SPECIFIC OBJECTIVES 76
3.3 MATERIAL AND METHOD 77
3.3.1 Bamboo harvest 77
3.3.2 Morphology 78
3.3.3 Anatomy 79
3.3.4 Silica 79
3.3.5 Mechanical characterization 80
3.4 RESULTS & DISCUSSION 83
3.4.1 Gross morphology 83
3.4.1.1 Inner and outer culm form 83
3.4.1.2 Estimation of woody volume 85

3.4.2 Anatomy ... 90
3.4.3 Silica ... 92
3.4.4 pH-value and sugars ... 94
3.4.1 Mechanical characterization ... 94
3.5 INTERMEDIATE CONCLUSION ... 100

4 | Process engineering ... 102

4.1 INTRODUCTION ... 103
4.1.1 Production parameter screening ... 103
4.1.2 Process engineering ... 104
4.1.3 Industrial upscaling ... 104
4.2 SPECIFIC OBJECTIVES ... 106
4.3 MATERIAL AND METHODS ... 107
4.3.1 Experimental design and statistical analysis ... 107
4.3.2 Scrim strand production ... 110
4.3.3 Heat treatment ... 111
4.3.4 Resin systems ... 112
4.3.5 Wax addition ... 112
4.3.6 Mat formation ... 113
4.3.7 Press parameters ... 113
4.3.8 Industrial upscaling ... 115
4.3.9 Test procedures ... 116
4.4 RESULTS AND DISCUSSION ... 117
4.4.1 Tentative production ... 117
4.4.1.1 Resin application trial ... 117
4.4.1.2 Press production trial ... 118
4.4.2 Production parameter screening ... 120
4.4.2.1 Resin system selection ... 120
4.4.2.2 Effect of heat treatment ... 123
4.4.2.3 Effect of wax addition ... 125
4.4.3 Effect of resin concentration and layered panels ... 126
4.4.3.1 Thickness swelling and water absorption ... 127
4.4.3.2 Internal bond ... 128
4.4.4 Influence of the fiber bundle morphology from different culm height sections ... 131
4.4.4.1 Flexural strength and elasticity ... 133
4.4.4.2 Thickness swelling and water absorption ... 134
4.4.4.3 Internal bond ... 135
4.4.5 Industrial upscaling ... 138
4.4.5.1 Hot pressing ... 138
4.4.5.2 Resin application ... 140
4.4.5.3 Heat treatment ... 141
4.5 INTERMEDIATE CONCLUSION ... 145

5 | Export market requirements ... 147

5.1 INTRODUCTION ... 148
5.1.1 Towards an export standard for outdoor bamboo scrimber ... 148
5.1.2 Flexural performance ... 152
5.1.3 Mechanical surface characterization ... 152
5.1.4 Humidity and weathering ... 153
5.1.5 Biological performance ... 154
5.2 SPECIFIC OBJECTIVE ... 156
5.3 MATERIAL AND METHODS ... 157
5.3.1 Panel production ... 157

5.3.2 Flexural properties ... 158
5.3.2.1 Moisture resistance under cyclic test conditions ... 158
5.3.2.2 Bending creep ... 158
5.3.3 Mechanical surface characterization ... 158
5.3.3.1 Hardness and elastic recovery ... 158
5.3.3.2 Abrasion resistance ... 159
5.3.3.3 Impact resistance ... 159
5.3.3.4 Pull-through resistance of fasteners ... 159
5.3.3.5 Sliding friction ... 159
5.3.4 Humidity and weathering ... 160
5.3.5 Resistance to fungal attack ... 160
5.3.5.1 Screening ... 160
5.3.5.2 Basidiomycete monoculture test ... 161
5.3.5.3 Soft rot soil bed test ... 161
5.3.5.4 Durability classification ... 162
5.3.6 Statistical analysis ... 163
5.4 RESULTS AND DISCUSSION ... 164
5.4.1 Flexural properties ... 164
5.4.1.1 Static bending ... 164
5.4.1.2 Creep behavior ... 166
5.4.2 Mechanical surface characterization ... 167
5.4.2.1 Hardness and elastic recovery ... 167
5.4.2.2 Abrasion resistance ... 168
5.4.2.3 Impact resistance ... 169
5.4.2.4 Pull through resistance of fasteners ... 170
5.4.2.5 Sliding friction ... 170
5.4.3 Humidity and weathering ... 171
5.4.3.1 Dimensional stability ... 171
5.4.3.2 Weathering resistance ... 172
5.4.4 Resistance to fungal attack ... 174
5.4.4.1 Screening ... 174
5.4.4.2 Basidiomycete monocultures ... 176
5.4.4.3 Soft rot soil bed test ... 178
5.4.4.4 Durability classification ... 180
5.5 INTERMEDIATE CONCLUSION ... 183

6 | Final remarks ... 185

6.1 ECONOMIC CONTEXT ... 186
6.2 OUTLOOK ... 189

List of figures ... 190

List of tables ... 196

Literature ... 199

Appendix ... 217

A2. STATE OF THE ART ... 218
A3. RAW MATERIAL STUDY ... 219
A4. PROCESS ENGINEERING ... 223
A5. EXPORT MARKET REQUIREMENTS ... 233

Statutory declaration ... 235

1 | Introduction

Ato Hamuso and Weyizero Bange are Ethiopian villagers with a family of nine. Living in the Southern remote highlands their family uses small amounts of bamboo as fuel to prepare meals and to construct their livelihood. As with most rural Africans practicing subsistence agriculture, they work with forest products every day. Bamboo forests guarantee livelihood in many regions in East Africa (Teshale 2015). Nevertheless, population growth, land reforms and foreign investments in infrastructure and agriculture have taken over lands. Out of about 10,250,000 km² arable land in Sub-Saharan Africa (SSA), an estimated 1,340,000 km² suffered from land-grabbing (Batterbury and Ndi 2016, World Bank 2018). Additionally, the extreme weather-related crop shortfalls in normally food-secure regions exacerbate the already critical situation for the rural population (Deressa *et al.* 2008). Rural communities now face an enormous challenge: Change the focus from a traditional subsistent forest-based and agricultural form of living to a microentrepreneur model. They need to add value to local resources, commercialize them (Teshale *et al.* 2017) and make them accessible for emerging industries with export ambitions (Siba and Gebreeyesus 2016). This challenge bears the potential to transform a rural agrarian society into an industrial one. Development banks, policy makers and economists across the African continent aim at industrializing their economies. Industrialization has been shown to bring prosperity, create jobs and develop social standards. However, parts of SSA are structurally less industrialized today than they were in the 1980's. Figure 1 shows an increasing trend of the Ethiopian industrial GDP share in the last five years. Nevertheless, just like in other "lion economies" (Economist 2011) this development based on the construction sector and steadily increasing commodity prices. About 70 % of African exports are commodities and only 25 % come from manufactured goods, while imported manufactured goods account for 56 % (African Development Bank Group 2018). In fact, the continent's manufacturing sector actually declined from 12 % in 1980 to 11 % in 2010 of GDP (Shiferaw 2017, Tafirenyika 2016, World Bank 2018). Industrialization does not only mean to increase the GDP share of the industrial sector, but to reorganize the economy for manufacturing more complex (UNIDO 2016) and renewable products from biomass-based value webs (Virchow *et al.* 2014). The vertical integration of value-chains - comprising the farmer, the factory worker and the surrounding service environment - is crucial for human development (Shiferaw 2017, Virchow *et al.* 2016).

The wood and bamboo based panel industries are good examples of manufacturing operations which comprise many different sub-sectors (Müller *et al.* 2012, Thoemen *et al.* 2010, Zhu and Jin 2018). It connects land-use stakeholders (agriculture, forestry), the service sector (logistics, maintenance) and commerce (sales, export). One may ask, why there is not one single panel producing factory neither in Ethiopia nor whole East Africa? It is not a problem of corruption as Brittell *et al.* (2013) described it in the timber sector, though the situation is as complex as the continent itself. Sampath and Oyelaran-Oyeyinka (2016) summarized the perspectives on sustainable industrialization in SSA in need of more than only copying established concepts (Shiferaw 2017, Zhu and Jin 2018).

1.1 Ethiopia

Over the last 20 years, the Ethiopian economy has grown its GDP by roughly 10 % annually, nearly double as much as the average regional East African growth rate of 5.4 %. However, the GDP growth has not led to game-changing structural transformations in the industrial sector yet. Figure 1 shows Ethiopia's industrial GDP growing, yet the manufacturing share still stagnates. Industrial GDP comprises of extraction (mining), secondary (manufacturing) and tertiary (service) sectors. Manufacturing covers the conversion of raw materials into finished products. The manufacturing sector, although part of the industrial GDP, did not contribute to the Ethiopian industrial growth. The UNIDO (2016) and the African Development Bank Group (2018) assume agricultural mechanization and the construction boom being responsible for the GDP growth in Ethiopia, similar to whole SSA (Tafirenyika 2016). Additionally, high commodity prices driven by the strong demand from China had supported the apparent industrial growth. The important value-adding activities however happen in the manufacturing sector where agricultural raw materials are processed to high-value export products.

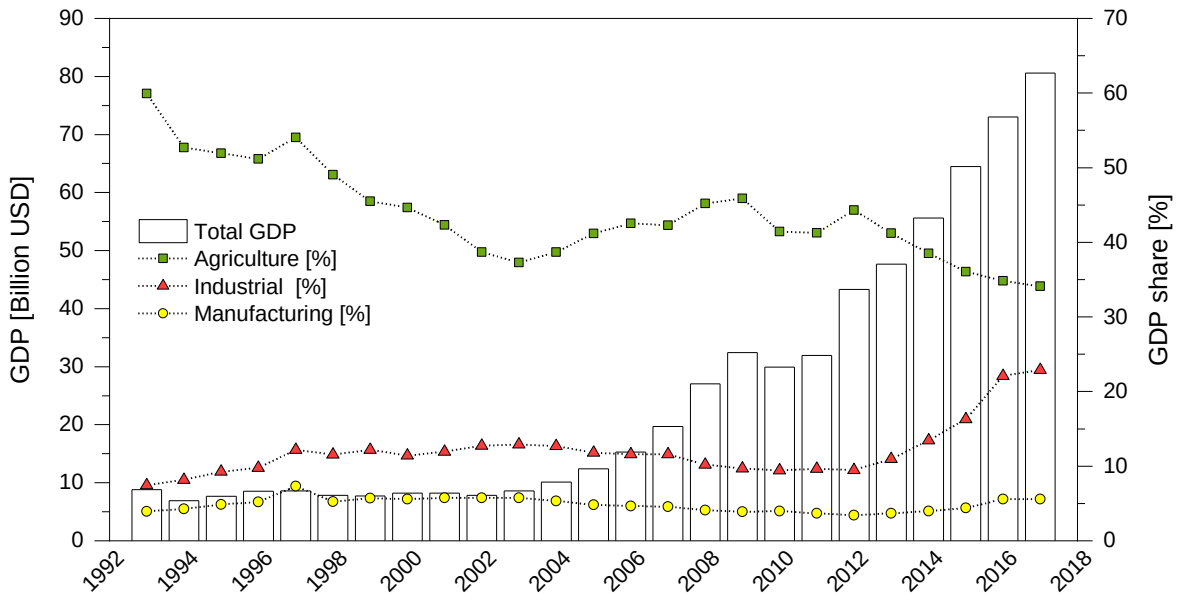

Figure 1: Total gross domestic product (GDP) and the cumulated shares of agriculture, industrial and manufacturing sector in the Ethiopian economy from 1993 to 2017, adopted from World Bank (2018) data

At the same time, the demographical and geographical situation gives Ethiopia a key function in the East African region. It neighbors the Middle East region and its markets, while at the same time standing as a stable anchor for the surrounding nations. Ethiopia borders Eritrea, Djibouti, Kenya, Somalia, South Sudan and Sudan. Ethiopia's huge and young population of about 104 million makes it the second most populous nation in Africa after Nigeria. Although it is the fastest growing economy in the region, it is considered an economically lesser developed country with an annual per capita income of USD 783. The Ethiopian government aims to reach lower-middle-income status by 2025 (National Planning Commission 2016, World Bank 2018). Sustainable effects on employment rate and income will happen once national industries start producing renewable building materials from their own resources. The worldwide increasing demand for sustainable construction materials and efficient value-chains closely interlocks with the social and economic benefits for rural populations in the global South (Hannula 2012). The industrial utilization of agricultural and forestry raw materials in Africa is in its infancy with a strong development potential. Products made from bamboo offer market potentials, but also

social and business perspectives for micro-enterprises in Ethiopia. A rural bamboo value-chain would benefit thousands of Ethiopian farmer families (Gatzweiler and Braun 2016, Mekonnen *et al.* 2014). Ethiopia has a very high potential due to its vast raw material stock and the relatively stable political setting (Prunier and Ficquet 2015). Even though forestry research in Ethiopia started in the late 1960s (Heske 1966) under the umbrella of his imperial majesty Haile Selassie I., the industrialization perspective was added much later by the Ethiopian Growth and Transformation Plans I and II (Prunier and Ficquet 2015).

1.2 Problem and objective

Continental Africa has only five native woody bamboo species (Bystriakova et al. 2004) with two of them being native to East Africa (Liese 2005). The industrial utilization of Ethiopian highland bamboo *Yushania alpina* (K. Schum.) W. C. Lin and lowland bamboo *Oxytenanthera abyssinica* (A. Rich.) Munro was barely explored for high-value products (Kelemwork *et al.* 2005), raw material pre-processing (Schmidt 2013), forestry aspects (Zhu and Jin 2018) or in socioeconomic studies (Mekonnen *et al.* 2014). The Ethiopian bamboo and wood processing sector is a net importer and does not contribute to industrial employment and notable value creation (UNcomtrade 2018). Fu (2019) estimated the employment potential at 2.5 million people working in a future Ethiopian bamboo industrial sector producing a potential USD 7 billion revenue and a 0.5 billion export value. A lack of knowledge about processes as well as barriers for industrial players had limited the bamboo sector in East Africa to low-value products in the past (Mekonnen *et al.* 2014, Schmidt 2013). These deficits motivated Mulatu and Kindu (2010) to identify major research gaps for bamboo in Ethiopia. These gaps were updated according to the state of the art of bamboo research. The identified deficits concern:

- Databases on type, use, harvest, processing, storage and properties of bamboo resources
- Information on seasonal fluctuations, harvest yield, high yield regions and mobilization of untapped highland bamboo resources
- Comparative economic analysis, market information and feasible product options; Industrial processing technologies for efficient utilization
- Technologies for large-scale silviculture
- Holistic and conclusive concepts from industrial production to consumption
- Economic applicability of research results to industrial development projects on the ground

The present work aims to tackle those deficits. Thus, the overall goal of the present work is to develop a building material for an industrial scale production based on the African highland bamboo *Yushania alpina* (K. Schum.) W. C. Lin. This goal was subdivided into technological and market related objectives. These aspects will be worked out to specific objectives within in the following empirical chapters.

- MARKET ASPECTS
    - Analyze the Ethiopian construction sector in regard of renewable building materials and determine a potential bamboo-based industrial panel product
    - Identify export market entrance hurdles for building products made from Ethiopian bamboo and elaborate the technological research part to overcome those hurdles

- TECHNOLOGICAL ASPECTS
    - Investigate raw material characteristics and their suitability for the industrial processing
    - Show the technical feasibility of a tangible bamboo-based panel production by combining existing technology, develop the process and initiate industrial scale engineering
    - Design a testing scheme and examine the product quality of the bamboo-based composite panel

1.3 Project context

The strategic alliance “Development of the industrial bamboo sector in Ethiopia” was initiated by the Deutsche Gesellschaft für Internationale Zusammenarbeit (GIZ) GmbH and a private startup company was founded. An experimental pilot plant was installed in Addis Ababa in 2013 inspired by Chinese producers and facilitated by financial support from Germany (develoPPP, BMZ), Netherlands (Ministry of Foreign Affairs, PSI Fund) and the US (USAid). The project network was accompanied by Fraunhofer WKI, glue suppliers (Dynea AS, Solenis, BASF), machine manufacturers (Michael Weinig AG, BigonDry, Dieffenbacher GmbH, Raute Oyi) as well as research entities (FH Rosenheim, TU Dresden, University Hamburg).

Instead of developing new concepts from the scratch, the actual innovation challenge in this project was the combination of 1. Process engineering using state-of-the-art technologies, 2. A new unstudied raw material, 3. Product quality issues and market entrance facilitation as well as the 4. Technical and economic feasibility. The expected project result is the first large-scale industrialized bamboo building product from Africa. Furthermore, the GIZ project intended to build local expertise to bring this industrial manufacturing branch to the East African reality. More insights into the practical project context was given in technical reports and publications (Böck 2014a, 2014b; Schmidt 2013; Schmidt et al. 2016b; Schmidt et al. 2016a).

1.4 Structure

The present work encompasses the above described objectives in five chapters. Figure 2 reflects the branched structure of the chapters and their topics. It divides in introduction, state of the art, three empirical chapters and final remarks. The introduction gives an overview of the regional context, explains the problem and the corresponding project. The specific research objectives derived from this are further discussed and defined in each chapter. The state of the art chapter (2) begins with an analysis of the Ethiopian construction sector and describes the its trade deficit. Raw material potentials in the bamboo sector are critically examined and an overview of bamboo composite panels in connection with a possible production in Ethiopia is shown. The product development strategy is worked out details of the scrimber technology are presented.

From here on, three experimental chapters follow. These chapters are structured in a typical article pattern (introduction, objective, material and methods, results and discussions, conclusion). In each experimental chapter's introduction, its contents and structure are explained. Chapter 3 represents the work done studying the raw bamboo, its gross morphology, anatomy, mechanical properties and process-critical characteristics such as silica. Chapter 4 evolves the production process engineering from a trial stage to the industrial scale. Chapter 5 then discusses the export market requirements, analyses standards and identifies weaknesses and strengths of highland bamboo scrimber (BS) as a construction material with emphasis on resistance against biological attack. The last chapter recaps the empirical results and then closes with a compact economic analysis about its commercial potential in export markets.

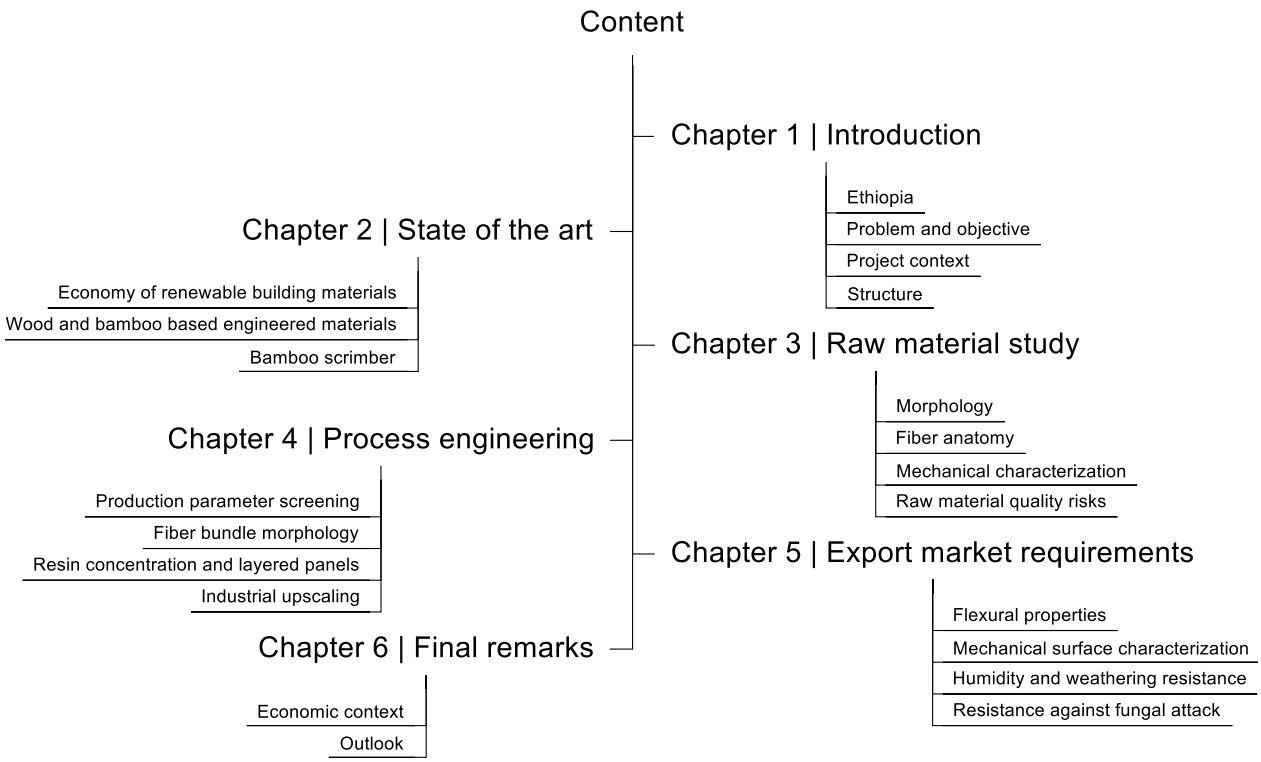

Figure 2: Structure of this work

2 | State of the art

This chapter builds from three sub-chapters as shown in figure 3. The first part reflects on the economic aspects of wood and wood-based panels as renewable construction materials in the context of the recent Ethiopian GDP boom. It shows the trade deficit and reveals the untapped potential of native bamboo in East Africa and helps in identifying a promising development strategy. The second part then provides an overview on conventional wood- and bamboo-based engineered panel products in the context of Ethiopia. The last part reviews bamboo scrimber as a development option, introduces the several process steps, raw materials and applications.

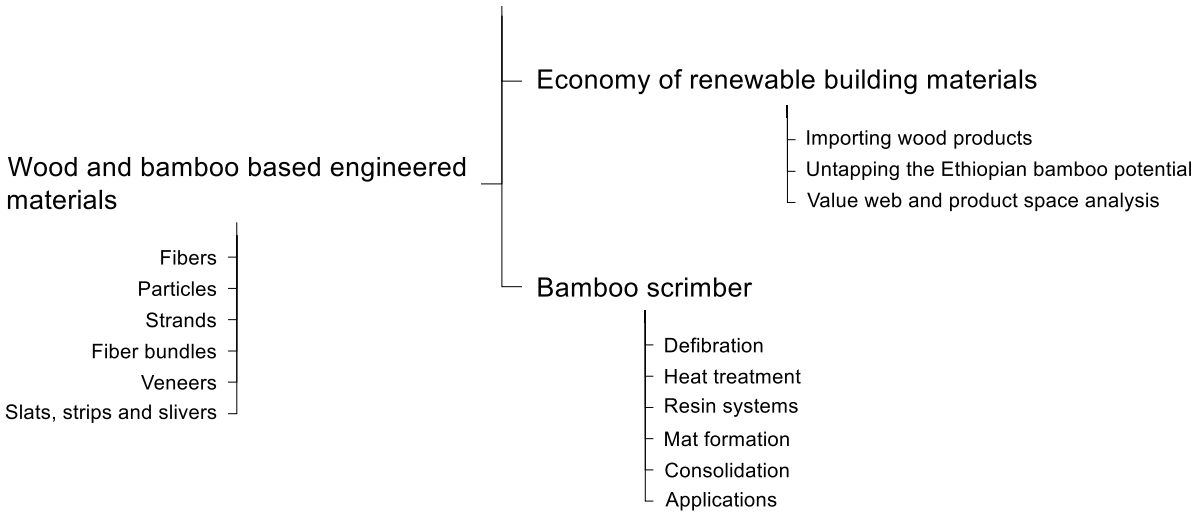

Figure 3: Structure of the state of the art chapter

2.1 Economy of renewable building materials

Ethiopia has been the least urbanized country in the world, but at the same time, the one with the highest urbanization rate. The enormous shift from rural areas to the cities in Ethiopia requires immediate action promoting renewable building materials from national sources and industrial construction methods (McKinsey 2017). Cherenet and Helawi (2015) estimated that there is a lack of at least 900,000 urban living units, with drastically increasing tendency. With the GDP growing fast, the pressure on the construction and manufacturing sub-sectors increases. Sustainable solutions for sourcing renewable building materials from regional industries must be established urgently (UNIDO 2016). The use of wood and bamboo may benefit the booming economy and at the same time reduce the environmental impact of the construction sector (Kedir *et al.* 2020).

In lack of complex industrialized products Ethiopia imports goods and services. The Ethiopian economy is a net importer and holds the 76th rank in the global ranking of importing countries. Figure 4 illustrates that about one third of Ethiopia's import comes from China (PRC), ca. 10 % from Europe and only 2.1 % from Germany (UNcomtrade 2018). Intra-African trade is meanwhile below 5 %. While imports were USD 17.9 billion, exports sum up to USD 3.13 billion, resulting a trade deficit of USD 14.8 billion in 2016. Ethiopia is strongest in exporting coffee (763), oil seeds (470), gold (397), dry vegetables (247) and horticultural products (173) [USD million], i.e. agricultural products and raw materials with a very low value added (National Planning Commission 2016). At the same time its top imports are petroleum (1810), aircrafts (648), medicaments (639), trucks (587) and fertilizers (502) [USD million], i.e. manufactured or semi-finished goods which cannot be provided nationally (National Planning Commission 2016, UNIDO 2016).

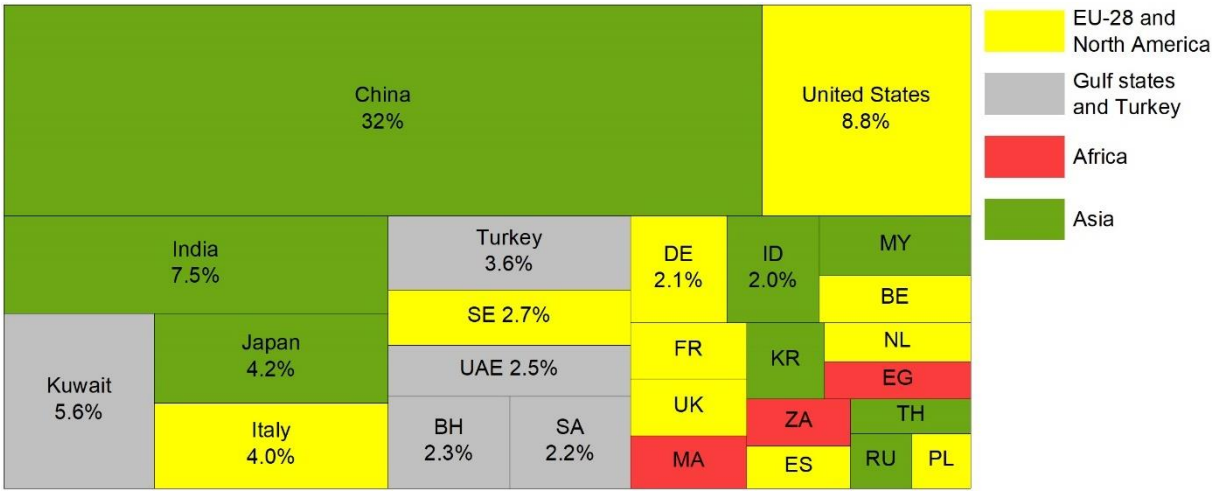

Figure 4: Import share by origin country with import volumes higher than USD 100 million in 2016 (UNcomtrade 2018)

The PRC is engaged in political and infrastructure issues in SSA and Ethiopia (Hess and Aidoo 2015). The typical trade channels for above mentioned import and export goods are going through the port of Djibouti, currently the only military presence of the PRC in whole SSA. The railways from Djibouti to the Ethiopian mainland were completely renewed by Chinese investors, hence the transport costs sunk to a minimum.

The manufacture GDP share remains at 5 % in Ethiopia. The structure of manufactured exports still bases on resources, a relatively low technology level and less value added. The country depends on crude oil imports, machines, engineering and construction materials. For the

emerging building industry, this new situation is a chance and a risk at the same time. A causal association of growing foreign direct investments in infrastructure (FDI), import of construction materials and the subsequent deterioration of local entrepreneurs in the Ethiopian building industry leads to a vicious self-sustaining cycle of economic dependency (Gebreyouhanes 2016, Lopes *et al.* 2017). SSA is the second largest FDI destination in the world and inflows to SSA rose from USD 10 billion in 2000 to USD 55 billion in 2015. This development favored a growing GDP (figure 1) and a booming building sector (African Development Bank 2018). The building boom and its value-adding activities remain in the service sector and do not impact the industrial manufacturing structure. The sustainable development of the Ethiopian construction sector depends on the maturing of its whole economy. It is well known that the construction sector's GDP share should be about 5 to 6 % to keep it in balance with the overall development of an African country (Lopes *et al.* 2017). Once as the "Dubai fever"[1] cools down, the trade deficit, inflation and currency crisis may govern the GDP development. Even though the economic wealth of the Ethiopian nation seems to grow, the potential young workforce generation does not participate appropriately in this development yet. This heats up social conflicts and promotes an anti-Chinese (Hess and Aidoo 2015) and anti-Western (Reuters 2016) atmosphere resulting in vandalism against companies, damaged infrastructure and interethnic rioting.

2.1.1 Importing wood products

The Ethiopian economy consumed around 124 million m³ wood and wood products in 2013, or 1.22 m³ per capita. Compared with the German wood consumption per capita of 1.87 m³, the Ethiopian figure seems to be relatively high. At the same time, the share of fuel wood is roughly 90 % in Ethiopia, which is a typically high figure in lesser developed countries with a mainly rural profile. After fuel wood use, construction purposes demanded 6.6 million m³ wood in the same year (Ministry of Environment, Forest and Climate Change 2017). Nevertheless, the dynamic population growth and the economic development expectations will continue driving the demand for wood and wood products and a consumption increase of 27 % over the next 15 years is expected. The construction sector consumes more and more industrial round wood and the fuel wood share is expected to decrease due to rural electrification. The Ethiopian Ministry of Environment, Forest and Climate Change (2017) estimates an annual consumption of wood and wood products up to 158 million m³ by the year 2033. Because of lacking national resources and manufacturers, the demand for imported wood products constantly increased from 2000 to 2010 and reached USD 107 million during the last decade. Figure 5 illustrates the structure of this remarkable development by showing the import value shares of the five largest wood product categories and the progress of the overall wood products import value (excluding paper products[2]). Whilst export of wood and wood products accounted to only negligible USD 3.15 million export (0.15 %), import was 30 times higher in 2016. The import value constantly increased from USD 7.26 million (0.48 % share) in the year 2000, showing an enormous peak in 2013 and currently amounts to USD 104 million (0.58 %). Sawn wood, wood fiberboard and plywood hold the biggest shares in this development. Sawn wood (mostly coniferous) has grown from 32 % in 2000 to 43 % in 2016 being stable for the

[1] The term is often used among stakeholders in the building industry to describe the fast construction of high-rise buildings in capital cities with lacking urban planning concepts.

[2] Pulp and paper accounted to USD 211 million which represents a 1.1 % share of the total import volume.

last couple of years. Wood fiberboards (mainly MDF) share 21 % nowadays which has to do with the fast-growing middle class demanding modern furniture and interior from molded MDF products. Plywood share decreased from roughly 50 % to only 17 % in 2016. However, the actual total imported plywood increased in volume during the same period which basically has to do with the price decrease on the world plywood market. Coniferous sawn wood was imported mainly from Austria, Croatia and Slovenia and sums up to USD 40.5 million in 2016 (UNcomtrade 2018). This timber is used in representative elements of private estates or in porch roof in hotels, restaurants and others. Despite the high price (USD 500 to 800 per m³), the demand for European grown timber assortments is growing every year. The reason for this choice is rather a quality aspect, which must be taken into consideration when developing a regional substitute product.

Cherenet and Helawi (2015) stated that Ethiopia offers a huge diversity of renewable raw materials for the building sector, such as rammed earth, clay, sorghum straw and bamboo. In combination, one traditionally uses them as a mortar-like material in affordable constructions. Additionally, a selection of Ethiopian indigenous tree species is currently being reforested (Negash 2010). Those raw materials are only available in small decentral patches providing heterogenous quality to potential building products. The urban African building industry is very static and consumes standardized assortments only and hence requires constant qualities (Cherenet and Helawi 2015). Nationally available, renewable construction materials with a controlled quality range, e.g. low-diameter eucalypt logs, remain auxiliary means for scaffolding or temporary poles. This is an odd situation, one of the poorest nations in the world importing timber from one of the wealthiest nations in Europe. Negash (2010) interprets the Ethiopian dependency on external timber sources to have three causes: the historical deforestation, contemporary environmental destruction and weak forestry institutions. In fact, lessons learnt from South American tropical forests show that the strictly controlled utilization of selected wood species can lead to sustainable forest management practices (Elias 2004). The emerging African bamboo processing industry faces similar concerns: The demand for constant quality raw material competes with the need for fuel of rural communities leading to unsustainable harvest cycles and degraded remnant bamboo forests (Gebru 2013, Zhao *et al.* 2018).

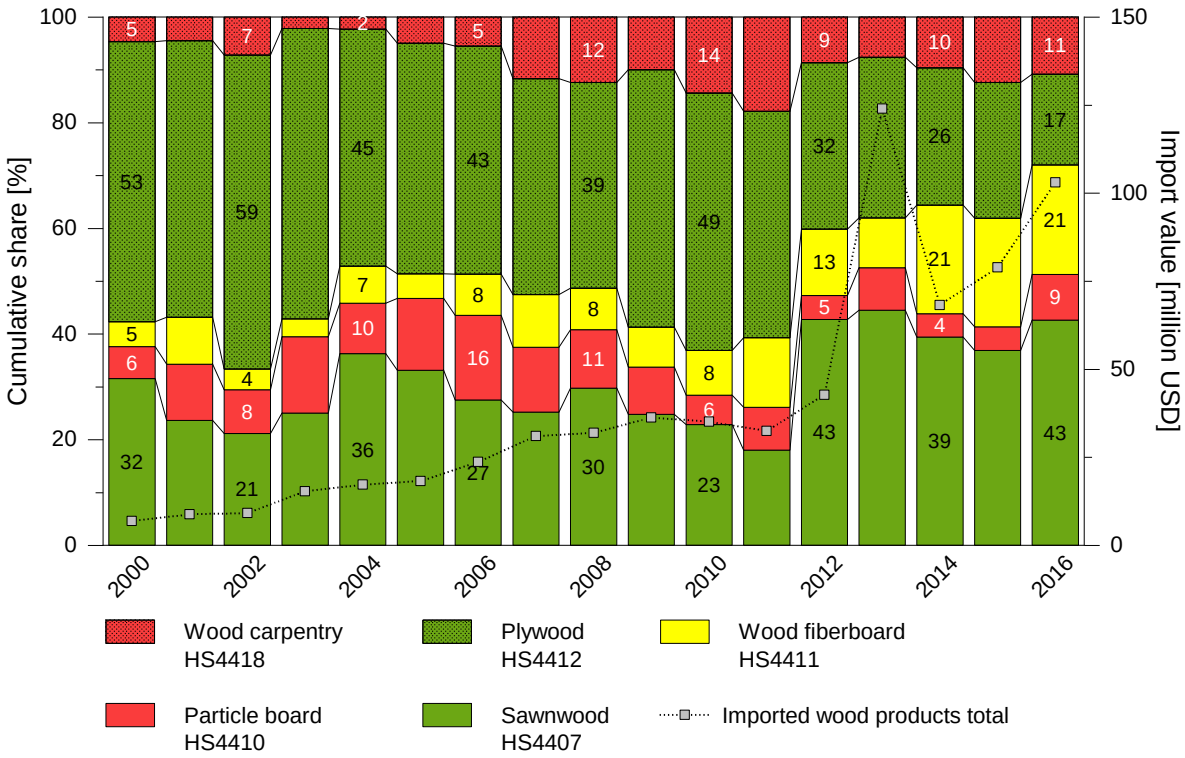

Figure 5: Normalized value share of Ethiopian wood products import of the five largest categories (left axis) and the total value of the imported wood products (right axis) using HS92 codes from 2000 to 2016 (UNcomtrade 2018)

2.1.2 Untapping the Ethiopian bamboo potential

From the point of view of vernacular architecture, renewable building materials already start in a relatively simple form. A woven mat made of bamboo splits and slivers together with a skeleton made of bamboo culms and eucalyptus poles is enough to construct traditional houses in communities all around the world (Hannula 2012, Joffroy 2016). Specialized architects and carpenters able to build complex structures (Janssen 2000) are rare and still lack even in bamboo rich Ethiopia. Although there are significant efforts to make Ethiopian vernacular bamboo architecture a viable element in modern urban constructions (Dalbiso and Addissie 2019, Harries *et al.* 2012, Joffroy 2016) there is an undeniable demand for manufactured, standardized and high-value building products (Cherenet and Helawi 2015).

- BAMBOO FOREST AREA

Eastern Africa is covered by 27 % forests and woodlands, while bamboo shares less than one tenth of the total area (FAO 2006). The deforestation rate in Ethiopia reached 2 %, or 140,900 ha/a from 1990 to 2010. FAO (2015) stated that the deforestation rate in Ethiopia decreased to 40,300 ha/a from 2010 to 2015. The heavy decline of Ethiopian forests seemed to have had eased between 2010 and 2015. Being that as it may, stocks of wood still decreased by 1.3 % per year and reached the all-time low record of 251 million m³ in 2015. The political structure changed in that time and the Ministry of Environment, Forest and Climate Change (2017) was recently founded. Ethiopia is one out of the ten nations worldwide with the largest

non-forest woodlands[3], hence this resource should be covered by statistics as well. The definition of forest cover was adapted, and new inventory data was analyzed. Hence, the FAO (2015) reports 12,499,000 ha forest, which equals 11.3 % of the country's total area. However, it is not without discussion that not only growing stocks but also growing political interest in inventories might have led to the increase. The African continent is considered to be covered by roughly between 1.5 and 2.8 million ha bamboo forests (FAO 2015, Mulatu and Kindu 2010). The East African macro-region is the largest bamboo patch on the continent with a growing industrial interest especially for the two native bamboo species in Ethiopia, the highland bamboo *Yushania alpina* K. Schumann Lin, and the lowland bamboo, *Oxytenanthera abyssinica* (A. Rich) Munro, as described in the literature (Embaye 2000, Liese 2005, Liese and Köhl 2015, Schmidt 2013). In the past it was generally accepted that roughly 1 million ha of bamboo covered land is found in Ethiopia, accounting for two thirds of Africa's bamboo resources and 7 % of the world total (Embaye 2000, Liese 2005). This number is based on a three decades old study (LUSO consult 1997) and was discussed controversially. Bamboo industrials (Gebru 2013) or researchers (Böck 2014a) doubt that the bamboo area in Ethiopia has increased during the last two decades.

Table 1 Extent of bamboo forest cover in SSA by country (top 5) and the world total according to Lobovikov *et al.* (2007) and FAO (2006) for 1990 to 2005 and Zhao *et al.* (2018) for 2017

Country	**Covered area [10^3 ha]**			
	1990	**2000**	**2005**	**2017**
Nigeria	1,590	1,590	1,590	-
Ethiopia	849	849	849	1,439
Tanzania	128	128	128	-
Kenya	124	124	124	131
Uganda	67	67	67	55
Total SSA	2,758	2,758	2,758	-
World	23,988	35,656	36,777	-

However, national (Teshale *et al.* 2017) and international (Zhao *et al.* 2018) authors recently published a total bamboo coverage in Ethiopia of 1.1 and 1.44 million ha, respectively. The latest study provided a very recent mapping analysis of Ethiopia, Kenya and Uganda using a multi-temporal landsat imagery. Inaccuracy and controversial study results are caused by the color coding of canopy covers being mistaken in mixed stands. Those studies carried out analyses with contemporary methods of remote sensing and ArcGIS using grid maps with a 25 to 50 m spatial resolution. Stands narrower than that (riverbanks) are usually overestimated. Additionally, lowland bamboo often is confused with grass- and shrublands, whereas highland bamboo is counted as part of a regular forest. The risk analysis in the study (Zhao *et al.* 2018) explains this with the low resolution of their satellite images. The highland bamboo covers approximately 300,000 ha out of which a small amount of 19,000 ha is planted in small-scale plots by rural communities. The lowland bamboo covers an area of approximately 700,000 to 850,000 ha accounting for more than 80 % of the land covered with bamboo. In the literature, controversial information is found on those figures (Desalegn and Tadesse 2014, Embaye 2000, Mekonnen *et al.* 2014, Mulatu and Kindu 2010, Teshale *et al.*

[3] FAO (2015) defined as "Land not defined as "Forest", spanning more than 0.5 ha; with trees higher than 5 m and a canopy cover of 5-10 %, […] or with a combined cover of shrubs, bushes and trees above 10 %."

2017, Zhao *et al.* 2018). Additionally, Ethiopia started introducing ten exotic species with the aim to cope with different climate and soil conditions (Mulatu *et al.* 2016a). The current afforestation rate (2,000 ha/a) is rather of experimental nature, but first results showed the potential of filling ecological niches with more than only the two native species (FAO 2015, Mulatu *et al.* 2016a).

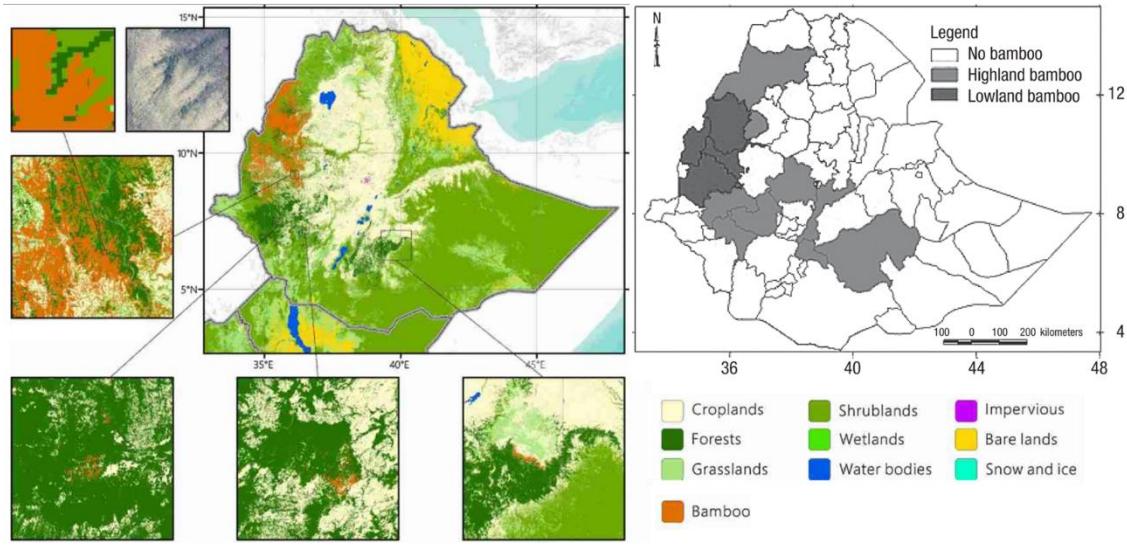

Figure 6: Landsat imagery bamboo mapping using data from 2016 extracted from Zhao *et al.* (2018) and the occurrence of the two native bamboo species in Ethiopia by federal districts (Desalegn and Tadesse 2014)

- FROM "SUPPLY PUSH" TO "DEMAND PULL"

Even though forestry research has been done in Ethiopia for about three decades, bamboo is yet a neglected research topic. The East-Africa bureau of the International Network of Bamboo and Rattan (INBAR) focuses on business development, skill training and technology transfer. Nevertheless, up to now, no national Ethiopian institutional entity is officially assigned to conduct bamboo research. Such institutional support, in research as well as in policy and implementation is essential for marginalized bamboo smallholders (Gatzweiler 2016) and especially for the bamboo-based value web in Ethiopia (Lin *et al.* 2019). A new impulse might improve the situation in the near future, since the PRC announced the establishment of a USD 60 million investment in a China-Africa Bamboo Center (INBAR 2018) which is going to be constructed by 2021. The Ethiopian bamboo-based value web is restricted to informal and local uses (also see figure 7). The Ethiopian highland bamboo was treated as a forestry topic Obvious that technological and financial capacities have been reserved for forestry research, but not for bamboo industrialization. To date the existing research in Ethiopia comprises:

- Sustainable management, cultivation and biomass (Embaye 2000, Embaye *et al.* 2005, Katumbi *et al.* 2017, Kigomo 2007, LUSO consult 1997, Mulatu 2012, Mulatu *et al.* 2016b, Mulatu and Fetene 2013, Seyoum *et al.* 2018, UNIDO 2009a)
- Propagation techniques (Ayana 2014, Kebede *et al.* 2017, Kigomo 2007, Mulatu and Feng 2014, Negash 2010)
- Raw material characteristics and processing (Kelemwork *et al.* 2008, Schmidt 2013, Starke *et al.* 2016)
- Engineered panels (Böck 2014b, Kelemwork *et al.* 2005, Schmidt *et al.* 2016a, Stute 2018)
- Value chains and socio-economic studies (Endalamaw *et al.* 2013, Mekonnen *et al.* 2014, Teshale *et al.* 2017)

Evidence from other developing countries showed that the “supply push” policy has to change to a “demand pull” approach (Tambe *et al.* 2020). The supply of raw culms has increased while the industrial utilization has declined. Similarly, the Ethiopian research and policy priority on the supply-side may successively switch to the opening of new markets. Like Ethiopia, China had used traditional bamboo products based on barely processed bamboo for centuries. The industrialization of large bamboo plantations in the 1990s shifted the focus to paper, textile, charcoal and engineered composite panels. The success of the Chinese bamboo industry and its manufacturing boom results from a subsidized, innovative export-based economic model (World Bamboo Organization 2018). The historically grown cultural identity and the fast integration of research into business models helped to grow the total value of China’s bamboo industry. It is a common fact that the Chinese bamboo industry is world leader with 7.75 million employees with a net value of USD 19.5 to 30 billion in the years 2015 and 2016, respectively. In the same years China exported USD 1 to 1.5 billion in bamboo and bamboo products (World Bamboo Organization 2018, Zhiyong and Junqi 2017) representing two thirds of the global market. To date, the Chinese export numbers are probably more reliable than any other import figures in the Western world due to lacking HS codes for bamboo-based products (Liu *et al.* 2015b, van der Lugt and Otten 2006). Global trade in bamboo is valued at USD 60 billion including intra-country trade especially in India and China. Although these figures seem to be relatively high, export of bamboo products accounts to less than 1 % of the world wide traded forest products value (World Bamboo Organization 2018). A potentially emerging bamboo industry in East Africa is endangered to be cannibalized by the outdistancing cost and innovation performance of the Chinese bamboo industry. The superior size of wood-based panel industries is known to directly correlate with the export success of Chinese companies (Qin *et al.* 2015). Zhiyong and Junqi (2017) explain the Chinese bamboo development policies: Between 1978 and 2000, the number of bamboo-related research papers exploded, though the Chinese bamboo industry mainly commercialized low grade products. There was a discrepancy between published research papers and actual entrepreneurship. The strengthening of independent innovation capabilities and a massive investment in implementation measures adjusted industrial structures and currently transforms China’s growth strategy. The Ethiopian bamboo sector is difficult to analyze due to lacking market information, diffuse institutional organization, the mainly informal sector and poor industrial structures. However, Fu (2019) prospectively sees a potential USD 7 billion annual income and 2.5 million laborers in the long run of the Ethiopian bamboo industry. To identify appropriate product opportunities the value web concept (Virchow *et al.* 2014) was combined with the product space theory (Hidalgo *et al.* 2007).

2.1.3 Value web and product space analysis

The value web approach uses a multidimensional framework to understand the interdependencies between several value chains. The web approach covers the various products obtained from a single raw material, analyzes the potential product portfolio, their value chains and how to potentially link them. This perspective helps to explore the synergies between these value chains, identifying resource inefficiencies instead of showing only the linear pathway of a product (Virchow *et al.* 2016).

The product space theory explains the development of an industry with the relative comparative advantage and the degree of similarity (raw material, process and market) of the emerging industry and the existing economy. Hidalgo (2011) looked at macroeconomic

indicators and identified the best industrial development opportunities in East Africa. The author recommends that emerging industries must not be decoupled from the agricultural product portfolio. Bahar *et al.* (2014) explains this effect with a knowledge diffusion mechanism which facilitates the establishment of “neighboring” branches. The industrial development policy has to focus the promotion of goods and services adjacent to existing branches. Siba and Gebreeyesus (2016) showed the learning effect which benefits the emerging manufacturing sector in Ethiopia once pioneer firms are exporting processed goods.

Based on literature review and expert interviews, the Ethiopian bamboo-based value web was analyzed for existing products, interdependencies between them, their processing depth and economic impact. The results were illustrated in figure 7. The supply relations (black arrows) and potential connections (grey arrows) have been worked out in accordance with the principles of a force spring algorithm. The processing depth of each product or intermediate is highlighted by color coding. Red stands for a highly intense processing, i.e. at least four distinguishable process stages; yellow stands for medium processing intensity and green for low intensity, such as simple drying or splitting. The economic impact is indicated by the line thickness of each connection. The thicker the line, the higher the net value flowing from one (potential) production to the other. The grey domains enframe product spaces with either similar production technologies, complementary intermediate products or comparable market channels. Those product spaces were grouped irrespective of whether the product is currently being manufactured in Ethiopia or not.

Figure 7 shows a central product space containing typical bamboo uses which are closely associated to the informal sector, such as in handicraft and architecture techniques (Lin *et al.* 2019, Seyoum *et al.* 2018). They share the same rare market channels and are of low bulk value density. Moreover, utilities, such as curtains, incense sticks, toothpicks are in a direct cost competition with Indian and Chinese producers. Ethiopia exports such products solely regionally, e.g. to Sudan and the Middle East. Production is related to high amounts of residues and a very low added value. Furniture products mainly come from the informal sector. The first efforts for operating semi-industrial workshops were undertaken by Chinese trainers (Fu 2019) but did not show the desired effects yet. This traditional branch adds higher value but produces a bulky good, restricting its export prospect. Long distance transports impact the cost structure of traditional bamboo furniture and hence superregional or international commercialization is economically infeasible. The product space on the upper left of figure 7 represents subsistence bamboo uses. Using leaves for fodder and culms for fuelwood is an ancient habit in Ethiopian rural communities. Most of those products do not even have a market channel due to the local production-to-consumption chain. A relatively new product are bamboo shoots for alimentation, which can be produced from highland and lowland bamboo and are currently being commercialized in Asian expat restaurants.

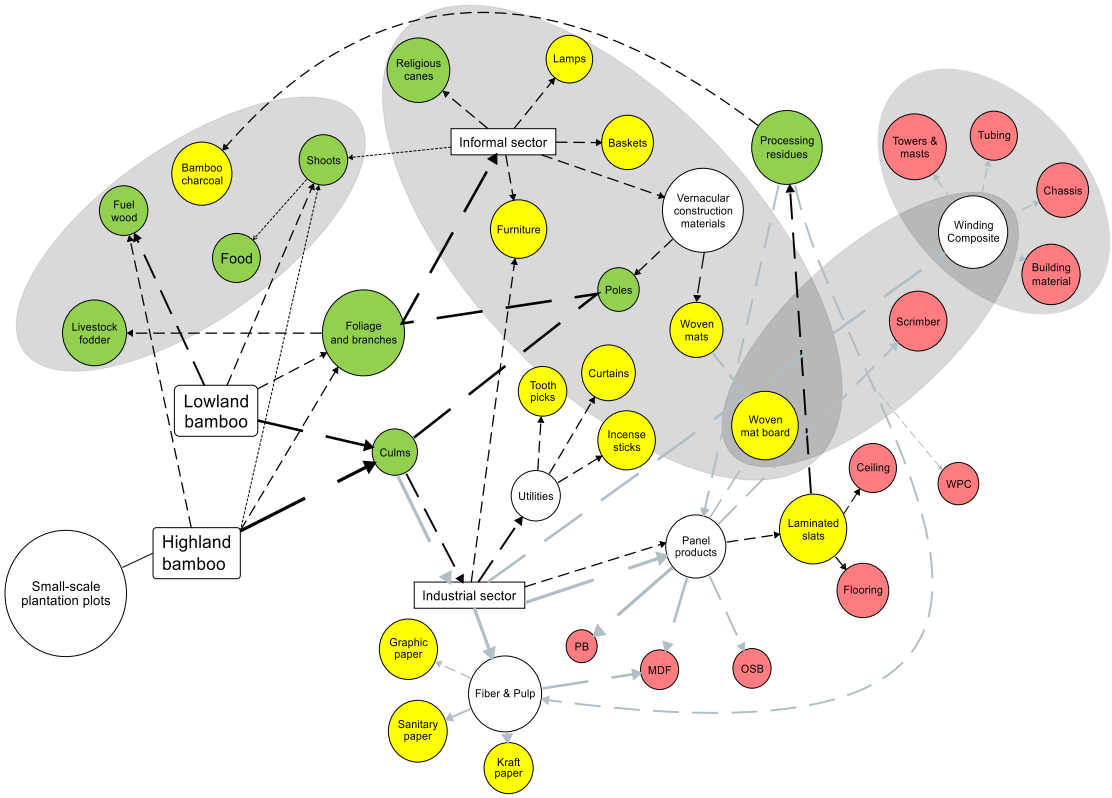

Figure 7: The actual and potential Ethiopian bamboo-based value web illustrating 1. Existing (black arrows) and potential supply relations (grey arrows), 2. Processing depth (red: highly intense; yellow: medium; green: low), 3. Economic impact (line thickness) and 4. Product spaces (grey domains)

Bamboo industrial activities in Ethiopia have declined lately. There were three bamboo processing factories: the first, Adal Industrial PLC, located in Oromia, about 20 km from the capital. The factory was set up in 2006 and is capable to process 500 to 1000 highland bamboo culms per day. The company produces utilities (sticks, curtains) and floorboards (laminated slats). The labor-intense production operates with simple machineries, UF resin and makes use of the relatively low labor costs. According to the owner (Berhe 2019) there are plans to expand the product portfolio to WPC and bamboo-based pulp and paper. The second factory, called SA Bamboo PLC, is located about 20 km west of the capital and was founded in 2017 (Fu 2019). To date, there was no notable production output, though the product portfolio seems to be similar. The third one has been operating in Asosa, in Western Ethiopia from 2007 to 2018. Bamboo Star Agro-Forestry PLC had overseen nearly 400,000 hectares of lowland bamboo natural forests in the Benishangul region. The company had started a completely new factory to produce laminated bamboo flooring, interior fittings, toothpicks and chopsticks. The factory had a planned annual capacity of 120,000 m² flooring and ceiling (laminated slats), doors, chopsticks and toothpicks. The cash cow of the factory was laminated bamboo floorboards. Though using Taiwanese processing machinery, the output quality (surface, color, consistency) did not compete with foreign competitors. Consequently, boards could only be commercialized on the Ethiopian market.

Products based on the mat-weaving techniques were developed mainly by rural women in the informal sector. These woven bamboo mats have been produced for the vernacular Ethiopian architecture over centuries. Rural communities use the mats for traditional housing, such as the so-called Sidamo dome houses shown left in figure 8, but also for coffee fermentation and

as containers. The mats are woven from the outer high-density sliver which was split off the bamboo slats (UNIDO 2008). Comparable methods are known from indigenous cultures in South America and countries in Asia (Hidalgo López 2003). Although, this advanced indigenous knowledge on fiber bundle splitting, knitting and weaving is used for traditional buildings, it may facilitate a value chain for technical fibers as well. The important role of traditional bamboo knowledge is highlighted in Seyoum *et al.* (2018). This is where modern manufacturing technology and indigenous knowledge may catch up. The production of bamboo fiber intermediate products, such as mats, filaments, fabric webs is in principal not that different from artisanal products.

Since the late 1990s research concerning bamboo composites has been focusing on fiber extraction techniques, high-value product applications (Abdul Khalil *et al.* 2012, Fan and Fu 2017, Jawaid *et al.* 2017) and textile applications. Bamboo textile fibers are either won mechanically (retting) or chemically (regenerated cellulose). In the mechanical process, the woody culms are crushed and wetted so that the fibers can be combed and spun using processes like those of flax production (Hu *et al.* 2019, Kaur *et al.* 2013). In the retting process, naturally occurring enzymes break down the parenchyma and cell middle lamella, facilitating the extraction of the fiber bundles (Müssig 2001). However, this process is work intensive and its economic feasibility will directly depend on labor costs. Swiss company Litrax together with Lenzing (Austria) was engaged in developing such fiber production (nova-institute 2010). Fabric made by this process is also called bamboo linen. It is a coarse but highly stiff material and provides a durable textile for clothing (Nayak and Mishra 2016).

Figure 8: Traditional Sidamo dome house made from woven bamboo strips (left) and mechanically extracted technical bamboo fiber (right)

For technical application, one major concern is the damage of fibers during extraction. A recently developed method of hydro-mechanical fiber extraction (Trujillo 2014) delivers technical fiber bundles shown in figure 8. The same research group investigated the major microstructural damages (Osorio *et al.* 2018) and their relation to the mechanical properties whilst other studies looked for culm height classified extraction grading to guarantee constant quality (Hu *et al.* 2019). Such intermediate technical bamboo fibers can be further processed to engineering composites (Fan and Fu 2017, Perremans *et al.* 2018), reinforced thermoplastic composites (Abdul Khalil *et al.* 2012) and large scale engineering materials. Most prominent applications promise enormous potential for lesser developed countries by solving three problems at the same time: a substandard electricity and water infrastructure and the import of engineering materials for piping and utility poles. Innovative engineering products from technical bamboo fiber composites may significantly contribute to develop sustainable solutions.

The bamboo fiber based winding composite was invented a couple of years ago in a Chinese patent (柃 叶刚 朱钟坚瑜陈文强 2010). Researchers started a research line on how to produce winding composites from technical bamboo fiber and a water-soluble resin. The innovator company Zhejiang Xinzhou Bamboo-based Composites Technology Co. Ltd. was listed in the first batch in the Chinese National Key Research & Development Plan (XZBBC 2016) and started operating in 2016. It was the first ever to set up a Chinese state research center installed into a private company infrastructure (Zhiyong and Junqi 2017). To date, the industrial hub has produced 300,000 units of stiff round elements for water pipes, electricity modules, train chassis or even modular buildings. Emerging economic development, substandard electric infrastructure and the urbanization pressure induce a demand for decentral power supplies in Ethiopia and other East African countries. Beronov *et al.* (2015) assumed the annual power demand would show an increase of 7.7 % by 2030. Wind energy utilization emerges in Ethiopia – two wind parks (324 MW) are already operating. One major constraint is the import of tower elements, generator compartments and rotor blades. The first approach of using bamboo-epoxy laminate composites for structural parts of wind turbine blades was published by Platts (2013). The technological requirements were proven (Platts 2014) and nowadays, bamboo wind rotor blades are produced by four Chinese manufacturers. Blades of 40 m length for stations of the 1.5 MW capacity class were installed in Hekou and Tiansheng, China, in 2010 and 2012 (Beronov *et al.* 2015). Since then the market is ever growing and dozens of stations have been put into operation. The combination of relatively high labor efforts (manual sanding and manufacturing), bamboo as main raw material and the emerging wind energy market in East Africa, make this technology a perfect fit for the Ethiopian industrialization case. Nevertheless, the relatively high skill level in such productions require long-term qualification.

Figure 9: View on infrastructure utility tunnel made from a bamboo-based winding composite (XZBBC 2016)

Shell core (recycled) bamboo plastic composite (BPC) are composites made from a recycled thermoplastic matrix and bamboo fibers or particles as a filler (Fan and Fu 2017). Just like wood plastic composites (WPC), such composites show a higher density than solid bamboo or neat plastic. They can be processed with technology from the plastic industry. Such BPC are produced in a co-extrusion process and consist of 90 % low-grade recycling materials in the core and 10 % virgin or high-grade polymers in the outer face layer. The usage of secondary resources, such as bamboo process residues and recycling plastics positively impact the product life cycle (Sommerhuber *et al.* 2017). Currently, the BioHome project (BMBF 2017-2021) deals with questions of composite development, frugal processing and mass-flow-analysis of such BPC from recycled resources (Schmidt *et al.* 2017).

The range of all industrial products made from bamboo is very wide and will not be displayed here. For a general overview, the bamboo encyclopedia by Hidalgo López (2003) offers the whole range of bamboo products. Further summaries on general industrial utilization of bamboo, including bamboo-based panels (BBP) are available from Zhu and Jin (2018), Liese and Köhl (2015), van der Lugt and Otten (2006), Zhang *et al.* (2002) as well as the somewhat aged INBAR study by Ganapathy *et al.* (1999).

2.2 Wood and bamboo based engineered panel products

The wood-based panel (WBP) industry processes fibers, particles, flakes, veneers, strands or even fine saw dust. The cutting, flaking, milling, peeling or defibering harms the natural structure of the wood and the panel product does not reflect the superior mechanical properties of the tree. Moreover, the pre-processing consumes energy to disintegrate the raw material to a low bulk density and small particle size. Afterwards the won particles are compressed into a relatively homogenous panel with controllable properties. The smaller the particles become, the better formable is the intermediate product. Particle size is an important factor to consider when developing new products and analytical models. Generally, the longer and slimmer a particle is, the higher the stiffness and strength properties of the panel (Bodig and Jayne 1993, Marra 1992, Niemz 2014). The stress distribution within a WBP made from slender strands varies with the element size distribution (Paton 1997). Marra (1992) pointed out that as the element size decreases, the stiffness and strength losses can be recovered by increasing density, adhesive content, aligning the elements, or reducing the variation in the product properties. Such structure-property relations should be applicable to bamboo-based composite products, too. The combination of bamboo and a resin results in a composite which can be used for construction in many applications, very similar to WBP (Fan and Fu 2017, Hannula 2012, Wegst 2011). Liu *et al.* (2015b) define engineered bamboo-based building products (also “engineered bamboo”) as “products that have undergone processing primarily to produce consistent, straight-edged building materials from round, irregular culms.” Just like many other authors (Fan and Fu 2017, Yu *et al.* 2018), they do mix up the terms “engineered bamboo”, “bamboo composite” and “bamboo-based panel”. In fact, “bamboo composite” can be referred to nearly all building products from bamboo, due to its natural composite structure on the one hand (culm-based products) and the two components, a resin binder and lignocellulosic element (panels). The focus of this chapter is on industrialized building products. The appended figure 96 shows the main difference between three main groups of industrialized engineered construction materials made from bamboo (World Bamboo Organization 2018). A classification of bamboo-based panels (BBP) was suggested by Zhang *et al.* (2002) who sub-divided BBP according to their raw material form into plywood (veneer), laminated (strips) and chipboard (particles) products. The primary industrial processes either chips, saws or crushes the bamboo culm. The largest amount goes to bamboo chips, either processed to fibers, pulp or particles. The traditional classification of WBP can serve as template for BBP. The categories suggested in figure 10 represent the intermediate raw materials and their element size. The large solid slats used in laminated bamboo lumber or slivers used in woven mat panels are found on the left and fiber-based products on the right. The following chapters introduce each category from the smallest element to the largest as classified in figure 10. Further literature provided plenty of insights into BBP and its processes (Ansell 2015, Fan and Fu 2017, Jawaid *et al.* 2017, Liu *et al.* 2015b, Paulitsch and Barbu 2015).

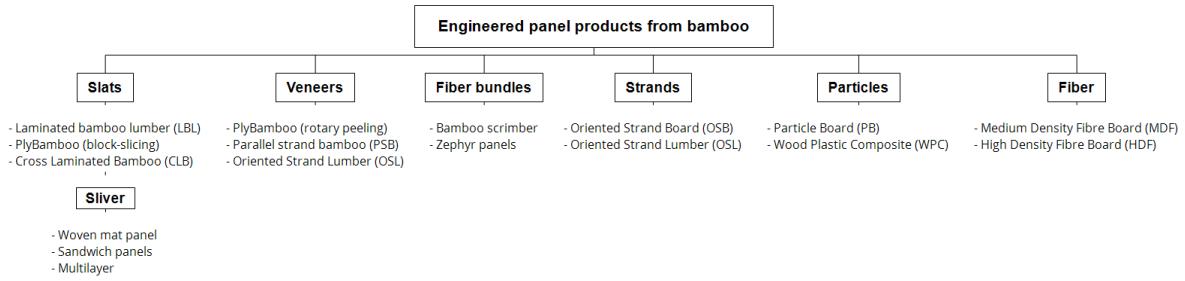

Figure 10: Classification of engineered composite panels from bamboo by their intermediate raw materials from large to small element size

2.2.1 Fibers

Fiberboards have gained higher attention in the last years, particularly in the indoor sector, construction and carpentry. Fiberboards are sub-divided by their panel structure and the production process. The highest market shares account to medium-density-fiberboards (MDF), thin high-density-fiber boards (HDF) and softboards for insulation purposes. Typical HDF panels show high densities of 0.8 to 1.05 g/cm³. Where MDF ranges from ca. 0.35 to 0.8 g/cm³ porous fiber boards are of low density (< 0.35 g/cm³). Those are a suitable substitution product for polystyrol or other petrol-based insulation panels.

Two decades ago, Ganapathy *et al.* (1999) classified bamboo fiberboards as an “experimental technology” and mentioned research in China and India. Back that time only minor quantities of bamboo MDF were produced in China. Today, India has built up the first MDF production using rubberwood and bamboo. Other non-wood alternatives on an industrial scale are straw-based MDF productions. Countries like India dispose around 80 million tons of rice straw every year (WBPI 2018). While involvement of big industrial players, such as Siempelkamp and Pallmann provided experimental know-how on silica sifters, retailers such as Ikea contracted high demand volumes. These dynamic developments accelerated the use of bamboo and straw in fiber boards. A new MDF/HDF plant in India’s Uttarakhand state started production in 2018 aiming at a 500,000 m³ annual capacity (WBPI 2018).

Generally, bamboo-based fiberboards are produced using similar equipment as known from wood fiberboards. Bamboo chips are water-soaked and hygrothermally treated at 130 to 170 °C. The steamed chips are defibrated in a refiner either solely mechanically (RM pulp), thermo-mechanically (TM pulp) or chemo-thermo-mechanically (CTM pulp) by adding an alkaline agent. Figure 11 shows RM pulp from highland bamboo processed on an atmospheric refiner. The mat formation can either happen in an aqueous emulsion (wet process) or using pre-dried fibers (dry process). Ganapathy *et al.* (1999) reports on 1 % PF resin and 1 % wax used for 4 mm thick board with 1.0 g/cm³ target density. Preliminary experiments on MDF production from highland bamboo were done by UNIDO (2009b) as well as at Fraunhofer WKI laboratories. The most important parameters that directly influence bamboo fiberboards performance are similar to WBP: resin content, density and hot-pressing procedure (Paulitsch and Barbu 2015). Bending strength (MOR) and modulus of elasticity (MOE) of highland bamboo MDF ranges from 16 to 20 N/mm² and 2.1 to 2.8 kN/mm², respectively. The regarding panels have been produced with 10 % UF and a target density of 0.75 g/cm³ (UNIDO 2009b). The same applies for internal bond (IB), thickness swelling (TS) and water absorption (WA) which range from 0.2 to 3.0 N/mm², 2 to 23 % and 12 to 82 %, respectively.

Figure 11: RM pulp produced with atmospheric pressure from Ethiopian highland bamboo (Kickhöfen 2019)

To date no MDF plant operation has been started in Ethiopia. The production processes for MDF, HDF or tHDF are economically only feasible investing in annual production capacities above 250,000 m³ using continuous hot-presses. An industrial MDF production of this size consumes ca. 800 to 900 kWh/m³ thermal energy and 280 to 350 kWh/m³. Interruptions in electrical energy or water supply would damage the equipment and lead to extraordinary costs. This production scheme continuously demands large amounts of fresh bamboo in a constant quality which currently is not possible in Ethiopia. Frugal process developments with low batch sizes can offer solutions by using extruder defibration technology (Trung Cong *et al.* 2006). They can be used decentral and can produce pulp in small batches based on seasonal demand. However, the geometry of extruder fiber was rather dull and not as slender as of RM pulp. The costs of such process must not be neglected but might be compensated by producing higher value products such as WPC. First investigations on highland bamboo WPC investigated lubricants and process fiber degradation recently (Kickhöfen 2019).

2.2.2 Particles

Particle boards (PB) made from bamboo were developed on commercial scale in China, Costa Rica, Malaysia and Vietnam. Commercial bamboo PB bulk density ranges from 650 to 800 g/cm³ and mostly uses UF and PF with resin concentrations varying from 4 to 12 % (Ganapathy *et al.* 1999). The most important parameters that directly influence bamboo particleboards performance are similar to WBP: resin content, density and particle size/morphology (Paulitsch and Barbu 2015). In general, bending MOR and MOE of bamboo-based particle boards range from 6 to 38 N/mm² and 0.7 to 5.8 kN/mm², respectively. This wide range owes to the use of alternative binders, such as castor-oil based polyurethanes or citric acid (Gauss *et al.* 2019). The same applies for IB, TS and WA which range from 0.2 to 3.0 N/mm², 2 to 23 % and 12 to 82 %, respectively. The raw material quality for PB is relatively low (see figure 12). Residues from other bamboo processing industries can be incorporated but do stand in competition with energetic uses. Factories in Africa produced no more than 73,100 m³ PB in 2015, mainly based on pine and eucalypt plantation wood. On the other hand, the market volume, which currently stands at about 250,000 m³, is growing strongly, but mainly demanded by countries in the Magreb region (Egypt, Morocco, Algeria, Tunisia). The demand gap was covered by European producers (European Panel Federation 2018) which represent an annual 32 million m³. This offers a vast potential for traders and producers in the region but hinders the establishment of PB productions in SSA.

Kelemwork *et al.* (2005) used 10 % UF producing a layered particleboard from *Y. alpina*. Their study was the first ever using Ethiopian bamboo in a wood-based panel. The study investigated bamboo growing site, board density, particle size, particle orientation and particle layering and their influence on mechanical and physical properties. With a 750 g/cm³ target density they achieved a flexural MOE of 2.1 to 6.8 kN/mm² and MOR ranging from 17 to 34 N/mm². The study confirmed basic structure-property relations for highland bamboo PB as they are known from WBP. Higher bamboo maturity (age) did not affect the panel mechanical properties but lowered IB and increased TS.

Figure 12: Hammer mill produced particles from Ethiopian highland bamboo (Stute 2018)

A second study done by Shimels and Woldesenbet (2014) used Ethiopian lowland bamboo *Oxytenanthera abyssinica* and 12 % UF on a standard lab hot press. The findings are not well evaluated but do show that lowland bamboo is on a par with the common products made from eucalypt. The authors intended to implement a bamboo PB production at Maichew PLC panel factory in Ethiopia's Tigray region. The project was stopped due to low competitivity and raw material supply problems. A common PB production consumes between 400 to 600 kWh/m³ thermal energy and needs an estimated 90 to 150 kWh/m³ electrical energy (Michanickl 2013). Production lines operate with continuously working hot presses and are highly sensitive to abrupt power cuts.

2.2.3 Strands

Strands are cut slender chips which can be used either for waferboards, single or multilayer oriented strand boards (OSB) and oriented or parallel strand lumber (OSL/PSL). Oriented strand boards (OSB) made from bamboo and their production methods were patented in China by the Yung Lifa Forest company and Hong Kong-based Panda Capital, a Swiss investor. To date, the only operating industrial scale production existed in China. The Chinese provincial authorities had initiated a bamboo commercialization project in 2008 and started planting 80,000 ha *Phyllostachys* spp. in the Yunnan province. After four years of development Yung Lifa started the first production in Luxi, Yunnan China in October 2012. The bamboo OSB panels were produced with a target density of 850 g/cm³ and were meant to be used as container flooring boards substituting high density tropical plywood (Grossenbacher 2012, Paulitsch and Barbu 2015, WBPI 2012). Thus far not one single OSB production plant exists in Sub-Saharan Africa using either wood or bamboo as a raw material. At the same time the demand for OSB in Africa is negligible and ranges below 1 % of the overall global demand volume (European Panel Federation 2018).

OSB productions in Europe commonly use pine wood, North American producers use aspen and yellow poplar whereas low density pine and eucalypt (short rotation plantation wood) is used in South America (Liu and Lee 2003). High quality OSB panels need homogenous and slender strands with controlled dimensions and a minimum of fines. Species with a homogenous density profile are favorable for strand production, i.e. flat density gradients across the stem and along the longitudinal axis (Paulitsch and Barbu 2015). In contrast, bamboo comes with a harsh density gradient in the transversal plane and adds the difficulty of handling the nodal areas. Typically, OSB strands are commonly produced with long log knife ring flaker, such as Pallmann's PZU universal flaker. First trials with bamboo have shown problems in homogeneity and yielded irregularly shaped strands shown in figure 13. The standard ring flaker knives have been worn resulting in short maintenance intervals and exploding costs. The strands break apart at the node and do not fulfill the requirements of OSB strands (slender, homogenous, low fines content, stable dimension ratio). Research focused on moso bamboo and a novel stranding method cutting out the nodal part of the culm and stacking the resulting cylinders in one another (Semple 2014, WBPI 2012). The new stranding knives cut horizontally into the culms and yield an homogenous quality shown in figure 13B.

Figure 13: Bamboo strands produced with a Pallmann universal knife ring flaker including nodes (A) and without nodes (B) on a Yung Lifa strander, adopted from Grossenbacher (2012)

Nevertheless, even when nodes are cut out, different bamboo species lead to different strand qualities (Semple *et al.* 2015) and subsequently different panel properties (Febrianto *et al.* 2015). Several pre-treatment methods (cold water extraction, acetylation steaming) may improve the stranding process quality as well as the final composite properties (Febrianto *et al.* 2012). Steam treatment plasticizes the lignin and hence facilitates the cut against the fiber grain direction which increases the strand yield (Fatrawana *et al.* 2019).

In contrast, production experiments at Fraunhofer WKI have shown the technical feasibility of a strand-based panel production with African highland bamboo without removing nodes or prior sorting. The single layer panels were produced by steaming culm sections (125 °C for 30 min) and three different PF resin concentrations applied in a rotating drum blender. The 19 mm thick bamboo OSB panels were hot pressed with 200 °C platen targeted a moderate density of 700 g/cm³ and temperature. The results in table 2 indicated that highland bamboo OSB panels fulfill OSB/1 standards defined in DIN EN 300:2006-09. Highland bamboo OSB showed to be feasible to compete with existing OSB made from moso bamboo. Nevertheless, laboratory research on Asian bamboo species (Lee *et al.* 1996), layer structure (Sumardi *et al.* 2015) and resin concentration (Sumardi *et al.* 2006) showed far better flexural properties than the present results. Further research on multi-layer highland bamboo OSB and alternative resins is needed. Nevertheless, important properties of OSB boards such as bending MOE and MOR are limited due to the restricted strand length.

Table 2: Bending strength (MOR) and elasticity (MOE), internal bond (IB) and thickness swelling after 24 h water immersion (TS) of oriented strand board from steam-treated Ethiopian highland bamboo produced with different resin contents (Fraunhofer 2014)

c_{resin} [%]	MOR [N/mm²]	MOE [kN/mm²]	IB [N/mm²]	TS [%]
10	20.87	3.09	0.25	6.0
13	22.90	3.60	0.21	6.0
16	25.68	3.19	0.45	3.0

This length restriction for OSB strands is a consequence of technical limits of the ring flaker. The parallel strand lumber (PSL) and oriented strand lumber (OSL) concepts overcome this by producing intermediate veneers which are subsequently cut into slender veneer strands. These processes commonly require raw materials with a constant quality and at least medium log diameters. Small diameter logs, damaged beetle wood or fast-growing species with high amounts of juvenile wood are not suitable to produce veneers or long strands (Liu and Lee 2003, Paulitsch and Barbu 2015). Nevertheless, the production of OSL and PSL from bamboo cannot be done via an intermediate veneer due to the technical restrictions of producing bamboo veneers described in the chapter 2.2.5. Up to now, research on long bamboo strand composite panels was carried out by Malanit *et al.* (2011) developing OSL and Ahmad and Kamke (2011) working on PSL. Both studies produced strands manually using *Dendrocalamus* spp. and pressed panels with different resins in a hot press with specific pressures around 4 N/mm². Commercial productions do not exist yet. Though there are publications mentioning “parallel strands” from bamboo (Dongsheng *et al.* 2013) the term was often used in a confusing context. Once long, slender strands have been produced by a non-cutting process, they should rather belong to the fiber bundle class. The structural differences of both product classes were described in the literature (Jin 2001).

An average OSB production consumes thermal energy in the range of 500 to 700 kWh/m³ and adds up another 130 to 180 kWh/m³ of electrical energy (Michanickl 2013). Wood-based OSB lines either work with multidaylight presses or continuous presses and require a constant fresh raw material supply. Power cuts or water shortage (steam) will cause remarkably high maintenance costs. The experimental bamboo OSB production at Yung Lifa is a multi-daylight batch press and thus produces at higher variable costs than continuous wood based OSB lines (Paulitsch and Barbu 2015).

2.2.4 Fiber bundles

The usage of fiber bundles in composite panels bases on an alternative technique. It makes use of the inherent fracture mechanisms in lignocellulosic plant stems. Instead of turning the eye blind on the precious wood structure, one takes advantage of its natural fracture behavior and crack propagation (Amada and Untao 2001, Liu *et al.* 2015a, Youssefian and Rahbar 2015). The general principle is to splinter the raw stem along its longitudinal axis instead of cutting perpendicular to the fiber. The so produced fiber bundles, also named scrims or scrim strands, are much longer than common wood particles (see figure 14). Together with a thermosetting resin the scrims are then consolidated to a billet under pressure and can be machined just like common sawn timber (Shang *et al.* 1998, Wagenführ and Scholz 2008). This process converts low grade timber into structurally strong composite beams utilizing around 85 % (Jarck 2017).

Figure 14: The scrims after being released from the crusher line (Hemmings 2019)

There are principally two ways of producing scrim strands. The decomposition can be either done in a roller crusher or with press plates. The basic ideas of the roller crusher are relatively simple and resemble the rudimentary sugar cane processing equipment (Miller *et al.* 1969). The first concept using wood and a roller crusher was patented by Harvey Jr (1972). The patent describes an apparatus for converting solid logs into splinter-like wood particles by passing them through a series of heavy rolls with controlled pressure. The logs enter a series of three roller crusher pairs (figure 15a) with a profiled surface, followed by four press rollers (figure 15b). The roller crusher applies pressure to the raw material by two counter rollers. The diameter, distance and speed of the roller pair forces the material to bend and subsequently generates tensile stresses perpendicular to its grain direction. Moreover, the press rollers cause normal stresses in the raw material and split it along the grain, resulting in a flat and disintegrated fibrous mat. The single scrim strands (Harvey calls them “splinters”) are then separated from each other with a scrubber device. The latter basically is a pair of metal plates with grooved profiles which moves in the y-z plane to scrub off the scrim strands from the mat (figure 15c). The apparatus had never been built at industrial scale. However, the idea of substituting lumber with composite based on a long, slender and non-cut fiber bundle, was developed parallelly in different parts of the world and inspired new processes to date (Joscak *et al.* 2006). The most important production concepts are introduced hereinafter.

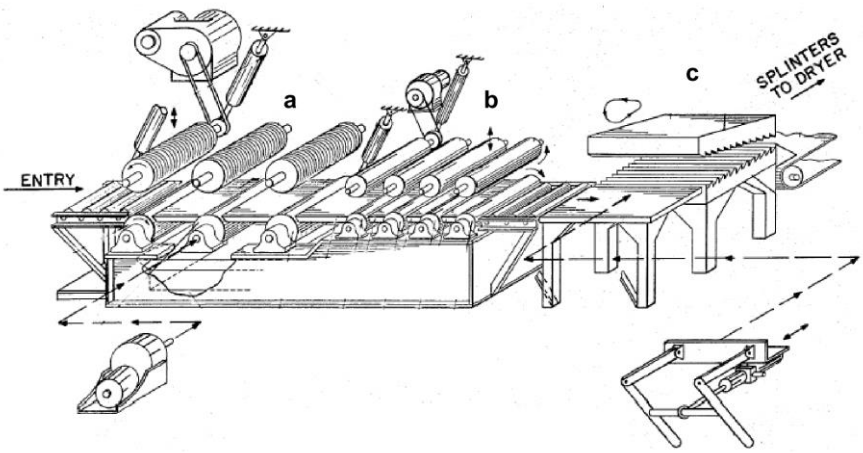

Figure 15: Apparatus described by Harvey Jr (1972) using three pairs of crusher rollers (a), four pairs of press rollers (b) and a scrubber device for strand separation (c)

- PRODUCTION CONCEPTS

The so-called "*Quetschholz*" process uses press platen technology and was developed in technical scale at the former Institute of Forest Sciences in Eberswalde, former German Democratic Republic. Figure 16 shows the basic principle described by Götze and Luthardt (1974) in the former German Democratic Republic. The process combines both principles, press plate and roller crusher, but lacks the scrubber device. These plates basically look like the scrubber station in figure 15, however do not separate the scrim strands from each other (Götze *et al.* 1980). The two angled, profiled plates periodically oscillate up and down and thereby apply compression force to the log. The laterally applied force then leads to rolling shear stresses and subsequently detaches the fibrous bundles from each other.

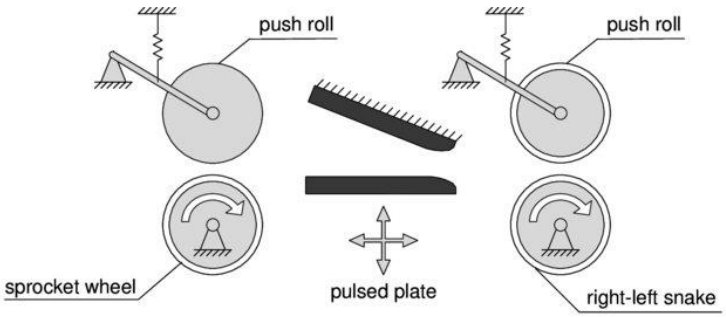

Figure 16: The two basic log disintegration principles in the Eastern German "Quetschholz" technology (Götze and Luthardt 1974 cited in Joscak *et al.* 2006)

In 1985 the Japanese Forest and Forest Products Research Institute (FFRRI) started their own research on scrim strand making. The FFRRI then patented the Superposed Strand Timber process (SST) using a press-split rollers (Fujii and Miyatake 1998). The abbreviation SST stands for "Small logs, Short logs and Twigs, producing Superior Strength Timber". Another specialty about the SST process are the two steps shown in figure 17. The first station divides the log in coarse pieces, followed by a second pair of rollers in which the discs are staggered in reverse order and produce finer scrims (Fujii and Miyatake 1993). Empirical studies on SST made from sawmill residues, namely *Cryptomeria japonica* slabs, showed to compete with high grade timber. With a density of 0.67 g/cm³ the SST achieved bending MOR and MOE of 75.6 N/mm² and 10.1 kN/mm², respectively (Suzuki 2005). A raw material yield of 90 % and above was reported for the SST process (Miyatake 2002). A pilot plant for SST with an annual capacity of 7,500 m³ started operations in 1997 (Miyatake 2004). However, according to Joscak *et al.* (2006) the production was ceased due to economic constraints. The authors commented that the technology is not robust enough to tackle with hard and highly dense raw materials. Sugi based SST were used in cement-bonded composites. MOR, MOE and especially fire resistance were higher than in common SST which makes a low-value resource interesting for high-rise buildings (Miyatake 2002). The hardest challenge is the problem of matrix compatibility. The highly alkaline matrix and the slightly acetous wood do not form a chemical interface. The relevant mechanism between geopolymer and lignocellulosic particles is mechanical interlocking (Fujii and Miyatake 2003).

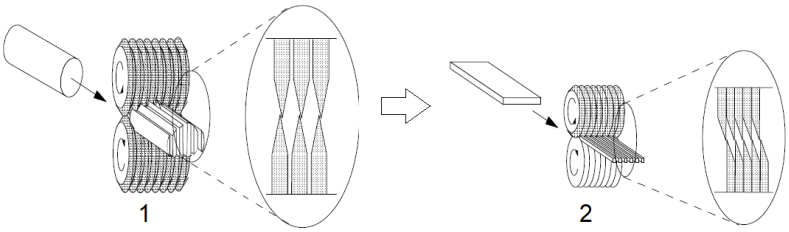

Figure 17: The two roll press splitters in the Japanese SST process disintegrating the log into slabs with a coarse disc profile (1) and a fine disc profile for transforming the slabs into scrims (2), modified sketch from Miyatake (2004) cited in Ceccotti and van Kuilen (2004)

Parallelly, experimental investigations on so-called "*zephyr*" were started by Japanese and Korean researchers (Kikata *et al.* 1989, Kim *et al.* 1998, Roh 2007, Roh and Ra 2009). They had started using fast-growing timber species, such as poplar (Kim *et al.* 1998), and produced low density panels (0.6 to 0.8 g/cm³) with a roller crushing technique and applying phenolic resins manually with a brush. The panel surfaces had a rough grain with an open structure which was prone to water penetration. To solve the issue, sandwich panels with *Dipterocarpus* spp. veneer face sheets were developed (Roh 2007). Other authors (Nugroho and Ando 2001) suggested to densify the zephyr mats in the hot press prior to laminating them to the core layers. Similar concepts using low technology levels (hammering by hand), were reported by Mahdavi *et al.* (2012). None of them have gained notable industrial attention yet.

The potential of these new technologies raised the attention of Chinese researchers in the late 1980s when China suffered a lack of high-quality timber. The Timber Research Institute of the Chinese Academy of Forestry advised the Northeast Forestry University in Harbin and Jiangxi Timber Factory to set up a consortium and a pilot plant was built in Xuanhua in the Hebei province (Li *et al.* 2001). They used *Pinus massoniana* with 6 to 8 cm diameter and produced scrims with a hammer crushing technique. Panels as well as billet blocks were produced on industrial scale. The equipment was designed under the assumption of isotropy of raw material and a waist-drum-shaped (腰鼓) roller crusher was constructed. Research in China has intensified due to the large amounts of plantation timber available, e.g. poplar and fir. The defibering method does not notably differ from the original patents (Zhang *et al.* 2018a), but resin concentration (> 14 %) and product density (1.13 g/cm³) were higher (Bao *et al.* 2019) which increases costs. Since the low grade plantation wood was so cheap at the time, the economic benefit of such operations was shown by Shang *et al.* (1998).

Recently, Austrian researchers had put notable efforts to push the technological development of the fiber bundle production from fresh logs. They developed roller pairs with cutting webs which encompasses the log in the circumference and rather breaks off the fiber bundles instead of squeezing them (see figure 18) to a scrim strand. The invention intends to yield more homogeneous elements of approximately 150 to 300 mm length and a slenderness ratio of about 20. The patent further describes hot-press configuration and a foaming resin, thus a complete production process (Graeter *et al.* 2012).

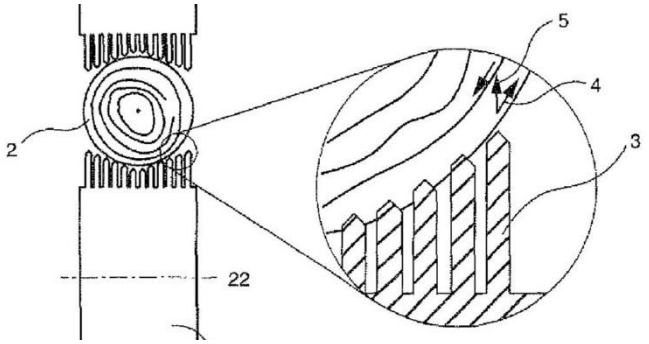

Figure 18: Device for the production of macro-fibers from wood trunks (Graeter *et al.* 2012)

- INDUSTRIALIZATION

Nevertheless, none of the above-mentioned production methods amounted to a significant commercial market volume. Simpler devices to produce scrim strands were studied at experimental stages at the German Fraunhofer Institute (Berthold 2013), in the Indian Forest Research Institute in Dehra Dun (Shukla and Prasad 1988) and some private initiative in Colombia (Hidalgo López 2003, Stamm 2019). All of them used a single pair of rollers with fixed distance and limited adjustment options. They are used for preliminary laboratory purposes and contract works.

The Australian Commonwealth Scientific and Industrial Research Organization (CSIRO) was after all the first to build a complete industrial process (Coleman 1980). The process offered a commercially and technically applicable concept to produce the so-called scrimber. The name composes of the English terms “scrim” and “timber” (Pardo 1987). A scrim actually is a heavy, coarsely meshed cotton fabric for reinforcement; Timber relates to the structural wooden beams, columns or rafters. The scrimber research and development process resulted in a pilot plant at Mount Gambier in South East Australia. The CSIRO consortium invested a lump sum of about USD 6.4 million to develop the product and process. Scrimber was introduced to the Australian market and more than USD 200,000 public money was invested for its promotion. The financial, technical and political (forestry) problems of the long-term research forced the initiative to close the production in 1992. The scrimber products disappeared from the market and were believed to have run into a dead end (Bowden 2007, Jarck 2017, Joscak *et al.* 2006).

Two decades later, the aforementioned returned to the fold of engineered wood products under the new brand name “ScrimTec”. A consortium was formed between the Australian TimTek Ltd. and the Mississippi State University (MSU) on whose campus a pilot plant was inaugurated (Jarck and Seale 2011). Commercial activities shifted parts of the project to Alabama where the Shuqualak Lumber Company bought a TimTek® patent and started putting efforts into realization of industrial projects in the region (Kryzanowski 2009). A first plant was built in Meridian, Mississippi. According to Jarck (2017), additional investments are projected in Quebec, Canada and in Malaysia (Tarmeze *et al.* 2016). The technology changed and where the original scrimber process used a high-frequency press, the new method now applied a steam-injection press. Typical quality problems had been caused due to poor resin penetration, high local resin concentrations and local low-density flaws. The scrimber technique had been re-engineered and yielded a group of patents in Europe and the US in which a complete process for the steam injection press had been developed (Coleman 2002,2011) and commercialized (Jarck 2009).

- RAW MATERIALS

The scrimber technology was a new approach for the utilization of poor-quality raw materials, such as *Eucalypt pilularis* and *Pinus radiata* or residues such as peeler cores, small and damaged logs. A scrimber mill converts low-grade raw materials into a wood product mechanically superior to the regarding lumber which could have been produced out of the same. Especially the weak diameters of plantation and thinning wood was in the focus of the scrimber technology. Typical processable log diameters are in range of 70 to 200 mm (Bowden 2007). In contrast to lumber sawmills which faced 40 % process residues, Harvey Jr (1972) claimed to reach a process yield up to nearly 100 %. The scrim strand thickness typically ranged from 0.25 to 20 mm and can theoretically be produced in various lengths. The rational handling in an automated production line necessarily limited the scrim length to below 1000 mm, although the log length is the theoretical maximum (Joscak *et al.* 2006). A fiber bundle based scrimber composite can be produced from a wide range of raw materials:

- Hardwoods, such as black oak (Harvey Jr 1972), eucalypt (Sheriff 1998, Shukla and Negi 1996), poplar (He *et al.* 2016, Kim *et al.* 1998, Zhang *et al.* 2018b), European ash (Berthold 2013), European beech (Benthien 2020) and black wattle (Tarmeze *et al.* 2016);
- Coniferous trees, such as radiata (Coleman 1980, Wei *et al.* 2019b), lodgepole and ponderosa pine (Linton *et al.* 2008), Japanese cedar (Fujii and Miyatake 1993), larch (Kikata *et al.* 1989) and hinoki cypress (Kikata *et al.* 1989);
- Industrial residues, such as saw mill slabs (Du *et al.* 2018), veneer rejects (Kim *et al.* 1998) mulberry branches (Yu *et al.* 2015a), cotton stalks (Zhang *et al.* 2016), Chinese desert shrub (Li *et al.* 2013);
- Non-wood resources, such as oil palm (Wardani 2014), coconut palm (Tarmeze *et al.* 2016) and bamboo (see chapter 2.3);

Figure 19 shows four semi finished billets made from softwood, hardwood and bamboo. In the 1990's the Australian scrimber development program tried to utilize many broadleaved wood species. In general, those with fast growth rates, either native or not, in the South Australian region around Mount Gambier were considered. This is where the first small-scale forestry and wood-processing enterprise was founded (Pardo 1987). In a study started in 1991 by Sheriff (1998), the researchers compared *Pinus radiata* and six hardwood species (three *Eucalyptus* spp., *Acacia mearnsii*, *Casuarina glauca*) for their forestry growth yield, utilization rate and wood properties. Besides the forestry aspects of such a project, Sheriff (1998) defined technological requirements. The author payed special attention to density, workability, durability, strength, stiffness and fiber grain. Density should be moderate to be able to compact the material properly. A value was not defined, but considering the chosen wood species, a basic density of 0.4 to 0.6 g/cm³ is typical. A high workability facilitates the machining of the scrimber product and avoids excessive abrasive wear of tool tips. Wettability and penetrability are needed to make a good bond quality possible. In his patent, Harvey Jr (1972) mentioned difficulties with spiral and interlocking wood fiber grain. The resulting scrim strands are distorted, and the scrubber device may cut unintentionally against the grain. The weakening effect of deviated wood fiber grain is known from natural timber and He *et al.* (2016) emphasized that a minor grain deviation will dramatically influence MOE and MOR of a scrimber product.

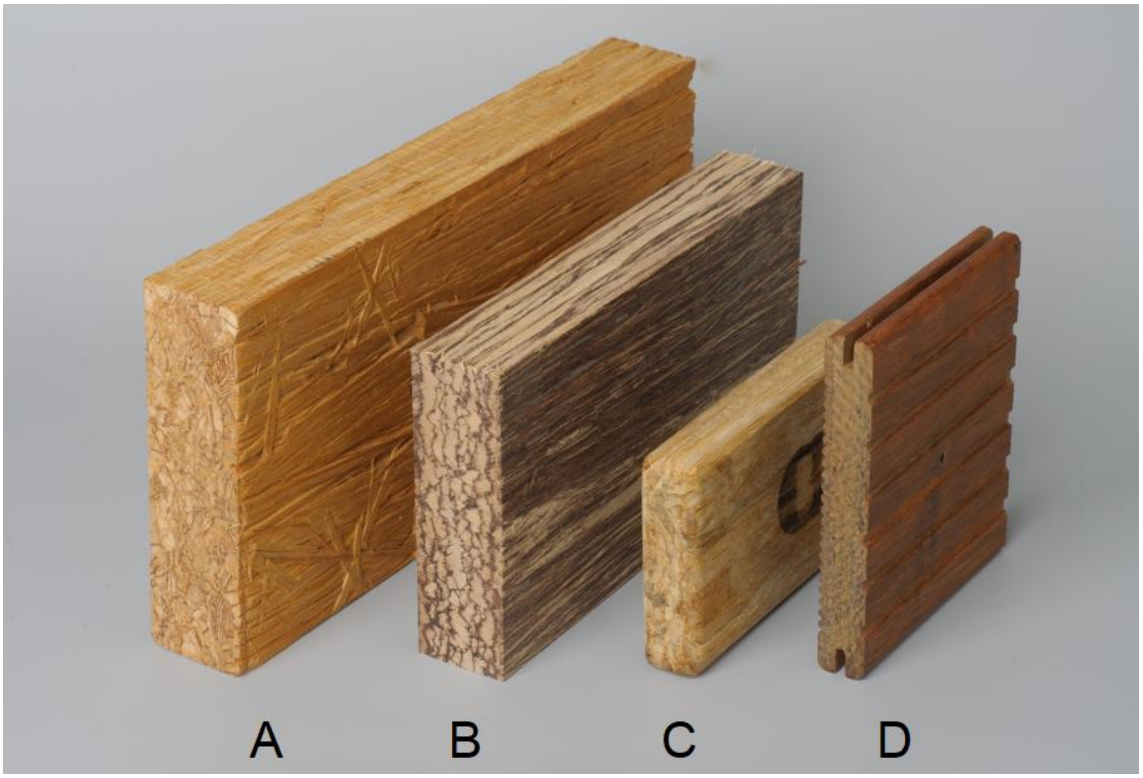

Figure 19: Scrimber billets made from pitch pine produced with the TimTek® technology (A), European beech produced in Fraunhofer laboratories (B), guadua bamboo produced with the GrassBuilt® process (C) and moso bamboo scrimber from a commercial batch from China (D)

2.2.5 Veneers

Wooden veneer plies are produced either by peeling tangentially, slicing with a veneer knife or sawing thicker veneer sheets from stems. To a certain extent, these three manufacturing methods work out for bamboo-based veneers too (Hidalgo López 2003, Paulitsch and Barbu 2015, Zhang *et al.* 2002). Most comparable with the classic wood method is the peeling of veneer sheets from a round culm. The challenges in such a production are the restricted culm wall thickness, the nodes and the relatively low yield due to the volumetric taper of the bamboo culm (Qi *et al.* 2014). The culm wall thickness along a 2.5 m height section reaches maximum of 30 to 40 mm, i.e. only 15 times the circumference length for a 2 mm thick veneer. The yield reaches around 50 % in a very optimistic case. In the nodes, separating the culm along its height axis, the fiber direction is rather unstructured compared to the linear orientation in the internodes. Curiously, these give the actual strength keeping the veneer sheet intact tangentially. The increased density in the node and the amorphous fiber arrangement results in rougher veneer surfaces than in the internodes. Such rotary sliced bamboo veneers are produced with a high manual effort and are economically feasible only for handicraft and decorative uses (Ganapathy *et al.* 1999).

Figure 20: The two most common bamboo veneer production methods (left): Rotary slicing of a culm (A) and fineline block-slicing (B), adopted from Hidalgo López (2003) and a Fineline veneer industrial plant in Hangzhou, Zhejiang (right), adopted from Fu (2008)

The more common production method is the sliced bamboo veneer manufacturing, similar to what Western markets known as “Fineline” technique (Cheng and Zhang 2011, Paulitsch and Barbu 2015). An intermediate block is glued from dried laminated slats and then sliced to sheets of 0.5 mm thickness and above. The slicing process happens in a wet state for better plasticity. The disadvantage of wetting the slats and the laminated block is the higher susceptibility to mold fungi. Li *et al.* (2012c) resolved the problem by combining a dry and a wet step and increased the veneer yield from 20 to 66 %. The so produced veneers are then coated with a hot-melt adhesive fleece and are sold for direct application on raw surfaces for decorative purposes. Alternatively, some niche products exist, such as decorative plybamboo with 3-plies and 0.5 mm thickness each. Most of these alternative methods take the internodal bamboo veneer from the culm surface by manually saw-flattening the internodal part of the culm and removing the internal tissue until the desired veneer thickness.

Often when bamboo fiber bundle mats or slats are getting plied and laminated, authors may use the term “veneer” instead (Deng *et al.* 2014, Qi *et al.* 2014, Zhang *et al.* 2018c). The latter produced bamboo plywood panel out of fiber bundle mats and investigated the role of bamboo culm characteristics (height, taper, fiber share) on the composite properties. Their results indicated that culm height could significantly affected the mechanical properties. The maximum bending and tensile strength of plybamboo were observed when producing the “veneer” from the middle culm part. The authors make the lower frequency of nodes and the higher fiber volume in the middle part of the culm responsible for the improvement (Qi *et al.* 2014).

So far, there is no industrial bamboo veneer or plybamboo production in SSA. The Ethiopian plywood export was regional and remained below USD 100,000 (UNcomtrade 2018). Nevertheless, the technology is robust and generally smaller than other WBP factories. Two thirds of the thermal energy demand in a typical plywood factory are generated from biomass. The residual cylinder (peeler core) supplies the main portion for heating steam boilers. The electricity accounts to ca. 140 kWh/m³ finished product (Puettmann *et al.* 2016). Nevertheless, the resource availability here again is the main reason why plywood is not being produced in Ethiopia. There is only scarce information regarding energy consumption of plybamboo production, but is assumable more than plywood due to the additional process steps.

2.2.6 Slats, strips and slivers

The first step to do with a bamboo culm is to split it. The strips can then be transformed into slivers by taking off the inner and outer cortex to improve gluability with a robust milling device simply called “knot remover”, In many factories, the 4-side planer then mills a slat with a rectangular cross-section out of the sliver. The oldest bamboo-based panels are produced from strips, slivers and slats. Another approach that needs to be mentioned here is flattening split bamboo (Kadivar *et al.* 2019, Liu *et al.* 2013, Parkkeeree *et al.* 2015, Zhang *et al.* 2014). This process describes a thermo-mechanical densification process. The technology is relatively new for bamboo but promised to provide dense and hard materials for flooring applications especially.

- GLUE LAMINATED BAMBOO LUMBER (LBL)

The most important of all the industrial processing methods of moso bamboo is glued and laminated bamboo lumber (Ma *et al.* 1976). Slats of 90 cm length and a 2.4 by 0.6 cm cross section were treated and laminated with UF, MF and PVAc. The results showed mechanical properties superior to wood products and the authors recommended using LBL in quality furniture making. Typically, slats are milled from strips and then glued to blocks either edgewise or horizontally with specific pressures from 0.4 to 1 N/mm². Figure 21 shows vertical and horizontal arrangements, parallel slats or plied ones. The arrangement of the lamella obviously impacts the mechanical properties whilst thickness swelling and dimensional stability remain untouched (Lee *et al.* 2012).

Such glue laminated blocks can be used to manufacture flooring, paneling, furniture, utilities and load-bearing elements. The product shows an ever-working economic success in a wide range of applications. Utilities, such as chopping boards are made from LBL but also structural elements in modern, earthquake-sage long-span constructions (Xiao *et al.* 2008). One of the constructional disadvantages is the dimensional limit of the beams due to the process-related length of single bamboo slats. Generally, large LBL elements are connected to each other by nail trusses. The production of “endless” slats was investigated recently applying three different connection types (Lin *et al.* 2020). The results showed that longitudinal joints of single slats weaken the LBL notably but do not depend on the type of connection. A very similar phenomenon was described by Anokye *et al.* (2016) who found that the distance of bamboo nodes in different layers of the LBL is of critical importance for its flexural performance.

The extremely low yield, resin-intense production and the economic relevance of LBL led to innovation pressure. Three recent examples out of innumerous patents and ideas are the flattening technology, bamboo welding and the arc bamboo concept (Yan *et al.* 2017): Instead of milling and planing, producers densify the raw strip with the help of heat, moisture or oil bath (Parkkeeree *et al.* 2015). The yield is obviously increasing from around 40 up to nearly 100 %. The flattened strip shows a strongly compacted parenchyma in the inner third of the cross-section, homogeneous fiber distribution, increased stiffness and strength (Archila-Santos *et al.* 2014) and can be used for laminated glue lumber or cross-laminated products (Liu *et al.* 2013). Instead of using PF or PUR, the welding technology as known from wood was applied for LBL too. Analogous to wood, a mechanical vibration (150 hz) induces friction heat which softens the lignin and provides a strong bond between two slats. Zhang *et al.* (2014) proved the concept for moso bamboo.

Frugal solutions such as the Colombian guadua plybamboo (Hidalgo López 2003) or low-technology LBL (Mahdavi *et al.* 2012) make use of hand tools to split and sand raw strips

as shown in figure 21. They can be used in the core layer or for low-grade construction materials. Nevertheless, LBL is often confusingly referred to products which are neither manufactured from slats nor slivers (Mahdavi *et al.* 2011) but from crushed fiber bundles (Nugroho and Ando 2001).

- BAMBOO MAT BOARDS

The earliest bamboo-based composite panels were produced from woven slivers and casein glue. Bamboo mat boards (BMB) are produced by splitting culms preferably with long internodes, into 5 to 6 mm wide strips and consequently tangentially cleaving those into slivers. The slivers are manually woven to mats (see figure 21) and then impregnated with UF or PF resin either by dipping or curtaining. Depending the product application, BMB are produced in thicknesses of 1 to 10 mm, hot-pressed in bamboo-typical density ranges from 650 to 850 g/cm³ (INBAR 2001). Productions exist in China, India, Thailand, and Vietnam but capacities are negligible compared to the before-mentioned bamboo-based panels. BMB are applied as face reinforcement of panels with a relatively low bending stiffness, such as particle boards. Such hybrid boards are produced in a 1-step hot-press and have been widely used in rail coaches in China. Innumerous other panel combinations are explained by Ganapathy *et al.* (1999). All in all, this technology is on decline due to high resin consumption, labor effort and upcoming more efficient products such as OSB. On the other hand, such production concept may easily be built up on the traditional handicraft processing of highland bamboo in Ethiopia. Woven highland bamboo mats are widely in use for fencing and traditional shelter construction in rural areas.

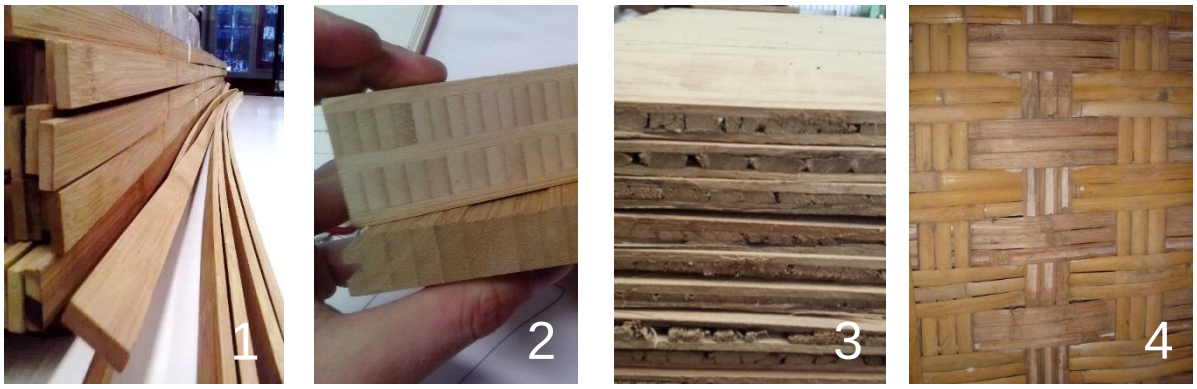

Figure 21: Planed moso slats (1) for Chinese glue laminated bamboo lumber (2) and Colombian ply boards made from raw guadua strips (3) and a hand woven highland bamboo mat produced for Ethiopian vernacular construction (4))

- COMPOSITE BAMBOO-CROSS-LAMINATED-TIMBER

Cross laminated timber gained global interest as a very versatile and well-studied engineered wood product. Full-size wall and floor applications are possible in high-rise buildings in Europe, North America and some parts of China (Li *et al.* 2019). The cross-wise lamellar structure allows to bear loads in various directions the plane. A recent review of production technology and standardization was provided by Brandner *et al.* (2016). Hybrid panels where bamboo layers may fulfill a reinforcement or high wear function have been explored very recently (Wei *et al.* 2019c). The combination of BS with spruce, kiri wood or oil palm as core material has shown to be technically feasible (Hoffmann 2018). Munis *et al.* (2018) applied bamboo LBL as face layers of a coniferous CLT. The authors showed a significant reinforcement in compression strength. The bamboo face layers hinder the timber lamella to buckle and hence stiffen the whole composite CLT. This is especially relevant for countries with a scarcity of

quality timber. Low-grade wood, such as palm or fast growing plantation timber, can be applied without notable stiffness and strength losses (Wang *et al.* 2015).

The energy uptake of a typical LBL production according to Xiao *et al.* (2014) is a total (electrical + thermal) of ca. 2.7 GJ/m³. That corresponds to 750 kWh/m³ and is less than OSB or MDF but notably more than a PB production. The only bamboo-based panel product in Ethiopia was LBL flooring made from lowland and highland bamboo (Fu 2019). Both had operated with first generation technology and did not develop any innovative approach in their productions. Although the Ethiopian factories rely on lower labor costs and the lowest energy price in the world, they do not compete well in quality with Chinese LBL producers.

2.3 Bamboo scrimber

Bamboo scrimber (BS) is a type of engineered composite panel formed by adding adhesive to fibrous bamboo particles and compressing them with high pressure. The original scrimber technology reached utilization ratios of 85 % and wood scarcity in China in the 1990s awakened the interest to utilize not only low-grade wood, but also bamboo. BS was developed at laboratory scale at Nanjing Forestry University in 1987. The product was named „重组竹", which literally translates „heavily reorganized bamboo". Chinese researchers translated it as „reconstituted bamboo lumber", „woven-strand-bamboo" and „parallel strand bamboo" but naming is still up for debate (Liu *et al.* 2015b). The production process is illustrated in figure 22. Raw bamboo culms (A) are split preferably in the green state (B). The split strips (C) are then occasionally softened (steam or water bath) and the outer terminal layer of the culm is removed with a tangential split knife (D). The outer sliver (E_2) sells to bamboo mat industries, the larger, inner sliver (E_2) enters a crushing device or "fluffer" (F). The crushed bamboo bundles (G) are thermally treated (H) and then enter a resin tank (I) to impregnate the bundles with an aqueous solution of urea or phenolic formaldehyde resin. They are then technically dried (J) to obtain press-ready scrim strands with a MC below 5 %. A certain risk of pre-condensation is considered during resin drying. The bundles are manually laid into steel molds (K_1) or press platens (K_2) and consolidated and cured.

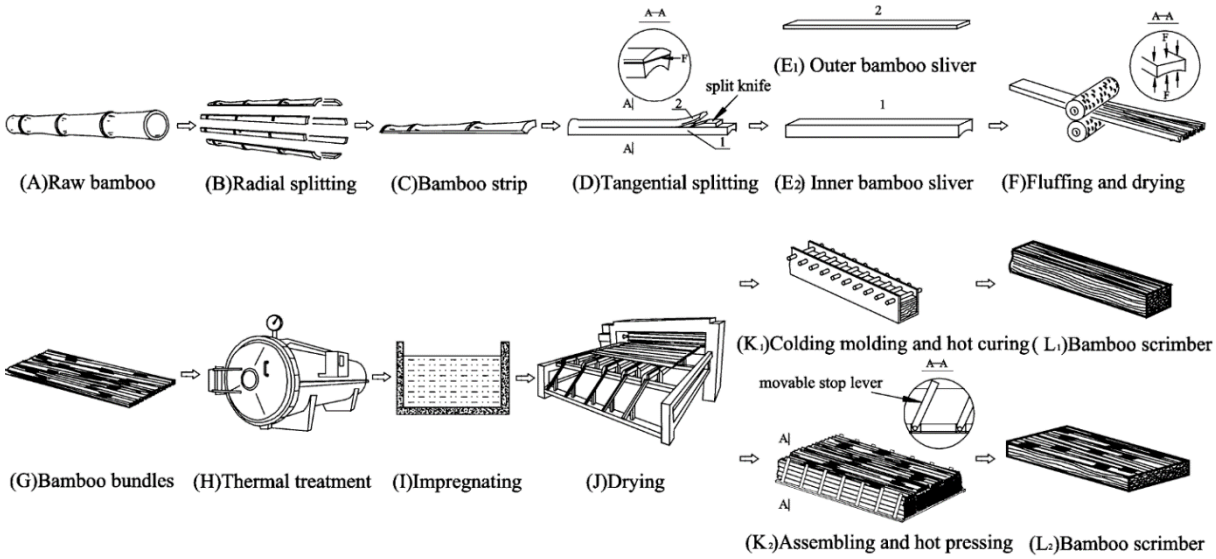

Figure 22: The hot press and cold molding process scheme in Chinese bamboo scrimber productions (Yu *et al.* 2015b)

2.3.1 Defibration

Shang *et al.* (1998) stated that raw material processing, i.e. the production of scrim strands from culms, is the primary development challenge for BS. The first generation of BS had used thin diameter bamboo culms with no splitting prior to crushing. The scrim strands were produced using entire culms in a roller crusher (Huang *et al.* 2019a). The applied pressure leads to shear stresses and promotes dotted and linear cracks along the longitudinal direction. Later, the negative impact of the inner and outer terminal tissue of the bamboo culm on the glue performance was recognized. Thus, the second generation of BS production then removed the outer and inner cortex in a planer and milled a rectangular intermediate prior to

crushing it. A comparable technique is in use when producing post-consumer bamboo panels[4]. In the third generation, the machines were combined, as shown in figure 23. An optional splitting knife removes the outer sliver (illustrated in step E_1 in figure 22). The outer perimeter of the bamboo culm contains substances which do not favor the resin penetration and steam diffusion across the material. Substances, such as wax, fatty acids and silica negatively affect the wettability and thus, producers in China usually remove it before further processing (Zhang *et al.* 2002). Chung and Wang (2018a) described the positive effects of peeling on mechanical properties and confirmed results of Deng *et al.* (2015). The combination of the planer and crusher in one machine increased the raw material yield and reduced manual handling between the stations. The bamboo slat enters the crusher and goes first through press rollers (no profile) which flatten the curved form. After that, the flattened slat goes through a spring-mounted planer station (see 2A in figure 23), one for the top and the bottom. The slat then goes through a series of coupled rollers with adjustable distances between them and pressure defined by the spring mounting (see 2B in figure 23). The more often the bamboo slat passes the crusher, the finer will be its texture, i.e. the single strand in the bundle is smaller and hence the number of fibers per strand is lower.

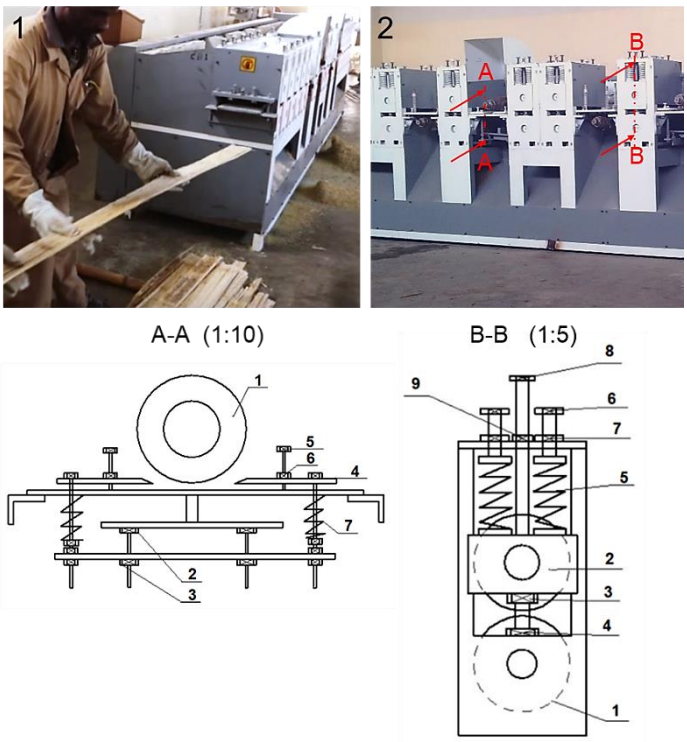

Figure 23: Highland bamboo scrims leaving the machine (1) and cross section of planer (A-A) and profiled rollers (B-B)) in the scrim crusher machine used in this study

[4] There are special bamboo composites made from fine rods with diameter < 2 mm Yang and Lee (2018) or post-consumer bamboo chopsticks Nguyen (2018). Both are produced in a similar manner as it is done with BS, PF resin impregnation, hot-pressing, very high density. Technically speaking, these post-consumer recycling products are no BS since they were made from milled elements rather than crushed scrim strands. Nevertheless, product properties are comparable to 1st generation BS and are utilized in furniture and indoor applications.

Natural plant fibers, such as flax, are mechanically extracted by first threshing the stalks, then scutching them in a swingle and then hackle them. Analog to flax threshing, bamboo splits can be crushed by hand with a hammer (Mahdavi *et al.* 2012) or in a roller crusher (Nugroho and Ando 2001). Different from flax fiber extraction, BS intentionally incorporates the non-fibrous matrix parenchyma instead of combing it off. Therefore, scutching and hackling are not done in BS productions. Where the extraction of technical long fiber is the focus, the flax process has got adopted and applied to bamboo. The hackling of bamboo scrims yields subtle long bamboo bundles (cross-sectional diameter < 1 mm) with only few parenchyma left as shown in figure 8 (Osorio *et al.* 2018). The latest innovation, also referred to as the 4th generation in BS, imitates this hackling step and fluffs the bamboo fiber bundle with fine-toothed roller crushers. Presumably, a wire brush is used to get rid of the internal and external waxy layer as well. The fluffing machine produces finer fiber bundles than a common bamboo crushing machine. One of these fiber bundles contains not more than five vascular bundles, i.e. approximately 2 mm thick elements (Yu *et al.* 2014a). The resulting fiber bundle mat (see figure 24) shows higher specific surface and allows a better distributed penetration of the resin. Nevertheless, the key advantage is the extremely high yield above 90 % (Yu *et al.* 2014a).

Figure 24: Bamboo scrim produced in a 4th generation fluffing machine comprising the epidermal green part of moso (Yu *et al.* 2014a)

The quality of the scrim depends on the applied technology but also whether the defibered bamboo species matches it. Even within the very same species, local proveniences may come with differences in morphology which lead to heterogenous qualities. Chung and Wang (2018b) compared two *Phyllostachys pubescens* (moso bamboo) proveniences from Taiwan and China as a function of density and found differences in the mechanical properties of the BS produced from those. Guan *et al.* (2012) studied Indian muli bamboo (*Melocanna baccifera*) for scrimber flooring fabrication. The species is of relatively low diameter (4 to 8 cm at breast height) and culm wall thickness (3 to 5 mm) compared to moso bamboo and thus not appropriate for the latest BS defibration technologies. The crushing machine had not been designed for such small-dimensioned bamboo species. The authors produced heterogenous scrim strands with dimensions ranging from 9 to 15 in width and 2 to 3 [mm] in thickness. However, surprisingly, the results of the muli BS flooring outperformed the moso alternative. African highland bamboo is of a medium diameter and culm wall thickness and its suitability for BS production was not yet studied.

2.3.2 Heat treatment

Heat treatment of bamboo aims to thermally modify its chemical composition and subsequently to reduce hygroscopic water uptake. Heat treated bamboo showed reduced hygroscopicity (Nguyen *et al.* 2012, Schmidt 2013), improved dimensional stability (Zhang *et al.* 2013) and reduced thickness swelling in scrimber made from it (Li *et al.* 2012a). Comparable results were achieved with different gaseous treatment media (Li *et al.* 2018). Colla *et al.* (2011) treated *Dendrocalamus giganteus* in inert and non-inert atmospheres for several hours resulting in improved thickness swelling and stable mechanical properties. According to the authors the ideal temperature for bamboo treatment ranges from 140 to 220 °C. On the downside strength properties might be weakened (Leithoff and Peek 2001) and a brittle failure can occur. For BS, Xu and Teng (2015) warned that treatments above 190 °C would degrade mechanical properties too much.

For highland bamboo, Schmidt (2013) showed that significant reduction of sorption behavior and hygroscopicity (EMC) was achieved at temperatures between 200 to 220 °C. A study conducted by Starke *et al.* (2016) analyzed the chemical composition of highland bamboo during heat treatment. The chemical composition of highland bamboo does not remarkably differ from other commercial bamboo species (Bremer *et al.* 2013, Zhang *et al.* 2013). Figure 25 shows the gradual decrease of the main chemical components with increasing temperature. Bamboo generally consists of 22 to 35 % hemicelluloses with high xylan content. The controlled degradation and modification of the hydrophilic hemicellulose is the main driver for all water-related material properties. Just like hardwood, bamboo is more susceptible to thermal hemicellulose decomposition than softwood. This may be a result of higher reactivity of pentoses which constitute the xylan backbone. The glucomannan based backbone of softwoods mainly consists of hexoses, which show less reactivity and therefore may be less degraded. Highland bamboo xylan share is between 10 to 20 % in (see table 42). Hemicelluloses start with deacetylation reactions in low temperature range, i.e. below 130 °C. The resulting acetic acids then additionally catalyze depolymerization of structural polysaccharides. The highland bamboo treatment at 160 °C affected thermally unstable extractives, such as starch or proteins[5] and may have affected hemicelluloses but without significant mass loss. At 220 °C, the hemicellulose components had nearly completely decomposed (Starke *et al.* 2016). Cellulose, due to its high crystallinity, is less susceptible to heat and keeps being stable up to 260 °C. Before that, amorphous regions of the cellulose degrade. Hence, the overall portion of crystalline cellulose increases. Subsequently, less free hydroxyl groups are accessible for water molecules. At temperatures above 200 °C, even lignin may cleave off polyphenolic components. Those rather cross-link with other structural molecules which leads to less accessible hydroxyl groups and an apparently higher lignin and extractives content (Esteves and Pereira 2009).

[5] Liese (1998) supposed that due to the high amounts of sap and carbohydrates, hygroscopic behavior of bamboo may be more influenced by thermal treatment than that of wood. Consequently, there must be a certain dependence of hygroscopic properties along the culm height as well. Most of bamboo extractives like lipids, resins, gum, starch and simple metabolic intermediates possess much lower decomposition temperatures than the structural polymers (< 130 °C)

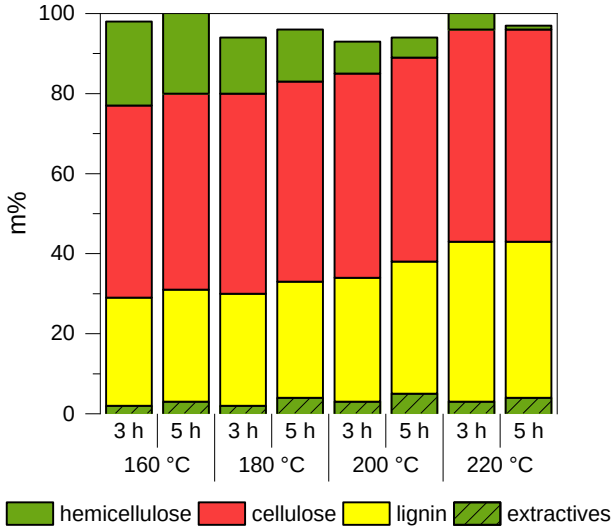

Figure 25: Chemical composition of highland bamboo after heat treatment at four temperature levels and two holding times, mass percentage related to the final oven-dry mass, modified from Starke *et al.* (2016)

Industrial modification is done by heat treating the manufactured panel inside the hot-press (Kitchens *et al.* 2016), after panel manufacturing (Lee *et al.* 2017) or by modifying wood particles *a priori* (Paul *et al.* 2006, Pelaez-Samaniego *et al.* 2013, Thoemen *et al.* 2010). However, a post-manufacturing heat treatment degrades cell wall components in the already consolidated composite panel leading to brittle fracture, lower MOR and higher water uptake (Shangguan *et al.* 2016). A post-manufacture treatment was therefore not considered in the present work. The common practice in fiber bundle heat treatment is a two-step batch process at medium temperatures (100 to 170 °C) and short duration (1 to 2 h). The scrim strands are either undergoing a saturated steam treatment (SST) or hot-dry air treatment (HDAT). Chung and Wang (2018a) steam treated at 120 °C for 6 h and produced scrimber boards from the treated *Phyllostachys makinoi* and *Phyllostachys pubescens*. The authors found a more homogeneous density profile, higher nail withdrawal resistance, increased IB and bending MOR and explained that with significant decrease in water absorption. Kumar *et al.* (2016) had used SST at 170 °C for 100 min with chamber pressure around 0.5 N/mm² to reduce oxidative effects during treatment. The main goal of such treatments is of aesthetic nature. The process is commonly referred to as “carbonization” and obtains a darker color. It is believed that the oxidation of sugar components and production of acetic acids mainly cause the discoloration of bamboo (Zhang *et al.* 2013). Li *et al.* (2012a) produced BS and investigated the effect of thermal modification of *Neosinocalamus affinisat* at temperatures between 160 and 200 °C and treatment durations of 2, 3 and 4 h. Thickness swelling (TS) and resistance to fungal decay improved significantly at 180 °C and 2 h and above.

The protection of mature bamboo against fungal degradation with preservatives was always difficult due to lack of cross sectional conductive tissue (Liese 1998), sealed vessels (Liese and Weiner 1996) and environmental concerns on impregnants (Liese and Tang 2015). Modification of wood via heat treatment is known to enhance durability against fungal attack without usage of impregnation chemicals (Candelier *et al.* 2016, Esteves and Pereira 2009, Kamdem *et al.* 2002, Paul *et al.* 2007, Pelaez-Samaniego *et al.* 2013) and similar effects were observed for heat treated bamboo (Liese and Tang 2015). Wood-destroying fungi require water and nutrients. Because heat treatment depletes hemicelluloses it reduces the number

of hydroxyl groups available for water sorption. For African highland bamboo the EMC at 85 % RH decreased from 12 to 9 % after 3 h laboratory heat treatment at 180 and 200 °C, respectively (Schmidt 2013). BS which was mildly heat treated with aqueous solutions showed improved resistance against mold fungi (Cheng *et al.* 2013). A strong effect was observed for similar non-wood lignocelluloses such as reed (Brischke and Hanske 2016) where fungal ML decreased by 95 % after being treated at 180 °C (Dosdall *et al.* 2015). A comprehensive study regarding oil-bath treatments above 200 °C reduced fungal ML to below 3 % (Leithoff and Peek 2001). For selected engineered wood products Barnes *et al.* (2018) showed higher durability after a post-manufacturing heat treatment.

Nevertheless, MOR, hygroscopicity as well as the biological durability are influenced also by resin, additives and hot-press parameters. Final product characteristics will have to be researched, since to date, only raw materials had been investigated.

2.3.3 Resin systems

Generally, the resin type and application do not differ too much from comparable wood-based panels, such as OSB or LVL. Urea- (UF) and phenol formaldehyde (PF) resins are generally used for the manufacture of plywood and other wood products such as flake board, oriented strand board and laminated veneer lumber. The PF dominates the bamboo scrimber market because of its relatively low cost, ability to achieve high quality bonds rapidly with the application of heat, and for its resistance against harsh environmental conditions. The PF resin is prepared in a resin kettle or batch resin reactor made of mild steel. After drying the fibers, a blend containing resin, wax and alkaline hardener applies to the bamboo scrim strands (Hu *et al.* 2018, Huang *et al.* 2019b, Li *et al.* 2001). In the original scrimber (Coleman 1980) and TimTek® (Jarck 2009) patent the typical application form is liquid impregnation by dipping the scrim strands into a tank containing a low viscosity resin solution (Dynea 2010) for 20 seconds. The practice was adopted for BS and is being performed to date. In common productions, the scrim strands are bundled and dipped into resin tanks for 6 min or more (Yu *et al.* 2015b). The bundles are then taken out and the excess glue simply drips off. The amount of resin in the final panel is mainly steered by the leaking time. The results are high resin contents (> 20 %), heterogeneous distribution and high process MC. The scrim strands show between 60 to 80 % MC after dipping and necessarily need to be dried before hot pressing. Consequently, uncontrolled pre-curing of the resin may occur (Li *et al.* 2001).

Solving novolac prepolymers (reacted particle of > 15 µm) in aqueous media instead of organic ones, made it possible to apply a low viscosity resin system with a high level of cross-polymerization (Fliedner *et al.* 2011). These resins work as a formaldehyde scavenger due to the phenol excess but do not react on a kinetic way. That means, they can be stored on long term and only start to polymerize when adding an alkaline activator. This makes it an ideal candidate for an industrial setting in rural Eastern Africa. Long transport distances and high risk of production delays require raw materials which can be stored for more than six months without major quality curtailments. Another PF system, Prefere 4976 (Dynea 2004), contains a large amount of phenol formaldehyde prepolymer (80 to 85 %). Free phenol (< 0.2 %) and free formaldehyde (< 0.1 %) are only minor shares of the resin powder. This way, a relatively low volatile formaldehyde can be achieved in the final product (Dynea 2004).

Figure 26 shows a vertical cross section as microscopic fluorescence photograph of the commercial bamboo scrimber product from figure 26D. The red lines indicate the glue lines

between the single scrim strands A, B, C and D. The parenchyma tissue was filled with phenolic resin which appeared as blue luminescence. The picture indicated the high degree of penetration into the ground tissue achieved by dipping the scrim strands in the low viscosity phenolic solution. Furthermore, one can observe a second phase which appears as beige-colored especially in fiber bundle C and parts of A and D. There are two possible explanations for this second resin phase. Either the resin wet parenchyma tissue contains precured phenolic resin as a result of the technical drying process after dipped in the solution tanks, or the beige-colored phase stands for a completely different resin. Many BS production use UF resins with the intention to lower the production costs. The microscopy provided a hint that UF has been used as a filler in the present BS decking product.

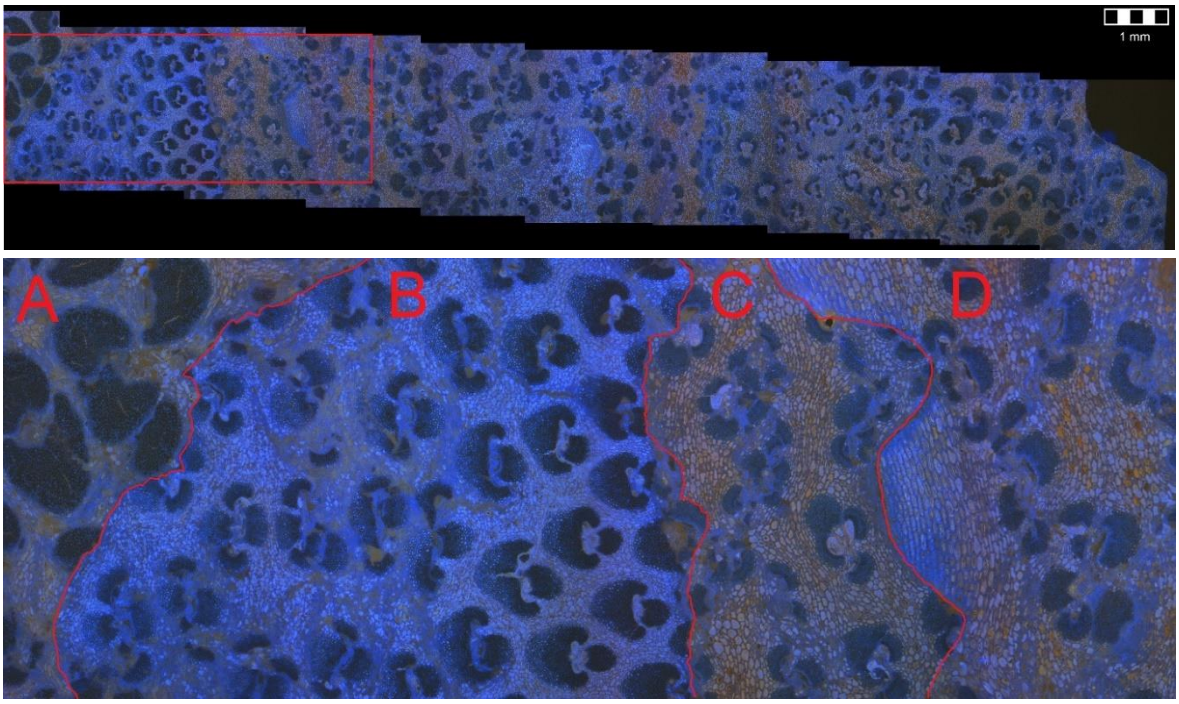

Figure 26: Fluorescence microscopy photograph of a cross section of a commercial bamboo scrimber decking product and a magnified section (red box) showing the distinct fiber bundle layers (A, B, C, D)

Beside the quality aspect, one major concern of using BS as a structural building material is its high density. Graeter *et al.* (2012) developed a new device for fiber bundle production which the authors denominated “macrofibers”. The invention comprises a pair of rollers with cutting webs which follow a dished template form. The authors optimized the scrim production by applying similar tensions to the lateral part as well as the central part of the log to be crushed. The so produced scrims measure 100 to 400 mm in length with a slenderness ratio of 20. The bundles were coated with a 2-component PUR expanding foam system and immediately pressed with low temperature. Depending the desired application, a target density of 0.2 to 0.55 g/cm³ (Bliem *et al.* 2019) can be achieved. Potential alternatives to phenolic resins with a comparable performance are acrylic resins (Böck 2014b), melamine- or isocyanate-based (Nugroho and Ando 2001). Technically promising results (internal bond above 0.5 N/mm²) were achieved with soy-based (Ashland, USA), melamine-formaldehyde (Dynea, Norway), acrylic resins (BASF, Germany) and blends of those systems and were part of project trials (Böck 2014b, Schmidt *et al.* 2016a). However, these alternatives had to be neglected in further studies due to higher costs and occupational safety reasons.

2.3.4 Mat formation

The BS panel shall show a homogenous density distribution across and along the grain direction of the scrimber composite, voids and uneven densification are undesirable. In case of bamboo, the fiber matrix anatomy is another challenge especially for high density raw materials such as bamboo. On the one hand consistent strand quality is needed, on the other hand the mat forming is a critical step for the following densification in the hot-press. The mat forms from the scrim strands which priorly were impregnated with resin and occasionally dried to press-ready moisture content. The mat is manually laid by the weighing method. The process is done manually, consumes time and labor and causes inconsistency in quality. This concerns all handling tasks when transferring an intermediate product from one station to the next one. However, especially the resin application and the mat formation tie up labor capacities. Graeter *et al.* (2012) stated that a continuous process would be possible using their macrofiber device, at least for common scrimber. To form the bamboo scrimber mat, the weighing method caused heterogenous fiber bundle distribution, hence results in density differences which in turn impacts the product properties (Yu *et al.* 2015a). For instance, the failure mechanics in a wooden scrimber beam depend on the overlap of particles and the capability of the glue to transfer the stress between the long, slender strands (Paton 1997). However, the heterogenous quality in bamboo scrimber is believed to be caused by local density extrema from overlapping fiber bundles in the mat. The vertical density profiles for a aleatorily stacked bamboo scrimber (a) and systemically arranged bamboo bundle veneer like mat (c) are shown in figure 28.

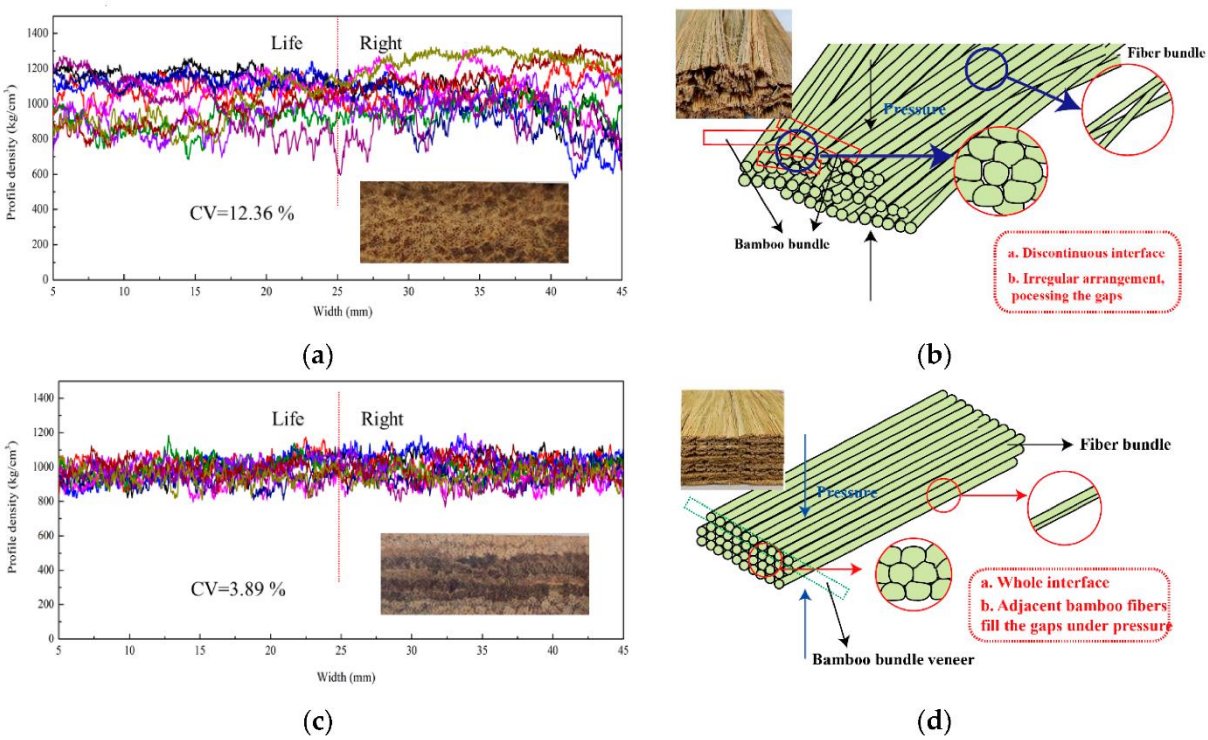

Figure 27: Vertical density profiles of aleatorily laid bamboo scrim mat (a, b) and a systemically layered scrim mat (c, d) as shown in Zhou *et al.* (2019)

A step towards automatization and homogeneous mat formation, demanded by different authors (Li *et al.* 2001, Shang *et al.* 1998, Xu and Teng 2015), has been taken into account lately: A lateral butt joint between the bundles is necessary to guarantee a homogenous

distribution in the mat. To do so, He *et al.* (2018) suggested a “weaving” or “knitting” technique connecting the fiber bundles as illustrated in figure 28. The machine’s principle works similar to the one used bamboo tablecloth production and sews the bundles laterally to each other so that a veneer like fibrous mat results. Zhou *et al.* (2019) tried to upgrade this concept with an online measurement concept using transmitted light and stiffness. The technique emits a light beam vertically through the formed mat and correlates the panel stiffness with the absorbed light of the mat. The technique is in its early days and might not be applicable in an industrial setting in SSA.

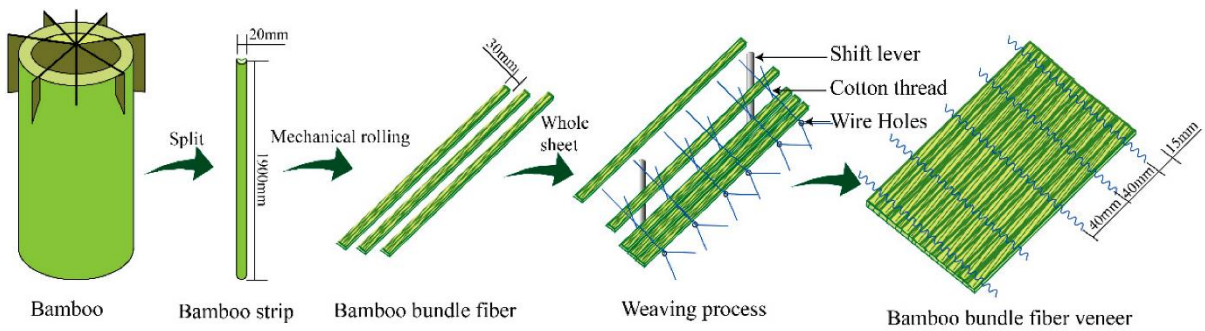

Figure 28: Illustration of the process scheme starting at the splitter and crusher, and then weaving or knitting single bamboo fiber bundles into a veneer like mat with a cotton lining, as shown in Zhou *et al.* (2019)

Zhang *et al.* (2018c) have produced PF-bond scrimber in a cold-in-cold-out process using scrims made from poplar veneers. They arranged the bundles parallel to each other and compared it to an aleatorily mat formation. In contrast to Zhou *et al.* (2019), they found only shear strength to be affected by the mat arrangement but not bending MOR or MOE. A particle grading is essential part of PB and OSB productions. In PB, fine particles form the faces while coarse particles are destined to the core layer. In OSB it is the other way around, large, slender strands form the face layers and give bending stiffness to the panel. Such particle sorting is not part of BS production so far. The “particle” handling is rather challenging compared to OSB or PB due to the bulky geometry of scrims. Moreover, the quality of bamboo scrims defines mainly by its fineness and homogeneity (density, impurities). The more often a bamboo slat passes a crushing device, the finer it will be. Investigating the mat arrangement, and the effect of different raw material qualities (e.g. height sections) on the novel highland bamboo BS panel quality will have to be investigated.

2.3.5 Consolidation

During consolidation, the mat compacts and the duroplastic resin condenses inside a press. The necessary thermal energy can be introduced via conductive heating, pressure-induced heat, high-frequency and steam injection. All of them are batch processes – continuous solutions are not in operation yet. For the Chinese BS industry, Yu *et al.* (2015b) differentiated two pressing processes: The batch hot-press using single or multi-daylight presses and the cold molding technique as described in figure 22. The very energy-intensive production process and the high amount of resin did not only raise concerns on the environmental impact but result in long pressing times > 100 min and thus inacceptable variable costs (Böck 2014b).

- COLD PRESS

Most of the factories in China still use the cold molding technique for BS production. The cold molding technique takes the impregnated and treated scrims to steel molds as shown in process step K_1 in figure 22, the fiber bundle mat is densified under high pressure. The pressure Yu *et al.* (2014b) mentioned goes up to 82 N/mm². The resulting compacted material now has a density close to cell wall density (1.4 g/mm³). The consolidated billet gets mechanically clamped in the mold with heavy metal pins and is then heated up to 130 °C in a chamber and cures for 10 h. The result is a strongly densified cuboid billet with excellent surface properties of roughly 2 m length and 15 cm width. There are some drawbacks of this methods, such as the very long curing and cooling time. Another problem is the high tooling costs. The metal molds and attachment bolts gradually deform with each batch produced due to the enormous pressure in the scrimber billet.

- STEAM-INJECTION PRESS

An alternative consolidation technique undertaken on industrial scale is a steam-injection press. The PF polymerization reaction is induced by increasing pressure, so that press platens can be heated up slightly to 110 °C to reach the needed condensation reaction energy (Pilato 2010). The whole press unit was encapsulated in a pressured vessel. The steam injection happens at 0.5 N/mm² saturated steam pressure in the vessel. This way the specific press plate pressure can be kept relatively low (ca. 0.7 N/mm²) compared to typical atmospheric wood-based panel hot-presses (Coleman 2011). The new technique achieves a more homogenous heat distribution across the fiber bundle mat and the batch press line needs only 60 s time for producing one billet. The resulting billets (figure 19A) have shown mechanical properties superior to commercial WBP. The steam penetration in the pressurized chamber allows the producer to introduce impregnants deep into the cross section, thus a durable product can be produced *in situ* (Kitchens *et al.* 2016). The major drawback is the restricted dimensions due to the closed pressure vessel system. According to Jarck (2017) beams with a length of up to 40 feet (ca. 12 m). This relatively new technology was used for BS lately, but no publications were available to date. The process is based on the original TimTek® process described in the patent US7537669B2 (Hemmings 2017, Jarck 2009). The plant in Meridian, Mississippi, produced billets of BS which are being sold under the brand name GrassBuilt® by Hemmings (2017).

- HOT-PRESS

In the hot-press, the necessary energy for the PF polycondensation reaction is transferred through the press platens which heat up to 180 °C or more. Li *et al.* (2001) recommend press temperatures around 150 °C in combination with a specific pressure of 3.5 N/mm². The used hot-presses are batch presses with multiple daylights of usually up to 16. The handling of the mats and loading of the press lacks automatization and takes at least a team of two laborers. On top of that comes the fact that the panel thickness is limited to a maximum due to the long pressing times. Specific pressing time is determined as per 60 s/mm panel thickness which causes excessive batch times. To reach a polycondensation reaction in the panel's core within economic time frames, a panel thickness below 50 mm is indispensable. The cold-in-cold-out process exacerbates the time consumption of the batch process since the curing is done inside the very same press. The advantage of the hot-press method for BS production is the potential formation of a density profile. In a mat-forming panel, such as PB (Iwakiri *et al.* 2014) or OSB (Akrami and Laleicke 2018), the bulk density of the mat increases when compacted in the hot

press. The fluffy uncongested material forms a vertical density profile with density peaks at both face layers and a valley in the core layer. The compaction ratio determines the quality in such mat-forming wood-based composites such as OSB, PB and MDF. Usually, the higher the compaction (mat) and densification (strand) ratio[6], the better the IB. It is important to note that mat-forming and veneer-like panels behave differently in this context. Compacting a veneer or a massive wooden board (see CLT production) works differently since cell walls are folded or even destroyed during densification. For this case, panel faces look darker than the core which indicates a stronger densification and thermal modification. It is yet not clear whether a BS panel consolidation rather works according to the principles of a mat-forming or a veneer-like composite.

2.3.6 Applications

In comparison to any other bamboo-based panel or raw bamboo as a building material, the BS application range has greatly expanded. Yu *et al.* (2015b) report more than 60 bamboo scrimber factories producing 600,000 m³ per year, while Hu *et al.* (2018) mention “hundreds” of factories producing 900,000 m³ in China only. The typical uses can be categorized in non-load-bearing, such as flooring, ceiling and façade cladding (outdoor/indoor), load-bearing and niche applications[7] (Huang 2019).

For load-bearing applications LBL had been successfully established as viable alternative on timber markets (Xiao *et al.* 2008, Xiao *et al.* 2014). Bamboo scrimber is still underrepresented in building structures and envelopes (Huang 2019). Although there have been reports on structural use of BS and high rise buildings were recently established in Chengdu, Sichuan province (China), it is questionable whether the high density of structural BS elements is not a drawback in comparison to timber. Fan *et al.* (2017) analyzed the current situation and trends from the architectural perspective and found a lack of harmonized standards nationally (China) and worldwide. At the same time, the authors identified a high potential for BS in prefabrication housing. So it is that BS was successfully used in 2 x 4 modular systems in combination with plybamboo and LBL (Huang 2019). A notable problem in this regard was the lacking proofs of fire resistance. The breakthrough for BS application in Western architecture happened when a certified cladding was installed in a large scale at Madrid Barajas International Airport in Spain (Zhiyong and Junqi 2017). BS showed advantages and disadvantages at elevated temperatures (500 to 900 °C). Due to the high density and resin content, the thermal conductivity is higher than timber (Cui *et al.* 2018). The charring rate on the other hand is lower compared with different timber species in the literature. That makes BS an interesting (Xu *et al.* 2018) alternative in non-structural architectural elements. Moreover, Huang *et al.* (2017) obtained hygrothermal parameters of BS and compared them to timber and wood-based panels in applications in building envelope. The study showed that BS had higher heat storage

[6] The compaction and densification ratio are two misleadingly used terms. Commonly authors use compaction ratio to describe the proportion of the raw material density to the finished panel density. In this study, “compaction ratio” refers to the height of the press-ready mat:panel thickness and “densification ratio” to the fiber bundle density:panel density.

[7] Huang *et al.* (2019b) mentioned BS utilization in wind power plants but no further details were provided. Since the second generation of BS is often confusingly denominated as “bamboo-fiber reinforced composite”, there might have been a mistaken attribution to ambitious engineering application.

but lower vapor permeability as well as thermal conductivity. The authors reasoned that BS would surpass timber in constructions especially in the tropical and hot regions which overlaps with most bamboo forest resources location. The potential in the construction sector implied a synergy effect benefitting both the utilization of regional resources and the structural-physical strength advantage of BS. However, due to the high cost of bamboo and wooden building structures, small market share, and low social awareness, the reorganized bamboo has not been widely used in construction. Therefore, it is necessary to strengthen publicity and increase the influence and market (Fan *et al.* 2017). The authors reviewed the situation of bamboo scrimber application in architecture and listed Chinese and international standards applicable to it. Further insights are provided in chapter 5.

- HYBRID COMPOSITES

The high density and relatively expensive resin make it an interesting candidate for hybrid solutions. Where stiffness and strength are still too low, Zhong *et al.* (2017) suggested to reinforce BS with iron rod bars by cold-pressing them into the scrimber matrix during manufacturing. Although the authors believe this to be a promising solution for long-span joists, it is highly questionable to reinforce BS with a material that it was supposed to replace in the construction sector. Hollow hybrid elements made from cold-formed thin-walled steel and BS laths make more sense. The scrimber keeps the steel wall from buckling and gives the hollow structure a frame (Li *et al.* 2012b). In combination with low density products, such as MDF or PB, sandwich panels are conceivable solution in many applications. The flanges of I-joists are usually made from PSL, LVL or finger-joint construction timber. Approaches using LBL in the flange showed to be expensive and overdesigned in bending tensions which leads to shear failure in the web (Schlegelmilch 2015). BS can substitute those composite materials and improves stiffness and strength. Sun *et al.* (2019) found notably higher maximum bending loads when using bamboo strand boards in the web, however emphasized the significantly higher impact of joint-type and flange material. Sugi-based SST (Fujii and Miyatake 1993) was successfully used in substituting veneer-based flanges in an innovative 1-step hybrid I-joist made with MDF and PB web (Abdalla and Sekino 2005). One of the main problems are the connection points along the joist length. In a preliminary work Lammert (2017) showed that simple but staggered lap joints between flanges achieved similar strength and stiffness as an “endless” joist would do. Such simple techniques (lap and butt joints) are easily applicable in low technology environments using hand tools.

- DECKING AND FLOORING

One of the commercially most established retail product classes is bamboo flooring (Guan *et al.* 2012). Producers and traders promote bamboo flooring performance in outdoor and flooring purposes due to its strong densification, high contents of phenolic formaldehyde resin and a thermal modification. BS shows high strength and stiffness (Li *et al.* 2012a) which is not too surprising considering the densification process and the correlation of mechanical properties with density (Chung and Wang 2018b, Kumar *et al.* 2016). Commonly, such products show densities of up to 1.2 g/cm³ but suffer brittle properties, lower MOE (> 10 kN/mm²) and flexural MOR (> 50 N/mm²). On the other hand, BS products with high density usually show low abrasion and high impact toughness. This makes them suitable for heavy wear applications in agricultural construction, garden and landscaping or footing exposed to moisture and weather. A very challenging application was demonstrated using scrimber from bamboo in horse stabling infill and lagging. The technical requirements mainly refer to impact strength (Benthien *et al.* 2019) and durability against fungi and insects (Benthien *et al.* 2018). Other very

successful hard-wearing applications are railway sleepers, container floorings and even as base mat for track vehicles on construction sites.

BS are believed to possess excellent biological resistance, especially against basidiomycetes. Jacobs *et al.* (2011), Meng *et al.* (2017) and Kumar *et al.* (2018) reported mass loss (ML) of less than 5 % for commercial BS. It is believed that this apparent resistance is mainly attributed to the lack of moisture in the substrate. Water hardly penetrates the highly densified, PF impregnated BS and hence hinders fungi from degrading the structural polymers (Meng *et al.* 2017). Once this physical barrier is taken (long term), moisture enters, and fungal hyphae follow. Surface degradation by weathering, tension cracks due to seasonal swelling and shrinking, as well as different thermal expansion coefficients between glue and bamboo, can lead to such openings. This effect on scrimber surfaces is riskier for low and moderate densities than for high densities (Wei *et al.* 2019a). Analogously to a wood-based panel (WBP), the face layer (FL) of a scrimber panel is believed to be densified stronger than the core layer (CL) although previous results indicated a heterogenous vertical density profile (Schmidt *et al.* 2016b, Schmidt *et al.* 2016a). This reminds products such as Delignit® (Blomberger Holzindustrie GmbH, Germany) or Werzalit® (Werzalit Austria GmbH, Austria). In such panels resin content far beyond 15 % and densification up to 1.3 g/cm³ are common practice to make the product durable. Nevertheless, fungal attack on BS panels has not been studied sufficiently yet.

Figure 29: Flooring products from bamboo scrimber in three market typical sortiments: Bleached with tongue and groove, carbonized click parquet and a three layered product with MDF base layer and poplar counter veneer

This is undoubtedly the reason that BS is mainly sold as a substitute product for parquet floors and terrace decking for indoor and outdoor purposes. The bamboo flooring producing enterprises in China alone account to more than 1,000, producing about 780,600 m³ annually (Jin 2001), however not all of them solely produce bamboo scrimber flooring. Most of them are small-scale companies manufacturing laminated strip boards with relatively low production volumes. From the 600,000 to 900,000 m³ bamboo scrimber produced most of the volume goes to flooring and decking uses. Important players in this industry are the Chinese Dasso Bamboo Technology Co. Ltd. from Hangzhou, Zhejiang and the European distributor Moso International B.V. in Zwaag, Netherlands. The many years of cooperation ended up in a patent lawsuit recently. Yet 97 % of the global bamboo flooring trade is still controlled from China (Fordaq 2018).

3 | Raw material study

The raw material study chapter divides in three main aspects as shown in figure 30, the gross, structure-property relation and quality risks. The first part analyses culm diameter, wall thickness and its taper along height. On this basis the actual woody volume of the bamboo culms was approximated using different methods. The second part starts with investigations of the anatomy, with special attention to the fiber cells of the culm. The results are then later related to the mechanical properties of the scrimber elements, namely the crushed bamboo fiber bundles or scrim strands. The investigations shall provide baseline information for the structure-property relation in bamboo scrimber composite panels with special regard to nodes, internodes, fiber volume and density. The picture complements with studies of the raw material quality risks. This part of the chapter investigated, amongst others, the silica content, its localization and concentration and presents a potential solution to reduce it.

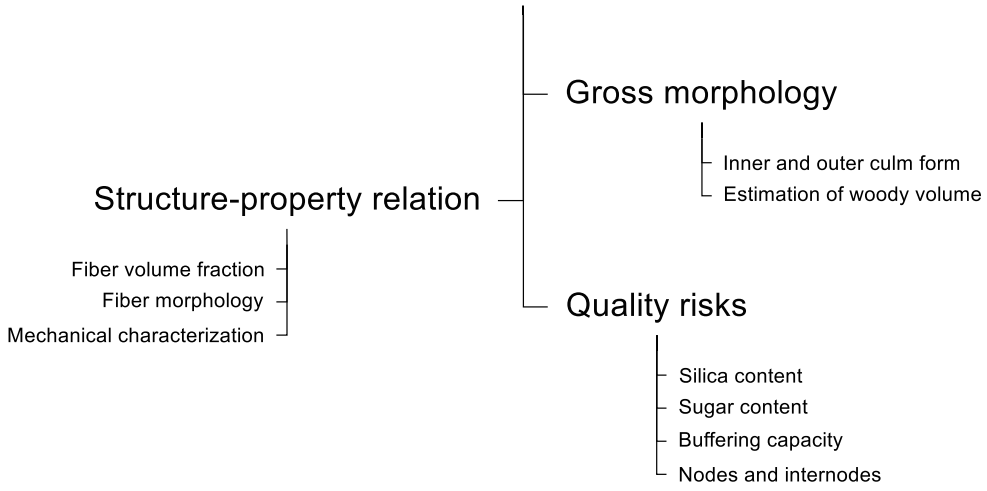

Figure 30: Structure of the raw material study

3.1 Introduction

Bamboo is a tall grass with no secondary growth, i.e. a single shoot consists of an apparently simple morphology. There are more than 60,000 wood species (Beech *et al.* 2017) of which 600 to 900 are observed in the commercial context (Haag 2020). In contrast, only a very few of the 1,200 bamboo species are being industrially utilized: The most important one is certainly Chinese moso, or *Phyllostachys edulis* (Carrière) J. Houz., which accounts for nearly 70 % of all Asian bamboo (Lobovikov *et al.* 2007). Giant sweet bamboo *Dendrocalamus asper* (Schult.) Backer is of high importance especially in India and South East Asia. Rather relevant in the informal sector, but not of minor importance are the South American *Guadua* spp., the worldwide spread *Bambusa vulgaris* Schrad. ex J.C.Wendl. and African species, such as lowland bamboo *Oxytenanthera abyssinica* (A. Rich.) Munro and highland bamboo *Yushania alpina* (K. Schum.) W. C. Lin. These priority species are characterized by their woody culm walls, large native and planted forestry stocks.

3.1.1 Culm biomass and volume

Highland bamboo management, its industrial utilization and the potential for carbon sequestration lacks a scientific fundament. For example, there is a widely held belief of bamboo superiorly fixing CO_2, still lacking comparative studies between bamboo and other woody plants. A comparison between bamboo and coniferous trees revealed that stands of 1 to 5-year-old culms yield 8.13 to 99.5 t/ha whilst in even-aged stands of China fir the stock develops from 3.35 to 40.6 t/ha in the age range from 15 to 54 years (Yen and Lee 2011). That belief is neither proven nor falsified due to enormous gaps in empirical data on actual bamboo biomass production and yield per hectare (Sanquetta *et al.* 2015). Bamboo's fast growth is not based on superior photosynthesis abilities, but rather on a storage system in which mature culms build up starch reserves (Düking *et al.* 2011, Liese 2009). These are then released in form of sucrose and transported to the active apical meristems of young shoots and lead to the extraordinary height growth. Hence, for biomass modelling, one clump must be seen as a whole production unit and not only the single culm increment. In fact, there is another underestimated variable - the rhizome. For non-woody plants and juvenile trees, Niklas (2005) found models predicting an isometric scaling relationship between belowground and aboveground biomass. For woody plants, a complex scaling function is predicted. Although the same authors found the reliability of estimates of below-ground biomass based on above-ground biomass increasing with overall plant size, estimates severely differ from measured values. For highland bamboo, Mulatu (2012) found the biomass allocation of plant parts to be $m_{culm} > m_{rhizome} > m_{branches} > m_{leaves}$. The highest biomass portion is found in the culms with 55 to 67 %. The rhizome shares 15 to 21 %, branches 11 to 14 % followed by leaves with 5 to 9 %. Since bamboo possesses rather shallow roots, the rhizome is limited to a certain soil penetration level. Therefore, the below-ground biomass of bamboo is suspected to show isometric relations with the above-ground biomass during the maturation phase of the clump, turning into an allometric relationship at maturity (biomass maximum). In forestry, commonly the outer diameter at breast height (D_{bh}) is used for estimations due to its simple measurement technique by tape (via circumference) or slide caliper. The only study regarding Ethiopian highland bamboo analyzed ecological gradients, land races and age class (Mulatu and Fetene 2013). For mature culms (> 3 years) the authors found exponential models

predicting biomass, i.e. the total dry weight of a plant, by using one-way equations with D_{bh} as best predictor variable.

Any value chain that is sustainable and economically viable stands on a questionable fundament when lacking harmonized information on the renewable resource. It is generally accepted that the overall worldwide market of bamboo and bamboo-based products accounts to roughly 20 million t/a with an increasing tendency. Since the weight of bamboo is significantly influenced by its fluctuating moisture content, a weight-based figure does not contain enough information. Although highland bamboo tends to have more homogeneous moisture distributions than tropical woody species, moisture content still ranges between 88 % in the top of the culm up to 129 % in the bottom portion. Bamboo density generally ranges between 0.4 and 0.9 g/cm³ at standard climate conditions (20 °C and 65 % relative humidity). Additionally, mass, basic and oven-dry density of highland bamboo have been misinterpreted in the past (Schmidt 2013). Where Liese (2005) stated an oven-dry density below 0.5 g/cm³ for highland bamboo, recent investigations found 0.85 to 0.9 g/cm³. The gradient along the height is nearly negligible with 0.93, 0.91 and 0.87 g/cm³ for top, middle and bottom portion of the culm, respectively. Technologically more relevant is the basic density which was determined 0.62 g/cm³ for highland bamboo (Schmidt 2013). When it comes to trade balances, industrial yield and carbon sequestration potentials, bamboo resources shall be expressed not only by weight, but also by woody, i.e. merchantable, volume (Inoue *et al.* 2011).

Research on taper function and volume modelling is widely available for economically relevant tree species, e.g. *Eucalyptus* spp. (Eerikäinen *et al.* 1999, Mabvurira and Eerikäinen 2002, Scolforo *et al.* 2018) *Pinus* spp. (Cutini *et al.* 2013), Chinese fir *Cunninghamia lanceolata* (Duan *et al.* 2016, Tang *et al.* 2016). For the priority woody bamboo species, *Phyllostachys* spp. and *Guadua* spp. in Asia and South America first approaches were presented by a few authors only (Inoue *et al.* 2011, Inoue and Suga 2009, Kleinn and Morales-Hidalgo 2006, Sanquetta *et al.* 2015). For highland bamboo there is no such study at hand, however, the shape of the culm is a crucial factor for the further processing. Too thin culm walls are not processible with common machines, too thick culm walls cause a low yield. The culm wall thickness from a basic unrepresentative dataset is presented in table 3.

Table 3 Descriptive statistics of highland bamboo wall thickness in three height portions according to Schmidt (2013)

[mm]	Top	Middle	Bottom
Mean	6.35	7.69	10.3
SD	0.91	1.27	1.63

The wall thickness changes by more than one third from the bottom to the top of the culm. However, information on the inner and outer culm form is needed for the accurate prediction of the woody, merchantable volume. To estimate the total tree volume, allometric models using diameter at breast height (D_{bh}) and total tree height (h) have been widely used (Kozak *et al.* 1969). Schumacher and Hall (1933) were the first ones to show a two-way function $V(h,D_{bh})$ by describing the linear relation between their logarithms. Other models for the estimation of the apparent volume using D_{bh} and h have been developed for coniferous tree species and derived a modified one for bamboo species (Suga *et al.* 2011). The studies regarding two-way bamboo took form factors in account and estimated the volume for *Phyllostachys* spp. (Inoue *et al.* 2011). Whether the models could be applied to highland bamboo has not yet been researched. Moreover, the volume estimation mostly relates to the apparent, i.e. the outer, volume of the culm. This study will have to apply the existing models to estimate the actual woody volume instead.

3.1.2 Anatomy

The anatomy of a bamboo culm cross section certainly compares with a fiber reinforced composite. However, its function goes by far beyond mechanical performance, but also represents the metabolic, i.e. transportation, storage and biosynthesis requirements of the bamboo plant. The gross anatomical structure shown in figure 31 divides into a matrix, a foam-like ground tissue (parenchyma) and the axially oriented fiber sheaths (sclerenchyma) supporting the vascular bundle. The vascular bundles are composed of a pair of metaxylem vessels (1), phloem sieve tubes (2) and their accompanying cells. The phloem is responsible for transporting metabolic substances, such as carbohydrates and proteins. The water-carrying metaxylem vessels are surrounded by an outer (3) and inner (4) fiber strand and a lateral one neighboring the vessel (5) which hinder the tissue from buckling collapse. The matrix forms of vertically aligned parenchyma cells (6), most of them being slightly stretched. The voluminous cells are interconnected axially with simple pits, however radial connections are usually not found. The parenchyma saves metabolic substances, storage carbohydrates like starch and soluble carbohydrates and volumetrically accounts to 50 %, whereas fiber cells make up to 40 %. The leftover 10 % belong to conducting xylem and phloem tissue (Liese 1998). This ratio underlies basically two gradients[8]: The absolute number of vascular bundles decreases with culm height whilst their area density increases (Grosser and Liese 1971). However the change across the culm wall is notably stronger (Grosser and Liese 1974). So it is that the vascular bundles form changes, too. They not only become more in number from the center to the outer perimeter but also smaller. Where they are visible to the bare eye in the inner part, one could hardly distinguish them in the outer part. The formal composition of vascular bundles, i.e. the manner of how vascular elements are surrounded by their supporting sclerenchyma tissues, differs depending on the species. Grosser and Liese (1971) had introduced four distinct types and modified sub-types were described later (Liese 1998). Figure 31 shows the different forms in a lowland (A) and highland bamboo (B). Both samples came from the geometrical mid of the culm, in terms of height and across the culm wall. It is that the vascular bundles of lowland bamboo *O. abyssinica* are of type Ill according to the classification and belong to the group C. Their vascular bundles consist of six fibrous parts. The large strand at the outer part (3) and a separate smaller one at the inside (3a) of the bundle supporting the protoxylem. At the inner side of the vascular bundle, the phloem is supported by another medium sized strand which occasionally is supported by a free fiber strand (4a) detached from the actual vascular bundle. The pair of lateral fiber sheaths (5) which encapsulate the large metaxylem vessels are rather small but distinguishable from the other sclerenchyma tissue. This vascular bundle is typical for sympodial bamboos (pachymorph genera) where culms mostly grow in narrow clumps.

[8] The role of the density gradient across the culm wall for the resistance against external load was subject to biomechanical research for more than a century now Amada *et al.* (1996),Ueda (1980). The whole culm is known to be hierarchically organized following principles of functionally graded materials Amada *et al.* (1996),Tan *et al.* (2011) of which some authors even grant natural intelligence behind their design Nogata and Takahashi (1995). Its property gradients on micro, meso and macro-scale had shown superior efficiency against bending loads than trees and palms Ghavami *et al.* (2003),Gibson (2012). The FGM design of bamboo culms has inspired researchers to design mechanically optimized wood-based panels Wegst (2011) and cylindrical large scale components of wind energy towers Sato *et al.* (2017).

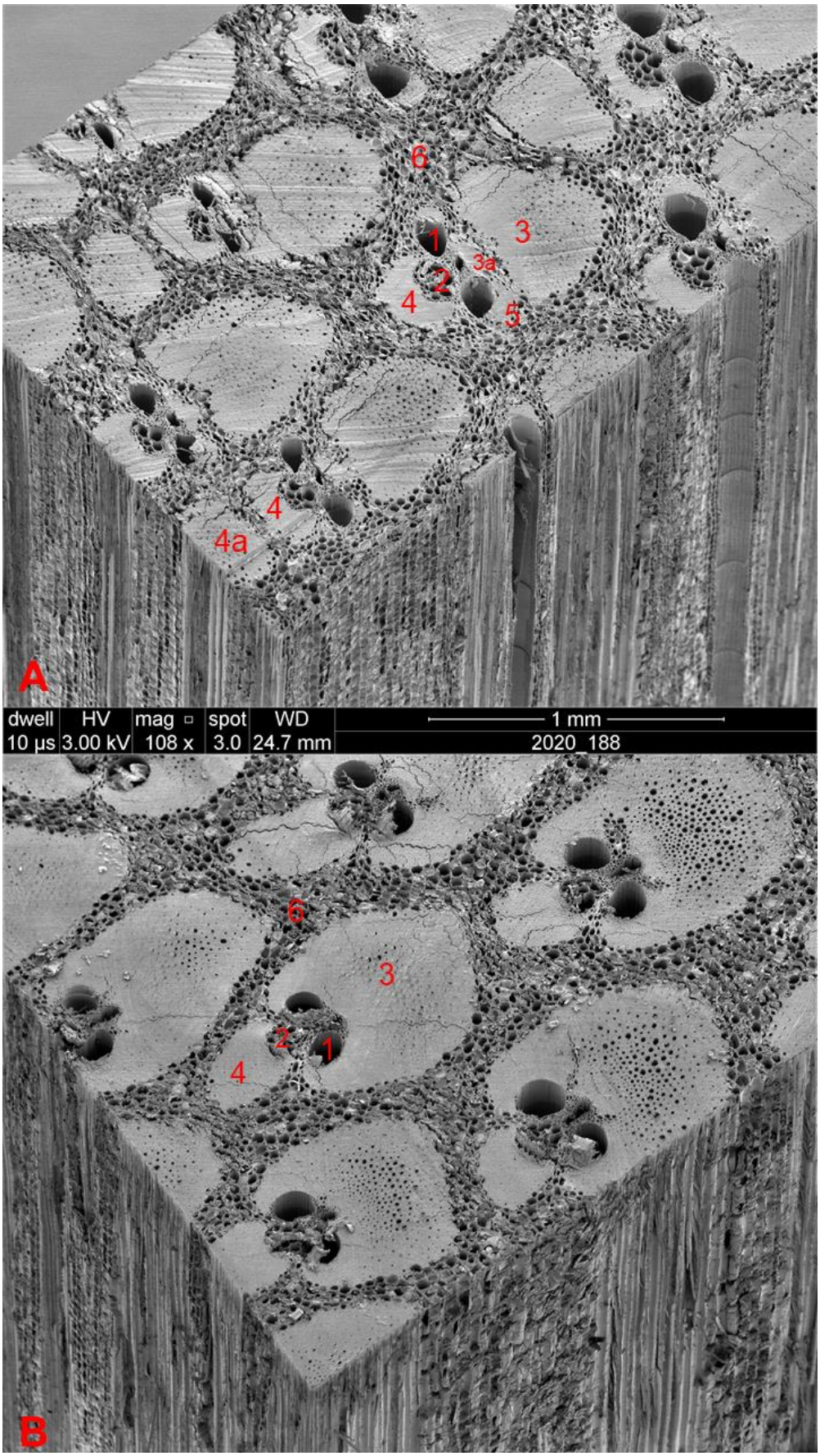

Figure 31: Isometric view on FESEM pictures of culm tissue with vascular bundles embedded in a parenchymatic matrix in African lowland bamboo *Oxythenantera abyssinica* (A) and highland bamboo *Yushania alpina* (B)

The reinforced anatomical structure is what gives bamboo the enormous axial tensile strength. The matrix strength is more than 10 times lower than fiber strength. MOE may even be 20 times lower in the parenchyma than fiber cells (Amada *et al.* 1997). By applying the rule of mixture Nogata and Takahashi (1995) and later Zhou *et al.* (2012) showed that tensile strength of fiber cells is between 450 and 810 N/mm² whilst parenchyma only from 11 to 25 N/mm². The fiber strands consist of sclerenchyma fiber cells with a long slender form. The length of those is gradually distributed along the cross section, too. At the inner portion of the cross section, fibers can be shorter by 40 % compared to the outer perimeter. The different average fiber lengths of some commercially relevant species are shown in table 4. The difference between species can be notable from 1.3 to more than 3 mm - up to threefold and can also be notably different between node and internode section within the very same species and culm (Grosser and Liese 1971).

Table 4 Mean fiber lengths of some major commercial bamboo species selected from Liese (1998)[A], Liese and Grosser (1972)[B] and Osorio *et al.* (2018)[C]

	Fiber length [mm]	**Diameter** [µm]
Bambusa vulgaris	2.3[A]	10[C]
Yushania alpina	2.3[B]	23[B]
Guadua angustifolia	2.1[C]	11[B]-25[C]
Oxytenanthera abyssinica	1.5[B]	12[B]
Phyllostachys pubescens	1.3[A]	13[A]

Due to their aspect ratio (length:width), the cross sectional area obviously changes in a comparable way. The slenderness of Ethiopian highland elementary fibers was not studied yet. For Colombian guadua bamboo Osorio *et al.* (2018) found a heterogeneous distribution, with longer fibers in the outer and shorter in the inner third. They calculated an asymptotic relation between aspect ratio of the elementary fiber and stiffness of a technical fiber bundle. When fiber cells slenderness was below 75, the MOE and MOR of the technical composite had drastically sunk. Other possible causes on cell wall level were discussed elsewhere (Wang *et al.* 2014b). Different to wood, the bamboo fiber cell wall consists of lamellated secondary layers especially in the S2 wall (Liese 1998).

3.1.3 Raw material quality risks

Raw material characteristics presumably fraught with quality risk may affect the production process and differ between bamboo species. Highland bamboo has only been researched very little in this regard before (Schmidt 2013). The quality-to-design approach adopted from biochemical industries (Bansal *et al.* 2019) defines what a critical raw material attribute (CMA) is: “A physical, chemical, biological or microbiological property or characteristic of an input material that should be within an appropriate limit, range, or distribution to ensure the desired quality of output material”. This part of the chapter summarizes bamboo attributes which are suspected to critically affect the processing of bamboo scrimber, as there are maturity (Huang *et al.* 2018), nodes (Qi *et al.* 2015), sugar (Okahisa *et al.* 2006), pH-value (Chaowana 2013) and silica (Müller *et al.* 2012).

- SILICA AND ASH

The outer perimeter of the culm, namely the cortex, protects the underlaying tissues and blocks water. The terminal layer of the cortex, the epidermis, consists of axially elongated cells, stomata and the paired cork and silica cells. Those silica cells contain hard particles of silicon dioxide, varying in size and shape (Liese 1998). This silica is just one out of several inorganic inclusions in bamboo tissues. The ash of bamboo contains as well metal components, such as Cu, Zi, Fe, K, Ca, Ma, Mg and commonly correlates to the amount of silica in the plant. The overall ash content of a bamboo culm may vary from 0.8 to 9.7 %, showing a higher amount in the nodes than in the internodes. The amount of silica, and hence the ash content, increases along the culm height, which might have to do with the thinner culm walls in the top (Liese 1998, Zhang *et al.* 2002). However, one will not find any silica crystals within the bamboo tissue across the culm[9], but only in the cortex terminal layer where it accounts to the high hardness of the culm. Processing tools in the production may suffer wear caused by silica particles in the plant tissue. It was noticed that tool wear with particleboards from agricultural residues was just moderately increased compared to wood, even though their silica contents were many times higher. For finished particleboards Müller et al. (2012) found that the panel density intensifies the negative impact of abrasive substances with respect to tool wear. On the other end of the cross section, the tissue facing the lacuna is protected by considerable amounts of sclerenchyma tissue and a waxy endodermal terminal layer, which makes it less permeable. To produce a panel, these protective coatings must be removed for better glue penetration and consequently improved adhesion (Chung and Wang 2018a, Deng *et al.* 2015). The problem is well known from chemical bamboo preservation where liquids do not penetrate the culm tissue radially (Liese and Kumar 2003).

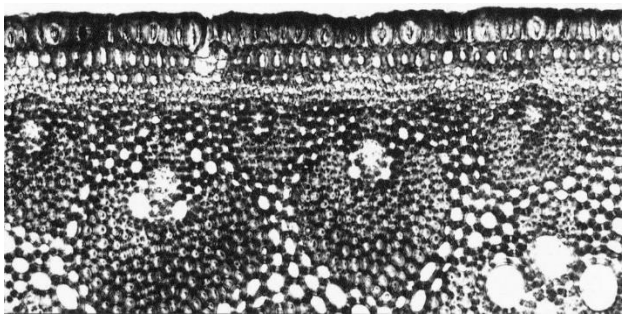

Figure 32: Light microscopy (200x) of the cortex, epidermis and hypodermis of *Bambusa polymorpha* (Liese 1998)

The hardness of the cortex is a great protective advantage for the plant but hinders industrial processing. In chemical and pulp industry, recent research resolves this challenge with an alkali pre-extraction, which removes nearly all silica (Yuan *et al.* 2016). In the (Chinese) bamboo panel industry, one way to deal with the silica challenge is to cleave off the outer perimeter with a splitting knife (see also step E_1 in figure 22) and subsequently use the residue for woven bamboo mats (Deng *et al.* 2015, Yu *et al.* 2015b, Zhang *et al.* 2002). Since the silica amount is closely related to the ash content, species with low ash value should be considered for panel and composite production. The silica content varies between species, e.g. 1.5 % (*Bambusa vulgaris*) and 6.4 % (*Schizostachyum lumampao*) and is influenced by the age and site conditions of the clump. In general, mature culms contain more silica than

[9] One exceptional feature of some bamboo species is the presence of a massive siliceous deposit in the lacuna known as “tabashir”. This phenomenon is still not understood and is observed especially in sympodial taxa from tropical climates which is not observed in *Y. alpina* so far

younger culms (Liese and Weiner 1996). For *Phyllostachys nigra* found that the overall ash content of mature culms is significantly higher than in young culms, but the share of silica is four times higher (Scurlock 2000).

- NODES

The culm shape is determined by the intercalary growth for which nodes are of special importance. At the same time nodes fulfill metabolic functions. The nodes contain the only cross sectional conducting tissue due to the lacking radial cells in internodal bamboo anatomy (Liese 1998). The morphology of the node influences aspects of bamboo utilization, especially in terms of drying, impregnating and in load-bearing applications. Where the macroscopic anatomy of the internode is axially aligned, vessels and fibers deviate from longitudinal axis in the nodal region (André 1998, Peng *et al.* 2014). The nodes are stiffening elements to protect the culm wall from torsion and macro-buckling (Harries *et al.* 2017). Figure 33 illustrates the nodal anatomy: The node consists of a diaphragm radially connecting the culm wall, a sheath scar and a nodal ridge which basically represents the upper edge of the diaphragm. When a standing culm breaks due to flexural loads, then interlaminar fracture in the internode is the relevant failure mode. At the same time, this apparently low interlaminar strength makes it possible for the culm to adapt to large flexural deflection (Shao *et al.* 2009). Wang *et al.* (2014a) has later shown that nodes contribute to fracture toughness in the standing culm avoiding the excessive propagation of cracks. The axial fracture toughness of the nodal region is nearly three times higher than the internode which attributes to the unoriented, intertwined vascular bundle organization and the resulting radial density profiles (Huang *et al.* 2015).

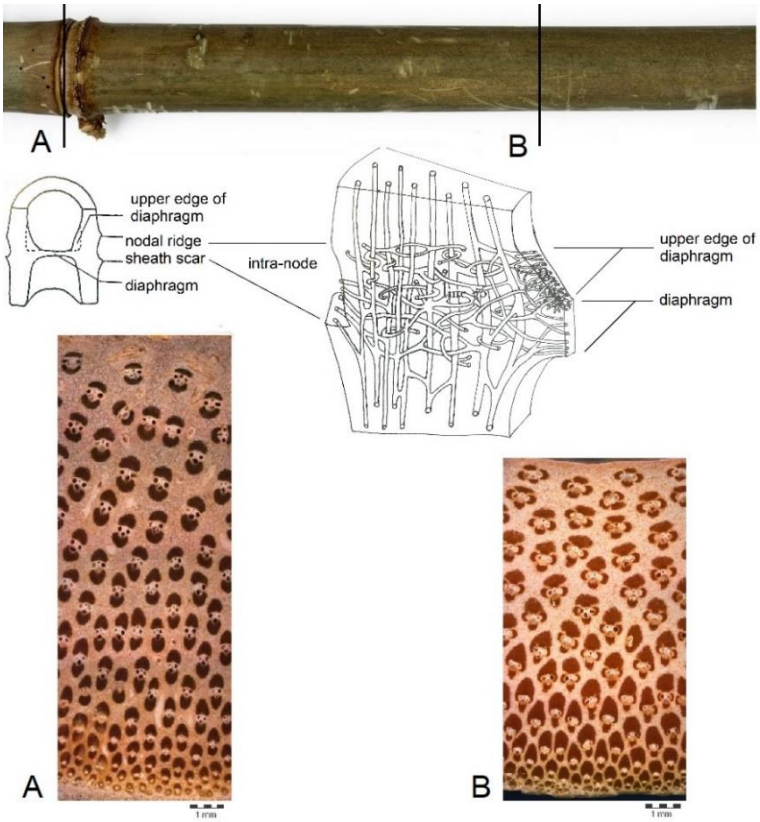

Figure 33: The macroscopic and microscopic anatomical structure of a node (A) and internode (B) of African highland bamboo showing a cross-section (10x) and a modified schematic draft based on Liese (1998)

Nodes are of special interest for the industrial processing of a composite. Although they are a stiffening element in the standing culm, they might weaken the scrim strand in a composite panel. Taylor *et al.* (2015) investigated the mechanical role of nodes in the culm and stated that they must be rather seen as a necessary weak point instead of reinforcement. The authors explain that with its biological necessity due to its functionality as a starting point for branches or culm sheaths (Wang 2017). Qi *et al.* (2015) found reduction in axial tension, compression and bending by at least factor 0.3, 0.8 and 0.5 when used in a bamboo fiber reinforced composite. The authors produced panels containing nodes of *Dendrocalamus farinosus* and *Phyllostachys heterocycla* and compared them to node-free panels. It is a rather theoretical work, since there is no realistic way to avoid presence of nodes in a bamboo scrimber panel. Anokye *et al.* (2016) found a relationship between distance of nodes and flexural MOR in laminated bamboo lumber (LBL) and defined minimum interval distances between them to mitigate the mechanical loss. Hence, to understand the impact of nodes on highland bamboo scrimber mechanical properties, the single scrim, strand or fiber bundle should be investigated. The influence of nodes to fiber length, the volume fraction (density) and the axial MOR and MOE in compression, tension and bending has not been studied for highland bamboo.

- SUGAR CONTENT

Ethiopian highland bamboo was chemically characterized by Starke *et al.* (2016) who found 48 % cellulose, 25 % hemicellulose, 27 % lignin and 4 % extractives. A processing-critical component are metabolic sugars which are believed to inhibit resin curing and of course happen to attract biodegrading agents, such as *Dinoderus* spp. and molds (Schmidt 2013). Metabolic sugars occur in all bamboo species enabling the immense height growth of culms in the early stage. Mature (>3 years) culms store energy in the form of starch and mobilize them as soluble carbohydrates (sucrose) through the rhizome. Commonly, the starch reservoirs are found in parenchyma cells and microscopic images show that those are accumulating in single cells instead of being dispersed across the parenchymatic tissue (see figure 34).

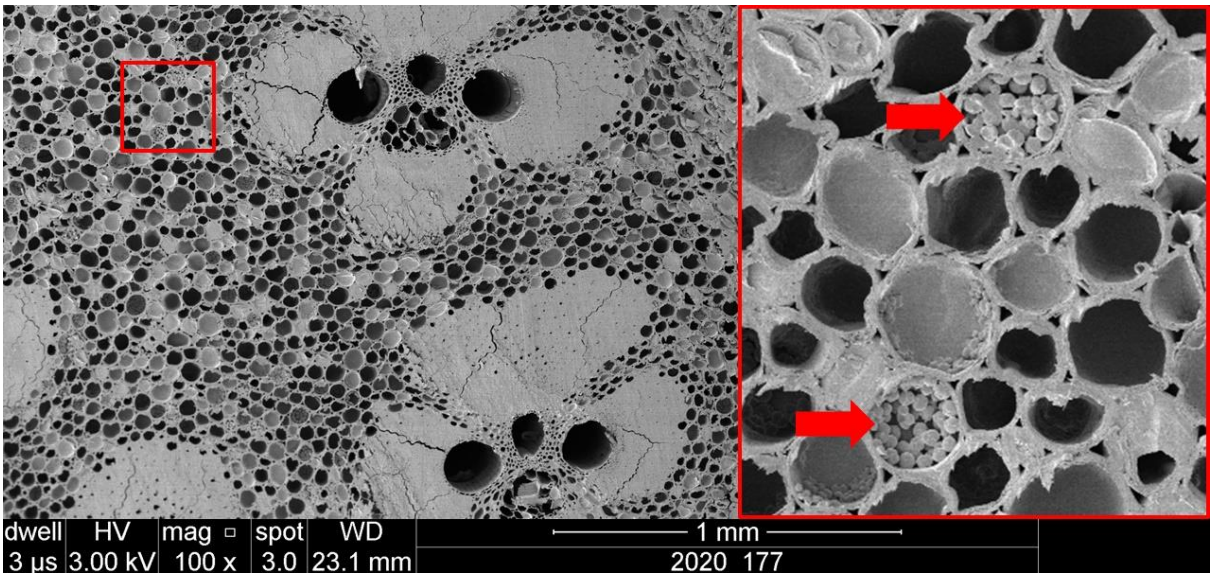

Figure 34: Crossectional FESEM picture of a 4 years old internode indicating parenchymatic cells filled with starch granulate in African highland bamboo *Yushania alpina*

During the vegetative season sucrose is transformed into monomeric sugars, especially glucose, which is needed mainly in the apical meristem where the main growth happens (Magel *et al.* 2005). A thin layer chromatography combined with an enzymatic-assay analysis showed

that the fluctuation happens in between dry and rainy season. During the rainy season, highland bamboo culms contain 3.05 % starch, 1.14 % sucrose, 0.66 % fructose and 0.77 % of glucose related to the culm dry mass. Glucose and fructose content slightly decrease during dry season whilst sucrose is nearly halved. The starch content is significantly higher in culms harvested in the dry season (Schmidt 2013). The sugar analysis was done with bamboo sample material taken at breast height. Only one single site and age class were considered. Thus, height dependent figures as well as difference between age and harvest sites are needed.

- BUFFERING CAPACITY

The pH-value of wood and bamboo plays an important role in resin curing. Typical polycondensation duroplastic resins (Hocking 2005) use catalysts to increase the pH value. The commercially frequently utilized bamboo species show acetous pH values (Chaowana 2013) comparable to wood species (Rowell 2005). First observed on plywood bonding strength, the acidic nature of bamboo can notably weaken the long-term mechanical performance (creep) of bamboo-based composite panels (Wang and Hu 2007). The high buffer capacity of bamboo requires a higher amount of sodium hydroxide catalyst for controlling pH-value and initiate the polymerization. Earlier studies have investigated the buffering capacity and found bamboo strongly resisting pH-value changes when comparing to wood species (Chaowana 2013).

3.2 Specific objectives

Based on the state of the art of bamboo scrimber reported in chapter 2 and related to the presented literature aspects of the raw material, the following questions shall be addressed:

- **Morphology**
  - What does the inner and outer culm taper of highland bamboo look like?
  - What volumes can be expected for the industrial process?
- **Anatomy**
  - What form do the highland bamboo fiber cells show?
  - Does the fiber volume distribution follow a characteristic gradient?
- **Raw material quality risks**
  - Is the silica content lower or higher than in other woody bamboo species?
  - What is the pH value and sugar content in highland bamboo and do growing site, age or the position in the culm influence it?
  - Can a simple process step like washing remove silica components?
- **Mechanical characterization**
  - What axial compressive, tensile and bending MOR and MOE do industrial bamboo scrims have?
  - To what extent do fiber fraction, density and presence of nodes impact the mechanical properties?

3.3 Material and method

The material and methods part documents the raw bamboo origin, harvest and sample processing. Furthermore, the methods of morphology, anatomy, mechanical analysis and others are presented in this sub-chapter.

3.3.1 Bamboo harvest

Bamboo culms were harvested in three phases in 2014, 2015 and 2016 from two semi-managed stands in the Sidama Zone of the Southern Nations, Nationalities and Peoples' Region. The main portion of bamboo culms was harvested in the Hula woreda[10] between Aletta Wondo (also known as Wendo) and Hagere Selam (also known as Hula)[11]. The closest village to the harvesting site is known as Teticha. The exact coordinates of the local are 6° 30' 8" longitude and 38° 29' 50" latitude. The Hula site is denominated as site “A” throughout the thesis. The second stand served for comparison and is in the Bursa woreda, Sidama Zone, neighboring the Oromia Zone (Amharic: ኦሮሚያ ዞን). The access to this region goes through the village of Arbegona. This site is referred to as “B”. The culms were purchased from local production cooperatives for Birr 15 or approximately USD 0.4 per culm[12].

The culms were harvested according to sustainability standards to not harm the clump and ensure a further growth of shoots (Desalegn and Tadesse 2014, Seyoum *et al.* 2018). The culms were first selected by a team consisting of experienced local elders, one cooperative representative and a purchasing agent for translation. The harvest team marked mature culms (4 to 5 years) only and took them from several clumps where possible. The selected culms needed to fulfil an ovality criterium and must not have been bent by external influences. Culms with broken apices or other visible damages (borers, ruptures) were discarded as well. The culms were cut at the second internode above ground with a machete and the tip end was cut off and discarded after an apical diameter of approximately < 5 cm.

[10] A woreda (ወረዳ) is a district and stands for the tertiary level in Ethiopian administration

[11] Hula and Wendo are former Italian names from the 1940s in which the colonial commanders tried to wipe out Amharic names and substitute them by “Italian” names

[12] The issue of currency exchange rates was addressed at the end of chapter 5

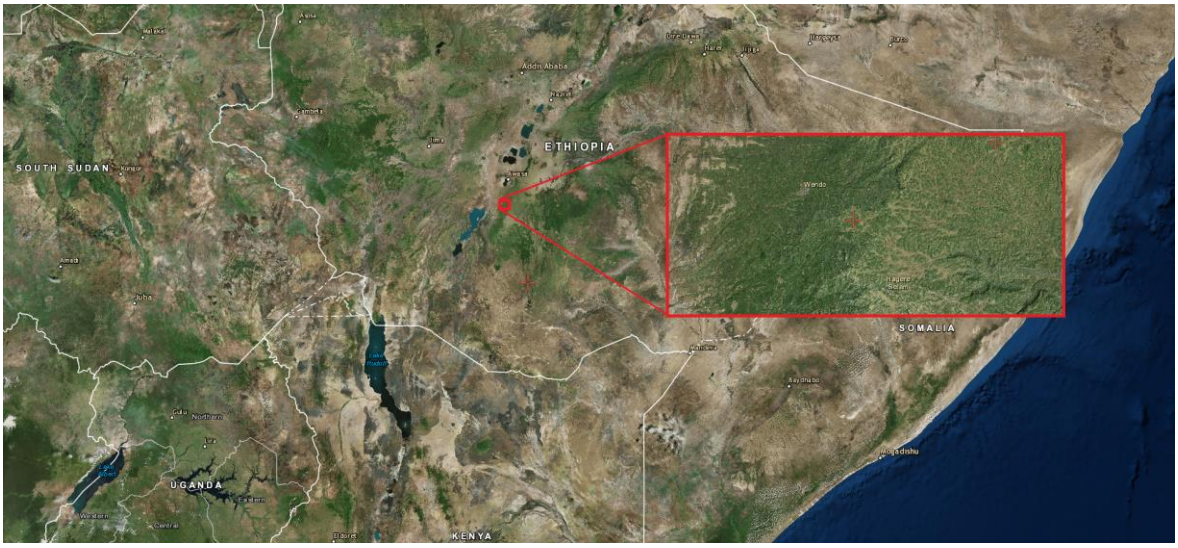

Figure 35: Edited map section of the harvest region in Southern Ethiopia (Earthstar Geographics 2018)

3.3.2 Morphology

The macroscopic study was carried out on site A in December 2015. In total, 11 mature culms were randomly taken out of a batch of 36 culms. The batch was harvested according to the prior chapter. In this stand vital and undamaged were felled above ground and utile length and diameter were recorded with a tape measure and a caliper. Commonly, the outer diameter at breast height D_{bh} is taken at a fixed height (1.3 m) defined a priori. Bamboo outer and inner diameter locally changes at the internode/node transition zone. The variation which can be expected from the fixed height measurement is obviously higher than the one resulting from a slight height alteration. The D_{bh} was therefore measured at the internodal, longitudinal middle at a variable culm height as close to the actual value as possible. The measurement height was recorded.

On the same day, the culms were sawn with a circular saw lengthwise into single height portions (sections). These sections had a length between $70 < L < 150$ cm and contained $4 \leq n_{in} \leq 7$ internodes each. The section was cut at the position with the thinnest culm wall within the middle of the internode. The length of each section was taken with a tape measure. The weight of each section was recorded with a lever spring balance. The outer diameter was measured crosswise with a caliper. The culm wall thickness was measured with a caliper at the same spots where the diameter was taken. The measurement was done at the top and bottom grain end of the height section. The apparent volume (solid truncated cone with outer section diameter $D_1 < D_2$), was calculated adopting the sectional measurement methodology described by West (2015). The inner volume (void) was calculated with the same technique and then subtracted from the apparent volume to yield the woody volume (hollow truncated cone). Due to the outer diameter increase and inner diameter decrease at the nodal transition zone, it is believed that the calculated volumes underestimated the actual woody volume.

3.3.3 Anatomy

The number of vascular bundles, the amount of fibers, the fiber wall thickness, the fiber diameter as well as the fiber length were analyzed. For measuring the number of vascular bundles, the percentage of fibers, the fiber wall thickness and the fiber diameter cross sections of both samples were produced and inspected by digital reflected-light microscopy. Pictures were taken with a ProgRes® C14plus Microscope Camera (Jenoptik, Jena) at 25x and 500x magnifications and then analyzed with the open-source platform for biological-image analysis, Fiji with the GPL v2 license, developed by Schindelin *et al.* (2012). The number of vascular bundles in a specific area over the whole culm wall thickness was counted and translated into an area of one square centimeter. The amount of fibers was measured according to ASTM E562-01:2001. Therefore, a measuring grid with 200 μm^2 arrays was applied to the photograph. Only those arrays were counted, where fibers were found in the bottom right corner of the array. From the ratio of counted arrays with fibers to the total number of arrays, the nominal fiber bundle density (FBD) was calculated according to:

$$\mathrm{FBD_{nom}} = \frac{\mathrm{n_{fiber}}}{\mathrm{n_{total}}} \qquad [-] \qquad (3\text{-}1)$$

where

n_{fiber} is the number of arrays which contained fiber cells

n_{total} is the total number of arrays within the grid

The fiber length was measured by transmitted-light microscopy at 25x magnification. In general, 70 measurements were taken for each sample. The samples were cut into matchstick size, boiled in a beaker with distilled water for 2 h and decanted afterwards. The samples were then immersed in 100 ml of a 5 % CH_3COOH (acetic acid) and 5 g $NaClO_2$ (sodium chlorite) was added. The whole beaker containing the sample was placed in a boiling water bath under a fume hood. After 1 h, 2 ml glacial (anhydrous) CH_3COOH followed by 5 g of $NaClO_2$ added. Gradually, glacial CH_3COOH and $NaClO_2$ were repeatedly added until the samples softened and disintegrated with ease. Diluted with distilled water, a drop with several fibers was placed on a slide and subsequently analyzed. The fiber wall thickness and the fiber diameter were measured at a magnification 500x.

3.3.4 Silica

A reliable method comes from the fiber board sector, where siliceous contents are a problem due to abrasiveness. For bamboo in its raw material form, there is no own method. Hence, we determined the silica and ash content according to ISO 3340:1976-04. The sample material was taken from nodes, internodes of thin-walled and thick-walled culms. The material was cut out with a circular saw and then milled with a cross-beater mill. Hereafter, approximately 10 g of air-dry material were burned at 550 °C in a muffle oven. The combustion product was then boiled with 20 ml hydrochloric acid (HCl) and the dissolvable components were washed out with distilled water. The acid-insoluble part (sand) was then dried in the oven and weighed out. A duplicate determination was done. The ash and sand content calculated as:

$$\text{ash content} = \frac{\mathrm{m_{ash}}}{\mathrm{m_{ws}}} * 100 \qquad [\%] \qquad (3\text{-}2)$$

$$\text{silica content} = \frac{m_{sand}}{m_{ws}} * 100 \qquad [\%] \qquad (3\text{-}3)$$

where

m_{ash} is the weight of ash

m_{ash} is the weight of ash

m_{ws} is the absolute dry weighted sample

3.3.5 Mechanical characterization

All mechanical tests were conducted on a Zwick/Roell Z050 universal testing machine (Ulm, Germany). Prior to testing all specimens were conditioned until weight constancy at a standard climate of 20 °C and 65 % relative humidity. The cross-sectional images were taken from all bending, tension and compression samples. The cross section of each specimen was analyzed and the actual fiber bundle volume fraction was computed using an adopted formula (3-1). An algorithmic procedure (script) was developed in FIJI similar to methods described in the literature (Schindelin *et al.* 2012). The script contrasted the image and transformed it into a binary (8-bit) file. The result of such process is shown for a compression sample in figure 36. The binary file was then used for counting all fiber bundle sheaths as well as determining their mean area percentage of the whole cross section. Information on slenderness or cross-sectional gradients were not recorded. The density and moisture content were determined according to ISO 22157:2019-01 for all tested specimens right before the actual test.

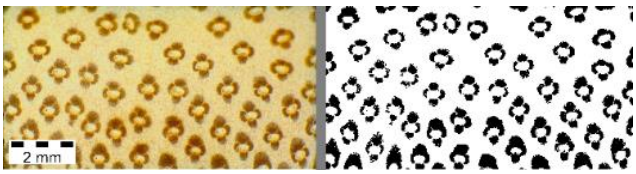

Figure 36: Microscopic image and processed binary image of a compression sample cross section

- BENDING

The static bending test was performed respecting the sampling and naming principles described in ISO 22157:2019-01. However, the tests were conducted on specimens with the dimensions 80 x 10 x 4 mm as described in EN ISO 178:2006-04. A 5 kN load cell was used and crosshead speed was set 3 mm/min.

- TENSION

The tension tests were conducted on long, slender specimens with 120 x 10 x 3 mm. One group contained the internode, the other a node in the middle. The test was done using a 50 kN load cell and with 3 mm/min crosshead speed. Due to the different gradients in the specimen, stress is expected not to evenly distribute in the cross section and a kind of warping (inherent bending) may occur accordingly (Richard and Harries 2015). Thus, for strain determination two methods were tested, one with a mechanical lever gauge sensor (“Macro”), comparable to the one used in bending and a contact-free method via video monitoring (VideoExtens). This was

additionally necessary due to the abrupt tensile failure which may have damaged the mechanical levers. The actual strain gauge length was set at 50 mm and the specimen strain was measured parallelly with both methods. An example of the curves was compared in figure 37. The optical measurement shows more noise than the mechanical method. However, a regression analysis showed nearly perfect linear correlation between both with a constant but negligibly small bias. Each tension specimen was cut to length and two portions of 10 mm length each were cut off at both ends of the specimen. These pairs were marked and stored in the same controlled ambient as the actual mechanical specimen. The two end pieces were then taken to the microscope and their fiber bundle density was determined according to the aforementioned method.

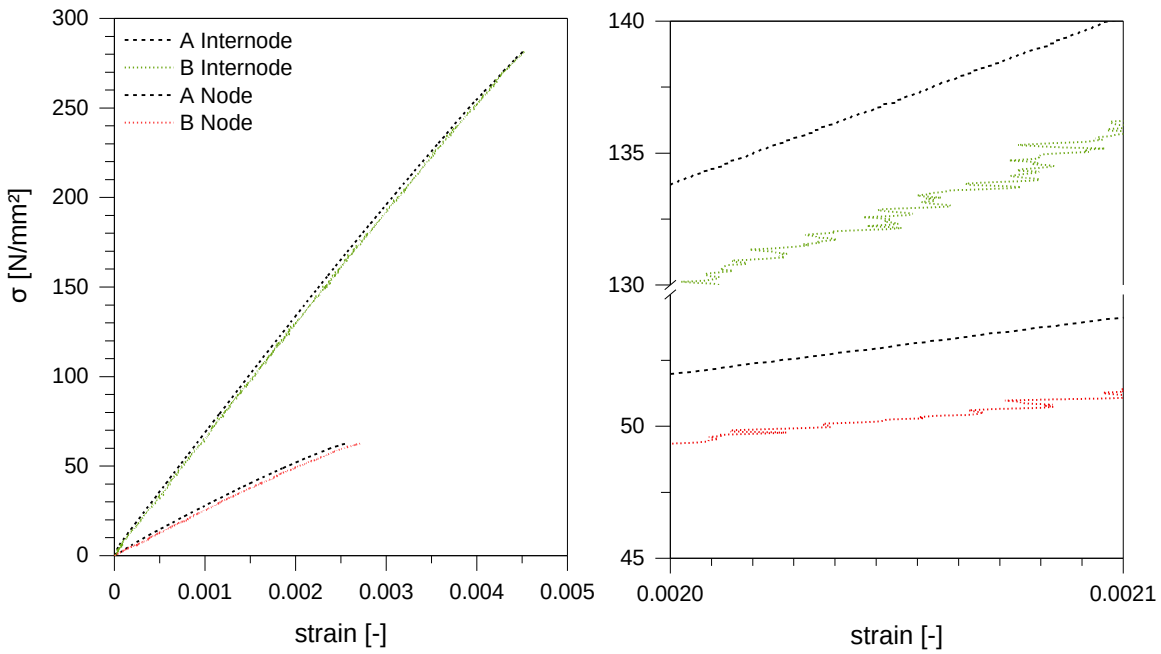

Figure 37: Stress-strain curves for bamboo internode (green) and node (red) samples in tension measured with mechanical lever gauge sensor (A) and a contact free method via video monitoring (B)

- COMPRESSION

Compression was tested on short, longitudinally oriented specimens. On the one hand, the geometry should mimic the form of a slender bamboo scrim. On the other hand, a compression sample, if too slender, tends to buckle before reaching its actual compressive strength. A compromise between specimen thickness (radial) and length (longitudinal) was found, yielding a relatively thick-walled and short specimen (15 x 10 x 5 mm). This makes it difficult to clearly distinguish between the nodal and internodal zone, since the anatomic and physical characteristics of the node (twirled fibers, density change) turn into the internode type (aligned fibers, constant density) along an axial distance more than 15 mm. To cover this transitional area as well, specimens for node only, internode only and the transition zone were tested. The compression strain was monitored through two techniques: A mechanical makroXtens extensometer and electronic speckle pattern interferometry using the videoXtens extensometer. An artificial speckle pattern was applied to the samples since a CCD camera and no laser was used (Müller *et al.* 2005). The pattern was sprayed to the longitudinal-tangential plane manually using white and red acrylic paint as shown in figure 38A. The tests respected the principles of ISO 22157:2019-01 using a hemi-spherical loading head to

guarantee a uniform stress distribution when compressing the sample. To determine the axial compression stiffness (MOE), the downer (F_1) and upper limits (F_2) in the linear stress-strain relation needed to be defined first. Thus, four scenarios were tested according to appended table 43.

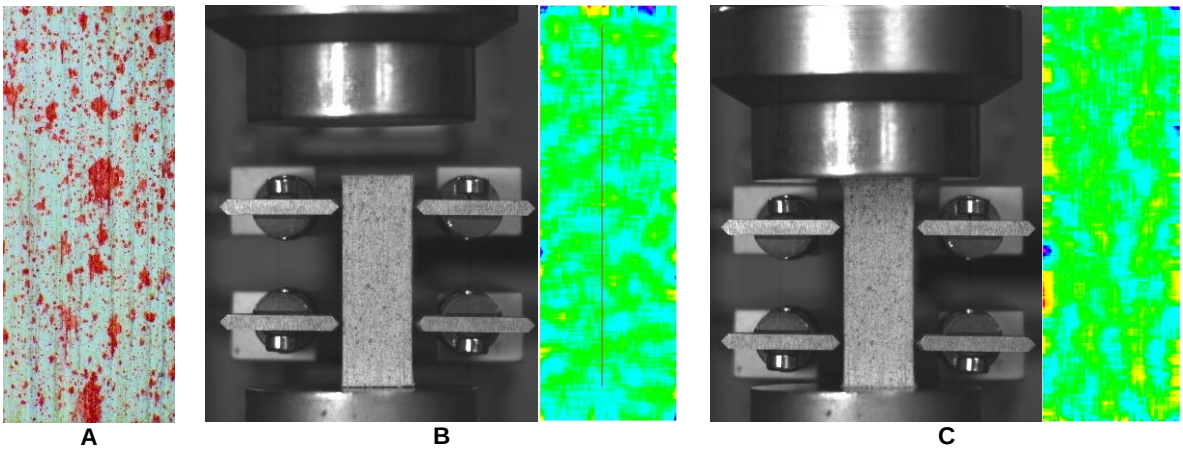

Figure 38: Strain measurement on a compression sample prepared with a speckle pattern (A) through makroXtens extensometer and videoXtens, showing the strain heat map before load was applied (B) and when the sample reached 0.2 x F_{max} (C)

3.4 Results & discussion

The raw material study results are sub-divided in three fields. The forestry part presents new macroscopic shape parameters and taper functions and their potential role in volume estimation. The second part presents material characteristic values of highland bamboo fibers and their role in nodes and internodes. Those results are then connected to compression, tension and bending tests of small defect-free specimen. The third sub-chapter then deals with localization and treatment of silica, pH-value and sugar in highland bamboo.

3.4.1 Gross morphology

The total height (h), the outer (D_{bh}) and inner (d_{bh}) diameter at breast height and the green weight of the culms (m) are shown in table 5. The mean height of 9.9 m ranged between a minimum of 8.2 and maximum 11.6 m showing a variation of 9 %. Though the mean height was within plausible values, the variation is double as high as found in the study of Mulatu and Fetene (2013). A mean D_{bh} of 50.9 mm was recorded. The very few studies on *Y. alpina* showed slightly lower, but comparable D_{bh} of 50 mm and less (Muchiri and Muga 2013) even when looking at very distinct highland bamboo landraces (Mulatu 2012).

3.4.1.1 Inner and outer culm form

Each culm was divided into industrially relevant sections of defined length along its height axis as described under 3.3.2. The segmented portions were analyzed for their inner and outer shape. The mean outer diameter (D), wall thickness (wt) and internodal length (L_{IN}) are plotted against culm height (h) in figure 39. The outer diameter is the mean of two cross-wise measurements at each bottom and top end of the height section. The same applied for the wall thickness. The minimum wall thickness of 10.9 mm was found in culm 1, height section 8, internode 37. As expected, this wall thickness was measured at the tip end of the culm. The basal area of culm 8, height section 1, internode 2, showed the maximum with a wall thickness of 14.3 mm.

Table 5 Descriptive statistics of culm form parameters culm height (h), outer and inner diameter at breast height (D_{bh}, d_{bh}), wall thickness (wt), breast height (h_b)

	h [m]	**D_{bh} [mm]**	**d_{bh} [mm]**	**h_b [m]**	**wt_{bh} [mm]**
Mean	**9.9**	**50.9**	**36.4**	**1.6**	**12.3**
SD	0.9	4.6	3.4	0.1	1.2
COV	9%	9%	9%	6%	9%
min	8.2	44.7	32.7	1.4	10.9
max	11.6	62.3	44.8	1.7	14.3

Diameter, wall thickness and hence cross-sectional area decreased with height. The bubble size in figure 39 shows that the culm diameter decreased less along the culm height than the wall thickness did. An outlier test was conducted for wt_i, D_i and L_{IN} to exclude values which do not serve for developing the taper volume function. When looking at the probability density function, one recognizes (see figure 97) that the distribution shows a diameter tail on the bottom of the culm and a wall thickness tail at the top of the culm. Hence, outer diameter and wall thickness rather follow a Weibull density function with $2 < k < 5$. The internodal length showed a typical Gaussian normal distribution and no outliers were identified. The modified

Weibull distribution fits wall thickness and diameter better than Gaussian normality and should be considered for future studies. The internodal length followed a polynomial function. The coefficient of determination rose with increasing function power, which is a known and often misinterpreted phenomenon. With a degree 4 and higher, the function yielded an R^2 of 0.68 which was acceptable in the context.

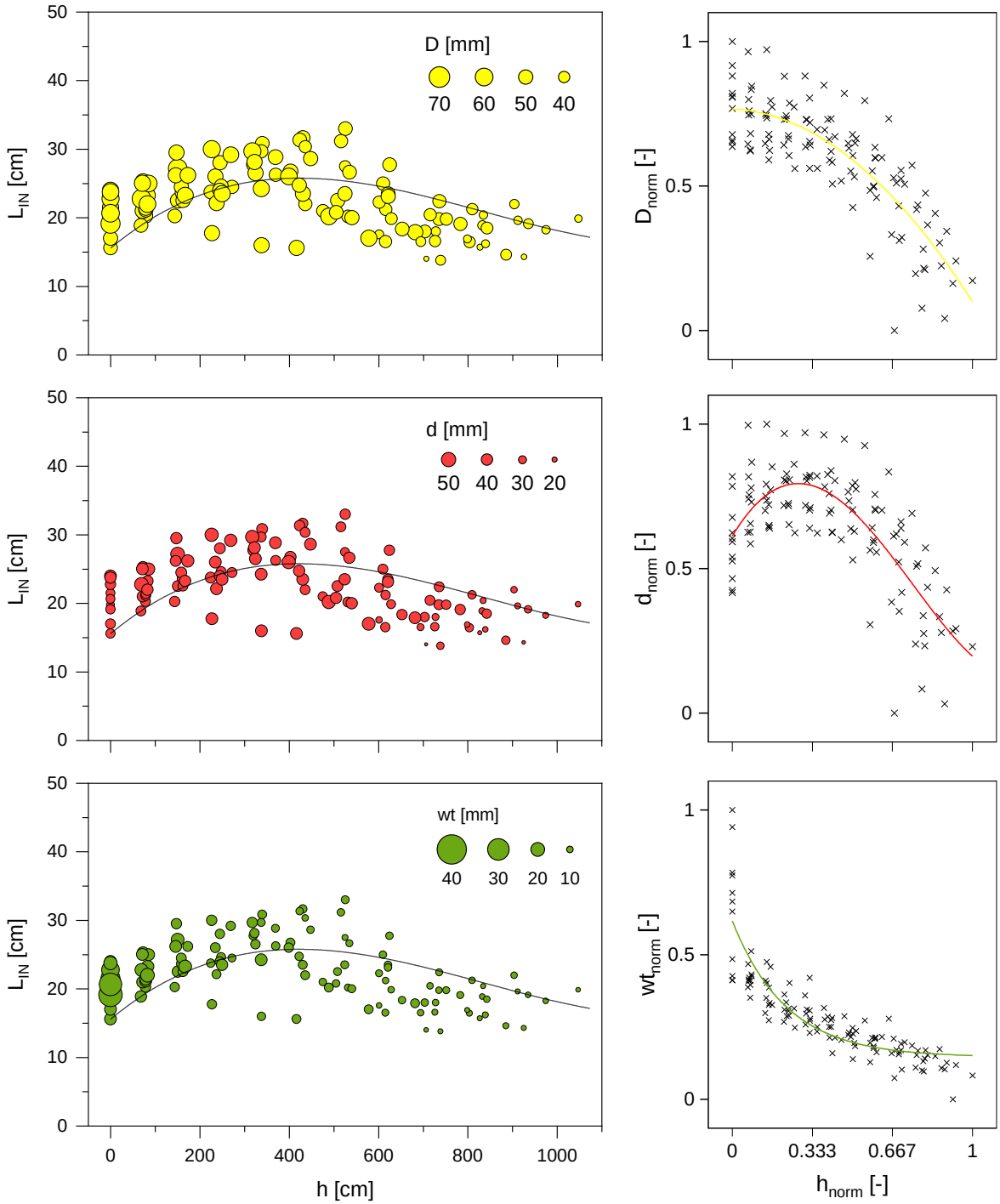

Figure 39: Internode length (L_{IN}) and the regarding outer diameter (D), inner diameter (d) and culm wall thickness (wt) represented by the bubble size (left) and its normalized height curves (right)

To be able to compare the culm form the graphs in figure 39 (right) describe the normalized (related to its maximum) inner and outer form parameters against its normalized height. The

negative slope of D more than doubled from the first to the second third and was strongest in the last third. The inner diameter d instead showed a positive slope in the bottom third, reached its inflexion point between bottom and middle third. Then the negative slope only slightly increased from the middle to the top third. This means that the actual wall thickness was strongly reduced in the first three meters along the culm and only slightly reduced in the middle and top portion of the culm. Outer diameter as well as inner diameter followed polynomial functions. Where a second-degree polynomic described D, a fourth-degree equation applied for d. Wall thickness fitted best an exponential decay function, as expected from the Weibull density distribution. To a certain extent it was surprising that wt was not functionally being described by a combination of D and d instead. The parameter and regression quality of inner diameter, outer diameter and wall thickness along the height are described in appended table 40. The form of the culm in terms of internodal length is favorable for a composite production especially in the first two thirds of the culm height. Since wall thickness showed a nearly constant curve in the upper two thirds, it is believed that those are height sections may produce different qualities in a scrim strand production.

3.4.1.2 Estimation of woody volume

As shown above, the bamboo culm shape followed an inner and outer taper function along its height corresponding to inner and outer diameter, wall thickness and axial curvature. Out of three characteristic culm shape irregularities, two have been neglected: curvature of the culm and ovality are of less relevance for industrial processing than the taper. The apparent volume of the bamboo culm is of importance for logistical questions where the bulk density of stacked culms must be known. However, the effective merchantable woody volume of a culm must be known to be able to build a substantial process and cost model. In a rural industrial setting, it is obviously impracticable to measure each section's diameters and wall thicknesses to determine the actual woody culm volume.

The volume of each height segment was calculated by simplifying each section geometry (neglecting the diameter change at the axial node-internode transition zone as well as axial culm curvature). The culm section was therefore simplified as a truncated cone. The woody volume of the section can then be the calculated by subtracting the inner truncated cone from the outer one (substitutional method). The culm actual woody volume is then the sum of the sections as per:

$$V = \sum_{i=0}^{n} V_i = h_i * \pi/3 * [\left(\frac{D_i}{2}\right)^2 + \frac{D_i * D_{i+1}}{2} + \left(\frac{D_{i+1}}{2}\right)^2 - \left(\frac{d_i}{2}\right)^2 + d_i * \frac{d_{i+1}}{2} + \left(\frac{d_{i+1}}{2}\right)^2] \text{ [m}^3\text{]} \quad (3\text{-}4)$$

with D being the outer diameter

d the inner diameter

and h the length of the culm section

The resulting volumes for inner and outer hollow truncated cone as well as the actual woody volume are statistically described in table 7. The mean volume reached 2.17 x 10^{-3} m^3 with a COV of 16 %. The method followed the principles of West (2015) and delivered plausible results. However, it made no claim to reflect the real woody volume and should be critically reviewed. The apparent and actual woody volume was thus modelled through three approaches: (1) an artificial form factor derived volume V(f) estimating the apparent volume of the culm; (2) a reduction factor V(α,D) comparing the calculated volume from equation (3-4)

with the ones estimated by using form factors; and (3) a two-way equation with V(D,h) using Kunze's form equation (West 2015).

- FORM FACTOR APPROACH

Once the outer form of a stem was known then the volume could be estimated with high accuracy. The form could be expressed by form quotients, taper function equations and form factors (West 2015). The use of a form factor adjusted the volume overestimation which is usually a result of using only D_{bh} and h (Socha and Kulej 2008). Classical forestry modelling distinguishes three form factors with each relating to a different relative height: The normal form factor (0.1 x h), the absolute form factor (< 0.1 x h) and the artificial form factor (breast height). All of them compose of the volume ratio with the respective reference diameter as per:

$$f = \frac{V(D)}{V_{cyl}} \qquad [-] \qquad (3\text{-}5)$$

Where V is the apparent culm volume (i.e. neglecting the hollow of the culm) and V_{cyl} the volume of a solid theoretical cylinder with a basal area of

$$A_{cyl} = D^2 * \frac{\pi}{4} \qquad [-] \qquad (3\text{-}6)$$

The artificial form factor therefore calculates by

$$f = \frac{\sum_{i=0}^{n} V_i\,(D_i; h_i)}{V_{cyl}(D_{bh})} \qquad [-] \qquad (3\text{-}7)$$

However, different to solid wood logs, the form and taper functions in bamboo not only depend the outer diameter, but the inner diameter as well as wall thickness. Figure 40 shows their relation to total culm height. It is obvious that the larger scale causes a higher spread for the outer diameter. The respective artificial form factors have been calculated according to the equation (3-5) as well as h, D_i and d_i as described in table 5. The artificial form factor of the apparent culm volume was 0.223 and for the inner hollow 0.026 with a respective variation of 12 and 6 %. This indicated that the inner diameter at breast height was slightly more accurate than the outer diameter. The wider spread of the outer diameter D than the inner diameter or the wall thickness (also see figure 40) supported this argument.

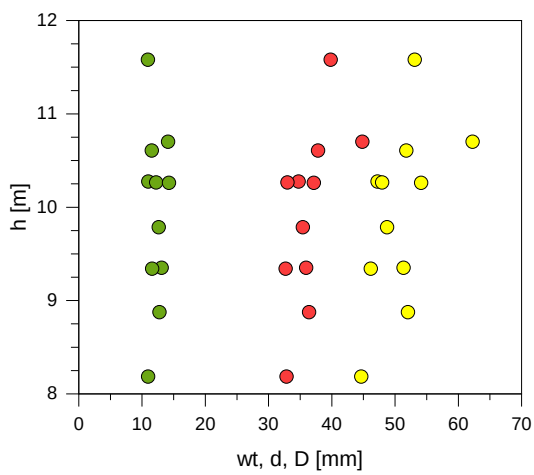

Figure 40: Wall thickness (green), inner (red) and outer diameter (yellow) at culm breast height against its total culm height

- REDUCTION FACTOR APPROACH

It was suspected that the ratio of cross-sectional area of the annulus defined by wall thickness $\mathrm{A(wt)}$ and the apparent cross-sectional area defined by the outer diameter $\mathrm{A(D)}$ was constant independent of height. To calculate $\mathrm{A(wt)}$ it is necessary to either involve d or D. Figure 41 shows the relationship between both for each variant. It can be generally accepted that if $\mathrm{A(wt)} = 0$ then $\mathrm{A(D)} = 0$. The data was fitted to linear functions by resetting its root to zero the linear relationship. Both showed approximately linear relationships but stronger determination (0.99) for $\mathrm{A(wt, D)}$ whereas $\mathrm{A(wt, d)}$ had scattered especially at high area values above 0.5 dm² with R^2 being 0.93.

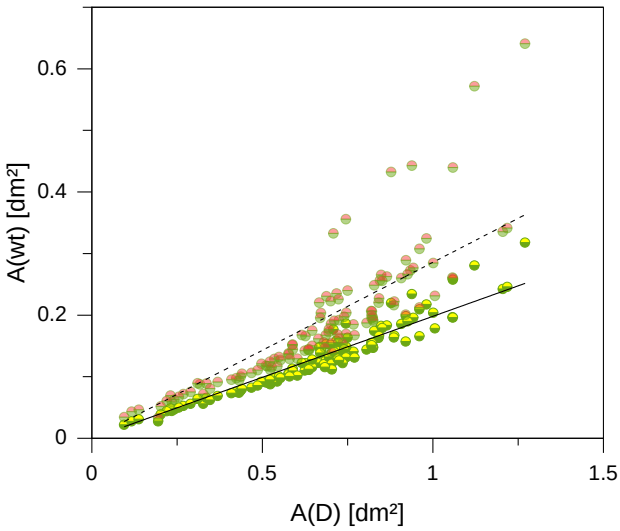

Figure 41: Cross-sectional area of annulus defined by wall thickness with inner diameter (green/red circles) and with outer diameter (yellow/green circles) against apparent cross-sectional area computed through outer diameter D and their respective linear relationship

The resulting relation between both showed that the area fraction becomes a constant as shown in equation (3-8) and indicated in figure 41. Obviously, the apparent cross-sectional area of the culm could be transformed into culm wall area independently from the culm height. The reduction factor was assumed to be 0.198 according to the same equation. The reduction factor then applied to each section apparent volume and integrated along the height. Subsequently, the reduction factor $\alpha_i(d_{bh})$ was calculated for each culm and used to reduce the apparent culm volume into the woody volume. The results are summarized in table 7.

$$\alpha = 0.198 \frac{\mathrm{A_{culm}}}{\mathrm{A_{wall}}} \qquad [-] \qquad (3\text{-}8)$$

The estimated mean woody volume was found at 1.06 x 10^{-3} m³ with a variation of 22 %. In comparison to the empirically determined sectional woody volume, it was lower by approximately factor 2 and showed higher deviation. This might have been the result taking the apparent volume, i.e. related to the outer diameter at breast height (D_{bh}) into account and reproducing its statistical error.

- TWO-WAY EQUATION APPROACH

It can generally be assumed that the culm form can be expressed by Kunze's equation with two parameters determining the relation between total height and diameter at breast height.

$$D_{bh}^2 = a * h^b \qquad [-] \qquad (3\text{-}9)$$

Instead of using the artificial form factor at breast height, the two-way equation estimates the apparent culm volume by using two form factors at two different relative heights above breast height. The form factors must not be dependent to the culm shape variables. Spearman's test investigating the correlation of total height, breast height diameter and the respective form factors at indicated significant correlation at all relative heights (0.1 to 0.9). Nevertheless, the form factor at the height section above breast height as well as the form factor at 0.9 relative height showed the lowest correlation and are suspected to be nearly constant independent of height and diameter. Respecting the dynamic nature of the actual breast height in this study, the apparent volume of the culm calculated according to:

$$V = \frac{\pi * D_{bh}^2 * h * \lambda_i}{4 * \left[\frac{1 - \frac{h_b}{h}}{j}\right]^x} \qquad [-] \qquad (3\text{-}10)$$

where x is the divisor power $x = \frac{\log\left(\frac{\lambda_i}{\lambda_j}\right)}{\log\left(\frac{j}{i}\right)}$

with λ being height dependent form factors at i and j being two relative heights at constant positions above breast height

Table 6 Descriptive statistics of artificial form factor f with reference to breast height (bh) for the outer (D) and inner (d) shape and the height dependent form factor (λ) at two relative heights (i, j)

	f_D(bh)	f_d(bh)	λ_i	λ_j	i	j
		[-]			[m]	
Mean	0.223	0.017	0.248	0.592	2.433	7.824
SD	0.026	0.001	0.027	0.109	0.152	0.910
COV (%)	12	6	11	18	6	11
min	0.182	0.015	0.195	0.417	2.245	6.010
max	0.271	0.018	0.297	0.821	2.72	9.350

By inserting the mean form factors, relative heights and breast height in table 5 into equation (3-10) gives the two-way volume equation as per:

$$V = \frac{0.248 * \pi * D_{bh} * h}{4 * \left[\frac{1 - \frac{h_b}{h}}{j}\right]^{-0.743}} \qquad [-] \qquad (3\text{-}11)$$

The calculated apparent volume by sum of sections, form factor and two-way equation approach as well as the estimated woody volumes by substitutional (D,d) method and reduction factor (r) method are shown in table 7. The mean apparent volume of a culm calculated with the empirically determined section method was 0.00534 m³. The two-way equation and the form factor estimation delivered lower values in the order $\sum Vi(D) > \sum V\lambda(D) > \sum Vf(D)$. For the sectional (i), the form factor (f) and the two-way approach (λ), the substitutional method (D,d) delivered relatively high values which were about half of the apparent volume for

i and λ and nearly the same volume for f. Therefore it was obvious that the substitutional method (D,d) could not further be applied to calculate the woody volume. The method using a reduction factor (r) with the two-way approach resulted in an estimated mean woody volume was at 1.03 x 10^{-3} m³ with a variation of 19 %. The estimated volume showed lower deviation and was not significantly different from the empirically determined sectional woody volume.

In comparison to the sectionally calculated actual woody volume the two estimation approaches differed notably. Whilst the simple form factor approach was 16 % lower, the two-way approach did not differ significantly (2.8 %). Moreover, the forestry measurement for the two-way approach demands more work effort than the simple form factor. In addition to D_{bh} at least height and outer diameter must be taken at two culm locations. The form factor just asks for culm height. Hence, bamboo forestry industrialization research shall investigate one-way equations (D or h) for highland bamboo inspired by coniferous forestry (Inoue *et al.* 2013).

Summarizing, the substitutional method did not give satisfying results, whereas the reduction factor method seemed to have yielded more reliable information on the woody volume. Both methods were applied with the form factor and the two-way approach.

Table 7 Apparent volume V(D), actual woody volume calculated by the substitutional method V(D,d) and the reduction factor V(r) method for the sectional approach ($\sum V_i$), the form factor approach (V_f) and the two-way equation approach (V_λ)

[10^{-3} m³]	**$\sum V_i(D)$**	**$\sum V_i(D,d)$**	**$\sum V_i(D)_r$**	**$V_f(D)$**	**$V_f(D,d)$**	**$V_f(D)_r$**	**$V_\lambda(D)$**	**$V_\lambda(D,d)$**	**$V_\lambda(D)_r$**
Mean	5.34	2.17	**1.06**	4.47	4.3	**0.89**	5.22	2.54	**1.03**
SD	1.16	0.35	0.23	0.71	0.68	0.14	1.02	0.51	0.2
COV [%]	0.22	0.16	**0.22**	0.16	0.16	**0.16**	0.19	0.2	**0.19**
min	3.37	1.6	0.67	3.46	3.33	0.69	3.94	1.91	0.78
max	7.83	2.87	1.55	5.96	5.69	1.18	7.87	3.79	1.56

Although very accurate, the sectional method ($\sum V_i$) could ultimately only approximate the real volume. For an exact determination in an industrial context, solutions such as x-ray or similar would be necessary. Alas, such do not have a reasonable cost-benefit ratio to a bamboo scrimber production. Furthermore, the results are based on a relatively small sample and do not represent the complete Ethiopian highland bamboo stock. There is a certain diversity in highland bamboo stands due to management differences, so-called land races and environmental gradients, such as precipitation and slope. These factors affect the gravimetric and volumetric characteristics. This may especially become a problem in combination with varying plantation densities which range from 11,467 culms/ha for the *Wonde* (ዎንዴ) to 15,800 culms/ha for the *Enkotekot* (እንኮተኮት) landrace (Mulatu and Fetene 2013). However, the stand density varying by one third is at least three times higher than the variation due to uncertainties in the model estimation of woody merchantable volume. Considering 300,000 ha highland bamboo forests in Ethiopia and above-mentioned stand densities an estimated woody volume stock of about 4.25 million m³ can be expected.

3.4.2 Anatomy

The numbers of vascular bundles decreased from the outer towards the inner zones as shown in figure 42. Close to the outer periphery, the vascular bundles are small in diameter, numerous and concentrated, while in the inner zones of the culm they were larger and widely spaced. The form of the vascular bundle changes with the radial position with special regard to the fiber sheaths. Where the inner bundles clearly showed distinguishable fiber strands and supporting sclerenchyma, the vascular bundles in the outer third showed one large strand. The number of vascular bundles per cm² and the percentage of fiber cells are shown in table 8. Nodes showed 94 n/cm² vascular bundles whereas internode measurement resulted in 156 n/cm². The fiber share (volume fraction) was found 26.7 % in nodes and 36.5 % in internodes. The number of vascular bundles appeared to be relatively low compared to other species: Qi *et al.* (2014) found vascular bundle densities along the culm height ranging from 411 to 579 n/cm^2.

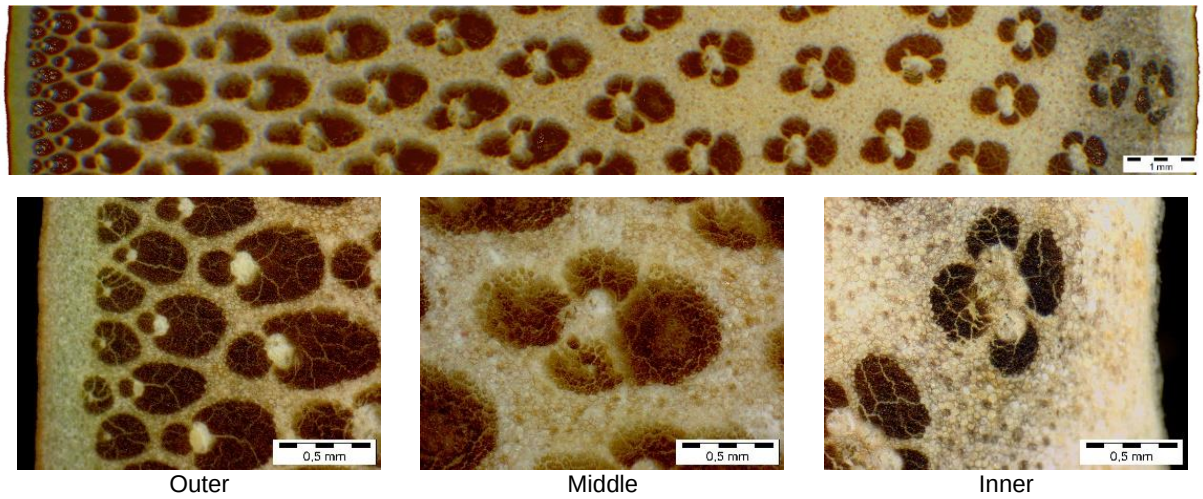

Figure 42: Reflected-light microscopy images (50x) from the outer (left), middle and inner (right) portion of the cross section of an internode of highland bamboo

The mean fiber cell wall thickness in the internode was 7.14 µm but showed a lower value in the node with 5.08 µm. The mean fiber diameter of 21.85 µm ranged between a maximum of 32.07 µm and a minimum of 15.49 µm for the internode. The nodal mean fiber diameter was significantly lower at 14.81 µm ranging between minimum 11.07 and 18.82 µm maximum. The mean fiber length of node and internode did not differ notably. Whilst the internodal fiber cells were measured 1.40 mm long, the node contained 1.45 mm long fiber cells. The main difference between node and internode is the statistical distribution. The nodes maximum fiber cell length is 2.54 mm whilst internodes reached a maximum of 3.03 mm.

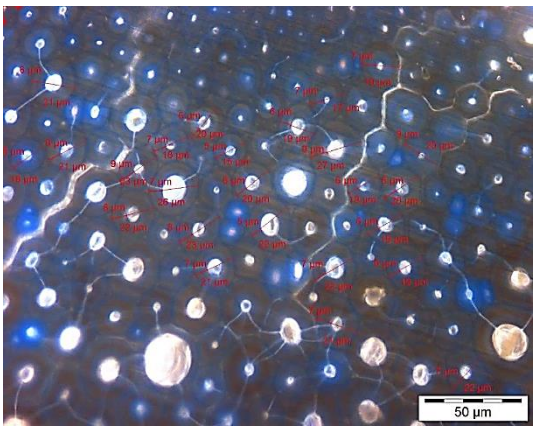

Figure 43: Transmitted light microscopy image (500x) of a fiber bundle cross section of *Y. alpina* for cell wall and diameter measurement

According to Liese (1998) fiber length, diameter and cell wall thickness differ with site, age and height section. Such differences were neither found significantly for Ethiopian lowland nor highland bamboo (UNIDO 2009b). However, fiber length is in between typical hardwood and softwood ranges. Though the values found for fiber cell length (see table 8) are slightly lower, they are in line with other results ranging from 1.57 to 1.80 mm for highland bamboo (Kelemwork *et al.* 2008, Kelemwork 2009). The opposite was observed for the cell wall thickness: Literature mentioned a range from 4.05 to 5.65 µm, however, the values found here were higher (see table 8).

Table 8: Number of vascular bundles, fiber fraction and morphology (cell wall, diameter, length) in internode (IN) and node (NO) as a mean across the whole culm wall thickness

			Mean	Min	Max	SD
Vascular bundle density	[n/cm²]	IN	156			
		NO	94			
Fiber fraction FBD	[%]	IN	36.5			
		NO	26.7			
Fiber cell wall thickness	[µm]	IN	7.14	5.00	11.62	1.29
		NO	5.08	2.87	7.85	1.08
Fiber cell diameter	[µm]	IN	21.85	15.49	32.07	3.46
		NO	14.81	11.07	18.82	2.21
Fiber cell length	[mm]	IN	1.400	0.622	3.030	0.393
		NO	1.447	0.511	2.538	0.431

Moreover, the cross sections were analyzed by counting vascular bundles and measuring their size and subsequently used for the calculation of the area share. The mean fiber area fraction in the internodes was 0.07 (0.02) mm² and 0.09 (0.02) mm² in the nodes. The cell wall diameter translated into area by simplifying the cross section of a fiber cell into a circular form. Simple geometry calculation then yielded 374.89 µm² and 172.27 µm² for the mean cross-sectional area of a fiber cell in internode and node, respectively. Thus, highland bamboo fibers from internodes and nodes did not notably differ in length but in slenderness. The volume of cell wall material in the internode was more than double as high in the node which may lead to significantly higher MOR and MOE.

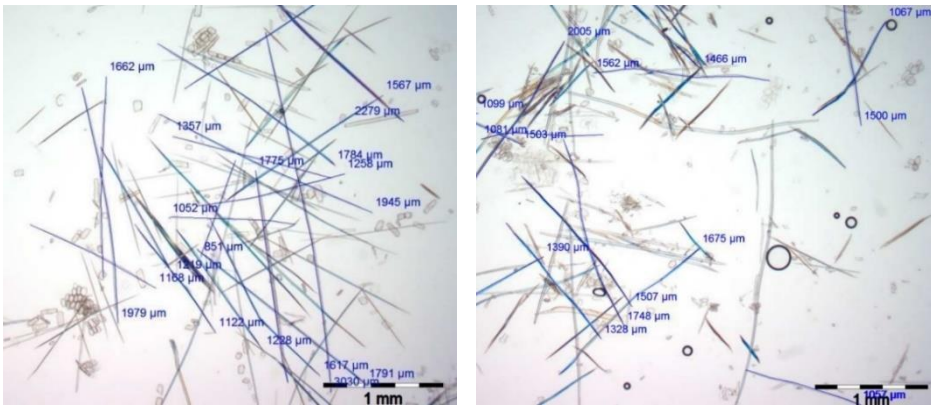

Figure 44: Transmitted light microscopy (25x) of macerated fiber cells from the node (left) and internode (right) of *Y. alpina* for fiber length measurement

Additionally, longitudinal shear cracks have been observed in the sclerenchyma fiber sheaths around the vessels. Figure 42 shows these cracks in all investigated samples in the inner, middle and outer part of the cross section. Apparently, such cracks were better visible in denser fiber bundles. They might have occurred in the parenchymatic matrix as well but were not observed due to the spongy structure of the low-density tissue. Figure 43 shows different cross sections and the regarding fiber sheaths surrounding the vascular elements. The higher resolution in the light microscopy indicates that the cracks occur in the middle lamella and grow not only axially but transversely to the plane. Depuydt *et al.* (2019) have found similar longitudinal cracks in samples from European grown bamboo species. A possible cause might be found in interfacial tension stresses perpendicular to grain induced by the drying. However, there was no difference found between kiln-dried, air-dried or heat-treated samples. All of them featured such longitudinal cracks. Shao *et al.* (2009) showed the weak interlaminar strength in bamboo and explains its cracking behavior with the energy model in mode I fracture. Following the energy model, nodes do show three times higher fracture toughness than internodes (Wang *et al.* 2014a) which is why those cracks are visible only in the internodal samples. The observed tissue damage prior to actual manufacturing must be kept in mind for the mechanical behavior of the bamboo scrims and final scrimber product. Several authors mentioned the presence of so called “dot-shaped” and “line-shaped” cracks after the crushing step to make scrims out of the strips in a bamboo scrimber production. The authors argue for the improved resin penetrability due to such tissue defects and the superior bonding as a welcome consequence. The here found cracks indicate that such defects are present in the tissue way before bamboo enters any mechanical processing and presumably have been caused by the simple fact of drying after harvest.

3.4.3 Silica

Figure 45 shows the silica mass share in nodes and internodes of thin and thick-walled culms before and after washing. The ash content was shown as a control parameter. The highest silica content of 1.54 % (based on dry weight) was determined in the nodes of thin-walled culms (wt < 10 mm), whereas the lowest value was found in the internodes of thick-walled (wt ≥ 10 mm) culms, with 0.17 %. The mean content in thin-walled culms was found 0.86 % and 0.33 % in thick-walled culms. Although this difference was shown to be statistically significant, the general ratio of lignocellulosic mass to content of inorganic substances must be considered different due to the localization of the silica in the outer cell layers of the culm

(see also figure 46). Figure 45 shows higher silica amounts in all nodes than in internodes. The mean silica content in nodes was 0.83 % while internodes contained about half with 0.36 %. The washing step decreased the sand and ash content by nearly half from 0.8 % to 0.39 %. Nevertheless, the general difference of higher silica in nodes and low in internodes did not change. Assumebly, washing had actually only removed superficial contamination or residual sand but not the silica contained in the tissue.

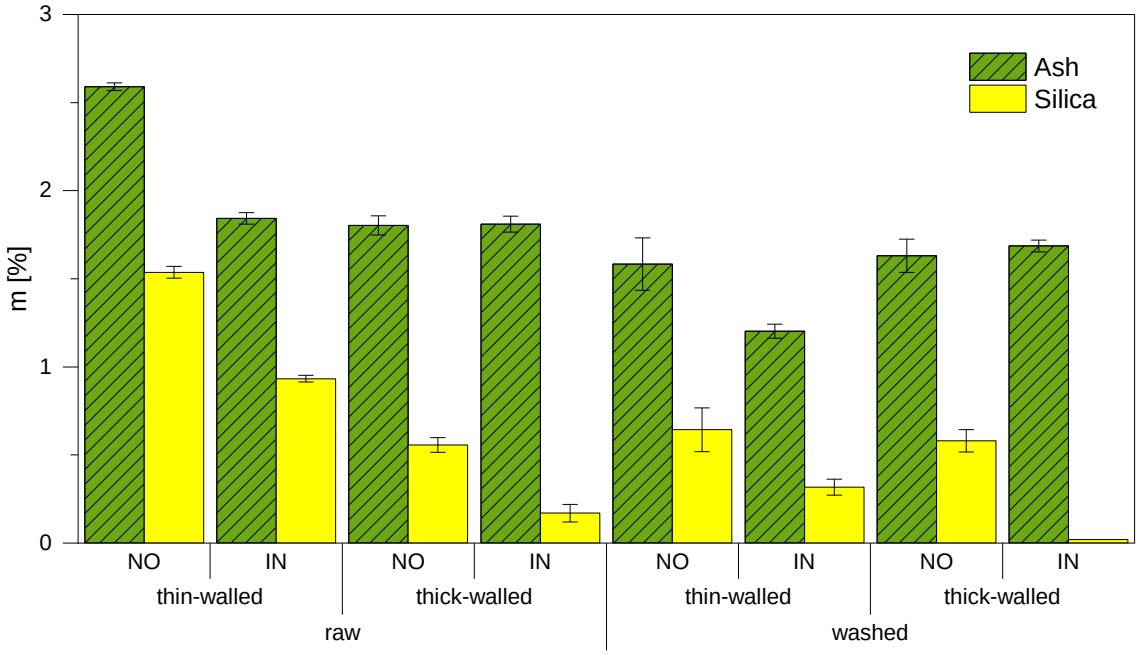

Figure 45: Mass percentage of ash and silica content of nodes (NO) and internodes (IN) in thin-walled and thick-walled bamboo culm before and after a washing step

In addition to the previous results, table 41 shows the silica content in the height sections (bottom, middle, top) of highland bamboo harvested from two sites (A, B) and two age classes (4 and 5 years). The highest content was found with 1.1 % on site A for the top section of 5-year-old culms. Surprisingly, the lowest silica share of 0.04 % was found in the middle section of the same site and age group. There have been generally no notable differences between the sites, the age class and the height sections.

Figure 46 shows the outer part of the cortex containing silica crystals especially in the terminal cell layer. The terminal, monocellular layer (up to 0.01 mm) consisted of epidermis cells filled with silica crystals as shown in figure 46. Beneath this terminal layer, the hypodermal parenchymatic layer (0.01 to 0.07 mm) can be found and from 0.07 mm depth the outer sclerenchyma fiber cells followed. Finnish and Chinese plant biologists investigated silica contents of leaves and culm biomass from the viewpoint of fauna diet. Helander *et al.* (2013) found that *Yushania* spp. contained relatively high silica contents of up to 10 %. In highland bamboo, most of the silica was concentrated in the outer perimeter of the culm wall. These are usually removed in the crushing machine. The machine uses a two-axis planing tool and rather strikes than cuts the outer tissue away. Although the silica amounts found in *Y. alpina* were relatively low, a washing step was considered to help further reducing it. The results in figure 45 show that the washing step decreased silica. Furthermore, Müller *et al.* (2012) showed that the impact of silica particle content is less influencing than the actual particle morphology. However, the actual removal effect of a washing step on final product quality or tool operational life was not proven.

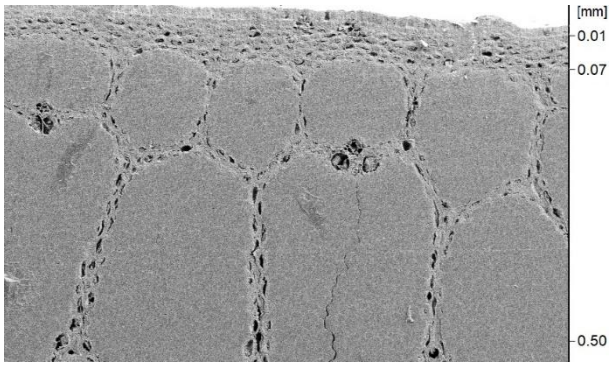

Figure 46: FESEM image (100x) of the terminal cortex cell layer containing silica crystals

3.4.4 pH-value and sugars

The pH values of highland bamboo from both harvest sites range in the slightly acidic side. No notable difference for different height portions can be observed. The mean pH-value for site A (Hula) was 4.97 whereas site B (Bursa) showed a pH-value of 5.52. The bad configuration of pH-value before resin curing leads to higher activation energy for the initiation of curing (polycondensation). This is especially relevant for novolacs. In contrast to resoles which are partly precured, novolacs cannot be cured just by cross-linking (He and Riedl 2004).

The results on the sugar analysis are displayed in appended table 42. For site A, the glucose content was lower in the bottom than in the middle and top sections. The same applies for site B, with one exception for the 4 years old culms. None of the differences found were statistically significant.

3.4.1 Mechanical characterization

For a better understanding of the bamboo scrim strands, small, defect-free raw bamboo samples were tested in tension, compression and flexural bending. All tests were carried out on nodes and internodes. The compression tests were sub-divided into nodes, internodes and a transition zone sample. Table 9 shows the fiber volume fraction (FBD) was slightly higher in internodes than nodes, however, the raw density was not notably influenced by that.

Table 9: Mean moisture content (MC), density (ρ) and fiber volume fraction (FBD) and their regarding standard deviation (in brackets) for node (NO), internode (IN) and transition (INNO) samples in three mechanical tests with n = 20 each

		MC [%]	ρ [g/cm³]	FBD [%]
Bending	IN	11.04 (1.29)	0.69 (0.07)	38.32 (5.46)
	NO	10.83 (0.88)	0.68 (0.08)	34.23 (8.79)
Tension	IN	11.12 (1.17)	0.72 (0.08)	34.25 (5.71)
	NO	10.92 (0.97)	0.71 (0.08)	29.83 (7.20)
Compression	IN	10.11 (0.77)	0.75 (0.12)	34.80 (5.60)
	NO	9.55 (0.71)	0.66 (0.09)	31.25 (5.24)
	INNO	10.69 (0.91)	0.68 (0.13)	31.73 (5.61)

This might be attributed to the different cell wall thickness (lumen size) in the fiber cells of node and internode. Nevertheless, the high SD indicated a variation of more than 15 % for FBD which is due to natural variation between culms and along the culm height. It is important to note that the anatomy chapter (3.4.2) found FBD with 26.7 in nodes and 36.5 % in internodes. The FBD of node and internode in the bending sample was 34.23 and 38.3 % which was obviously higher than before milling the specimen from the bamboo slat. The volume fraction relating to the complete cross-section was generally lower than the results in table 8. Those represent bamboo scrimber bundles of 3 to 5 mm thickness as they would be found in the later composite panel.

Table 10 shows the results on the axial MOR and MOE in bending, tension and compression of industrial highland bamboo. Whilst the tension MOR of the internode yielded 214.8 N/mm², nodes showed less than half with 99.2 N/mm². This difference explains with the load-bearing function of the aligned fiber sheaths in tension. Not only that the fiber bundle density was 5 % less in the node, the vascular bundles were not aligned in any direction. Moreover, the poor strength of parenchyma did not contribute notably when loaded axially which explains the minimum strength being nearly half of the mean value whereas the maximum is a third higher. The plot in figure 47 shows that the tensile strength of internodal samples increases nearly linear with a growing density whilst the slope for the nodal samples became less with increasing density. The higher density in the samples was mostly caused by the higher FBD. That in turn means that the higher amount of unaligned vascular bundles in the nodal area could not notably contribute to the tensile strength of the sample. To a certain extent the highest node strength was determined by the bond between parenchyma cells and a subsequent crack propagation (Shao *et al.* 2010, Wang *et al.* 2014a).

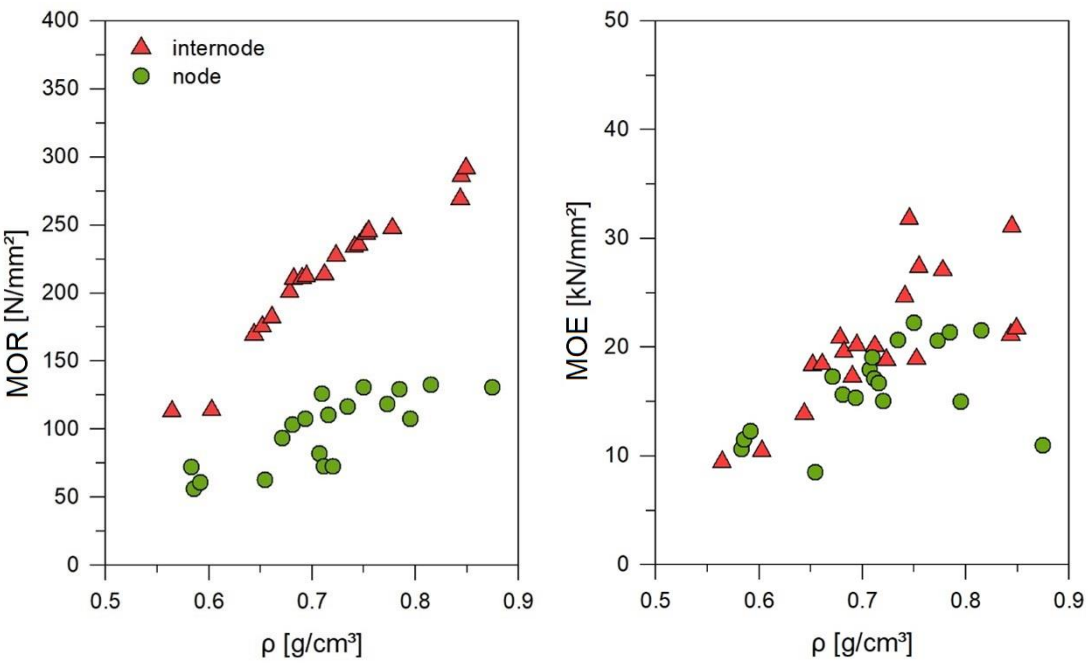

Figure 47: Axial tension strength (MOR) and modulus of elasticity (MOE) against density for highland bamboo scrims containing an internode (triangles) and node (circles)

Nevertheless, the maximum MOR of internodes loaded in tension was lower than comparable studies. Muche and Degu (2019) showed that the upper part of the highland bamboo culm contained a perceptually higher share of solid fiber cells and hence showed the highest axial MOR around 300 N/mm² in the culm. The primary failure mode in tension was fiber pullout and

interlaminar shear for internode samples as it is typical for high FBD samples (Shao *et al.* 2009). Most of the samples containing nodes ruptured in the parenchymatic matrix. The staged failure occurred often with a secondary stress-strain maximum. The yield strength was commonly below the primary stress maximum. The internode samples failed abruptly in the elastic range with a strain nearly double as high as it was with nodes. It is important to note that a potential damage from the clamping mechanism on a number of tension specimens was observed. Especially the specimens with high FBD were concerned. This problem is a renowned issue attributed to the stress peak at the transitory border between metal clamp and specimen. A theoretical tension MOR might thus be higher than measured.

Figure 48: Interlaminar shear and fiber pullout in a tension loaded bamboo internode sample with a high FBD indicating the initial location of failure occurred at the specimen clamping edge

The mean MOE of internodes and nodes was measured at 20.6 and 16.26 kN/mm², respectively, with a notably high coefficient of variation, being roughly 25 % in all samples. Figure 49 shows the stress-strain curves for internode (left) and node (right) loaded in axial tension. The lower curves (black) stand for a specimen with a low, the upper curves for a high MOE. The green curves in between showed a moderate MOE. The figure shows that higher fiber share obviously led to high stiffness in both, internode and node. The FBD of the plotted samples was approximately equal, however the density was not. The vascular bundles in the node sample was obliquely cut along the fiber grain which presumably over measured the FBD. While the tension MOR showed to be prone to the misalignment of vascular bundles the tension MOE of node and internode represented the sample density and FBD difference instead.

Table 10: Flexural, tensile and compression strength (MOR) and modulus of elasticity (MOE) parallel to grain for highland bamboo scrim strands containing node (NO), internode (IN) and transition zone (INNO) and their descriptive statistics

			Mean	SD	Minimum	Median	Maximum
MOR [N/mm²]	Bending	IN	229.91	68.67	123.83	231.82	388.29
		NO	178.51	41.47	99.19	180.47	256.66
	Tension	IN	214.80	48.96	112.95	213.65	291.72
		NO	99.17	26.66	55.97	107.56	132.72
	Compression	IN	57.93	14.16	31.48	56.46	81.92
		NO	60.37	14.17	36.77	62.20	87.52
		INNO	55.10	17.25	27.66	58.04	84.92
MOE [kN/mm²]	Bending	IN	21.51	4.51	13.70	21.64	29.70
		NO	16.76	3.27	9.09	16.54	20.58
	Tension	IN	20.58	5.98	9.43	20.09	31.80
		NO	16.26	4.11	8.48	16.67	22.22
	Compression	IN	22.59	13.45	3.13	19.40	57.41
		NO	16.61	7.67	9.00	11.24	28.89
		INNO	13.33	9.57	2.22	12.60	39.64

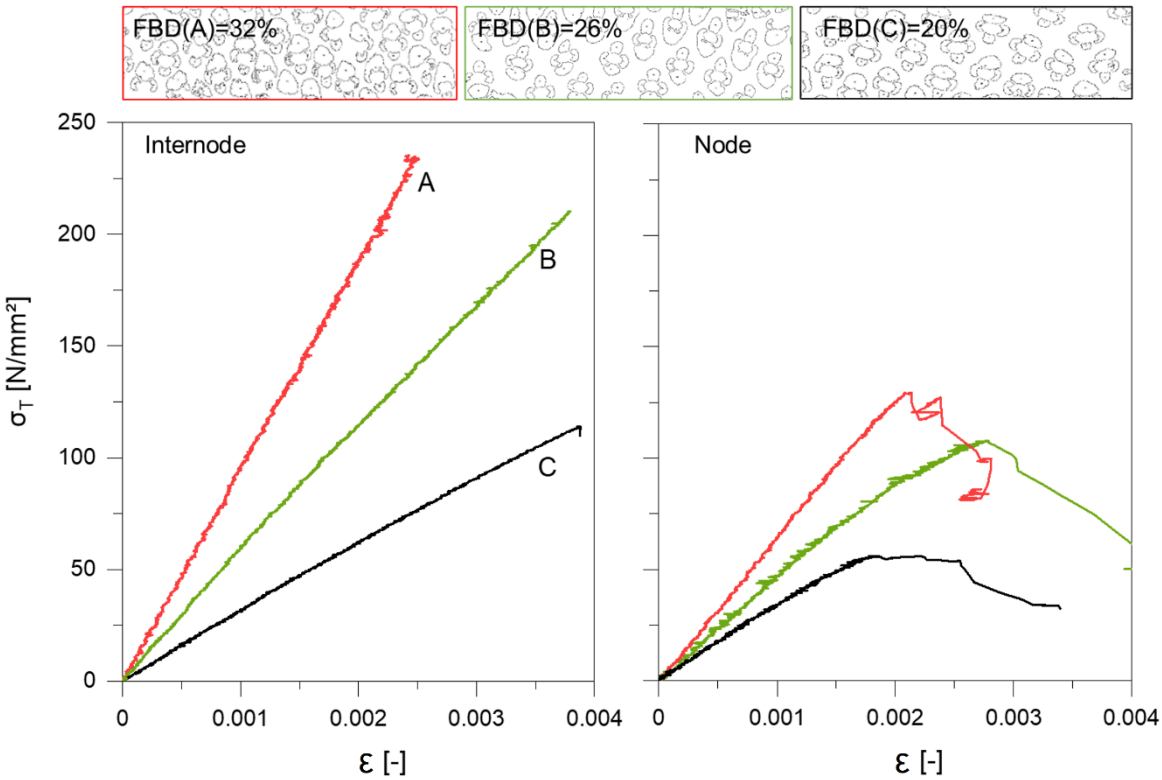

Figure 49: Stress-strain curves for tension loaded bamboo internode and node samples with a high (A), moderate (B) and low (C) fiber share (FBD)

Additionally, the axial compression MOR and MOE were tested and results plotted against density in figure 50. The FBD in internodes of the compression sample mean of 34.79 % ranged between minimum 24.5 % to a maximum 47.37 %. The mean raw density was 0.66 for internodes, 0.72 g/cm³ for the nodes and in between the transition zone sample. The nodes showed a compression MOR of 60.37, internodes 57.93 and transition zone 55.10 N/mm². A statistical difference was not found. The relation of compression MOR and density was obviously linear for all groups, node, internode and transition zone. Comparable result were observed for moso bamboo culms. Deng *et al.* (2016) investigated the compression MOR of node and internode and found no differences either for yield strength nor for failure load. Notably different mean MOR was solely found at different culm height, position, namely 48, 55 and 62 N/mm² for top, middle and bottom. The absolute values however were very close to the ones found for the here investigated material.

The compression MOE was tested in the present study but in contrast to compression MOR, no clear relation with density could be found. The stress-strain diagrams for the compression sample were very heterogenous and the elastic linear share could not be easily defined (see also figure 50). As shown in appended table 43, the correlation was best when using $F_1 = 150$ N and $F_2 = 0.5 \times F_{max.}$ However, the strong spread of results did not seem reliable which presumably explains with a not adequately suited test setup. For bamboo in compression ISO 22157:2019-01 recommends modifying the load bearing block using a hemi-spherical element equipped with a disc which is able to move in the plane perpendicular to the load axis. A tilting of the sample is thus prevented and potentially the two cross sectional grain end areas of the

sample that are not perfectly parallel would be compensated. The used apparatus featured a hemi-spherical movable block, but no disc as described above (also see figure 38).

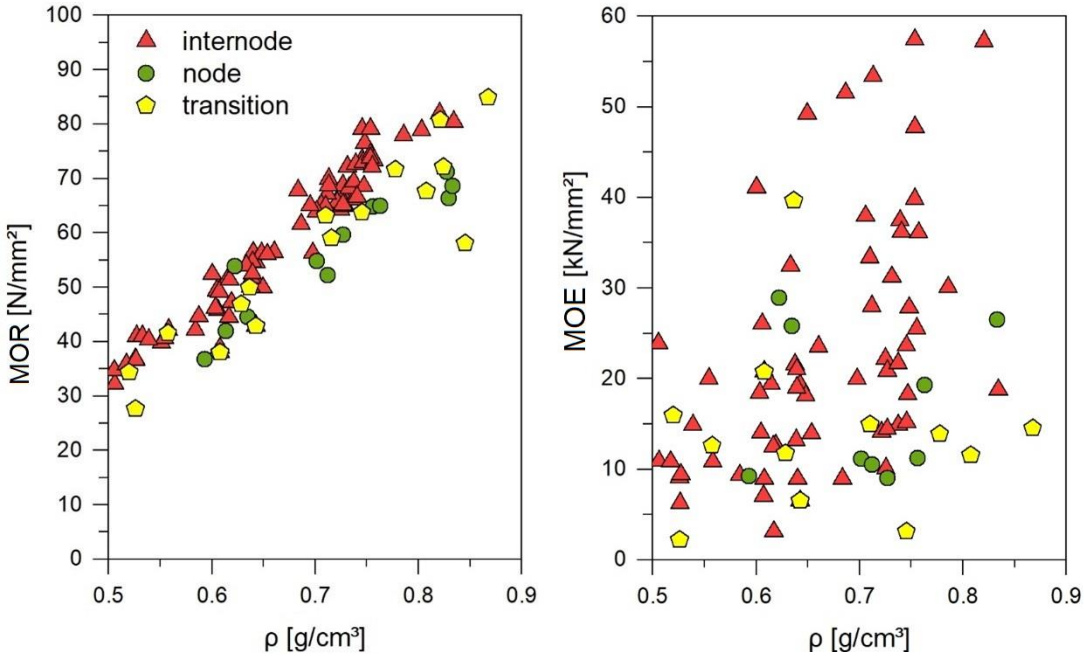

Figure 50: Compression strength (MOR) and modulus of elasticity (MOE) against density for highland bamboo scrims containing an internode (triangles) and node (circles) and transition zone (pentagrams)

Bending samples showed the highest MOR for nodes and internodes with 178.51 and 229.91 N/mm², respectively. When loaded in bending the scrims reflected the tension and compression behavior from the prior tests. The phenomena described mixed up and resulted in a slightly lower MOE for nodes. The results for bending MOE (nodes 16.76 and internodes 21.51 kN/mm²) did not differ notably from the compression and tension tests but indeed for MOR. The results were plotted against density, however, no additional insights were gained, so that can figure 98 be found in the appendix. Figure 51 then summarized the results and shows the mean values for MOE and MOR in bending, tension and compression. All values were normalized to the internode and node bending reference. The graph visualizes that the compression stress in bending was least affected by the nodes, whereas tension stress was highly prone to the presence of nodes. For MOE results, the effect of the nodes cannot be clearly classified. Despite reduced values being measured when nodal tissue was contained, the MOE loss turned out to be nearly equal for all load types. However, at least the MOE measurement of the compression sample must be critically reviewed due to methodological challenges. The results indicated that the role of nodes and internodes in a bamboo scrimber composite are not as crucial as expected. Once a bamboo scrimber composite is loaded in bending (which is the case for flooring and decking), the tension stresses will be halved, while compression stress rather depended on density and moisture content.

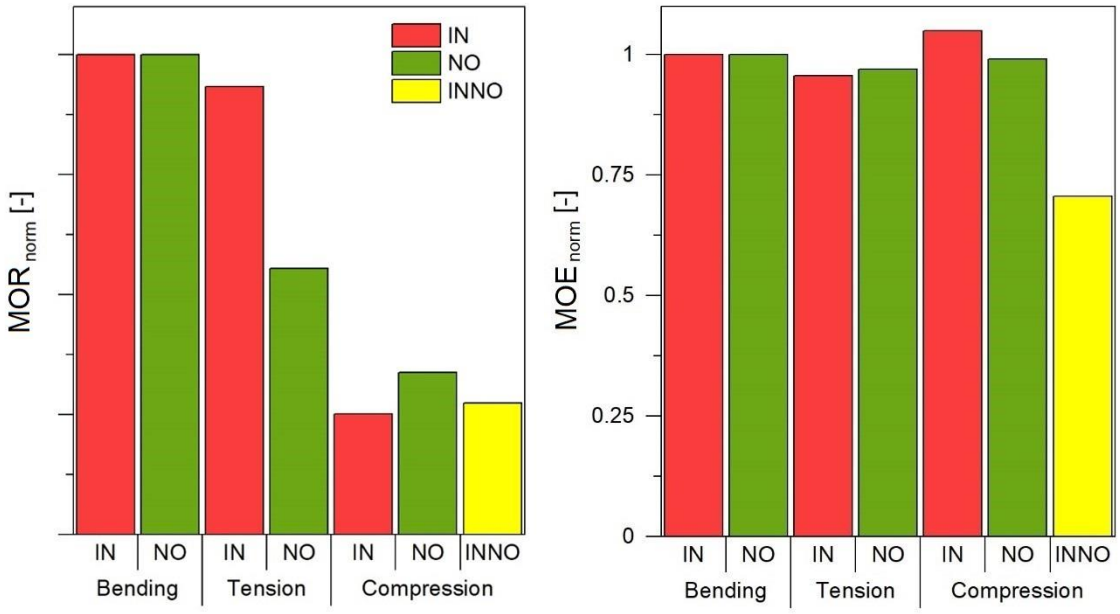

Figure 51: Mean strength (MOR) and modulus of elasticity (MOE) of highland bamboo internode (red), node (green), transition (yellow) loaded axially and normalized to flexural means

3.5 Intermediate conclusion

Highland bamboo culms are of moderate height (about 10 m) and thickness. At breast height, the culms were measured 5 cm thick and had about 12 mm strong culm walls. Proportionately, the culm diameter decreased less along the culm height than the wall thickness did. The form functions of inner diameter, outer diameter, internode length and culm wall thickness showed that especially the middle and top portion of the culm are of interest for scrimber processing. Although the greatest volume portion of the culm was found in the bottom, the wall thickness strongly reduced in the first three meters. Since the constant wall thickness is of high concern for the scrimber crushing process and yield aspects, commercially alternative uses for the bottom portion must be found. Bamboo scrimber production will have to use the whole culm length for lacking economic alternatives and also to avoid unnecessary depletion of the resource. Thus, the woody volume of the entire highland bamboo culm was estimated by using form factor, diameter and height. The apparent volume of a highland bamboo culm was about 5.34×10^{-3} m³ whereas woody volume of the culm was empirically determined between 1.06×10^{-3} and 2.17×10^{-3} m³. The estimation model using a two-sided equation approach was only slightly lower than the empirically determined one ($V_\lambda = 1.03 \times 10^{-3}$ m³) but showed more plausible results than the volume determined by form factor ($V_f = 0.89 \times 10^{-3}$ m³). Based on the results, it will be possible in the future to calculate the almost exact industrially usable volumes, even for small plots using plantation stock densities. A total highland bamboo volume of about 4.25 million m³ can be projected for the national woody stock. However plausible, the results generally seem to be relatively low. The examined stand potentially belonged to one of the smaller landraces of highland bamboo and other plots must be included in such studies prospectively.

The study of highland bamboo vascular bundles showed that their form changed from type 1 to 1a across the culm wall and the typical exponential FBD gradient was found. Moreover, notable differences between node and internode cross section were found. While fiber cell diameter and cell wall thickness differed significantly, the fiber length of 1.4 mm was nearly the same in node and internode. However, the presence of longitudinal cracks in all tissue samples independent from the radial or longitudinal position left open questions for the product side. The bamboo slat presumably enters the scrimber processing chain with defects which is neither favorable nor preventable, since the defects were observed at air dried raw material, not kiln-dried. The bamboo scrimber composite panel produces from those bamboo scrims. The scrims were milled on an industry typical equipment and analyzed regarding density, fiber fraction and nodes. The processed scrim strands showed densities between 0.66 and 0.75 g/cm³ with FBD ranging from 29.83 to 38.32 %, thus higher than the culm wall mean. When solely looking at the internodes, their MOR ratio against loads in bending, tension and compression was about 4:4:1 and MOE was determined almost equal 1:1:1. The negative impact of nodes was confirmed for tension, compression and bending. The results indicated that their role in a bamboo scrimber composite is relevant mainly for bending and tension stresses. The flexural and tension MOR was halved while compression MOR was not affected and congruently increased with density. The negative impact of nodes on the raw material MOE was less and decreased by one quarter in an equal manner for all tested loads.

Additionally, other bamboo raw material characteristics known to fraught with quality risks were investigated. Typical process critical raw material properties, such as pH-value, sugar, wax and silica content showed to be not riskier than in other commercial bamboo species. For example, the silica content did not exceed 1.5 % and, except for nodes, a notably lower content was found. Growth location, altitude section, age or morphology did not reveal differences and

a simple raw material washing step even reduced the anyway low risk. In contrast to other tropical species Ethiopian highland bamboo had proved to be very well suited for industrial processing.

4 | Process engineering

Essential part of the technical feasibility study of this project was to screen existing panel production processes for parameters, adjust them for the highland bamboo scrimber and investigate challenges for transformation to an industrial scale. Since own previous experience with bamboo-based scrimber was unavailable, first approximations (pressing temperatures, specific pressure, panel thickness) are made. After conducting those rudimentary production trials, this chapter divides in three main stages shown in figure 52. At first, production parameters are screened on laboratory scale. The panel composition is defined for resin and wax as well as heat treatment temperature and duration are determined. Secondly, a confinement phase in which bamboo raw material influences and questions related to resin distribution are researched. The culm height dependent raw material is investigated for influences on the panel. Problems from the parameter screening are further analyzed for resin related factors since resin is expected one of the key challenges when it comes to production costs and environmental impact. The third part of this chapter, the industrial upscaling, deals with the equipment which would be used during implementation of an operational production in Ethiopia. Due to the applied research character this part uses quasi-industrial equipment. Specifically the heat treatment, resin application and hot press steps are expected to differ notably from laboratory scale.

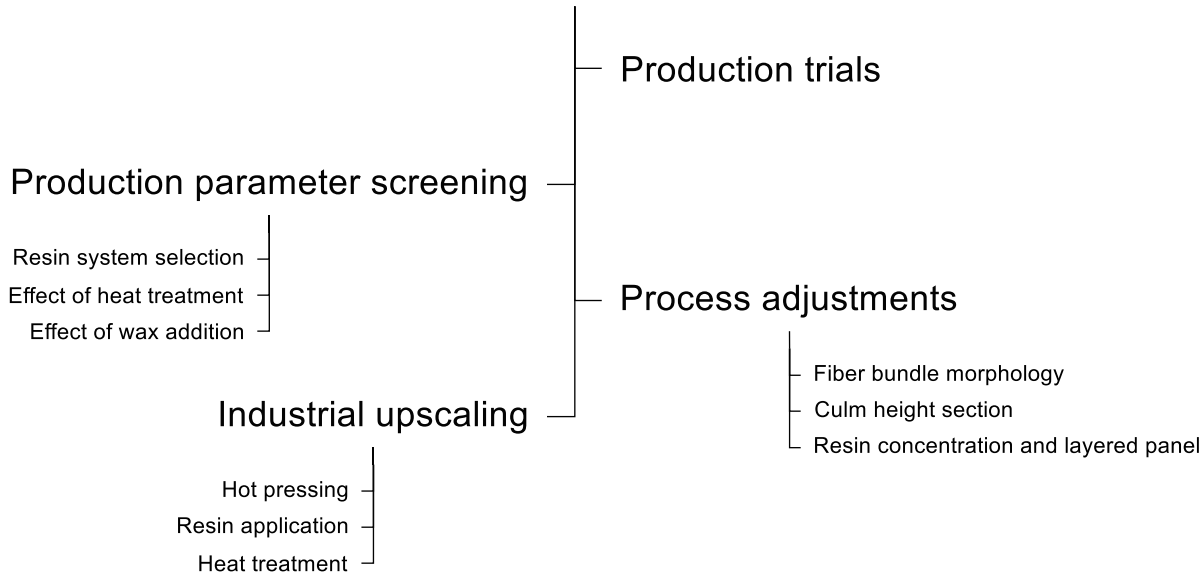

Figure 52: Structure of the process engineering research

4.1 Introduction

The experiences gained with Ethiopian bamboo for WBP productions, previously described in chapter 2.2, did not suffice to provide clues for a scrimber production. Thus, a novel process workflow was worked out for African highland bamboo scrimber as shown in figure 53. The shown process starts at the supply and ends with the semi-finished raw scrimber panel. First, the bamboo culms are delivered to decentral collection centers or left at the roadside after harvest. The logistical advantages of decentral pre-processing prior to factory transport was shown earlier. According to Schmidt (2013) the maximum distance for culm transportation should not exceed 280 km. Once arrived at the factory yard, the first step is to cut the culm into industrial segments of 2.60 m length each. The culm segments are then split into 4 to 6 strips which are checked for damages and deformations. The crushing station shown in figure 23 produces scrim strands from the strips which after inspection are loaded into a combined kiln-dry (KD) and hot-dry air treatment (HDAT) chamber. The HDAT used in the present process is similar to what Li *et al.* (2012a) introduced. In common productions the dry scrim strands are then impregnated with resin by dipping them into tanks, dripping them off and technically dry them afterwards. The present work instead applies the resin solution by spraying. This way, the resin-applied scrims can be laid up in a mat to the multi-daylight press immediately without an additional drying step. A batch hot-press similar to the one described by Yu *et al.* (2015b) consolidates the mats which are removed still hot (< 100 °C) for continuous stack curing. Before inspection, the conditioned panels get formatted prior to machining and sanding.

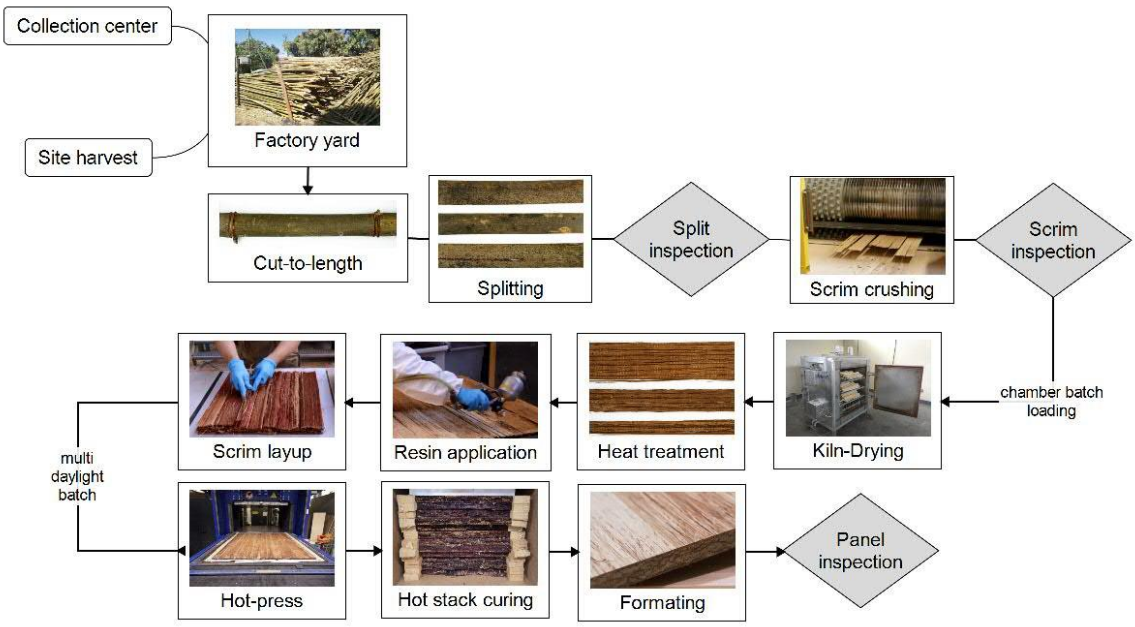

Figure 53: Workflow scheme for the African highland bamboo scrimber process development

4.1.1 Production parameter screening

Working with a new bamboo species and production scheme needs a new set of production variables especially for the secondary processing (see table 11). These variables comprise

press parameters (T, t, $t_{cooling}$), panel composition (resin type, additives, concentrations) and heat treatment parameters (T, t). Since complete heat curing of the PF polymer requires a panel core temperature of 110 °C, the press plate target temperature influences the whole process. A turnoff temperature needs to be found, which overcomes the thermal lethargy of the press and initiates the resin curing. Then press parameters need to be screened within a typical range for high-density wood-based panels. Furthermore, the type of resin has a large impact on the press program and must, if necessary, be adapted to the individual type subsequently selected in each case in order to achieve satisfying bond within an economically acceptable pressing time. In the presented case a panel of 22 mm thickness will be targeted and thus a batch time of less than one hour should be complied with to stay within economic limits.

4.1.2 Process engineering

With the results of the screening, the composition and the potential set of production parameters must be reduced to economize irrelevant tests in the following investigations. Table 11 presents the expected degree of impact of process control variables on the intermediate and final product. For the process engineering chapter, the secondary processing steps have been considered. Culm harvest, air-drying and splitting influence the process (e.g. different MC and particle geometry) but are, however, unlikely to be controlled in the rural context of forest industries in Ethiopia. The most important ones are expected to be the raw material density, bamboo fiber bundle quality and resin concentration and distribution. Typically, bamboo scrimber is produced from a relatively uniform raw material. In Asian factories, the culm middle section usually offers a relatively constant culm wall thickness and hence, more uniform radial and axial density gradients. The raw material investigations in this work showed that the two upper thirds of the highland bamboo culm are of better suitability. However, for reasons of yield and raw material costs, the culms will have to be used entirely. This implies gradients in density, moisture content and morphology along the axial and radial direction of the bamboo culm as shown in the prior chapter.

4.1.3 Industrial upscaling

The results from the screening and engineering parts cannot fully reflect the challenges happening at later industrial implementation level. Heat treatment, resin application and hot press differ notably between laboratory scale and industrial scale. Especially, chamber size and heating rates (K/min) of the heat treatment may affect the process and product quality. For wooden scrimber, Joscak *et al.* (2006) observed that MC before glue application may range from 3 to 15 % which in some cases can only be achieved by technical convective drying. In current bamboo scrimber factories the resin applies through dipping into tanks filled with an aqueous resin solution. This causes the problem of high MC of the press-ready fiber. The countermeasure, technical drying of impregnated scrim strands can cause pre-polymerization of resole PF resins and requires additional energy. The spray application in the screening seems rational, however, at industrial scale is not without problems. The resin-containing spray obviously cannot thoroughly hit the fiber mat and may spread uncontrollably in the factory environment. That makes cleaning intervals necessary and may waste resin. An alternative at industrial scale would be curtaining as it is known from plywood and glulam producers. A

recovery system may save excess glue. Feasibility trials at an industrial scale will have to be conducted. Once the resin applied mat enters the hot-press, high pressure and heat vaporize most of the remaining moisture. The vapor pressure in the panel is extremely high and might lead to local steam explosions (“blow-outs”). In an OSB plant the moist strands are dried down to 3 % MC for the core layer and 8 % for the deck layers (Ansell 2015, Paulitsch and Barbu 2015). The tertiary process steps will not be part of the investigations.

Table 11: Process control variables and estimated process impact on the final product quality and/or the following process step intermediate product (+ low impact, ++ medium impact, +++ strong impact)

Process step		Control variable	Estimated impact degree on product and/or intermediate good
Primary processing	Culm harvest	Green MC	+ weight, mold
		Maturity, age	++ mechanical properties
		Height portions	++ fiber bundle mat quality
	Air-Drying	MC_{in}	+ drying time
		MC_{out}	++ crushing quality
	Splitting	Outer diameter	+ width of split
		Number of knives	+ width of split
Secondary processing	Crushing	MC_{in}	+ amount of dust and splinters
		Number of passes	+++ slenderness of scrim
	Kiln drying & Heat treatment	MC_{in}	+ energy uptake, thermal conductivity
		MC_{out}	+++ MC before press
		T	+++ Degree of modification
		RH	+ Steam pressure/Oxygen level
		t	+ Degree of modification
		Heating rate	+ time → energy costs
	Glue formulation & application	Solid content	+ viscosity
		Line speed	++ Spread rate
		Viscosity	+++ Degree of distribution
	Mat formation	Layer structure	+++ Physical, surface and mechanical properties
	Hot-pressing	MC_{in}	+++ vapor pressure → blow outs
		T	+++ Curing of the resin
		Closing speed	+ Process energy, batch time
		p	+++ High pressure → high densification
		t	+++ vapor pressure → blow outs
		Panel thickness	+++ Pressing time, cooling time
Tertiary processing	Curing	t	++ Bonding quality
		T	++ Bonding quality
	Conditioning	t	+ Dimensional stability
		RH	+ Dimensional stability
	Machining & Profiling	Feeding speed	++ Surface quality
		Sharp tools	+++ Surface quality
	Finishing	Spread rate	+++ UV resistance

4.2 Specific objectives

The following questions were addressed:

- **Screening of production parameters**
  - Which production parameters, namely press parameters, resin selection, additives, heat treatment temperature and duration lead to acceptable results?
  - Which parameters can be neglected for later development stages?
- **Process engineering**
  - Where are the technological weak points of the production?
  - Can glue distribution help overcome a heterogeneous property profile?
  - To what extent do the bamboo raw material properties influence the process and the product properties?
- **Industrial upscaling**
  - Which production steps differ between industrial scale and laboratory scale?

4.3 Material and methods

In this material and methods section, the whole experimental design of all sub-topics in this chapter are given. Furthermore, the origin of raw materials and processing and production methods are explained in detail. The standard test procedures were defined in the last sub-chapter.

4.3.1 Experimental design and statistical analysis

The only empirical experiences with this new type of composite panel are superficial impressions from Asian factories and theoretical information from old patents. This lack of practical knowledge on the pre-treatment, resin and pressing procedures led to the pragmatic decision to not exclude specific factors or levels. Hence, a full factorial experiment design including four variables (T, t, resin, wax) was chosen. The pre-treatment with heat combined four discrete treatment temperature levels (160; 180; 200; 220 °C) and two duration levels (3; 5 h). Furthermore, four different resin systems (PF1-4) as well as a hydrophobization agent (no wax or 2 %) was put into the experimental matrix. One exception is the treatment at 220 °C which was done only for 3 h duration. The fully crossed design was intended to show the single effect of each factor on the tested variables (internal bond, thickness swelling, bending MOR, MOE) as well as the interaction effects between the factors. The used standards for testing and sampling can be found in the table in 4.3.9. The screening a total of 60 panels was produced. For the findings of press parameters additional eight panels were produced. The raw material grading experiments produced 18 panels. The vertical resin distribution experiments resulted in another 25 panels in lab-scale. For the industrial upscaling, six laboratory-scale panels have been compared with six industrial-scale panels per treatment and another two panels were produced in an external industry to verify the results. The detailed production recipe for the screening BS panels and the resin gradient panels can be found in appended table 44 and table 45.

All results were first tested for outliers either in a Grubb's test ($n > 10$) or in a Nalimov test ($n \leq 10$). Subsequently, descriptive statistics were produced (median, mean, SD, min, max) and data was checked for normal distribution and equal variance of means. Where box plots were used, the box stands for the 25/75 % quantile, mean as "x", median as horizontal line, the whiskers are the 1.5 x SD interval and outliers are marked as circles. The figure below summarizes the meanings of box plot symbols.

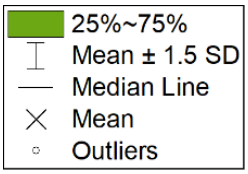

Figure 54: Meaning of symbols in box plots throughout the study

The significance of mean differences was then either checked using (2-w)-Anova, Kruskal-Wallis-Anova (KW-Anova) or a χ^2-test ($\alpha = 0.05$) for categorical factors. Dunn's post-hoc test identified the mean differences. Screening results have been checked for plausibility

and median values were calculated. No further statistical analysis was applied. All graphs, diagrams and analyses were produced using OriginPro 9.1 (OriginLab Corporation, USA).

Table 12: Full factorial experimental matrix for the screening of production parameters

Heat treatment							Resin parameter				Wax	
T [°C]				t [h]		Appl.	Type				c [%]	
160	180	200	220	3	5		PF1	PF2	PF3	PF4	0	2
						Spray	X				X	X
								X			X	X
X				X					X		X	X
						Powder				X	X	X
						Spray	X				X	X
								X			X	X
X					X				X		X	X
						Powder				X	X	X
						Spray	X				X	X
								X			X	X
	X			X					X		X	X
						Powder				X	X	X
						Spray	X				X	X
								X			X	X
	X				X				X		X	X
						Powder				X	X	X
						Spray	X				X	X
								X			X	X
		X		X					X		X	X
						Powder				X	X	X
						Spray	X				X	X
								X			X	X
		X			X				X		X	X
						Powder				X	X	X
						S	X				X	
								X			X	
			X	X					X		X	
						P				X	X	
						Spray	X				X	X
								X			X	X
			Untreated						X		X	X
						Powder				X	X	X

4.3.2 Scrim strand production

The bamboo for the process engineering was harvested to equal portions at the same two locations as in the prior chapter. The scrim strands were produced from split *Y. alpina* by passing the slats through a crusher machine once. The very first trials were done using scrim strands produced on the WKI crushing device (Berthold 2013). All further tests were done on an industrial scrim crusher. The crusher aggregate ZCZK190 (Anji Yukang and Luan Wobam Machinery, China) pulls the bamboo strips through eight stations with a pair of rollers each (see figure 23). These rollers are driven by propeller shafts (Cardan joints) which transmit the power from a heavy-duty chain. The inner and outer wax containing layer is removed. Differently profiled rollers crush down the scrim strands either by squeezing or defibering. The lateral and frontal section view into one roller pair (1 and 2) is shown in figure 23. By adjusting the bolts (6) onto the springs (5), one controls the crushing pressure and the thickness of the strand. The machine can process one strand at the same time at a maximum feed rate of 40 m/min (Xiao 2013). The crusher is designed for the Asian bamboo-processing industry, i.e. the raw material parameters (width of slat, wall thickness, taper) of typical commercial species used in China are the reference for the design and configuration of such a machine. The major species used, i.a. *Phyllostachys pubescens*, have larger culm diameters and yield bamboo slats with higher wall thicknesses on the one hand, and less curvature on the other hand. Hence, the adaption of the machine configuration to Ethiopian highland bamboo was an iterative process recorded in the appendix.

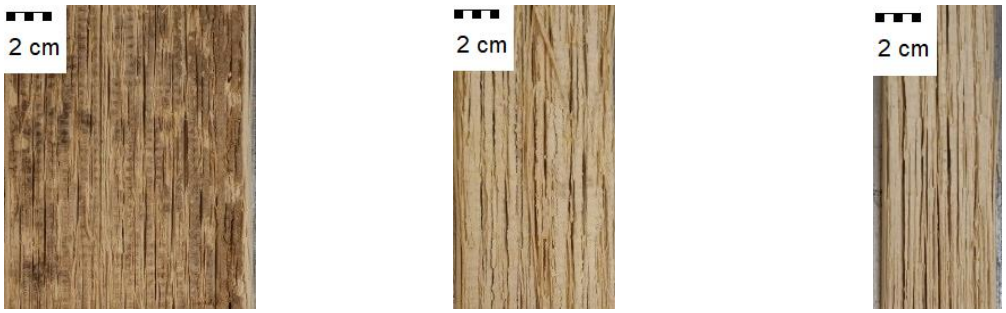

Figure 55: Broad, medium and narrow (f.l.t.r.) width classes of scrim strands used during the screening of production parameters

The width of the slats depends on the one hand on the number of splitter knives and on the other hand the culm diameter. Hence the process yields different width classes with different thick fiber strands. For the screening experiments, the strands were classified in three width classes, broad, medium and narrow. It is not clear whether the different widths of the strands correlated with their original vertical position in the culm. Although, bamboo species, growth location and height section may affect the process, those parameters were neglected in the screening investigation.

A series of culms was separated along the height into three height sections. The sections were named top (T), middle (M) and bottom (B) and measured 2.70 m each. Another set of samples from the top section was taken through the crusher aggregate four times instead of only one. Those strands consist of finer distributed fiber bundles and were suspected to show a better compression behavior. They were named fine (F). The scrims were air dried and showed a mean MC of 8 %. They were then treated with heat or kiln dried. The scrims for the height grading have not been heat treated prior to hot-pressing.

4.3.3 Heat treatment

Depending on the research question, two different treatment chambers were operated. Chamber volume and heating rate did notably differ, however treatment temperatures and durations did not.

For the laboratory scale boards scrims were treated in a chamber with dry steam and ambient pressure (Liyang Forwood Drying Equipment Co. Ltd, Liyang, PRC). The inner dimensions of 600 x 640 x 750 mm limited the batch size to 15 kg material per batch. The chamber coils operated with electricity (15 kW) which guaranteed high heating rates and a short heating cycle. Hence, one process took only two hours plus treatment time. The chamber was heated up to target temperature with a heating rate of 4 K/min. The temperature was measured via a chamber internal thermoelement. The total treatment time varied according to the target temperature level. The total time calculates through:

$$t_{total} = t_{treatment} + t_{heating} + t_{cooling} \qquad [N/mm^2] \qquad (4\text{-}1)$$

The treatment temperature (chamber) and the actual treatment time $t_{treatment}$ was varied. The experimental variants are summarized as per below. Variant V0 served as control for V1.

V0: untreated bamboo, KD only

V1: Treated at T=160; 180; 200; 220 °C for t=3; 5 h

Figure 56: The lab-scale kiln chamber (left) and treated strands after 3 h / 160 °C (right)

The scrims used in the industrial scale batch were treated in container-size treatment chambers in Cartigliano, Italy. Therefore, scrims were prepared in Ethiopia and then shipped overland via Addis Ababa through Djibouti and then on seaway to the destination port in Venice, Italy. The shipped samples have been sealed and controlled before and after every transport station. The treatment chambers are normally used for kiln drying and thermal modification of solid wood (BigonDry SRL, Italy). The industrial-scale chambers used high temperature heat exchangers and are fed with thermal oil. The chambers had a thermal capacity of 800 kW and a gross volume of about 30 m³. Due to the volume of those chambers, the heating rate was lower than the lab-scale (1 m³). To be able to guarantee a holding time of 3 h at 160 °C or above, the whole batch process took several days. The temperature probes used in the stacks as well as the probe measuring chamber air temperature were observed continuously during the entire process through a company-own virtual remote desktop system-

A psychrometer, i.e. a dry and a wet temperature bulb, measures the relative humidity. This measurement only works reliably in temperature ranges below evaporation. Controllable variables in this context are the oxygen content, which depends directly on the vapor pressure

in the chamber. Oxygen concentration was kept below 2.5 % and a water spray nozzle was used to correct when necessary. A fan forces the heated air through the stacks where the airstream loses heat and velocity before it enters the heating coils again. Each hour the direction of the airstream changes to guarantee a homogenous vapor and heat distribution through the scrimber strand stacks.

4.3.4 Resin systems

The four phenolic resin systems shown below were screened. Two of them, the BD 984 and BD 837, are used in OSB production. They were applied directly in powder form since no additional moisture must enter the system. The Prefere 4976 was used together with a hardener, Prefere 5909 as recommended in the product datasheet (Dynea 2004). Additionally, the liquid PF system EXP 3G was used in the screening. This resin system was widely used by Asian bamboo scrimber manufacturers. The typical application form is liquid impregnation by dipping scrimber strand bundles into a tank containing a very low viscosity resin solution (Dynea 2010).

However, the production parameter screening at laboratory scale was done by spray-applying the resin solution with an atomizing spraying gun and compressed air as shown in figure 57. Resin concentration (dry bamboo:resin) was controlled at 10 % and steered by solving in deionized water. All resins were provided by Dynea AS (Lillestrøm, Norway) and former Prefere Resins Holding GmbH (Erkner, Germany). The panels with spray-applied phenol resin were defined as V2, whereas the powder-applied variation was called V3.

V2: Spray-applied PF1 (Exp. 3G) and PF2 (Prefere 4976)

V3: Powder-applied PF3 (BD 984) and PF4 (BD 837)

4.3.5 Wax addition

As an additive during the screening as well as in later stages, a hydrophobization agent was used in the panels. The used HydroWax ProA18 (Sasol Wax GmbH, Hamburg, Germany) is a white, homogeneous aqueous dispersion of micro-fine particles and was introduced as an emulsion into the aqueous solution of the resin paste. The synthetic wax is a relatively high-dosed blend with a pH-value around 9.3 and a bulk density of 0.95 g/cm³. It contains ca. 50 % water and shows a Brookfield viscosity of 480 mPas at ambient conditions. It is typically used in MDF or HDF productions. Concentrations in the wood-based panel industry commonly range from 0.5 to 3.0 %, depending the later application (Sasol 07/2013). Thus, for this work a concentration of 2 % was chosen. The results on wax treated panels were defined as V4.

V4: Additive; HydroWax Pro A18

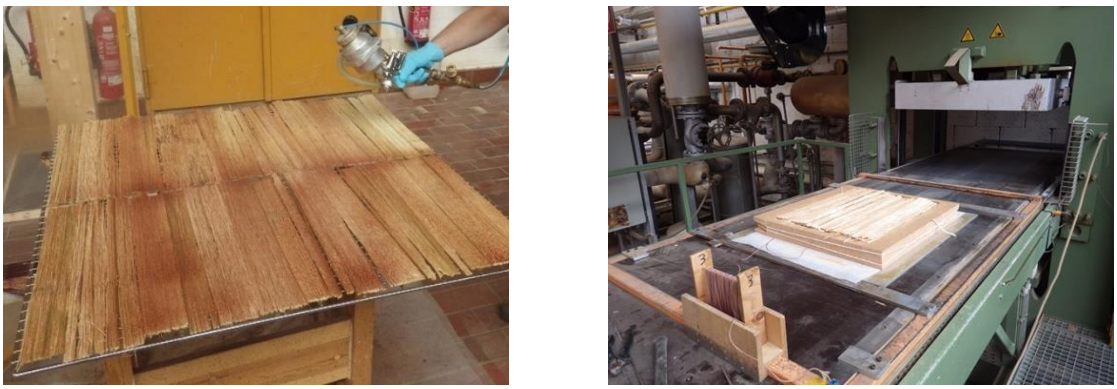

Figure 57: Resin spray application on lab-scale scrims (left) and the press-ready mat with a temperature probe in the core layer (right) at Fraunhofer WKI laboratory

4.3.6 Mat formation

The crushing processed yielded strands with different dimensions. The strand width depended on the number of knives in the splitting machine and the diameter of the culm section. Broad strands in the face layers should seal a homogenous face layer. Each subsequent layer was offset to one another. The scrim strands were arranged in a brick manner (also see figure 58). Smaller gaps were filled with narrow strands. We avoided overlapping layers to prevent density peaks across the panel. No attention was paid to the height section of the scrim strands in the screening part. In the lab-scale, the layers were arranged to yield panel dimensions of 500 x 500 x 22 mm. Additionally, to the lab-scale panels, two types of industrial-scale panels were produced. One set coming from the same facilities, but hot-pressed on a larger format and without active cooling.

Figure 58: Mat formation with narrow scrims in the core, medium strands in the center and broad strands in the face layer (left) using a softboard template (right)

4.3.7 Press parameters

The panels for all lab-scale boards were produced in the facilities of Fraunhofer WKI (Braunschweig, Germany) and the Thünen Institute (Hamburg, Germany). The panels produced for the screening and the vertical glue distribution analysis were produced at Fraunhofer WKI and Thünen Institute on a laboratory scale Siempelkamp hot-press (Krefeld, Germany) with active cooling. All lab-scale panels targeted a dimension of 500 x 500 x 22 mm whereas the industrial-scale panels were produced externally on a large-scale industrial hot-press measuring 4 x 8 feet which translates to the metric dimensions of 1.2 x 2.4 m. Target thickness was set constant at 22 mm. The configuration of the three main phases, compression

(1), heating (2) and cooling (3), is shown in table 13. The press was configured isochor to the target thickness but without distance templates. The untreated scrim strands were kiln-dried and showed an average MC of 3 % before resin application. The treated scrims came from the same batch as in the prior experiments and belong to the 180 °C / 3 h group. Their MC was slightly lower (2.6 %), measured in an off-hands sample. The resin increased the MC before pressing. The resin used in this part was the PF2 system. The supplier recommends MCs of 3 to 8 %.

Table 13: Hot-press phases configuration at laboratory scale

Phase	Press plates	Parameter	End condition
1	Close	-	Until mat contact
	Compress fast	1.0 mm/s	Pre-compression
	Compress slow	0.4 mm/s	Compression/Heating-up
2	Maintain	> 110 °C	Heating-up to PF curing
3	Maintain	< 100 °C	Cooling-down below evaporation point
	Open	0.02 mm/s	Ventilation for at least 60 s
	Maintain	0.5 mm above target thickness	
	Open	0.10 mm/s	Open
	Open press	-	Discharge panel

The core temperature of the panel needed to pass 110 °C to reach the activation energy of the phenolic resin. The thermal lethargy of the system led to a holding time above 5 min (2) before entering the active cooling phase (3). Right after leaving the hot-press, the still hot panels were put into a warm veneer press at 80 °C for 20 min and subsequently stacked in conditioning cabinet overnight. Afterwards, the panels were sanded and cut into specimens with a circular saw according to the regarding standard. The phase values in table 13 are of parametric nature and might have altered slightly in absolute values.

Figure 59: Press-ready fiber bundle mat with a temperature probe in the core layer (left) and conditioning in a warm veneer press forming a hot stack for curing (right)

To find an optimum configuration for further lab-scale experiments, three “turn-off” temperatures were tested. They were tested using thermally treated as well as untreated

scrims and two distinct resin concentration levels. This fully crossed design intended to reveal the effect of the temperature adjustment on the tested variables (IB, TS, MOR, MOE). It was not intended to find interaction effects between the parameters.

Table 14: Full factorial experimental matrix for the screening of press temperature

Pre-Treatment	Resin parameter				Press turn-off temperature		
	Appl.	Type	c [%]		T [°C]		
			8	10	120	130	140
untreated	Spray	PF2	X		X	X	
				X	X	X	X
							X
heat treated			X		X	X	
				X	X	X	X
							X

4.3.8 Industrial upscaling

During the project implementation phase industrial experiments were conducted for heat treatment, resin application and hot-pressing. The equipment used was analyzed in terms of practical questions. Only basic tests on IB were conducted to confirm the laboratory results.

- HEAT TREATMENT

The air-dry bamboo scrims were first pre-dried in the very same kiln at relatively low temperatures (75 °C), And then a high temperature phase modified the scrims during a holding phase of 3 to 5 h. The combination of both steps delivered “press-ready” scrim strands. Kiln-drying and thermal modification happened in one chamber, hence in one single batch. Two protocols of treatment cycles at 160 and 180 °C were appended in figure 103. The manner of packing the strands into stacks was crucial. For this purpose, spacing and layer thickness were investigated and presented. The stacking and loading process of the chambers is one of the production bottlenecks. The stacks dimension is 300 x 120 x 90 cm each. One single chamber module took 2 by 2 stacks. The spacing between the stack layers (LY) was set either 20 or 30 mm, defined by the aluminum spacer between the layers shown in figure 74. The stack layers were either 20, 40 or 100 mm thick. This way it was ensured that the overall stack loading resulted in comparable total mass balances.

$$t_{total}(160°C) = 1d\ 10h\ 9'59'' \cong 34.17\ h \qquad \text{and}$$

$$t_{total}(180°C) = 2d\ 5h\ 17'10'' \cong 53.29\ h$$

- RESIN SYSTEMS

For the industrial application, the PF2 resin system (Prefere 4976) was applied to untreated bamboo scrim strands at Raute Oyi technical laboraties (Nastola, Finland). The resin mixture

recipe was the same as in the screening. However, the application methods and equipment differed from the laboratory technique. Two continuous systems were used: The circular jet gun spraying (CJG) and curtaining, also called liquid extrusion gluing (LEG). The latter is an inhouse patent also used in the plywood industry. Figure 60 shows a LEG and CJG station in action. The viscosity of the resin solution was kept constant and did not differ from the before productions.

Figure 60: Resin application by liquid extrusion gluing pushing the glue paste through several fine nozzles composing a pseudo-curtain (left) and the bottom side of the circular jet gun station atomizing the resin solution with pressurized air (right)

4.3.9 Test procedures

The screening based on the fast testing of a wide range of variants. For overall physical and mechanical performance, common tests on thickness swelling (TS), water adsorption (WA), flexural strength (MOR) and modulus of elasticity (MOE) were conducted. Internal bond (IB) was tested to yield first results on the process (pressure, heat, treatment) parameters. We applied a series of working standards for repetitive procedures throughout the whole thesis, e.g. determination of panel and specimen density, moisture content, sampling, cutting and inspection. The implemented standards for sampling and measurement are compiled in table 15. The sampling and cutting of specimens happened according to the regarding standard.

Table 15: Test and measurement standards as well as total plan number of specimens during the screening phase

Tested property	n_{panels}	$n_{specimens}$	**Standard method**
Thickness swelling Water adsorption	60	480	DIN EN 317:1993-08
Internal bond		480	DIN EN 319:1993-08
Moisture resistance		480	DIN EN 1087-1:1995-04
Flexural MOR Flexural MOE		240	DIN EN 310:1993-08
Density		480	DIN EN 323:1993-08
Moisture content		240	DIN EN 322:1993-08
Sampling and cutting (total)		1200	DIN EN 326-1:1994-08

4.4 Results and discussion

The results are presented in five sub-chapters. First, two tentative pre-experiments on hot press temperature and resin application were conducted. This first set of BS panels was therefore produced by tank dipping, using two panel thicknesses, resin concentrations and three press temperatures. The then following chapter iteratively screened a set of parameters to produce highland bamboo scrimber on laboratory scale. It dealt with press temperature, resin, additive and heat treatment and provided a full-factorial experimental outcome.

Based on the lessons learned from the screening the next sub-chapter then investigated the influence of the fiber bundle processing and origin. Hereafter, the fourth sub-chapter looked at the effects of altered resin concentration and distribution. In the last part, a technical outlook to the industrial level was given. Technical challenges with industrial scale equipment for heat treatment, resin application and hot pressing were identified and discussed.

For each production parameter variable (V0, V1, V2, V3) one single panel was produced. For the thickness swelling as well as water adsorption tests eight specimens were tested per panel, resulting in total 480 specimens for the screening. The press temperature (turn-off) experiment was designed in a similar way and thus resulted in 12 panels and 96 specimens. The resin application trial was conducted on four panels. The below table summarizes the mean MC and density of the panels.

Table 16: Mean and standard deviation (in brackets) of moisture content (MC) and density for all specimens tested coming from panels for the production parameter and press temperature investigation

	n_{panels}	MC [%]	ρ [g/cm³]
Resin application trial	4	n/a	n/a
Press production trial	12	11.3 (0.5)	1.01 (0.07)
Production parameters	60	10.9 (0.4)	1.04 (0.04)

4.4.1 Tentative production

Two tentative experiments mimicked existing techniques known from Asian producers but using African highland bamboo: unmodified scrim strands were prepared with the in-house crusher at Fraunhofer WKI.

4.4.1.1 Resin application trial

The preliminary results on thickness swelling (TS), water absorption (WA), bending strength (MOR) and elasticity (MOE) as well as internal bond (IB) are found in table 17. Not surprising, a very high resin concentration (20 %) led to notably low WA (2 %), TS (13 %) and high IB (1.8 N/mm²). Although MOR reached more than 120 N/mm², MOE was the lowest for the high resin concentration. This corresponds with results from Yu *et al.* (2017) who found increasing bending MOR with increasing resin concentrations but no correlation with MOE. The thicker panels (40 mm) showed nearly no IB and an excessive WA which led to the conclusion that heat conduction was not achieved sufficiently, thus resin did not completely react.

Table 17: Mean thickness swelling (TS), water absorption (WA), internal bond (IB), bending strength (MOR) and modulus of elasticity (MOE) for scrimber panels hot pressed with three target temperatures (120, 130, 140 °C) using two resin concentrations by tank dipping untreated bamboo scrim strands

c_{resin} [%]	Panel thickness [mm]	TS [%]	WA [%]	MOR [N/mm²]	MOE [kN/mm²]	IB [N/mm²]
15	20 mm	7	28	74.7	16.8	0.7
20	20 mm	2	13	121.7	14.9	1.8
15	40 mm	4	33	26.1	62.0	0.2
20	40 mm	8	42	27.1	56.9	0.1

The air-drying of scrim strands after tank dipping resin application takes time, occupies space and labor[13]. Chinese producers use kilns for drying the resin-wet scrim strands. For future research, resin concentrations must be decreased and panel thickness shall not be far in excess of 20 mm when using conductive hot pressing. An alternative application form, such as spraying, must be used to avoid excessive process moisture.

4.4.1.2 Press production trial

Another simple experiment was made at the beginning to determine the turn-off temperature for the laboratory scale hot-press. During the heating phase, water vaporizes, and pressure increased. The maximum system pressure was 250 bar, or 25 N/mm². Considering the panel dimensions press cylinder diameter, the system pressure corresponded to a specific pressure of 15 N/mm² in the hot press. This relatively high pressure was reached solely during the compression phase. The same applies for the results shown in 4.4.3. The target temperature in the core layer must reach 110 °C and stay above this level for approximately one minute to accomplish the minimum activation energy of the polycondensation reaction of the free phenol and formaldehyde and subsequently cross-linking it with the prepolymer. Three turn-off temperatures were tested and screened for their suitability at laboratory scale hot-pressing.

Table 18: Mean and standard deviation (in brackets) of moisture content (MC) and density (ρ) for panels produced with three hot-press target temperatures

T_{target} [°C]	n_{panels}	MC [%]	ρ [g/cm³]
120		13.4 (0.5)	0.94 (0.07)
130	4	12.0 (0.3)	0.92 (0.04)
140		10.7 (0.3)	0.89 (0.04)

Table 19 shows the screening results for different press temperatures. The highest IB was found in heat-treated scrims and 130 °C, being 0.93 and 0.83 N/mm² for 10 and 8 % resin, respectively. These values were double as high compared to the other turn-off temperatures in their respective group. In the control group, the 130 °C reached the highest values with

[13] Phenolic resin powder (PF2) was dissolved in deionized water and the scrims were dipped into resin tanks. The viscosity was steered by changing the resin solid content. The 20 and 40 mm thick panels contained 15 and 20 % resin and targeted a density of 1 g/cm³. The phenolic resin was applied by immersing the scrim strands in a dip tank for half a minute. The impregnated scrim strands were air-dried and a mat was formed. The mat entered a laboratory scale hot press and pressing temperature was set 180 °C with a pressing time of 30 s/mm panel thickness.

0.51 and 0.59 N/mm² for the two resin concentrations. The lowest mean IB around 0.25 N/mm² was produced with 8 % resin concentration and 120 °C for both, heat treated and control strands. The water adsorption values of the untreated panels produced with 120 °C ranged between 31.3 and 41.1 %. For the treated variant, these values went down to 31.6 and 20.7 % for the two resin concentrations, respectively. The WA and TS for 130 and 140 °C produced from untreated scrims and 10 % resin showed nearly equal values.

Table 19: Mean thickness swelling (TS), water absorption (WA), internal bond (IB), bending strength (MOR) and modulus of elasticity (MOE) for scrimber panels hot-pressed with three target temperatures using two resin concentrations, untreated (Ctrl.) and heat treated (HT) scrims

	c_{resin} [%]	T_{target} [°C]	TS [%]		WA [%]		IB [N/mm²]	MOR [N/mm²]	MOE [kN/mm²]
			2 h	24 h	2 h	24 h			
Ctrl.	8	**120**	19.2	30.6	23.9	41.1	0.26	92.6	22.1
		130	4.7	**10.5**	8.9	**21.8**	**0.51**	**108.3**	23.5
		140	9.1	17.3	15.4	30.1	0.24	106.1	23.5
	10	**120**	10.9	19.2	16.1	31.3	0.36	122.2	21.9
		130	3.9	10.1	8.9	21.6	0.59	155.3	22.8
		140	4.1	9.7	9.1	20.8	0.49	113.8	22.9
HT	8	**120**	7.6	13.2	18.5	31.6	0.26	75.4	19.5
		130	1.8	**5.6**	6.5	**18.5**	**0.93**	**142.9**	20.9
		140	3.8	9.9	10.1	23.7	0.52	124.0	22.2
	10	**120**	3.3	9.2	8.0	20.7	0.51	97.4	22.0
		130	2.3	**5.9**	5.9	**16.9**	**0.83**	**140.6**	20.7
		140	3.3	8.6	9.8	22.6	0.47	112.8	21.1

The results for 120 °C press temperature have led to higher TS and WA, lower IB and worse flexural properties than the 130 °C sample. The 140 °C sample showed higher TS and WA than the 130 °C sample, but lower than the bamboo scrimber pressed with 120 °C. It is possible that the slighter heat gradient between press platen and fiber bundle mat slowed down the conductive heat transfer and hence lowered the quantitative activation energy available for the polycondensation of the phenolic oligomers. The observed effect was stronger in the control sample. More water available might have led to more impregnation of the scrim strands than in untreated ones. The resin might have had enough time to diffuse into the dry scrims. Due to the lowered hygroscopic potential of the thermally treated strands, the effect is not visible as distinct as it is in untreated ones. Nevertheless, the turn-off temperature is a very equipment-specific figure and cannot be transferred to other systems. The combination of the specific thermal lethargy of the press system, reaction kinetics (activation energy) of the used resin and the thermal conductivity of raw materials may have influenced the results. Summarizing, the results indicated that the turn-off temperature set at 130 °C produced bamboo scrimber panels with better properties than 120 and 140 °C. The turn-off temperature was consequently used for all following experiments.

4.4.2 Production parameter screening

The entire mean results of the screening can be found in appended table 46. This table summarized the mean values of all panels produced for the screening. In the below sub-chapters, results were analyzed iteratively with the aim to identify promising parameters.

4.4.2.1 Resin system selection

Two spray (V2) and two powder (V3) applied phenolic resins were investigated. Firstly, the thermally untreated group (V0) without wax was analyzed for mean differences. The mean IB was found with 0.7, 0.9, 0.4 and 0.7 N/mm² for PF1, 2, 3 and 4, respectively. The PF4 resulted in the significantly lowest IB, whilst the high value seen in PF2 did statistically not differ from PF1 and PF3. However, the PF2 system was found to produce the highest MOR with 195.5 N/mm² and MOE with 26.49 kN/mm². On the other hand, the mean TS were lowest for PF1 with 1.8 %. In short, the untreated group showed a better performance of the spray-applied PF1 and PF2 whilst PF4 might be of less interest. However, the results did not provide statistical explanatory power which legitimates a sound choice of resin.

Secondly, the heat-treated groups (V1) were analyzed. The entire mean results for each group are shown in appended table 46. In contrast to the priorly shown results on V0, here, the PF2 showed the lowest mean TS of 4.3 and 3.2 % in the lowest temperature group V1(160 °C; 3, 5 h). The same analysis was done in the 180, 200 and 220 °C group but showed controversial results. Significance between means was found inconsistently during post-hoc analysis, i.e. the remaining heat treatments impeded further understanding of the phenolic resin system's impact on BS properties. Since there was no possibility to repeat empirical parts and increase the sample size, it seemed reasonable to continue with cluster analyses instead. A cluster analysis basically describes a grouping of sample treatments in such a way that samples in the cluster are more similar to each other than to those in other clusters. Hence, the V2 and V3 groups were clustered incorporating all heat-treated samples (V1) analyzing all treatment duration and temperature levels as one. The full descriptive statistics for IB, TS and WA are shown in table 20.

Table 20: Descriptive statistics of the effect of four different phenolic systems (PF1-4) on thickness swelling (TS), water absorption (WA) and internal bond (IB) of scrimber panels produced from all heat treated V1(T; t) bamboo scrims grouped in one cluster with means in the same column sharing same letters are not significantly different at $p \leq 0.05$

		Mean	SD	Minimum	Median	Maximum
TS [%]	**PF1**	4.0^{A}	2.0	0.9	3.7	8.7
	PF2	3.7^{AB}	1.8	1.1	3.2	8.0
	PF3	5.5^{C}	2.6	1.4	4.9	11.4
	PF4	3.2^{B}	1.0	1.3	3.1	5.2
WA [%]	**PF1**	14.1^{A}	4.5	5.6	13.8	24.2
	PF2	13.4^{A}	3.9	7.2	12.0	22.3
	PF3	16.8^{B}	3.3	9.2	17.6	23.5
	PF4	13.5^{A}	2.8	7.6	13.8	18.8
IB [N/mm²]	**PF1**	0.6^{A}	0.3	0.0	0.5	1.4
	PF2	0.7^{A}	0.4	0.1	0.5	1.5
	PF3	0.4^{B}	0.2	0.0	0.3	0.7
	PF4	0.6^{A}	0.3	0.1	0.5	1.2

The heat-treated cluster V1 based on 56 specimens each instead of only 8 in the untreated V0. In contrast to the untreated sample, the lowest cluster TS was found for PF4 with 3.2 % whereas the lowest WA was found for PF2 with 13.4 %. The IB was found 0.6, 0.7, 0.4 and 0.6 N/mm² for PF1, 2, 3 and 4, respectively. As expected, standard deviation was higher in the cluster means than in the untreated group. The min-max span for TS was largest in the PF3 cluster and lowest for PF4. The IB min-max span was comparably large for PF1, 2 and 4, but notably low in PF3. Figure 61 illustrates this spread in the four cluster means. However, at the same time it shows that there obviously was no density related correlation that caused the mean values to scatter. The high SD and spread raised notable doubts on the explanatory power of the mean values. The lowest mean IB (PF3) and the highest mean TS (PF3) differed significantly from the other systems, however, no other difference was noted (also see table 20). Thus, it was indicated to exclude PF3 from further utilization.

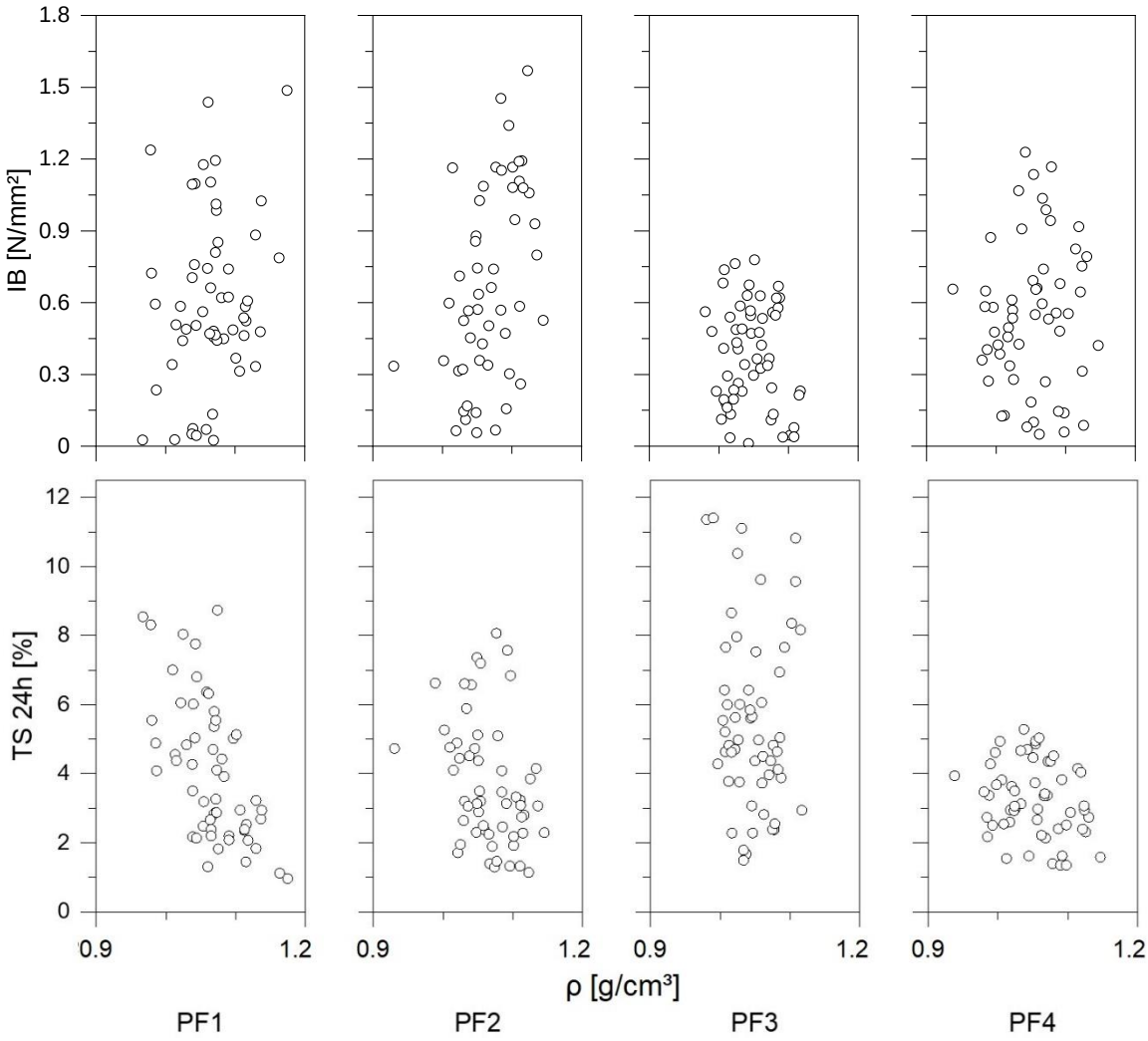

Figure 61: Thickness swelling (TS) and internal bond (IB) of scrimber panels against density produced with four different phenolic systems (PF1-4) shown as cluster for all heat-treated samples (V1)

Summarizing, the investigation of the control group (n = 8) favored spray-applied resin PF1 and PF2, whilst PF4 performed worst. The comparison within the single heat-treated groups delivered controversial results. The heat treatment cluster indicated to exclude PF3, however, failed to proof statistical validity. Consequently, the third and last step was to analyze distinctly sized clusters in between n = 8 and n = 56. The columns in table 21 present the mean results

and standard deviation of the untreated group (first column) and the three clusters composed of heat-treated sample groups with different size each. In each column means were either marked green as best or red for worst result. The means were only marked if there was a significant difference to the other resin systems in the same column. The first column represents the untreated sample group described earlier. The 160 °C cluster in the second column indicated best results for PF2 in TS, WA and IB, whilst PF3 had performed worst. This confirmed the result of the large heat-treatment cluster described previously. For the cluster in the third column sample size was larger, but no significant differences were found in TS, WA or IB. Only flexural MOR showed to be higher for PF2 as it has been in the untreated group also. The cluster in the last column contained four sample groups. Here again, PF3 showed the highest TS and WA and lowest IB with significant mean difference to all other resins and confirmed the explanatory power of the results in table 20.

Table 21: Descriptive statistics of the effect of four different phenolic systems (PF1-4) on thickness swelling (TS), water absorption (WA), internal bond (IB), flexural strength (MOR) and modulus of elasticity (MOE) for scrimber panels produced from untreated (V0) as well as heat treated (V1) bamboo scrims grouped in differently sized cluster

			V0 (untreated)		**V1 (160 °C; t)**		**V1 (200, 220 °C; t)**		**V1 (160, 180 °C; t)**	
Cluster sample size			1 group n = 8		2 groups n = 16		3 groups n = 24		4 groups n = 32	
			Mean	SD	Mean	SD	Mean	SD	Mean	SD
TS [%]	**V2**	PF1	1.8^{A}	0.6	5.2^{A}	1.9	4.0^{A}	2.0	4.0^{A}	2.1
		PF2	5.8^{B}	1.6	3.2^{B}	1.6	3.6^{A}	1.4	3.7^{A}	2.1
	V3	PF3	5.5^{B}	0.9	8.7^{C}	2.0	3.6^{A}	1.4	7.0^{B}	2.4
		PF4	3.0^{AC}	0.5	4.0^{AB}	0.9	2.9^{A}	1.1	3.5^{A}	1.0
WA [%]	**V2**	PF1	11.0^{A}	2.2	15.9^{A}	4.0	14.0^{A}	4.7	14.1^{A}	4.6
		PF2	17.8^{B}	4.1	11.8^{B}	3.3	13.6^{A}	3.9	13.2^{A}	4.0
	V3	PF3	22.5^{B}	1.5	19.0^{C}	2.3	14.6^{A}	3.4	18.4^{B}	2.3
		PF4	13.5^{C}	1.4	13.0^{AB}	2.3	13.4^{A}	3.1	13.6^{A}	2.7
IB [N/mm²]	**V2**	PF1	0.7^{A}	0.4	0.5^{AC}	0.5	0.5^{A}	0.1	0.6^{A}	0.5
		PF2	0.9^{A}	0.3	0.9^{B}	0.5	0.7^{A}	0.3	0.6^{A}	0.5
	V3	PF3	0.7^{A}	0.1	0.3^{A}	0.3	0.3^{B}	0.1	0.4^{B}	0.3
		PF4	0.4^{B}	0.2	0.7^{BC}	0.3	0.3^{B}	0.2	0.7^{A}	0.3
MOR [N/mm²]	**V2**	PF1	126.1^{A}	25.2	153.6^{A}	25.8	85.5^{A}	13.2	139.6^{A}	31.0
		PF2	195.5^{B}	27.6	111.6^{B}	32.6	106.4^{B}	31.2	118.3^{A}	25.2
	V3	PF3	128.4^{A}	19.5	119.1^{AB}	32.3	76.4^{A}	17.0	113.8^{A}	28.6
		PF4	132.6^{A}	40.3	138.5^{AB}	24.4	81.4^{A}	16.2	124.3^{A}	25.4
MOE [kN/mm²]	**V2**	PF1	19.2^{A}	2.7	23.6^{AB}	2.9	23.3^{A}	2.5	23.4^{A}	2.5
		PF2	26.4^{B}	0.8	20.1^{A}	2.8	24.5^{A}	3.2	22.7^{A}	3.6
	V3	PF3	22.8^{AB}	1.3	22.5^{AB}	2.5	22.0^{A}	2.6	22.8^{A}	2.0
		PF4	18.9^{A}	3.2	24.3^{B}	1.7	22.6^{A}	2.3	23.7^{A}	1.9

It remains to explain how the untreated PF1 group could have come to the notably low TS (1.8 %) and WA (11 %). Density differences between the four resin sample groups could be not be observed. Though, the mean density of the PF1 group (1.015 g/cm³) differed from

PF2 (1.039 g/cm³), PF3 (1.063 g/cm³) and PF4 (1.042 g/cm³), taking the variation of less than 5 % in all groups into account the difference was negligible. This difference would not explain the deviation of TS. A potential explanation might have been a man-made experimental error or an unknown cause in the sample composition. The atypical absence of hygroscopic active substances in the bamboo fiber bundle lot from which the panel was made might have been responsible for the unexpectedly low values.

4.4.2.2 Effect of heat treatment

Four temperature levels and two treatment durations (V1) were investigated and compared to the control group (V0). Figure 67 shows the surfaces of the scrimber produced with heat treated highland bamboo. The treatment was done for 3 and 5 h at four temperatures levels. The heat treatment at 220 °C and 5 h was not tested, because samples proved to be too brittle during saw formatting. The results were then further analyzed for the spray-applied resins PF1 and PF2 (V2) and without addition of wax (V4). The complete results for each group's mean are shown in the appended table 46.

The TS of panels produced with PF1 was found with 5.8, 3.2, 5.6 and 3.2 % for 160, 180, 200 and 220 °C, respectively. The thickness swelling of heat-treated samples were all higher than the control group which was at 1.8 %, reminding that this value seemed to not be plausible. Nevertheless, technically there was no notable improvement of TS observed from the heat treatment. In contrast panels produced with PF2 the TS were 4.3, 3.2, 6.4 and 3.6 % for the same temperature levels. The control in this group showed TS of 5.8 % which was three times higher than the control group pressed with PF1 resin. Although some heat-treated samples showed lower TS than the control group, the results showed to be inconsistent due to the great difference between the control group values of the two resin groups. For the treatment duration, in a combination of V1 and V2, controversial results for 3 and 5 h treatment were observed, too. The values in the PF1 group for 3 h were lower than the 5 h, which further did not match the expected effects of such a heat treatment. A similar result was obtained for PF2: However, the 5 h treatment caused 3.22, 4.21, 3.93 and 3.19 % TS and 3 h duration led to 4.3, 3.2, 6.4 and 3.6 % for V1(160, 180, 200, 220 °C), respectively. The treatment duration was disregarded as relevant variable. Temperature level is of higher impact on swelling than duration which was shown for wood and wood-based panels (Esteves and Pereira 2009, Pelaez-Samaniego *et al.* 2013) as well as African highland bamboo before (Schmidt 2013, Starke *et al.* 2016).

Figure 62: Surface photography of lab-scale scrimber produced of heat-treated highland bamboo (160, 180, 200, 220 °C)

The in-panel deviations showed to be higher than expected. Exemplarily, the appended table 47 shows the complete descriptive statistics of the V1(160 °C; 5 h) sample produced with PF1 resin. It shows that the SD not only of TS means, but also of WA, IB, MOR and MOE were notably high. The coefficient of variation was more than 50 % for TS, between 20 and 70 % for IB and below 10 % for the mechanical properties. This is not too surprising for a veneer-based layered panel, but indeed for a mat-forming composite. The high mean deviation of TS and IB are unusual even for a badly densified wood-based panel. Consequently, the comparison of single mean values from groups, whose differences were too scattered, seemed pointless. Remembering that due to the low statistical sample size (only one panel per variation), comparison of mean results was made on the base of only eight specimens. Which is why a coarser clustering of values had to be done. The treatment temperatures 160 and 180 °C were clustered and denominated as the low temperature group (LT) on the one hand. On the other hand, the 200 and 220 °C treatment datasets were combined and constituted the high temperature group (HT). Both treatment durations (3; 5 h) were joined in the same cluster. This way it should at least be possible to screen how untreated, mild or strong harsh heat treatment regime would affect the panel properties. Table 22 shows the mean and SD of the three separate clusters for Control, LT and HT produced with resin V2(PF1) and V2(PF2) and, respectively, the combined cluster sample V2(PF1, PF2) containing both resin systems. The cluster sample sizes differed inside the column since control group and heat-treated groups were not of equal specimen number. In the first and second column, significant differences were found for TS and WA between the mild heat treatment and the control group. The same applies for the harsh heat treatment and the control group. Nevertheless, there was no significant difference between the mild and the harsh heat treatment. The TS of the V2(PF2) cluster reduced from 5.8 to 3.7 and 3.6 % for LT and HT, respectively. The WA decreased from 17.8 to 13.2 and 13.6 % accordingly. It was known from the previously conducted resin analysis, that the PF1 control and PF2 control notably differed in TS, WA, MOR, and MOE, though there was no significant difference found for density. The reasons for this remained indeterminate.

Table 22: Descriptive statistics of mean thickness swelling (TS), water absorption (WA) and internal bond (IB) of scrimber panels produced from scrim strands priorly treated at low temperatures 160, 180 °C (LT) and high temperatures 200, 220 °C (HT) for the cluster comprising V2, V3 and V4; Means in the same column sharing same letters are not significantly different at p ≤ 0.05

		V2(PF1)		V2(PF2)		V2(PF1, PF2)	
Cluster sample size		1 group n=8; 24; 32		1 group n=8; 24; 32		2 groups n=16; 64; 56	
	V0; V1(3, 5 h)	Mean	SD	Mean	SD	Mean	SD
TS [%]	Control	1.8^{A}	0.6	5.8^{A}	1.60	3.8^{A}	2.3
	LT	4.0^{B}	2.1	3.7^{B}	2.09	3.9^{A}	2.1
	HT	4.0^{B}	1.9	3.6^{B}	1.42	3.8^{A}	1.7
WA [%]	Control	11.0^{A}	2.2	17.8^{A}	4.12	14.4^{A}	4.7
	LT	14.1^{B}	4.5	13.2^{B}	4.01	13.7^{A}	4.2
	HT	14.0^{B}	4.7	13.6^{B}	3.85	13.8^{A}	4.2
IB [N/mm²]	Control	0.7^{A}	0.4	0.9^{A}	0.27	0.8^{A}	0.3
	LT	0.6^{A}	0.4	0.6^{A}	0.48	0.6^{AB}	0.4
	HT	0.5^{A}	0.1	0.7^{A}	0.30	0.6^{B}	0.2
MOR [N/mm²]	Control	126.0^{A}	25.2	196.0^{A}	27.6	161.0^{A}	44.4
	LT	140.0^{A}	31.0	118.0^{B}	25.2	129.0^{A}	29.8
	HT	85.6^{B}	13.2	106.0^{B}	31.2	96.0^{B}	25.8
MOE [kN/mm²]	Control	19.2^{A}	2.7	26.4^{A}	0.78	22.8^{A}	4.2
	LT	23.4^{B}	2.4	22.7^{A}	3.63	23.1^{A}	3.0
	HT	23.3^{B}	2.5	24.5^{A}	3.16	23.9^{A}	2.8

When the two clusters were combined (third column) the gain in PF2 had offset the loss of PF1. Due to the implausible control group in the PF1 group, no different TS or WA was observed between control, LT and HT anymore in the combined cluster. A reduction of IB from 0.8 to 0.6 N/mm² was at hand, with clear statistical significance only between control and HT treatment. The HT group decreased flexural MOR the by more than one third for all clusters, namely from roughly 196 N/mm² to 106 N/mm² in the PF2 cluster. Taking this MOR loss into account, the HT treatment had considerable impact on properties. Although there are unclear effects interfering with the resin selection one can see that the results for TS, WA and IB were at comparable level for the cluster in the third and fourth column in the resin chapter cluster analysis. The low number of tested specimens in the control group (n = 8) have obviously caused

4.4.2.3 Effect of wax addition

All mean results on the effect of wax can be found in appended table 46. The TS after 24 h for scrimber from untreated bamboo (V0) produced with sprayed resins increased from 1.8 to 2.3 % and 2.3 to 3.1 % when wax was added, for PF1 and PF2 respectively. An inverse effect was observed for the powder resins (PF3 and PF4), where wax addition caused a slight decrease in TS. The same applies for WA, whilst for IB no consistent pattern could be observed.

The TS after 24 h for scrimber from heat treated bamboo (V1) was not distinct. The sample made from 160 °C (3 h) treated bamboo showed lower values once wax was added. The two samples produced with PF1 and PF2 reduced TS from 10.0 to 4.2 % and 4.3 to 2.8 %, respectively. Similarly, the powder resins PF3 and PF4 showed a reduction from 9.5 to 5.2 % and 4.5 to 3.3 % when adding wax to the paste. The 160 °C (5 h) delivered controversial results: The samples glued with PF1 showed increased TS when wax was added. The remaining heat treatment groups (V0; V1) tended to show lower TS but could not unambiguously be assigned to the wax itself. Nevertheless, the lowest TS in the 160 °C (3 and 5 h) group was found for PF2 and wax.

To confirm the results with an Anova, all samples (V0; V1; V2; V3) were clustered and descriptive statistics have been produced (see table 22). The mean TS decreased from 4.1 to 2.7 % when using wax. A similar effect was observed for the WA of the clustered sample. The WA dropped significantly from 14.6 to 10 %. The median as well as the span from minimum to maximum behaved similarly and showed that the mean results were plausible. Internal bond was not affected. All values (mean, min, max, median) for wax samples were apparently higher, but the spread of values for IB showed that wax did not have notable influence on the internal bond. A statistically significant difference could not be shown.

Table 23: Descriptive statistics of clustered mean thickness swelling (TS), water absorption (WA) and internal bond (IB) of scrimber panels produced with and without wax for all variants V0, V1, V2 and V3

	Wax	n	**Mean**	SD	Minimum	Median	Maximum
TS [%]	n	256	4.1^{A}	2.1	0.9	3.7	11.4
	y	224	2.6^{B}	1.6	0.3	2.2	9.5
WA [%]	n	256	14.5^{A}	4.1	5.6	14.5	26.7
	y	224	10.0^{B}	3.6	4.0	9.5	23.8
IB [N/mm²]	n	250	0.5^{A}	0.3	0.0	0.5	1.5
	y	210	0.6^{A}	0.3	0.0	0.5	1.6

In short, adding 2 % wax in the resin solution to produce bamboo scrimber resulted in lower TS and WA. The IB showed no significant difference, thus resin performance was not affected. The same applied for the bending properties which have not been further displayed here. Thickness swelling was improved by 35 %, the WA by 31 % within this cluster analysis.

4.4.3 Effect of resin concentration and layered panels

Three bulk resin concentrations and two vertically layered concentrations were tested for their effect on TS, WA and IB. Table 24 summarizes the sample density and MC prior to testing. A significant difference between the samples could be rejected. Nevertheless, the deviation observed in MC was in between 0.7 and 1 % basis points which corresponded to a variation of 5 to 8 % and might have influenced especially the IB. This experimental part used scrim strands heat treated at 180 °C for 3 h, since the production parameter screening indicated that LT heat treatment would improve hygroscopicity sufficiently. Different from the before screening where only one panel was produced per group, the n was increased to 5 panels avoiding statistical spread effects seen earlier.

Table 24: Moisture content (MC) and density (ρ) for panels produced with different resin concentrations in core (CL) and face layer (FL)

Resin content FL-CL-FL [%]	n_{panels}	MC [%]	ρ [g/cm³]
12-12-12	5	12.2 (0.9)	1.11 (0.05)
14-14-14	5	13.4 (1.0)	1.12 (0.06)
16-16-16	5	14.5 (0.9)	1.10 (0.07)
14-12-14	5	12.4 (0.7)	1.06 (0.05)
16-12-16	5	12.8 (0.8)	1.09 (0.06)

4.4.3.1 Thickness swelling and water absorption

Figure 63 shows TS and WA tested after 2 and 24 h water storage. For the 24 h test, the highland bamboo scrimber returned mean TS of 1.9, 1.5 and 1 % and WA of 10.2, 8.2 and 6.6 % for the 12, 14 and 16 % resin concentration, respectively. The observed tendencies were similar for 2 h WA, but not for TS. When the resin concentration increased only in the faces, the thickness swelling was the same (1.5 %) for both, the 14-12-14 and 16-12-16. Compared to the 1.9 % TS in the 12 % monolayer panel and 3.7% TS from the 10 % resin panels from the prior chapter, the TS had significantly been reduced. To go below 1 % TS more resin, namely 16 %, was needed. The absorbed water has mainly swollen the less impregnated and densified core of the panel. A similar observation can be made in the results of Hu *et al.* (2018) where different vertically graded and bulk resin loading levels were compared, though their findings on TS were not consistent[14]. The two curves in figure 71 comprise results of the whole chapter and show the different slopes of TS and IB with increasing resin concentrations. Irrespective of density related differences, the TS decreased linearly from 5 to 12 % resin content with a slope of -1, while raising the resin concentration beyond 12 % would flatten the linear slope to -0.25. In other words, increasing resin concentration by 1 % returned a TS decrease of 1 % in concentrations below 12 %. Beyond that, the effect of resin is 4 times weaker presumably owed to a complete fiber impregnation at this level. This fact points out, that high resin concentrations in bamboo scrimber do not impact properties notably, but possibly serve to guarantee

From a product view, neither thickness swelling, nor water adsorption could be identified as technological bottlenecks for the highland bamboo scrimber. The OSB standard DIN EN 300:2006-09 requires for application in humid environments a TS below 12 % for OSB/4 and 15 % for OSB/3. These values would have been fulfilled for untreated BS with 8 % resin.

[14] In their study a 10 to 18 % bulk resin concentration decreased TS from 7 to 3.7 %, whereas a 14 % concentration reached TS above 8 %. On the other hand, a panel with 18 % in the FL and 10 % in the CL showed 4.3 % TS.

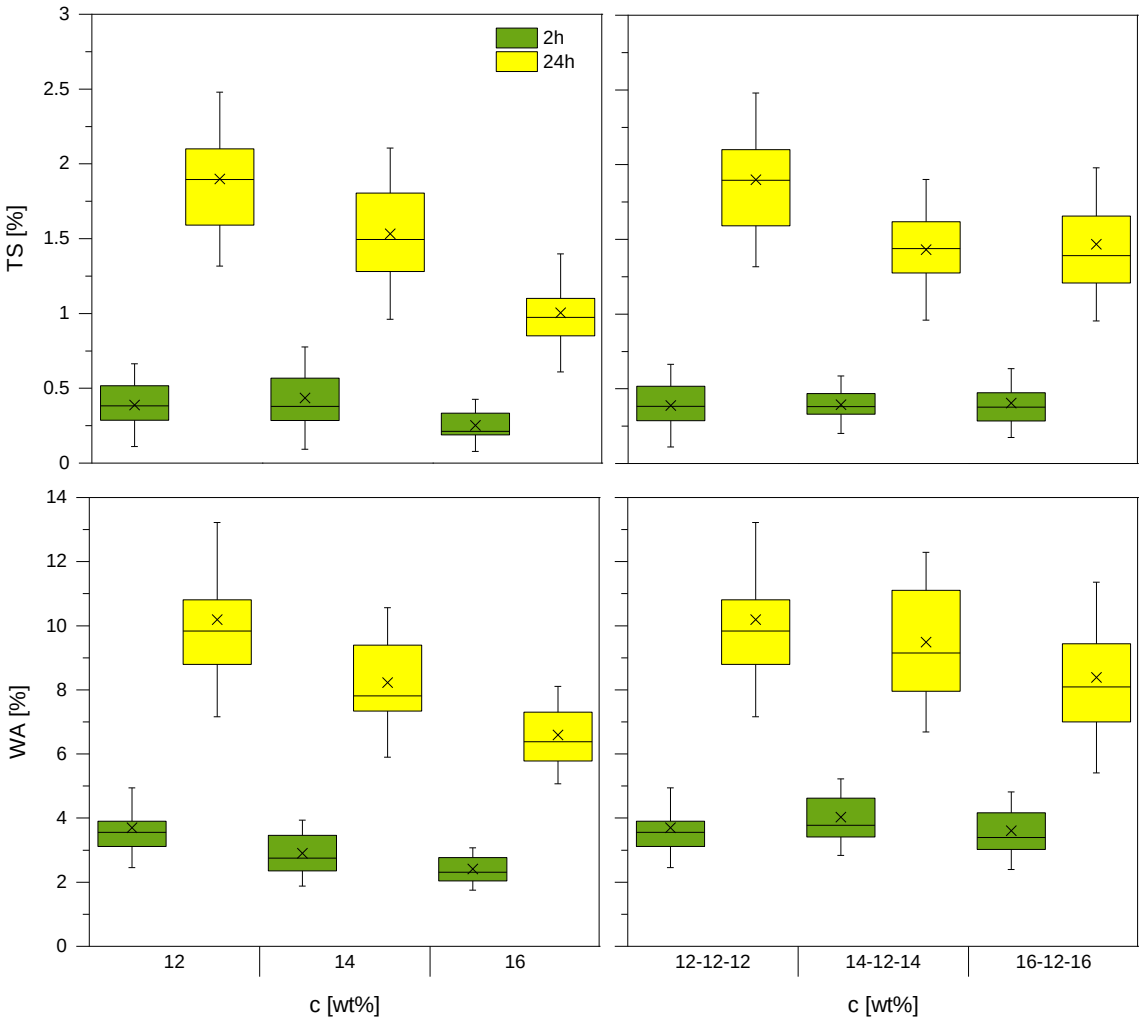

Figure 63: Thickness swelling (TS) and water absorption (WA) of highland bamboo scrimber with three different resin gradients and concentrations tested after 2 and 24 h

4.4.3.2 Internal bond

The resulting IB of three bulk resin concentrations are shown on the left in figure 64 and vertically layered concentrations on the right. The samples were tested in standard climate condition (20 °C/65 %) and after water bath boiling for 2 and 5 h. For standard climate, figure 64 (left) shows the 16 % resin concentrations reached the highest IB with 1.9 N/mm², followed by 1.5 and 1.2 N/mm² for the 14 and 12 % sample, respectively. A similar pattern was observed for the samples which were stored in water baths for 2 and 5 h prior to testing. The means of all treatments within the regarding group were significantly different from each other. For the samples tested after wetting, the IB for 12 % resin dropped to below 0.5 N/mm², whilst the IB of 14 % samples dropped to 0.61 and 0.59 N/mm² and for 16 % to 0.89 and 0.77 N/mm², after 2 h and 5 h water bath, respectively.

In figure 64 (right), the face layer resin concentration was increased to 14 and 16 %, whilst the core layer was kept constant at 12 %. The 14-12-14 reached a dry IB of 1.1 N/mm² but did not differ significantly from the 12-12-12 sample. The 16-12-16 sample reached dry IB of 1.5 N/mm² which was significantly higher than the 12-12-12 sample. Nevertheless, the layered

16-12-16 sample and the 14 % monolayer sample showed similar mean when tested in dry IB. Also, the 14-12-14 sample did not significantly differ from the 14 % monolayer. This might have indicated that a certain amount of resin migrated into the core layer. However, all tested samples failed in the scrimber core layer. The increased resin concentration in the face layers was not expected to show notable effect on IB. And in fact, the water-stored samples of the 12-12-12, the 14-12-16 and 16-12-16 % resin were found with no significant differences neither for 2 h nor for 5 h water storage. Therefore, all resin variants after 5 h water storage and their regarding statistical meaningfulness were worked out in figure 65. Here one can see that the core layer concentration was the main determining factor and only a bulk concentration increase altered the IB significantly.

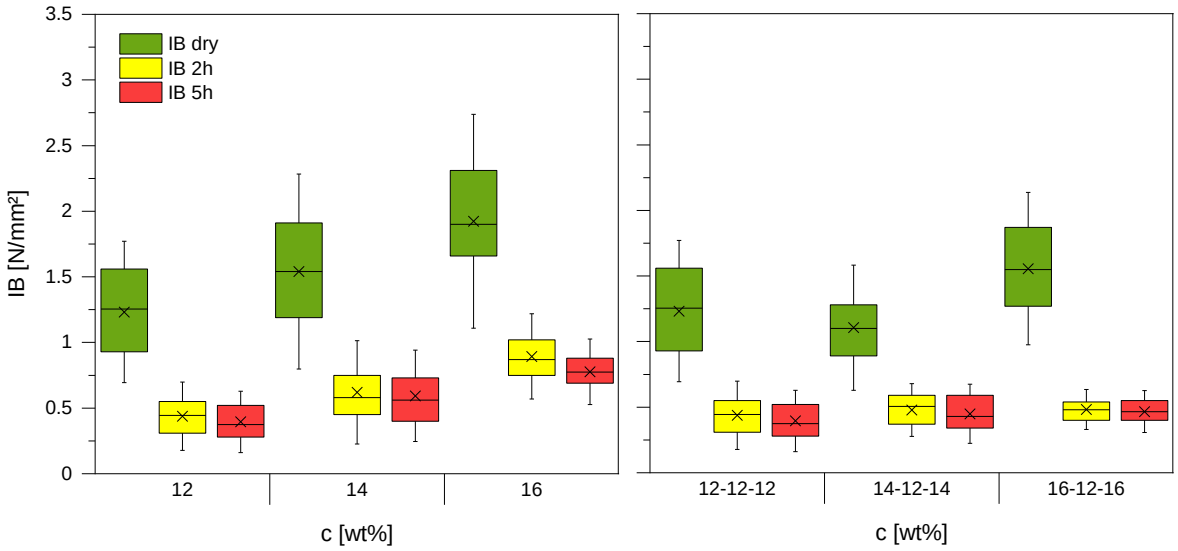

Figure 64: Internal bond (IB) of highland bamboo scrimber with three different resin gradients and concentrations tested in standard climate (20 °C/65 %), oven-dry and after 2 or 5 h water storage

To sum up, IB was not notably affected when face layer resin content was increased but did increase by 37 % once the resin concentration rose from 12 to 16 %. Comparable findings were made for interlaminar shear strength in veneer based scrimber composites from bamboo and poplar (Fan *et al.* 2011, Zhang *et al.* 2018c). It can be assumed that IB testing and interlaminar shear strength are both applicable methods for the assessment of the bonding quality in scrimber composites. The IB is commonly used to determine the bonding quality of mat-forming wood-based panel composites. The differences between testing IB of mat-forming panels (MDF, PB, OSB) and veneer-type panels (LVL, plywood) were illustrated by Suzuki and Miyagawa (2003). There is a strong relation between density and interlaminar shear strength in MDF and OSB which corresponds to IB in BS (Suzuki and Miyagawa 2003). In those panels IB obviously represents the weakest layer across the panel plane. In mat-forming panels, the weakest layer is in the vertical center, where density is lowest. This is why Lee *et al.* (2017) found a weak linear correlation (R^2 = 0.54) between peak densities and IB. In another study on layered resin concentrations from 10 to 18 % no such tendencies were found for bamboo scrimber. The authors showed that increasing resin concentration attained a strength maximum, independently of the core layer resin content (Hu *et al.* 2018).

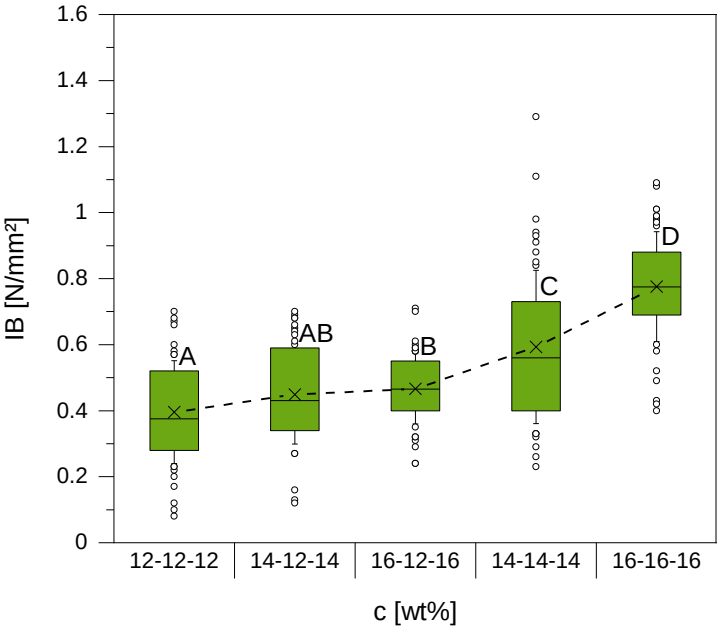

Figure 65: Internal bond (IB) of highland bamboo scrimber with three different resin gradients and concentrations tested after 5 h water storage; Means sharing same letters are not significantly different at $p \leq 0.05$

Figure 66 illustrates the layered bamboo scrimber cross sections with fluorescence microscopies where the color contrast was enhanced through a false-colored photography. The false coloration was a result of an individual choice at each picture to enhance visibility and did not stand for any different sample preparation procedure. The scrim strands formed mats with a distinct boundary in between them. These boundaries did not align horizontally but adapt the form and density of the neighboring layer. At the same time the pictures show that there was no clear evidence of the resin gradient across the board plane. Nevertheless, magnifying the core parts of the boards visualized the microcracks observed earlier. Those cracks run longitudinally through the fiber sheaths around the vascular bundles. They were observed in all examined samples and were already found in the raw material analysis. There was no further investigation to understand the importance of those microcracks to internal bond, but it is probable that the IB is directly proportional to fracture toughness. Amada and Untao (2001) showed that fracture toughness was higher in the outer perimeter of the culm where a high FBD can be found. Whether density, fiber cell anatomy or other factors are the reason for fracture toughness was not further researched. In the present study, the failure mode in low resin samples was commonly less brittle than high resin samples. Assumedly the failure started at the existing microcrack tips and then propagated along the grain axis. Due to the fact, that bamboo dries before processing, some fabricants (Rabik 2016) suspect the lacking impregnation of the initial crack void to be responsible for the statistical spread as seen priorly in the production screening.

It is however important to mention that the IB results were beyond the range of OSB/3 standards. The IB of OSB tested in standard conditions (without prior water storage) requires 0.4 N/mm² for usage in humid environments (DIN EN 300:2006-09). In the dry test and after 2 h water storage all IB means were above this threshold. After 5 h water storage only the 12-12-12 % mean value resulted slightly below this value. All other resin samples were higher in mean, but at the same time contained some outliers below 0.4 N/mm².

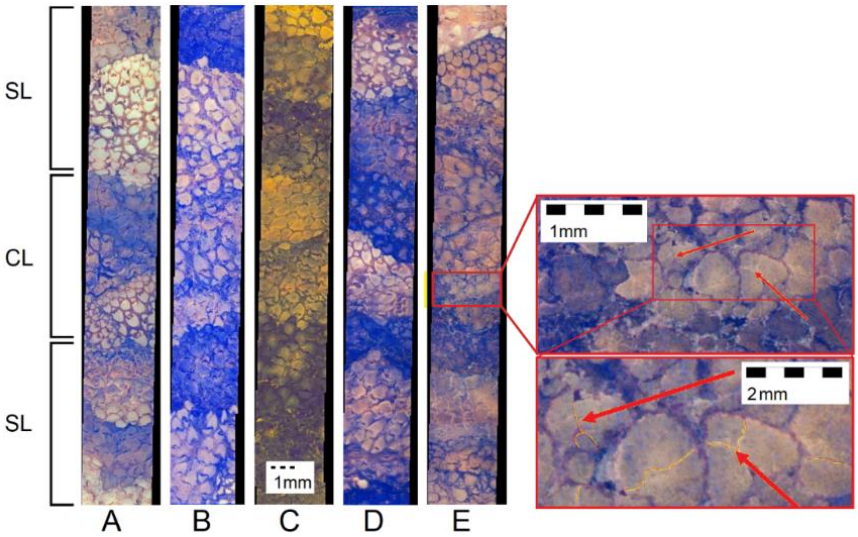

Figure 66: Cross section layers under fluorescence microscopy showing different resin concentration in the surface (SL) and core layer (CL) with 12-12-12 (A); 14-14-14 (B); 16-16-16 (C); 16-12-16 (D); 14-12-14 (E) in %

4.4.4 Influence of the fiber bundle morphology from different culm height sections

The results of the preliminary production trials (4.4.2) revealed a variation in properties which was on the one hand attributed to the low number of panels produced per variable. Additionally, the core layer of the BS panels produced during the production trials and screening seemed to have densified homogenously. Flaws at the panel surface and cavities ("*lunker*") were occasionally already observed in the production parameter screening (see figure 67). Some regions seemed to only have marginally densified, whereas others underwent an intense compaction. The particle geometry of the scrim strands was suspected to influence the panel compaction homogeneity. The effect of uneven density distribution among the sample groups and the specimens themselves might have caused variations in all density dependent properties. One major reason for uneven density distributions were heterogenous scrim mats of which the BS panel is hot-pressed. The cause of this heterogeneity could on the one hand be found in the manual mat formation, as argued by Shang *et al.* (1998) and Huang *et al.* (2019a), on the other hand, raw material related influences were described as potential cause of inhomogeneity in the property profile of BS (Qi *et al.* 2014, Qi *et al.* 2015).

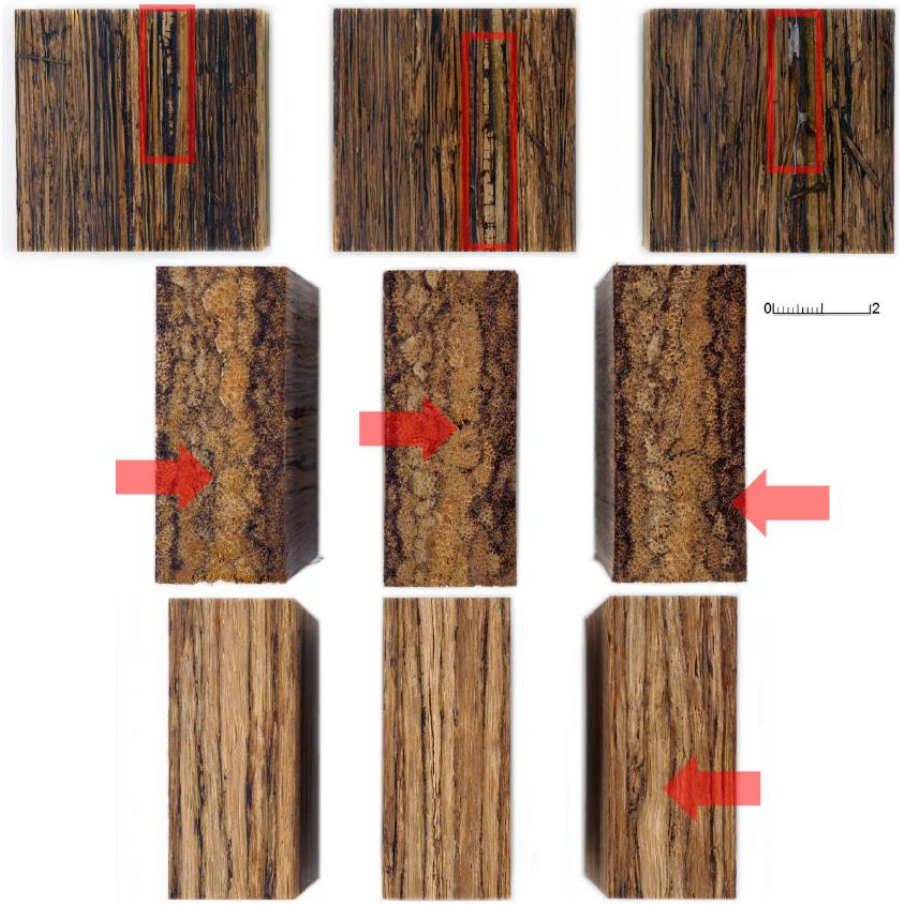

Figure 67: Surface, transversal and longitudinal section of laboratory scale highland bamboo scrimber with red boxes indicating superficial flaws, arrows pointing from the left to the right indicating low density and from right to left high compaction regions

Consequently, a grading of raw materials into height sections was done and scrim strands were produced from the top, middle and bottom portion (T, M, B) of the culm. Moreover, three additional panels were produced from T scrims which passed the defibration crusher four times instead of once. Figure 68 shows the finer scrims (F) in comparison to the T group.

According to the literature higher target density lead to homogenous property profiles which basically is associated to an even density distribution along and across the bamboo scrimber panel. On the other hand, decreasing element size leads to a more symmetrical and U-shaped vertical density profile. For that, an additional group of finely defibered bamboo scrims from the top portion was used to produce a control group. The target density was set to 0.9 g/cm³ and the resin concentration to 5 %, for the sake of understanding the sole effect of the raw material grading. High density and resin concentrations led to acceptable properties as shown in the screening part. However, resin and density were suspected to have overlapped the influence of the raw material. The hot-press reached a specific pressure peak of 7 N/mm². The panels produced in the screening showed more than double the pressure. Obviously, the lowered density and resin amount (moisture) resulted in less counter pressure of the BS mat during consolidation. The pressing diagrams are found exemplarily in the appendix.

Figure 68: Scrim strands from the top portion (left) and fine crushed scrims from the same top portion (right)

All in all, five additional panels were produced from each height class (T, M, B). Another three panels were fabricated from fine scrims (F) originated from the top section but passed the crushing device four times instead. The T group panels showed slightly lower MC, whilst the F group had a lower density than targeted (see table 25). The panels were all produced without a soft frame, so that the mat suffered lateral spreading during the compaction phase in the hot-press. The lesser densified margins were removed when edge-formatting the conditioned panels, however, it seems that the effect had decreased the bulk density of the panel.

Table 25: Sample size, mean and standard deviation (in brackets) of moisture content (MC) and density (ρ) for bamboo scrimber panels produced with different fiber bundle classes and a lowered target density (0.9 g/cm³) and resin concentration (c = 5 %)

Fiber bundle class	**n_{panels}**	**MC [%]**	**ρ [g/cm³]**
Top (T)		10.9 (0.4)	0.85 (0.08)
Middle (M)	5	13.3 (0.5)	0.91 (0.07)
Bottom (B)		12.4 (0.3)	0.86 (0.06)
Fine (F)	3	12.2 (0.3)	0.75 (0.05)

4.4.4.1 Flexural strength and elasticity

The results on MOR and MOE of T, M, B and F fiber bundle based bamboo scrimber are shown in table 26. The mean MOR was 73.6, 80.6 and 78.9 N/mm² for B, M and T respectively. The SD was relatively high for all three groups with a COV of roughly 25 %. The median MOR for the T group seemed to be higher than the others. The minimum and maximum MOR values of M showed a higher trend. In general, B samples performed worse than T and M. The MOE of T, M and B samples was between 18 and 20 kN/mm² with no significant difference between the three. The SD was surprisingly lower than the one for MOR. However, the analysis of variance showed that means of T, M and B did not differ significantly. The fine fiber sample produced a flexural mean MOR of 39.28 N/mm², i.e. half the T group mean where F scrims were derived from. This mean MOR difference of F was found highly significant against all other groups. Additionally, the F sample SD was found to be only a fourth of the T, M and B sample SD. It was obvious that the resin concentration was too low to cope with the highly elevated surface area of the fine fiber bundle in the F sample. Consequently, there was no sufficient load transfer between neighboring scrim fibers and hence, cracks would propagate with ease along the longitudinal panel axis.

The samples were grouped according to their density, and their relation with MOE and MOR is shown in appended figure 99 and figure 100. Overall, the functional relation between MOE and density was linear independent of the culm height section. Flexural MOR of the T sample was highest at a density level above 0.7 g/cm³, followed by the M sample. The B sample MOR was significantly lower than T. The difference between B and M was not significant at any density level, though MOR of B slightly tended to be lower than M. At the higher density samples above 0.9 g/cm³ a slight trend was observed. Each point in the graphs represents means with different n. Consequently, figure 99 and figure 100 (to be found in the appendix) could not give final answers but only trends.

Table 26: Flexural modulus of elasticity (MOE) and strength (MOR) for panels from bottom (B), middle (M), top (T) and fine (F) scrims; Means sharing same letters are not significantly different at $p \leq 0.05$

	Class	Mean	SD	Minimum	Median	Maximum
MOR [N/mm²]	**T**	78.92^{A}	21.39	37.37	80.22	131.88
	M	80.58^{A}	19.81	47.14	73.83	130.04
	B	73.6^{A}	18.43	37.93	73.31	112.86
	F	39.28^{B}	4.97	31.3	39.37	47.54
MOE [kN/mm²]	**T**	18.03^{A}	3.44	8.99	18.38	26.03
	M	19.57^{A}	2.76	13.02	19.10	26.56
	B	17.78^{A}	2.32	13.19	18.40	23.28
	F	11.69^{B}	1.61	9.47	11.68	14.80

The mechanically degrading effect of a strong defibration (or “brooming”) on MOR as it had happened to F scrims was documented in Fan and Fu (2017) and explained with the increasing width (tangentially) of bamboo fiber bundles. Whether this damage or the badly bonded fibers as it is known from wood scrimber (Paton 1997) were the main reason for the low MOR and MOE of the F sample had not been conclusively clarified. The culm height section of the raw material (T, M, B) did not seem to be relevant for the bending properties.

4.4.4.2 Thickness swelling and water absorption

The mean TS (24 h) of T, M and B scrimber was 8.9, 8.7 and 9.1 %, respectively. Figure 69 shows that the TS did neither notably differ for a short-term (2 h) nor for a long-term test (28 d). The same picture was observed for water adsorption. The F sample showed 12.3 % swelling in thickness after 24 h water immersion. The difference was significant for all test durations. The F and T sample are visualized in a density related comparison in figure 69. The TS values after 28 d in water increased for all samples. The T sample did not depict a clear TS tendency between 0.6 and 0.8 g/cm³, but then increased TS until 0.9 g/cm³. Surprisingly, the T variant drastically decreased TS above 0.9 g/cm³. The minimum TS after 24 h (6.46 %) is found above densities > 1 g/cm³. After 28 d water storage, the minimum TS was 8.14 % at the 0.8 g/cm³ density and did surprisingly not differ from the 24 h water storage. The same applies for the fine scrims (F).

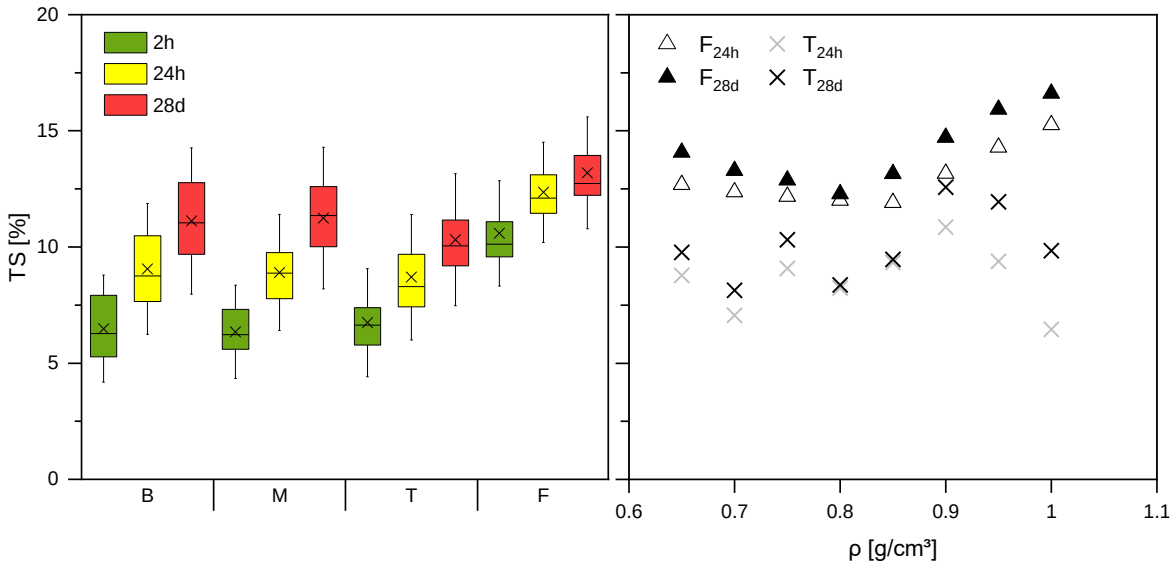

Figure 69: Thickness swelling (TS) for scrimber made from scrims coming from the bottom (B), middle (M), top (T) portion of the culm and a finer crushed (F) variant (left) and F and T means against sample density class (right)

The faster water uptake on the larger specific surface of the F panel can be disputed, since the TS was significantly higher than the T sample after all three TS (2 h, 24 h, 28 d) durations. The lower density compared to T (see table 25) might have additionally decreased the TS result for F which matches the macroscopic observation that F panels appeared more porous than others (see figure 102). The panels consisted of six vertically arranged mats which were generally more interspersed with voids than the ones seen in the prior chapters (higher target density). This observation especially applied for the F panel (see DF28 in figure 102). The resin impregnation degree of the single fiber (bundle) was nevertheless the key driver of higher hydrophobicity in the other (B, M, T) panels. The specific surface of finely crushed fiber bundles was not sufficiently impregnated so that water had easier access to them. Even a higher compaction and target density would not have prevented water from swelling the structure. For moso scrimber, Yu *et al.* (2017) confirmed that the effect of density on WA was more intense, especially at high resin contents. The authors revealed that increasing resin content decreased TS more so than density.

The two graphs in figure 71 show the different slopes of TS and IB with increasing resin concentrations. Irrespective of density related differences, the TS decreased linearly from 5 % to 12 % resin content with a slope of -1, while raising the resin concentration beyond 12 % would flatten the linear slope to -0.25. In other words, increasing resin concentration by 1 % returns a TS decrease of 1 % in concentrations below 12 %. Beyond that, the effect of resin is 4 times weaker presumably owed to a complete fiber impregnation at this level. At the low resin concentration, the finer scrims had a comparably strong impact increasing the TS value from 8.9 to 12.3 %. Further studies should be done on different resin impregnation levels.

4.4.4.3 Internal bond

The mean internal bond was 0.23, 0.29, 0.28 and 0.22 N/mm² for B, M, T and F respectively. The descriptive statistics in figure 70 show basically two things: Firstly, there is no significant difference between the B, M and T group, whilst T and F do differ. Since the scrims in group F were made from T, it is rather surprising that the T group achieved higher IB. Secondly, the IB results had deviated notably from their means. Outliers were found in in all groups which

supposedly was caused by the compaction and densification behavior in the panel. Figure 70 shows the IB against density classes, i.e. each specimen was grouped by its raw material origin and its actual density. This implies that each point in the figure represents the mean of a sample with varying specimen number. Hence, the lowest (< 0.75 g/cm³) density classes as well as the highest (> 0.9 g/cm³) density classes contain less data points than the moderate density classes. This way, the groups cannot be compared directly. Nevertheless, this way of displaying the results provides an indication on the different density dependent behavior of each group: Up to a density of 0.8 g/cm³ IB developed linearly depending on density with a slightly different slope for each group. From 0.85 to 1 g/cm³ the linear relation of the F group showed a higher slope than in the before interval. This does not apply for the M and T group. A regression analysis of all specimens within each raw material group was done to clarify the results. The resulting linear functions and confidence intervals are appended in figure 101 and table 48. Panels made from B and M deviated stronger from the linear relation than the T group. The F sample deviation coefficient (R^2) was highest (0.89) in comparison to T (0.78), M (0.57) and B (0.49). Suzuki and Miyagawa (2003) found that this effect on IB of wood-based panels depends strongly on the element type. In OSB, increased flake thickness would lead to increased IB since the specific area to cover with resin is lower. In contrast the IB in PB panels increases once the element geometry changes from large flake-like to small sliver-like particles. For PB there is a positive correlation between press time, temperature, resin content and IB as well.

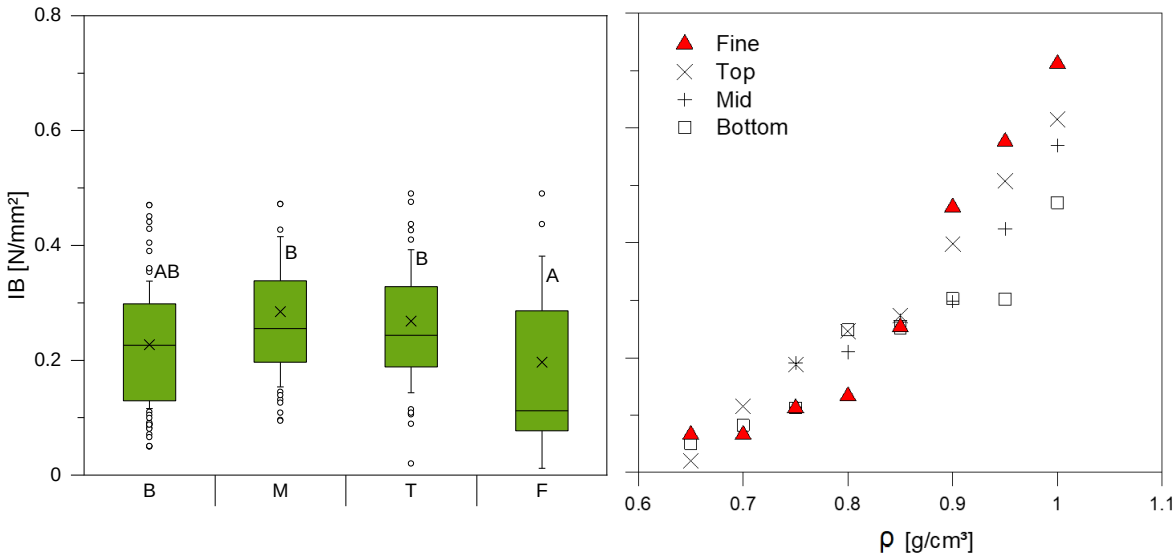

Figure 70: Internal bond (IB) for scrimber made from scrims coming from the bottom (B), middle (M), top (T) portion of the culm and a finer crushed (F) variant (left) and F and T mean against sample density class (right); Means sharing same letters are not significantly different at $p \leq 0.05$

Lee *et al.* (2017) found a moderate linear relation between mean density and IB = 0.007*ρ – 4.102 (R^2 = 0.74). Zeroing the function, i.e. considering a theoretical IB(ρ) = 0, the critical density would yield a nonsense value for the density. The IB(ρ) relation is only linear in a certain range, since their raw material (rubberwood) has an inherent internal bond which does not go down to zero even when the original raw material minimum density is reached (no compaction at all). The resulting IB values in a particle board are consequences of that inherent IB value and the (linear) increased IB value by densification in the hot-press (Lee *et al.* 2017). Based on the results, the principle seems to be not applicable to bamboo scrimber, although

the apparent compaction ratio[15] was above 3:1 which compares to mat-forming panels, e.g. OSB. The critical density (from linear regression with IB) ranged between 0.65 (B) and 0.69 (F) g/cm³ as shown in table 48. These densities reflect the raw density of scrims (also see chapter 3). Considering a target panel density of 1 g/cm³, the actual densification ratio ranges from 1.54 to 1.45 which means half the mat compaction ratio. Thus, principles of a mat-forming panel production cannot be transferred to scrimber production even for finely crushed scrims. For poplar veneer based scrimber He *et al.* (2016) and Zhang *et al.* (2018b) analyzed the influence of veneer thickness. Their findings support the present results since no significant change in bond performance was found with changing veneer thickness.

The low resin concentration in this chapter's experiment was intended to avoid overlapping effects on fiber bundle quality. The fine scrims showed better compaction and densification behavior. This effect was visible especially above a density of 0.8 g/cm³. Yet it was undeniable that the frayed out fibrous structure of the F sample (see figure 68) had increased the specific surface of the scrimber mat. To achieve the same hydrophobization (↓TS) and resin performance (↑IB) as it was found in the control group (T), the resin concentration must be higher than 5 %.

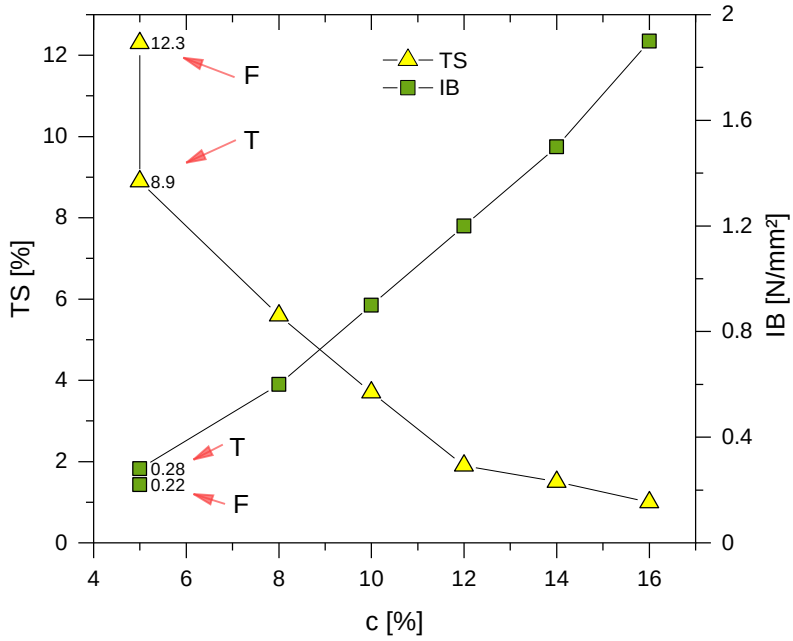

Figure 71: Thickness swelling (TS) and internal bond (IB) for scrimber made from heat treated (180 °C) highland bamboo produced with different resin concentrations and a sample of finely (F) crushed scrims

The two curves in figure 71 show the different slopes of TS and IB with increasing resin concentrations. The IB linearly correlated with the resin concentration with a constant slope throughout the function. With 1 % more resin in the panel, IB would increase roughly by 0.1 N/mm². The fine fiber bundle did not notably impact IB (reduced from 0.28 to 0.22 N/mm² at 5 %) in comparison to the effect that resin concentration had. When steering bamboo scrimber properties for different purposes, the functional influence of resin concentration will be helpful. However, a combined study of fiber bundle refinement and different resin impregnation levels will have to be done in the future.

[15] This results from mat heights between 60 to 80 and a final panel thickness of 22 mm.

4.4.5 Industrial upscaling

The empirical experiences at lab-scale are of only relative importance for industrial implementation. The last subchapter addresses implementation aspects of heat treatment, resin application and hot-pressing on industrial equipment. To reversely identify future process challenges, this chapter shows first hot pressing, then the resin application and lastly the heat treatment.

4.4.5.1 Hot pressing

Four test boards were prepared manually and pressed with an industrial scale hot-press (4 x 8 ft) using the protocols from the laboratory experiments (see also table 13 and figure 72). The press platens were heated up to 135 °C prior to press closing and heating circuit was switched off 10 min after press closing. The compaction ratio of about 3 was lower whereas the densification ratio of 1.4 was higher as in mat-forming panels (e.g. OSB, PB). In a laboratory press this consequently led to high specific pressure of up to 15 N/mm². The active cooling of the laboratory press allowed it to open after 34 min or earlier since the core temperature sank to 90 °C. On the industrial press, there is no active cooling circuit, thus longer press times were expected. Active cooling in a multi-daylight press necessitates a notable extra investment. In addition, the operational expenses due to energy costs (cooling-heating cycles) are undesirable. The peak specific pressure in the industrial press[16] reached 6 N/mm² as shown in figure 104 and must not pass 7 N/mm². To technically cope with higher pressure the stronger wall thickness of heating oil pipes would exceed standard sizes causing extraordinary costs.

The industrial press with passive cooling was then opened after pressing time of 45 and 60 min which led to core temperatures of 116 °C and above (see results in table 27). The internal bond of the panel was not sufficient at this stage yet, so the internal vapor pressure caused the entire panel to blow (see figure 72D). The temperature curves in appended figure 104 show that the core temperature dropped below the evaporation limit after roughly 90 min. The specific press pressure (0.5 N/mm²) measured at this stage was an average of the calculated from the cylinder and might consider local pressure maxima in the panel plane and still not low enough for opening. A practical technique from plywood producers who iteratively open their presses in 0.1 mm steps to release vapor pressure from the board might help at this stage. To get technically feasible panels, the press time went up to 240 min which is far from commercial viability.

[16] Reminding that production of first-generation BS was done with cold molding and pressure far beyond 15 N/mm² with values up to 80 N/mm². The pressure applied with steel molds was hold by massive bolts instead of a hydraulic system (see chapter 2.3.2).

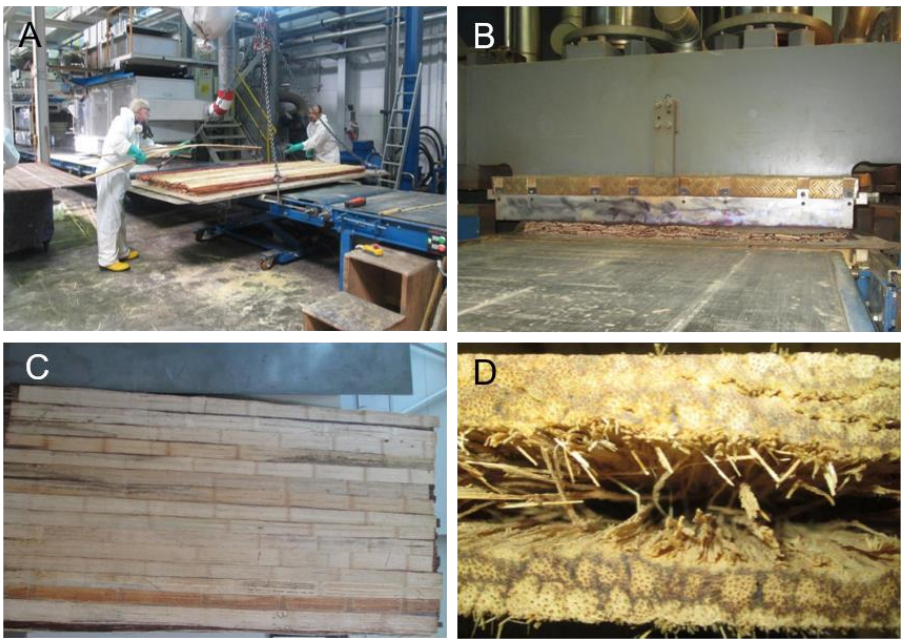

Figure 72: Manual fiber bundle layup (A), hot press compression (B), finished bamboo scrimber panel (C) and blow-out in the cross section from the industrial scale pilot production

Due to the relatively high specific pressures, another weak point in the industrial batch hot-pressing was identified. Once the press closed, the bamboo fiber bundle mat tended to spread laterally. Consequently, the produced panel showed an unfavorable in-plane density gradient. In other words, the density at the edges of the produced scrimber panel was lower than in the horizontal center of the panel. In a commercial stage, this may cause offcuts of up to 80 mm lengthwise. With a 22 mm thick panel this means roughly a 12 % production loss (0.069 m³ instead of 0.078 m³ per panel). This effect was observed in the laboratory press as well and was avoided by using a soft frame which is however no feasible solution at industrial scale. A soft frame made from foamy materials, such as low-density fiberboards is destroyed after each batch and cannot be recovered. The press manufacturer thus suggested a set of lateral self-retracting levers which hold the fiber mat in position.

After curing and conditioning the industrial panel IB was examined with 0.6 N/mm² which compared with laboratory results at similar resin concentration shown before (see figure 71). The too high vapor pressure cannot be resolved only by adjusting press parameters but needs special attention before the fiber bundle mat gets into the press. Though the press is the production bottleneck, the industrial heat treatment and the resin application are the key to reduce the cycle time by optimizing moisture content in the panel before pressing.

Table 27: Internal bond (IB) and press observations of industrial bamboo scrimber panels with different opening times (t) and opening temperatures (T) in the panel core

Panel dimensions [mm]	MC_{in} [%]	c_{resin} [%]	t [min]	T [°C]	IB [N/mm²]	Observation
			45	120	n/a	panel blow out; press time
			60	116	n/a	panel blow out; press time
1,400 x 2,550	13	10	240	84	0.5	untreated scrims
			240	89	0.4	heat treated scrims
			240	87	0.6	untreated scrims

4.4.5.2 Resin application

Two ways of industrial scale resin application, namely liquid extrusion gluing (LEG) which is an adoption of the curtaining technique and circular jet gun spraying (CJG) analogous to the laboratory technique were compared. Resin was applied to 1.6 m long scrim strands which were then cut in half to produce a hot-pressed sample on site in Finland. In both test cases the spreading rate was tuned by adjusting the conveyor belt speed and flowrate in the resin system. The scrim strands passed the application station lengthwise and made a homogeneous distribution challenging. The individual weight and geometry of each fiber bundle could not be included online. Consequently, the statically configured resin throughput rate caused different concentrations on each bundle. The results are presented in table 28. The results showed that the target resin concentration was not accomplished satisfactorily for neither method. The coefficient of variation of the resin concentration among the single scrims was notably higher for the LEG curtaining than for the spray application. On the other hand, the scrims used for curtaining showed lower dry mass and nearly double the variation than the bundles used for spray application.

Table 28: Weight of scrim and resin and the resulting resin concentration using two industrial application methods: circular jet gun spraying (CJG) and liquid extrusion glue curtaining (LEG)

n=15	**scrim strand [g]**	**resin [g]**	**c_{resin} [%]**	**scrim strand [g]**	**resin [g]**	**c_{resin} [%]**
	CJG spraying			**LEG curtaining**		
Mean	366.4	56.0	15.5	264.1	41.6	16.9
SD	62.8	7.4	2.0	88.6	5.6	3.5
COV [%]	17	13	13	34	14	21

The CJG spray application was done from the top and the bottom of the fiber bundle simultaneously. The nozzles were encapsulated, with an only narrow opening for the fibers to go through in lengthwise direction. In this manner an excessive atomized resin solution would be avoided in the factory environment. The complete resin amount was applied in one pass which caused small droplets forming on the fiber seen in figure 73A and B. It was expected that this would not cause problems during hot pressing where the resin would spread evenly with heat and steam. A lot of splinters had stuck to the cover on the infeed of the spraying box. Also, a lot of glue remained inside the housing metal sheets. A re-use in the industrial line would need a proper mechanical screen to get rid of the contaminating fibers. Especially the bottom nozzle of the spraying box would need frequent maintenance to avoid clogging and uneven resin spread.

LEG application was commonly used where one-sided spreading in plywood industries was needed. The resin solution pumps through a pipe system and the gradual inside design of the application heads ensures even glue spread in the width direction. The LEG applications heads are normally designed for 8 or 4 ft wide lines. For test purposes a 60 cm wide unit had been prepared with the same conveyor belt speed as it was done in the CJG application. Instead of stripe-formed adhesive lines the images in figure 73A and B the scrims showed large resin droplets. The used system was optimized for high viscosity resin solutions as used in plywood gluing. The low viscosity of the aqueous resin solution would have needed different kind of gluing application head design. Both application variants provided at least apparently similar adhesive lines and at first glance did not differ in cross-section (figure 73C) or side (D). However, the top side (F) of the one-sided LEG panel has revealed flaws that still need to be

assessed. The underside (E) of the LEG panel also showed the slightly poorer distribution of the resin on the surface. Whether and how this affects the panel properties could not be shown here.

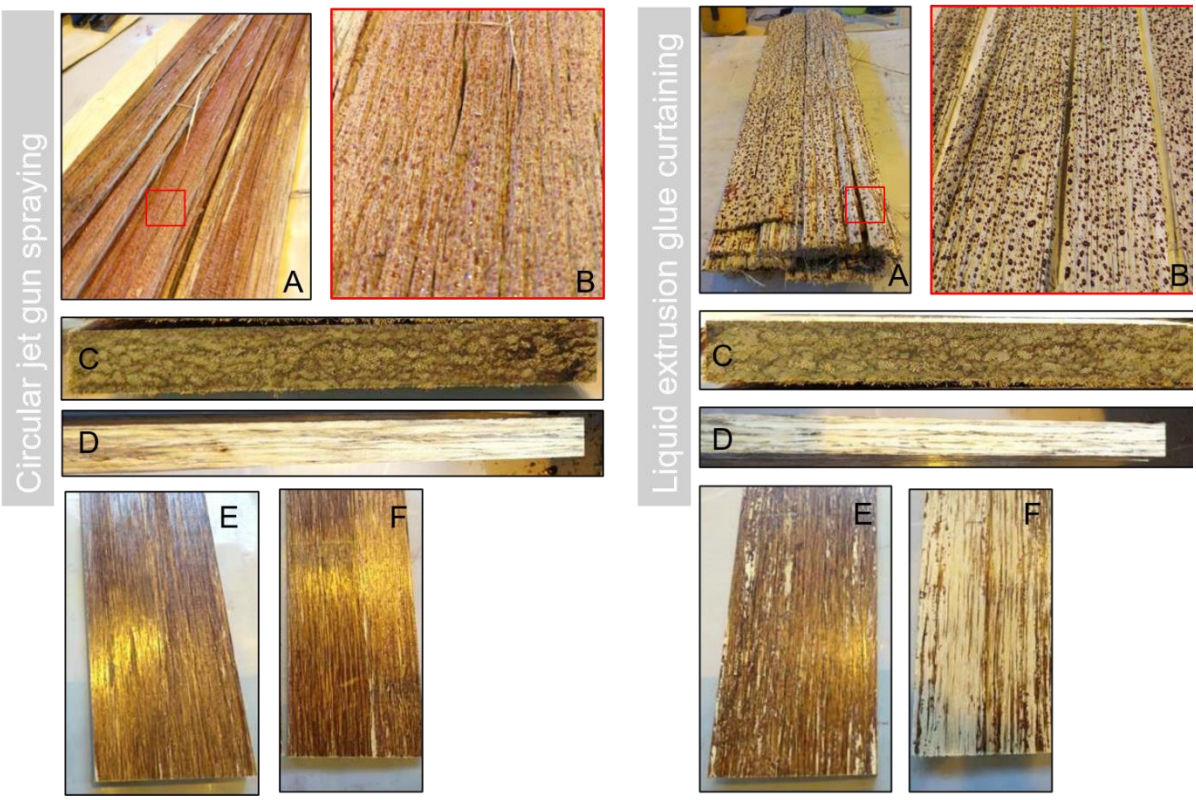

Figure 73: Resin impregnated highland bamboo scrims (A) in close-up (B) applied with industrial curtaining and spraying and the resulting hot-pressed panels as seen in cross-section (C), lateral (D), top (E) and bottom (F)

Compared to CJG, the LEG application method was the cleaner solution for the working environment, i.e. air and machinery. Nevertheless, both application methods struggled with a significant resin amount missing the scrim strands and would make a filter and recovery system necessary. To minimize this amount bundles might be fed sideways as full sheets like in a plywood line. This means that there would be always fibers under the application head and only minimal amount would miss the bundle at both ends of. With a cut 2.6 m long fiber bundle the application head could be 2.7 m wide with a 5 cm surplus at both ends. This relates to less than 2 % of the resin volume would potentially fall of the line. When feeding bundles lengthwise, the application area is narrow. Scrim strands are not equally wide and might change from 5 to 15 cm which consequently leads to glue recycling rates of up to 50 %.

4.4.5.3 Heat treatment

Before resin was applied, the air-dry bamboo scrims were treated in an industrial scale at 160 and 180 °C and the manner of packing the those was analyzed. Spacing and layer thickness were investigated and the difference of input and output weight (mass balance) was measured on site. The spacing and layer thickness is of high importance because it determines the tradeoff between heat treatment quality and batch size. The masses in table 29 contained the dry mass of scrim strands and the (presumably constant) weight of the aluminum spacers. The measured values thus contained the actual loss of volatile substances as a result of the heat treatment process. The mass balance in table 29 further shows the measured equilibrium

moisture content after conditioning the sample at standard climate (20 °C/65 %) and the regarding calculated dry mass as a mean of the four batches. The highest mass loss of 7.1 % was found with 20 mm thick layers and 20 mm spacing in between at the 180 °C treatment. Interestingly, the thicker layer of 40 mm resulted in a much lower mass loss of 3.94 %. The airflow seemed not to be able to transport all emergent gases anymore. The same layer and spacer setting and 160 °C treatment temperature yielded the lowest mass balance difference, namely 1.95 %. Despite the duration of the industrial scale treatment was nearly ten times more than in laboratory, the 160 °C seemed to be too low to notably degrade structural polymers in the fiber bundles. On the other hand, the EMC was nearly halved after treatment which indicated a substantial reduction of hygroscopicity. The low mass loss indicated that only accessory components as described in 2.3.2[5] were removed. Despite the actual treatment duration was 3 h, the whole batch took more than 24 h and other degradation effects might have played their role in reducing hygroscopicity as well.

Table 29: Calculated mass difference (Δm) and equilibrium moisture content (EMC) at standard climate (20 °C/65 %) of highland bamboo fiber bundle batches before and after heat treatment in an industrial scale chamber using different layer thickness (LY) and spacing distance (SP) between the layers for temperatures of 160 and 180 °C and 3 h holding time

T [°C]	**160**		**180**					
LY/SP [mm]	**40/20**		**20/20**		**40/20**		**100/30**	
m(u=0) [Mg]	Before	After	Before	After	Before	After	Before	After
Batch 1	0.535	0.519	0.527	0.502	0.554	0.537	0.534	0.522
Batch 2	0.545	0.540	0.478	0.440	0.537	0.503	0.459	0.448
Batch 3	0.472	0.468	0.502	0.469	0.554	0.513	0.614	0.597
Batch 4	0.474	0.460	0.479	0.435	0.545	0.551	0.688	0.653
Sum	2.026	1.987	1.986	1.845	2.190	2.104	2.295	2.221
Δm [%]	**1.95**		**7.10**		**3.94**		**3.25**	
EMC [%]	15.58	**7.56**	15.45	**3.52**	15.53	**5.29**	15.55	**7.18**

As mentioned earlier, the layer thickness and spacing distance is relevant to the batch size and thus has economic impact to the process (energy costs). An additional LY/SP setting was treated with 180 °C. The bundles were stacked in 100 mm thick layers and the spacer distance gap in between the layers was increased to 30 mm. The resulting mass loss of 3.25 % was close to the 40/20 mm setting but less than half the 20/20 mm setting. However, the EMC was at a relatively high 7.18 % and rather corresponded to the 160 °C treatment. The temperature inside the layer was not lower than at the surface which was made sure by monitoring with probes during the experiment. Consequently, the difference must have to do with the removal of degradation products. The hot air stream was presumably not as effective in the core of a 100 mm thick layer and might have left behind sorptives such as degraded hemicellulose fractions or degraded accessory substances. This presumption was supported by the slightly higher EMC in the 40/20 setting than the 20/20 setting.

Figure 74: A chamber-ready batch of manually stacked scrim strands with 20 mm spacing and 20 mm layer thickness separated by aluminum spacers

Generally, the fibrous nature of the treated material made the stacks less permeable for the airstream than solid timber would do. The desired laminar airflow at the layer surfaces was presumably disturbed and consequently hindered an efficient transport of volatile gases and steam. While only one fan with a capacity of 7.5 kW was installed in the single utilized chamber, the industrial project plant would potentially use two or four of these chambers. With a second fan, the transport of volatile gases might have been facilitated and the tests might have led to better results. Additionally, it needs to be taken in consideration that preparing (laying, handling, loading, unloading) a fiber bundle stack for thermal treatment is manual work. One single chamber (LY20/SP20) takes an untrained laborer nearly one working shift. Therefore, considering thicker layers would decrease the efforts. Nevertheless, a spacing of at least 20 mm was recommendable.

The desired EMC after heat treatment is another important criterion. For bamboo scrimber higher pressures are applied than in OSB productions. Based on empirical observations, the kiln-dried, heat-treated and resin wet scrim strands shall not exceed a MC < 13 %. Especially in tropical environments with high RH, the dry scrim strands leaving the chamber would take water up to EMC within a few hours only (Rabik 2016). The process is not a completely automatized and continuous one so intermediate stock of heat-treated scrim strands is indispensable. Hence, the thermal treatment should ideally lower the EMC of the scrim strands to a certain target level before resin application. Simple MC is calculated as per below:

$$\mathrm{MC} = \left(\frac{\mathrm{m_u} - \mathrm{m_0}}{\mathrm{m_0}}\right) * 100 = \left(\frac{\mathrm{m_u}}{\mathrm{m_0}} - 1\right) * 100 \qquad [\%] \qquad (4\text{-}2)$$

where

$\mathrm{m_u}$	-	Mass of wet sample	[g]
$\mathrm{m_0}$	-	Mass of dry sample	[g]
MC	-	Moisture content	[%]

The equation for a target MC after heat treatment then deduces by using the prior formula (4-2) and transform it with resin-applied and heat treated scrim strands:

$$\mathrm{MC}_{pressready} = \frac{\mathrm{c}}{100} * \left(\frac{\mathrm{m_{uPF}}}{\mathrm{m_{0PF}}} - 1\right) * 100 + \left(1 - \frac{\mathrm{c}}{100}\right) * \left(\frac{\mathrm{m_{uTM}}}{\mathrm{m_{0TM}}} - 1\right) * 100 \qquad [\%]$$

where

c	-	resin concentration	[%]

and then transposing to the summarized form of the target MC after heat treatment:

$$\mathrm{MC_{TM}} = \left(\frac{\mathrm{m_{u_{TM}}}}{\mathrm{m_{0_{TM}}}} - 1\right) * 100 = \frac{\mathrm{MC}_{pressready} - \frac{c}{100} * \left(\frac{\mathrm{m_{u_{PF}}}}{\mathrm{m_{0_{PF}}}} - 1\right) * 100}{\left(1 - \frac{c}{100}\right)} \quad [\%]$$

The planned industrial production may, for example, use a target resin concentration of 10 % (dry mass) and a water to resin ratio of 50:50. Inserting in the above equation the desirable moisture content after heat treatment (and moisture uptake to equilibrium in a standard climate) calculated $\mathrm{MC_{TM}} = 3.33\ \%$. The treatments at 180 °C from table 29 resulted EMC from 3.52 to 7.18 %. Sorption isotherms investigated at laboratory scale by Schmidt (2013) showed that a 2 h treatment at 180 °C resulted in EMCs between 5 and 7.5 %. This was notably higher than the calculated 3.33 % (all related to a standard climate 20 °C/65 %). Since the EMC value from that experiment based on an investigation of only 21 specimens, it can be assumed that the calculated value was correct in theory. Considering the practical aspects of the production however, a target MC between $3.0\ \% > \mathrm{MC_{TM}} > 5.0\ \%$ after thermal treatment and moisture uptake was recommended. Consequently, the LY20/SP20 and LY40/SP20 mm setting delivered suitable scrim strands for treatments at 180 °C. Thicker stacked layers and lower temperatures may not be appropriate for the industrial scale.

4.5 Intermediate conclusion

A tentative production was undertaken, followed by an extensive production parameter screening. The effect of resin distribution, fiber bundle preparation and sorting has been investigated, followed by upscaled pilot production on industrial equipment.

Firstly, the tentative production trials confirmed that panels produced with conductive heat cannot be much thicker than 20 mm, resin application in dipping tanks causes excessive process moisture and at least 130 °C panel core temperature was needed to sufficiently overcome the thermal lethargy of the laboratory system.

Secondly, the parameter screening returned ambiguous results with no evidence for resin selection, heat treatment temperature or duration and wax addition. Although clear statistical explanatory power was not at hand, a plywood resin (PF2) was selected for the further research steps. A cluster analysis then showed that addition of 2 % wax decreased thickness swelling by 35 % yet bond performance was not affected. Heat treatment had a comparable effect, reducing thickness swelling by 38 % but worsened internal bond slightly from 0.8 to 0.6 N/mm². Heat treatment influenced thickness swelling and internal bond equally whether, high (200, 220 °C) or low (160, 180 °C) temperatures were applied. Considering the high statistical spread in both groups, the lower temperature group seemed equally appropriate. Additionally, a significant drop in flexural MOR was observed for the high temperature cluster. Further investigations shall thus consider only untreated and mildly heat treated scrim strands which also offers cost advantages.

Thirdly, it was shown that differently resin-impregnated layers in the vertical plane can steer the thickness swelling and internal bond to a certain extent. For cost reasons the core and face layers shall be produced with as few resin as possible. Where a very low thickness swelling was desirable, especially the panel core layer resin content must be increased. Moreover, internal bond was not notably affected when face layer resin content was increased but did improve by 37 % once the resin bulk loading was increased from 12 to 16 %. Heavy exposure to moisture caused the bonding quality to drop by a third. This effect could only be counteracted by increasing the concentration in the core. The influence of the culm height section (top, middle, bottom) on thickness swelling and internal bond was negligible. The multiple crushing of the T strips yielded finer scrims which improved the panel compaction behavior but did not lead to better IB and TS. At low resin concentration (5 %), the finer fiber bundle texture (area surface) notably increased TS. The IB was not affected and developed solely congruent with resin concentration. Systematic investigations combining target density, resin concentration and fiber bundle geometry must be done to further understand the bonding mechanisms in the hot-pressing of bamboo scrimber.

The upscaling experiments then showed the technical constraints which hinder the laboratory knowledge to be transferred to industrial production. Press-ready scrim strands regained moisture in the resin application and led to notable vapor pressure in the press resulting in panel blows. Although resin spraying showed a slightly better distribution on the scrims, it was not essential whether it was applied by spraying or liquid extrusion. A spray applied to both sides of the bamboo fiber but at the same time was messy and process resin recycling challenging. The curtaining method was generally cleaner and recycling easy but the one-sided application must prospectively be investigated for bond quality.

The extensive pressing time was caused by the slow passive cooling and resulting pressure exceeding IB. The equilibrium moisture content of the non-impregnated fiber is therefore of greater importance and should be kept below 5 %. A heat treatment of at least 160 °C was

indispensable at industrial scale, but the effect was highly prone to the stack structure (gaps, package thickness). For optimal press-ready fiber bundle mats at given 10 % resin concentration, the most effective treatment was achieved at 180 °C with layered fiber bundle stacks not thicker than 40 mm and a spacer distance of 20 mm. Further systematic industrial tests on an installed line will be necessary to find the optimal tradeoff between heat treatment quality, energy consumption and process time. A direct link to the product quality requirement is needed for a goal-oriented process steering.

5 | Export market requirements

This chapter takes the boards from the upscaled, quasi-industrial production to a comprehensive testing program. The performance of highland bamboo scrimber (BS) used as flooring and decking product was assessed in the four branches shown in figure 75. In the introduction of the chapter the applied test program was developed from existing European, national and international standards, as well as informal regulation and certification systems. The present chapter comprises explanations on recent developments of test standards as well as results on flexural performance, surface resistance against mechanical wear, dimensional stability, resistance against weathering and biodegradation by fungi. The resistance of highland BS against wood-destroying fungi was examined and thus exemplified the current challenges of choosing the right standard and applying it to a new product.

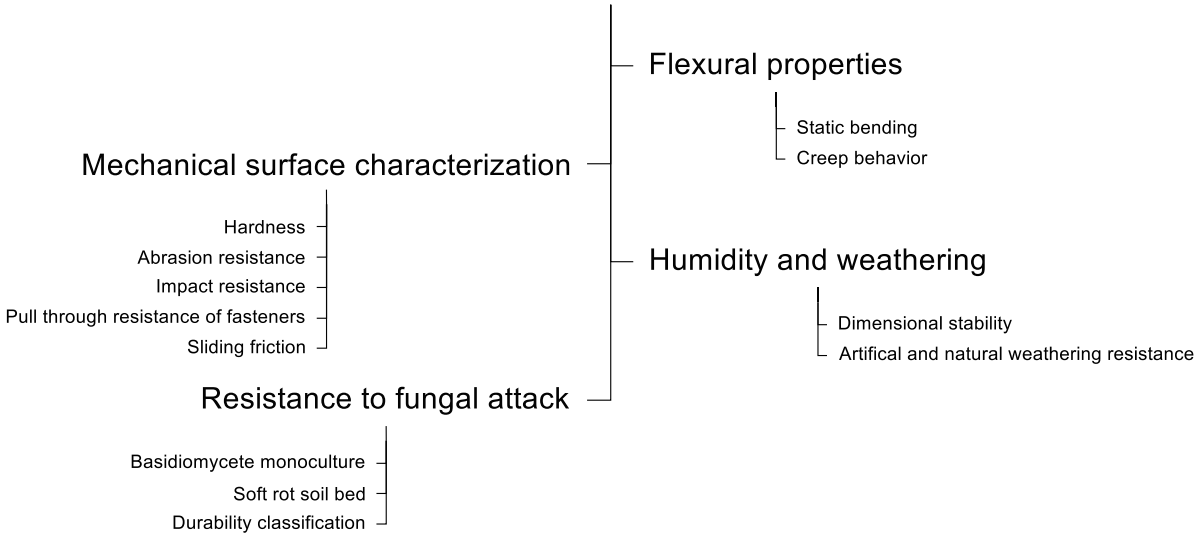

Figure 75: Structure of the export market requirements chapter

5.1 Introduction

Exporters from developing countries need to comply with international standards to successfully enter high purchase power markets. The facilitation of international trade in the last decades was accompanied by additional non-tariff barriers increasing in complexity. Those comprise technical regulations, consumer health or phytosanitary regulations. Additional voluntarily applied private and public standards, established by retail consortia, hinder companies from developing countries from export. Once the export product meets the technological requirements of the target market compliance must be proven. The CE-marking (*Conformité Européenne*) is obligatory and based on regulations which only accredited institutions can assess. Commonly, testing of a product at a certified laboratory determines whether the product fulfils the given requirements or meets the declared values. The responsible authority organ on national level in Germany is the *Deutsches Institut für Bautechnik* (DIBT), or Center of Competence for Construction. Such a “foreign” certification body must be consulted which consequently leads to high per unit costs especially for new market players with low trade volumes.

5.1.1 Towards an export standard for outdoor bamboo scrimber

Outdoor decking and flooring products are subject to various external stresses, loads and environmental factors. European standards for building products regulate which minimum requirements are obligatorily to be fulfilled. Outdoor decking made from wood is covered by the European construction products regulation no. 305 (European Parliament 2011). The mechanical and biological properties must fulfil requirements, which are given in standards covering sawn timber product. The comprehensive range of standards for sawn timber products across Europe developed historically, hence, producers of wooden outdoor decking products grade the sawn timber into specified classes expressing the mechanical and biological properties. It is not necessary to perform mechanical or biological tests for each lot since the usual properties can be taken from referenced table values. For wood-based panels use in construction a comprehensive standard is available with DIN EN 13986:2015-06.

For outdoor decking purposes there is only one comprehensive European standard developed for wood-plastic-composite (WPC). At the time when of market penetration the European standard body created a series of standards (DIN EN 15534-1 to -6) representing a comprehensive range of requirements and material tests applicable for outdoor products made from natural fibers and a thermoplastic matrix. For testing highland BS used outdoors, the DIN EN 15534-1:2018-02 provided the baseline set of methods.

The regulatory situation for bamboo products is totally different: International trade of bamboo and bamboo-based building products was always constrained by outmoded policy frames (Buckingham *et al.* 2011, Liu *et al.* 2015b) and low quality perception (Buckingham *et al.* 2014). Outdoor decking produced from non-wood lignocellulosic materials is not covered by a historically grown set of standards. For the sake of a wide range of technical export market requirements for bamboo scrimber outdoor decking a comprehensive testing program shall be addressed in this chapter. Therefore, legal standards for indoor bamboo and wooden flooring, Chinese bamboo scrimber, outdoor wood-plastic-composite decking as well as adjacent informal regulations and publications have to be analyzed and a blend of tests must be worked out for the present study.

- INDOOR FLOORING STANDARDS

The standard covering building products for flooring is DIN EN 14342:2013-09. However, the latter excludes non-wood lignocelluloses from examination and thus, new standards and methods were needed (Jones and Brischke 2017). For flooring products made from bamboo and other non-wood lignocelluloses DIN EN 17009:2016-07 was drafted and ratified lately in DIN EN 17009:2019-06. Though being intensively pushed by private initiative (MOSO 2017, SKH 2014), the European standardization process took more than five years and explicitly covered indoor products (use class 1 and 2) only. For outdoor uses, such as decking products made from bamboo a formal framework is still not available in Europe. A comprehensive branched brainstorming of market requirements can be found in figure 105 (appendix) and was extracted from the flooring standards and modified with experiences of retailers and consumers.

- CHINESE BAMBOO SCRIMBER STANDARD

Outside Europe there is a homegrown Chinese bamboo scrimber norm, namely GB/T 30364:2013-11, which creates a harmonized standard for wood-based panels (GB/T 17657:2013-11). Neither one of the two Chinese product standards[17] are of obligatory nature but provide orientation for technical requirements. Li and Chen (2010) cited the Chinese minimum requirements from GB/T 17657:2013-11 which in the case of BS asks for a density > 1 g/cm³, IB after wetting cycles > 0.3 N/mm², TS < 2 %, MOE > 10 kN/mm² and MOR > 100 N/mm². Remembering that these values are very close to what has been found in the prior engineering chapter. The explicit bamboo scrimber standard GB/T 30364:2013-11 then distinguishes between indoor and outdoor uses, but irrespective production method, fiber bundle treatment or coating (see figure 76).

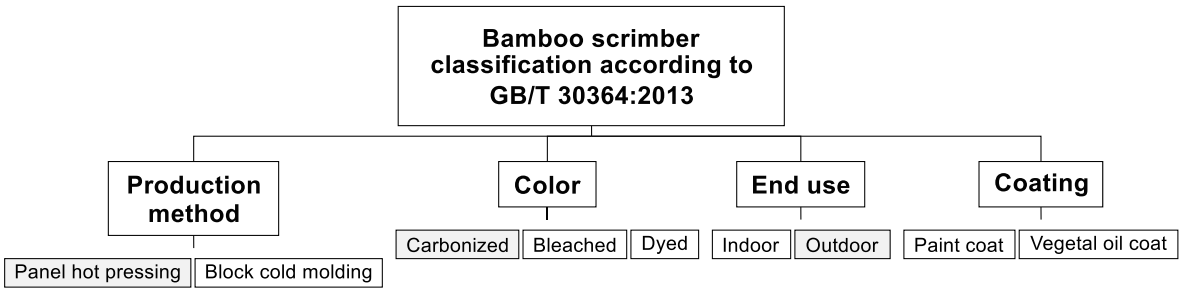

Figure 76: Bamboo scrimber classification with regards to the testing standard GB/T 30364:2013-11

For the here studied BS outdoor products, the standard demands density above 0.8 g/cm³ and EMC between 6 to 15 %. The standard additionally demands highest resistance against UV related discoloration (变色菌). For the dimensional stability and biological resistance, the standard defines an index value (指标值) which differentiates excellent quality (优等品) from qualified products (合格品). For example, thickness swelling must not pass 3 and 4 %, respectively. Regarding resistance against biodegradation (木材防腐性) the Chinese standard demands class 0 and 1 (growth density) for superficial mold fungi (霉菌) and a durability class 1 for decay fungi (腐朽). Generally, the test methods used for GB/T 30364:2013-11 cite from GB/T 17657:2013-11 which in turn is similar to their European counterpart, but do not explicitly

[17] The “GB” stands for national standard (国标) where both standards are nevertheless suffixed with a “T" which declares their optional nature as recommendable (推荐)

name them. Despite their technical and formal exclusiveness to the national context of the Chinese market, the relevance of the test topic towards the GB/T standards has been included in table 30.

- INFORMAL REGULATIONS AND PUBLICATIONS

The assessment base document developed by a Dutch certification consultancy (SKH 2014) stated that the following properties would affect the performance of decking in exterior use: Strength, stiffness, durability, hardness, impact energy of the break, wear resistance (abrasion), slipperiness, screw extraction resistance and UV resistance. Nevertheless, the Dutch guideline did not define minimum requirement for bamboo-based decking. For a technical feasibility study on highland BS for indoor and outdoor use Schmidt *et al.* (2016a) suggested a testing program comprising four categories: The mechanical performance (1), moisture and weather-related performance (2), performance against biological attack (3) and consumer health (4). On this base each topic relevance was reviewed in the priorly mentioned standards and regulations and a legal standard was derived in the four categories were shown in table 30.

In the following, the four categories flexural performance, mechanical surface characterization, weathering and biological durability will be addressed. The method procedures will be discussed and adapted to bamboo scrimber outdoor decking. Formaldehyde emissions were not prioritized due to the outdoor use. The resistance against discoloring micro-fungi, algae and termites were not included in the chapter for capacity reasons but should be considered prospectively. A test for pull through resistance of fasteners was included as recommended in DIN EN 15534-1:2018-02 and DIN EN 13986:2015-06.

Table 30: Potential test program for bamboo scrimber products in outdoor decking purposes, modified from Schmidt *et al.* (2016a)

	Topic	Relevant for	Common legal test procedure
1	Bending properties, deflection	DIN EN 15534-1:2018-02; DIN EN 13986:2015-06; GB/T 30364:2013-11; SKH 2014	DIN EN 310:1993-08
	Falling mass impact resistance	DIN EN 15534-1:2018-02	BS EN 477:2018-08
	Brinell hardness	DIN EN 15534-1:2018-02; SKH 2014	DIN EN 1534:2011-01
	Resistance against abrasion	SKH 2014	DIN EN 15185:2011-07
	Flexural creep behavior (WBP)	DIN EN 13986:2015-06	DIN EN 1156:2013-10
	Flexural creep behavior (NFC)	DIN EN 15534-1:2018-02	DIN 899-2:2015-06
2	Determination of moisture resistance under cyclic test conditions	DIN EN 15534-1:2018-02; DIN EN 13986:2015-06	DIN EN 321:2001-11
	Dimensional stability associated with changes in relative humidity	-	DIN EN 318:2002-06
	Resistance to weathering (natural)	DIN EN 15534-1:2018-02; GB/T 30364:2013-11	DIN EN ISO 877-2:2011-03
	Resistance to weathering (artificial)		DIN EN ISO 4892-2:2013-06
	Thickness swelling after immersion in water	DIN EN 15534-1:2018-02; DIN EN 13986:2015-06; SKH 2014	DIN EN 317:1993-08
	Moisture resistance: Boiling test	DIN EN 13986:2015-06	DIN EN 1087-1:1995-04
3	Use class	DIN EN 13986:2015-06; DIN EN 17009:2019-06; DIN EN 14342:2013-09	DIN EN 335:2013-06
	Durability class	DIN EN 15534-1:2018-02; DIN EN 17009:2019-06; GB/T 30364:2013-11; DIN EN 14342:2013-09	DIN EN 350:2016-12
	Resistance against basidiomycetes	DIN EN 17009:2019-06; DIN EN 15534-1:2018-02	DIN CEN/TS 15083-1:2005-10
	Resistance against soft rotting micro-fungi		DIN CEN/TS 15083-2:2005-10
	Resistance against discoloring micro-fungi	DIN EN 15534-1:2018-02	ISO 16869:06-2008
	Resistance against discoloring algae	DIN EN 15534-1:2018-02	DIN EN 15458:2014-11
	Determination of resistance against termites	DIN EN 15534-1:2018-02	DIN EN 117:2013-01
4	Formaldehyde emissions inside test chambers	DIN EN 14342:2013-09; DIN EN 17009:2019-06; DIBt/AgBB-scheme for VOC/sVOC emission	DIN ISO 16000-3:2013-01
	Sliding friction coefficient	DIN EN 15534-1:2018-02; DIN EN 14342:2013-09	DIN CEN/TS 15676:2008-02

5.1.2 Flexural performance

Decking planks need to be rigid. Both, in static bending as well as in the long term, i.e. bending creep, the BS must neither fail nor notably deflect. There are numerous studies on BS strength and stiffness, all hailing their excellent mechanical properties (Fan and Fu 2017, Huang *et al.* 2019a). It is not surprising since the high density and fibrous nature of BS consequently leads to high MOR and MOE (Chung and Wang 2018b, Kumar *et al.* 2016). The influence of a heat treatment on bamboo's nanomechanical behavior was studied (Li *et al.* 2017) but no implications for BS product performance (Li *et al.* 2012a) were given. Flexural properties of scrimber from heat treated bamboo was not tested under realistic outdoor conditions (seasonally changing precipitation, temperature) before. Artificial ageing treatment according to DIN EN 321:2001-11 emulates such conditions by alternate freezing and drying cycles. This treatment was integrated in Chinese BS examination as well (Fan *et al.* 2017). In Europe, static bending shall be tested according to DIN EN 310:1993-08 which is a simple three-point bending setup. The WPC standard, DIN EN 15534-1:2018-02, set requirements for single values of maximum bending force (at failure), as well as for mean values. Single specimens shall reach $\geq$ 3.3 kN, whereas the mean shall be $\geq$ 3.0 kN. Additionally, the standard provides a requirement for the deflection at a load of 500 N. The single value of each tested specimen shall be $\leq$ 2.5 mm whereas the mean value must be $\leq$ 2.0 mm at a defined span.

For bending creep there are at least two approaches to determine bending strain and stiffness: BS can be seen as a fiber-reinforced composite or a wood-based panel. Hence, an examination either be done through DIN EN 1156:2013-10, recommended for wood-based panels, or DIN 899-2:2015-06 for fiber-reinforced composites and WPC. In both methods, the creep behavior is determined in a constant climate in a flexural test by applying and keeping a constant load in the middle region of a test specimen. DIN EN 1156:2013-10 measures both, the time to break and the time-dependent increase in deflection in a four-point bending setup. The method according to DIN 899-2:2015-06, however, takes place in a three-point bending test in regard to its application. Another difference is the testing time. In contrast to DIN EN 1156:2013-10, where long-term tests of more than 26 weeks are usual, the DIN 899-2:2015-06 allows short procedures within two days. Additionally, the comparison of deflection results with WPC products allows to interconnect the numbers with the creep study.

For bending creep DIN EN 15534-1:2018-02 set two requirements: The difference between the deflection one minute after load application and at the end of the determination shall be below 10 mm and the difference of the deflection before the load and 24 hours after withdrawal of the load must not pass 5 mm. However, bending BS is expected to show by far lower deflection compared to WPC. This results from the thermoplastic nature of WPC. The density of WPC is often higher than that of BS. However, the duroplastic resin and the axial orientation of slender scrim strands along the bending axis make BS relatively stiff compared to WPC. Thus, a new set of bending creep criteria was set. A threshold of 50 % of the initial stiffness was set for the maximum creep stiffness loss. The deflection must not pass 1 % strain after load has been applied and shall then return to 0.1 % or below after a 24 h relaxation phase.

5.1.3 Mechanical surface characterization

The BS plank used in floors and terraces must withstand high mechanical surface exposure. Haptic impressions such as touch, smell and aesthetical look do play a major role which is why surface play a major role. The mechanical performance of the BS surfaces shall therefore be

characterized in terms of hardness, abrasion, sliding friction and impact resistance. Hardness, abrasion and friction vary with the substrate and are interconnected. Hardness can be measured with many different methods which will not be discussed here. The principle used for Brinell hardness is commonly accepted for wood and wood-based panels. Schwab and Schlusen (1999) have shown that hardness of broadleaved wood species is connected to density in the range of 0.58 to 1.04 g/cm³ following a simple linear function:

$$H_B = 76.2\rho_n - 25.5 \qquad [N/mm^2] \qquad (5\text{-}1)$$

Hence, applying the relation for a thermally untreated highland bamboo scrimber with a target density around 1 g/cm³ a Brinell hardness of roughly 50 N/mm² can be expected.

In daily life of the consumer, falling objects may worsen the aesthetic appearance of the product. Flooring and decking products shall withstand that kind of impact. A test with a defined mass, volume and height determines on how resistant the product is. When BS is used as decking or cladding it is fixed with fasteners onto a substructure. A frequently observed problem with brittle materials with low shear strength and fracture toughness (e.g. WPC profiles) is the pull-through of fasteners. Commonly, galvanized or stainless-steel screws are used. Heat treated BS is expected to be more brittle which might increase the risk of pulling the fastener head through the panel. Nevertheless, the effect of heat treatment on surface characteristics has not yet been sufficiently studied.

5.1.4 Humidity and weathering

Outdoor building products are exposed to sunlight, precipitation and temperature changes. Environmental conditions fluctuate throughout the year, e.g. ambient and surface temperature of the composite, relative humidity of surrounding air, ultra-violet radiation (UV) and precipitation. These natural phenomena can degrade the lignocellulosic polymers as well as the phenolic resin in BS. The effect of heat treatment on weathering, swelling and shrinkage of the BS surfaces has not yet been sufficiently studied. Once used in an outdoor setting, BS surfaces must not crack and shall withstand such weathering effects over a long period of time. For the sake of commercial application, it is crucial to understand the durability and potential service time with special regard to combined environmental factors. UV in combination with rainwater, leads to swelling, shrinking and bleaching of the exposed surfaces. Dimensional stability due to changes in relative humidity is not mentioned in the above standards. DIN EN 15534-1:2018-02 only relates to thermal expansion and DIN EN 14342:2013-09 refers to the regarding product standards. Schmidt *et al.* (2016a) applied DIN EN 318:2002-06 which actually is a fiber board standard although scope was extended to any kind of WBP.

The change of color is one of the most common phenomena and happens to be the simplest indicator of surface degradation. A human eye notices a minimum difference between two colors ΔE_{ab} of 1 to 3 (Best 2017). Values above are easily visible and may concern the aesthetic quality of a BS decking product. It is expected that the heat treatment improves the dimensional stability of the scrimber but make it prone to weathering degradation effects.

5.1.5 Biological performance

The environmental biotic pressure on the bamboo culm and its products make protective measures necessary. The number of insects that feed on bamboo is estimated to be at least 1,200 species. Fungal degradation accounts for more than 400 species (Shu and Wang 2015). During post-harvest processing, mold and micro-fungi cause severe damage to bamboo devaluating its economic potential (Liese and Tang 2015, Schmidt *et al.* 2015, Tang *et al.* 2009). Rot fungi inflict sever damage to bamboo and timber constructions and need expensive redevelopment procedures (Huckfeldt and Melcher 2008). Protective measures with low-emission impact are required especially for processed bamboo products since their carbon sequestration potential is already lower than raw bamboo (Gu *et al.* 2019, Liese 2009).

In contrast to many wood species, bamboo in general lacks inherent protective substances (Liese and Kumar 2003), as well as an effective encapsulation strategy as it is found in wood (Dujesiefken and Liese 2008). Once a culm is mechanically processed, most of its natural barriers against biodegradation are dismantled. Wood-destroying fungi may attack any lignocellulosic raw material or product and cause three characteristic rot types (Schmidt 2010): Brown rot (BR), white rot (WR) and soft rot (SR). Different to SR and BR, many WR causing fungi can metabolize all three structural polymers in bamboo, namely lignin, cellulose and hemicelluloses. The SR causing micro fungi degrade cellulose and hemicelluloses and slightly modify lignin. Fungi causing BR only attack cellulose and hemicellulose. The SR and WR fungi are found more often on bamboo substrates than BR (Schmidt *et al.* 2013, Schmidt *et al.* 2015). Wei *et al.* (2013) tested the resistance of five bamboo species against BR, WR and SR fungi according to DIN EN 350-2:1994-10, DIN EN 350-1:1994-10 and EN 113:1996-11 and determined durability class (DC) 2, 3 and 4. Durability against BR, WR and SR not only depends on bamboo species, but on location in the culm (Schmidt *et al.* 2011) as well as age. SR causes highest mass loss (ML), especially in young bamboo culms (Sulaiman and Murphy 1993). Similar observations were made for bamboo attacked by basidiomycetes. Young culms are highly susceptible to BR (Schmidt *et al.* 2013), causing higher ML loss than WR fungi do (Hamid *et al.* 2012). This is explained by increased local lignin concentrations in mature culms, physically blocking the growth of hyphae and reducing the local equilibrium moisture content (EMC). Although, anatomical (piths) and ultrastructural features (micro-fibril angle) determine hyphae growth direction and branching mechanism (Sulaiman and Murphy 1995), these barriers only delay (Hill 2006, Ringman *et al.* 2016) rather than hinder fungi to cause damage to the substrate (Hamid *et al.* 2012, Sulaiman and Murphy 1995). Okahisa *et al.* (2006) investigated seasonal sugar fluctuations in young culms and concluded that high glucose content benefits fungal decay. Further details on fungal biodegradation of bamboo culms and protection techniques are described by Liese and Kumar (2003), Schmidt *et al.* (2011), Liese and Tang (2015) and Schmidt *et al.* (2015).

- BAMBOO SCRIMBER AND FUNGAL ATTACK

In contrast, BS panels are believed to possess excellent biological resistance, especially against basidiomycetes. Jacobs *et al.* (2011), Meng *et al.* (2017) and Kumar *et al.* (2018) reported mass loss (ML) of less than 5 % for commercial BS. It is believed that this apparent resistance is mainly attributed to the lack of moisture in the substrate. Water hardly penetrates the highly-densified, PF-impregnated BS and hence hinders fungi from degrading the structural polymers (Meng *et al.* 2017). Once this physical barrier is penetrated (long term), moisture enters, and fungal hyphae follow. Surface degradation by weathering, tension cracks due to seasonal swelling and shrinking, as well as different thermal expansion coefficients, can lead

to such openings. This effect on scrimber surfaces is riskier for low and moderate densities than for high densities (Wei *et al.* 2019a). Analogously to a wood-based panel (WBP), the face layer (FL) of a scrimber panel is believed to densify stronger than the core layer (CL) although previous results indicated a heterogenous vertical density profile (Schmidt *et al.* 2016b, Schmidt *et al.* 2016a). Reminding why it is common practice using resin concentrations beyond 15 % and densification up to 1.3 g/cm³ to make the product durable. Nevertheless, fungal attack on BS panels has not been studied sufficiently yet. To date, scrimber made from heat treated bamboo has not been tested against decay fungi such as WR, BR and SR. The present work shall bridge the research gap between the effect of heat treatment of scrims and the durability of the product. However, there is no clear regulatory situation how to assess the durability of bamboo scrimber.

- FROM THE STANDARD TO THE DURABILITY CLASSIFICATION

The new standard DIN EN 17009:2019-06 requires applying DIN CEN/TS 15083-1:2005-10 for tests against basidiomycetes. Although the durability of WBP against basidiomycetes had been traditionally assessed according to DIN V ENV 12038:2002-07, it should not be used for BS. Scrimber has more in common with glue-laminated solid wood products than mat forming panel products due to its unique processing. Generally, the variability of solid wood products is higher than WBP which explains why DIN V ENV 12038:2002-07 requires using only three batches (trees) while for DIN CEN/TS 15083-1:2005-10 six batches (or production days) are needed. The DIN EN 17009:2019-06 exclusively covers products for use class (UC) 1 and 2 as defined in DIN EN 335:2013-06. UC 1 stands for a dry indoor environment, whilst UC 2 comprises applications under a rooftop with only occasional wetting by water condensation. Situations in which BS is used in weathered situations (UC 3) or in contact to the ground (UC 4) are not covered by an own standard. For products made from solid wood applied in UC 3 and 4, DIN EN 350:2016-12 recommends testing resistance against soil inhabiting organisms according to DIN CEN/TS 15083-2:2005-10. For wood-polymer-composites, requirements in DIN EN 15534-1:2018-02 ask for the same test. Large retailers selling outdoor decking materials apply DIN CEN/TS 15083-2:2005-10 and this way they try to make a comparison to solid wood products.

The way of deriving DC from the test data has been modified recently. For declaring DC of a product, the outdated DIN EN 350-1:1994-10 had considered the simple maximum median of the mass or stiffness loss. The variability of a timber species was not incorporated, and the DC referred to the statistically worst-case scenario. The latest DIN EN 350:2016-12 takes the mode of the distribution function of durability classes, i.e. the DC value that appears most often (Ushakov 2012). To what extent this methodological difference affects the classification of BS, has not been studied before. In general, the durability of BS against wood-destroying fungi has not been evaluated satisfactorily so far. The few investigations limit themselves to commercial batches in which the production parameters are insufficiently traceable (Jacobs *et al.* 2011), unsuitable test standards were applied (Kumar *et al.* 2018), or the method was irreproducible (Meng *et al.* 2017). The present study exclusively used BS which was developed in-house using industrial equipment but comprising full batch traceability of process parameters.

5.2 Specific objective

Based on the outcomes of chapter 4 and the prior explanation in this chapter, the following questions will be addressed empirically:

- **Flexural properties in the long and short-term**
  - What is the effect of heat treatment on the flexural performance?
  - Which variant fulfils the product requirements in bending?
- **Mechanical surface performance**
  - How does the heat-treated BS surface perform in everyday, application-oriented tests, i.e. hardness, abrasion, sliding, impact and connections?
  - Which variant fulfils the product requirements best?
- **Moisture and weather-related performance**
  - Is heat treated BS dimensionally more stable than untreated BS?
  - What effect does weathering have on heat treated BS?
  - Which variant fulfils the product requirements for moisture and weathering?
- **Resistance against fungal attack**
  - Does the industrial heat treatment of scrim strands increase the resistance against soft rotting fungi or wood-destroying fungi?
  - Can BS be tested as it would be softwood or hardwood?
  - Which durability classes can be achieved through thermal treatment and the current product configuration?

5.3 Material and methods

The material and methods chapter related to the export market requirements briefly explains the treatment of bamboo and production of scrimber panels. Moreover, the section reports on the test method and statistical analyses which have been applied for examining BS flexural properties, surface resistance against mechanical and weathering factors as well as its resistance to fungal attack. Commercial products were tested to set a benchmark for the product performance for the highland BS. The commercial BS COBAM® and WPC products were purchased from the Elephant® branch at Klöpferholz GmbH & Co. KG (Bremen, Germany).

Moreover, it is important to note standards which have been valid at the time of testing (2016 to 2018) were applied. DIN EN 15534-1:2014-04 and DIN EN 17009:2016-07 specifically were counter-checked with the latest versions of those standards, namely DIN EN 15534-1:2018-02 and DIN EN 17009:2019-06 and the differences were identified. Nevertheless, hereafter only the latest standard version will be mentioned.

5.3.1 Panel production

The panels tested in this chapter were produced according to the technical scale boards from the prior chapter. The scrim strands were prepared from African alpine bamboo *Yushania alpina* (K. Schum.) W.C. Lin. in an experimental pilot plant (Addis Ababa, Ethiopia) and then shipped through Djibouti on seaway to the destination port in Venice, Italy. The shipped samples have been sealed and controlled before and after every transport station.

The scrim strands were heat treated in industrial scale container-size chambers at Bigon Dry SRL (Cartigliano, Italy) as described in the prior chapter. The treatment temperatures at industrial scale ranged from 160, 180 to 200 °C with a holding time of 3 h. The heating rate (< 7 K/h) was lower than at laboratory-scale (Starke *et al.* 2016) due to the industrial chamber volume (ca. 33 m³). One single batch took > 24 h excluding loading. At least six temperature probes inside the stacked scrims monitored the treatment temperature online through a virtual remote system. Oxygen concentration was controlled below 2.5 % through steam injections.

The panels were produced in a single daylight batch industrial Dieffenbacher hot-press (Eppingen, Germany) at Fraunhofer WKI technical laboratories (Braunschweig, Germany). The panel dimensions have been on semi-industrial scale measuring 1,400 x 1,200 x 23 mm. For each treatment variant as well as the control, six batches were made. The target bulk density was 1 g/cm³ with a controlled resin concentration of 10 % (related to dry mass). The phenolic PF2 type resin (Dynea 4976) was dissolved with 50 % solid content and then spray-applied with an atomizing nozzle, as described in the prior chapter. More details on the industrial heat treatment and production methods are to be found in Schmidt *et al.* (2016a). The samples were not surface-finished before testing. They represent the semi-finished product which can potentially be transformed into BS flooring, decking or other final products. The panel density and moisture content were determined prior to testing according to DIN EN 323:1993-08 and DIN EN 323:1993-08, respectively. Sampling and cutting happened as defined in DIN EN 326-1:1994-08.

5.3.2 Flexural properties

The static bending samples were tested according to DIN EN 310:1993-08. The three-point bending test setup determined the apparent MOE of a specific transversal area as well as the deflection at a defined force of 500 N. The test specimen rested on two supports and was loaded at mid-span and consequently deflected. The loading at a constant rate continued until the maximum load was obtained or until rupture occurred. During the procedure, the force applied to the test specimen and the resulting deflection at midpoint was measured.

5.3.2.1 Moisture resistance under cyclic test conditions

A cyclic treatment according to DIN EN 321:2001-11 was applied to the samples. The samples were exposed to three moisture cycles. Each cycle comprised water immersion, a freezing period and oven drying. The treated samples were then stored in standard climate and their residual MOE and MOR was determined.

5.3.2.2 Bending creep

The BS was tested with regard to bending creep behavior according to DIN 899-2:2015-06. The flexural-creep modulus of elasticity was calculated according to:

$$\mathrm{MOE_t} = \frac{\mathrm{L^3 * F}}{\mathrm{4 * b * h^3 * s_t}} \qquad [\mathrm{N/mm^2}] \qquad (5\text{-}2)$$

In this context L is the distance between the supports, $\mathrm{s_t}$ is the deflection at mid-span at time t, F the applied force, b and h the width and thickness of the test specimens. In addition, the creep strain under a constant load of 500 N for 24 h, was analyzed. After releasing the load, the relaxing strain was recorded. The standard strain calculation was modified to yield a percentage based on the equation:

$$\varepsilon_\mathrm{t} = \frac{\mathrm{6 * s_t * h}}{\mathrm{L^2}} * 100 \qquad [\%] \qquad (5\text{-}3)$$

5.3.3 Mechanical surface characterization

The Hardness, resistance against abrasion, impact and pull-through of fasteners as well as the sliding friction were tested. The standards applied and technical requirements are mentioned below.

5.3.3.1 Hardness and elastic recovery

The industrial scale scrimber boards together with commercial products samples were tested for their resistance to indentation against DIN EN 1534:2011-01. A tempered high-strength steel ball of 10 mm diameter was forced into the material with 2000 N within 25 s. For each treatment, five specimens (n = 5) from five boards were tested. The indentation depth was measured at the force maximum. The Brinell Hardness (HBS) was then calculated according to:

$$\mathrm{HBS} = \frac{\mathrm{F_{max}}}{\pi * \mathrm{D} * \mathrm{h_0}} \qquad [\mathrm{N/mm^2}] \qquad (5\text{-}4)$$

where $\mathrm{F_{max}}$ is the actual maximum force at the end of penetration, D being the penetrating ball diameter and $\mathrm{h_0}$ the penetration depth in mm. Since lignocellulosic materials show relaxation effects after indenting, we decided to additionally test the elastic relaxation (ER) after 24 h. Therefore, we determined the share of ER by the quotient of the two indentation depths:

$$\mathrm{ER} = \frac{\mathrm{h_0}}{\mathrm{h_{24}}} * 100 \qquad [\%] \qquad (5\text{-}5)$$

The climate in the testing chamber was controlled at 23 °C and 50 % RH. Three repetitions at defined specimen locations were conducted.

5.3.3.2 Abrasion resistance

The samples were tested according DIN EN 15185:2011-07. This standard defines a method for the assessment of the abrasion resistance of surfaces. The test was carried out on a raw panel. Neither sanding nor finishing was carried out on the sample surfaces. A Taber® Abraser (Taber Industries, NY/USA) with a S-34 rolled zinc sheet with a thickness of 0.8 mm was used for the test. Two prepared wheels applied a force of 5.4 N each on the sample.

5.3.3.3 Impact resistance

The impact resistance was tested according to BS EN 477:2018-08. The requirements were defined according to DIN EN 15534-1:2014-04. A falling mass (steel ball) of 1 kg dropped from 700 mm height must not lead to an indentation spot with a depth (h) of 0.5 mm or more. Additionally, the occurrence of visible cracks may disqualify the sample material.

5.3.3.4 Pull-through resistance of fasteners

The pull-through resistance of fasteners was tested according to DIN EN 1383:2016-07. A fastener is drilled into a pre-cut sample at a defined position and with a standardized tool and a defined torque. Hereafter, the fastener head is pulled through the panel sample and the maximum load and deflection is recorded. Though the standard describes the overall setting it does not determine the exact type of fastener to be used. In this setting a standard stainless-steel counter-sunk screw with dimensions 4.5 x 60 mm was used.

5.3.3.5 Sliding friction

The slip resistance pendulum test was conducted according to DIN CEN/TS 15676:2008-02. A portable skid resistance tester (SRT 5800 by TRL Large Rubber Slider) with a rubber slider with the dimensions 76 x 25 mm was used. The specimens (136 x 86 mm) were wetted superficially and measured at a testing area of effectively 127 x 76 mm. The climate in the testing chamber was controlled at 23 °C and 50 % RH. Three repetitions at defined specimen locations were conducted. Before testing all samples were conditioned at standard climate for two weeks. The slip resistance value is the mean pendulum value obtained from 10 specimens per sample. To pass the requirements of DIN EN 15534-1:2014-04, the pendulum test must show at least a sliding coefficient of $\mu \geq 0.36$ per each side.

5.3.4 Humidity and weathering

The dimensional stability of heat-treated BS in change of relative humidity was tested according to the fiber board standard DIN EN 318:2002-06. Additionally, two different weathering methods were used, long-term natural weathering and short-term artificial weathering in controlled laboratory conditions. The resistance to natural weathering was determined following DIN EN ISO 877-2:2011-03. The test happened at Fraunhofer WKI's facilities rooftop in Braunschweig, Germany. The specimens were installed inclined at 45° and oriented facing south. For each variant, one specimen from three different batches (panels) was exposed for a one-year period from 05.10.2016 to 05.10.2017. During exposure, the specimens adsorbed a total of approximately 3700 MJ/m² of which 146.4 MJ/m² were UV.

Resistance to artificial weathering was determined following DIN EN ISO 4892-2:2013-06. The weathering effect of materials exposed to daylight, rain and temperature changes in end-use environments were reproduced in a controlled chamber. For each variant, one specimen from three different batches (panels) was exposed to filtered xenon-arc light under controlled environmental conditions (temperature, humidity and wetting cycles) for 300 h. The change of color of the weathered surfaces was characterized via the CIELab color model. In the L*a*b (LAB) space consists of three components or channels. The color differences correspond to the Euclidean distances in each single-color channel, according to:

$$\Delta L_{ab} = L_{ab1} - L_{ab2} \quad [-] \quad (5\text{-}6)$$

$$\Delta a = a_1 - a_2 \quad [-] \quad (5\text{-}7)$$

$$\Delta b = b_1 - b_2 \quad [-] \quad (5\text{-}8)$$

Two channels measure color differences and form a colorimetric plane, i.e. the "a" axis ranges from green (-a) to red (+a) and the "b" axis from blue (-b) to yellow (+b). The third channel, also called grey-scale, shows the luminance (L) which increases from the bottom to the top. ΔE is given by:

$$\Delta E_{ab} = \sqrt{\Delta L^2 + \Delta a^2 + \Delta b^2} \quad [-] \quad (5\text{-}9)$$

Additionally, change of gloss and the general appearance (intensity of change) were determined according to DIN EN ISO 2813:2015-02 and ISO 4582:2007-08, respectively.

5.3.5 Resistance to fungal attack

The effect of heat treatment on the biological resistance of engineered BS against wood-destroying fungi was assessed using two standard tests. Prior to incubating the major decay experiment, a screening was undertaken to evaluate test fungi, estimate the effect of densification and compare panel face and core layers.

5.3.5.1 Screening

Raw bamboo and BS without any heat treatment were cut into specimens (40 x 10 x 5 mm) and incubated for 8 weeks in Petri dishes. Field-emission scanning electron microscopy (FESEM) images were taken and the raw mass loss was recorded, i.e. mass loss from abiotic factors was noted but not subtracted from the values caused by fungi. Table 31 shows the test

fungi used in the screening: Brown rot fungi *Coniophora puteana* (Schum. ex Fr.) Karst., *Gloeophyllum trabeum* (Peerson ex Fr.) and *Tyromyces placenta* (Fr.) Ryvarden as well as the white rot fungus *Coriolus versicolor* (L.) are recommended for tests in UC 2 according to DIN EN 17009:2016-07. Although bamboo is known to be more susceptible to BR causing fungi than WR, *Donkioporia expansa* ((Desm.) Kotl. & Pouz.) was added to the screening. *D. expansa* causes white rot and is capable to moisten the substrate regardless of ML or visible mycelium growth (Stienen *et al.* 2014).

Table 31: Screened fungi, strain origin, white rot or brown rot (WR/BR) and obligatory use according DIN EN 17009:2016-07

Fungus		Strain	Type	Obligatory
Donkioporia expansa	(*De*)	P188	WR	No
Coniophora puteana	(*Cp*)	BAM Ebw. 15	BR	Yes
Tyromyces placenta	(*Tp*)	FPRL 280	BR	Yes
Coriolus versicolor	(*Cv*)	CTB 863 A	WR	Yes
Gloeophyllum trabeum	(*Gt*)	BAM Ebw. 109	BR	Yes

5.3.5.2 Basidiomycete monoculture test

During the main trial ML has been determined according to DIN CEN/TS 15083-1:2005-10 and consequently deduced the DC for UC 2 as recommended in DIN EN 17009:2019-06 and defined in DIN EN 335:2013-06. Pine sapwood (*Pinus sylvestris* L.) and European beech (*Fagus sylvatica* L.) served as virulence benchmark. The scrimber panels were conditioned at 20 °C and 65 % RH for two weeks and then cut into specimens of 50 x 25 x 22 mm. Those were first sterilized by gamma radiation, moisture content was recorded and then incubated on 60 ml of malt agar for 16 weeks at 22 °C and 70 % RH.

5.3.5.3 Soft rot soil bed test

The resistance against SR was tested through a soil bed test according to DIN CEN/TS 15083-2:2005-10. Specimens from the core and the face layer were prepared as shown in and figure 106. The modulus of elasticity and the mass was recorded prior to incubation and at week 16, 20, 24 and 28. The bending test for MOE determination based on EN ISO 178:2006-04. The linear stress-strain interval from 2 to 22 N/mm² was chosen for non-destructive elasticity determination for all samples. Expectable variations due to MC differences were equalized by fully saturating the specimens with an evacuation procedure according to DIN EN 84:1997-05 prior to flexural bending. The MOE loss was calculated for each specimen and paired with the initial MOE prior to incubation. The final determination was done after 28 weeks for the scrimber samples. Beech ML was measured with the same 4-weeks interval as stated above.

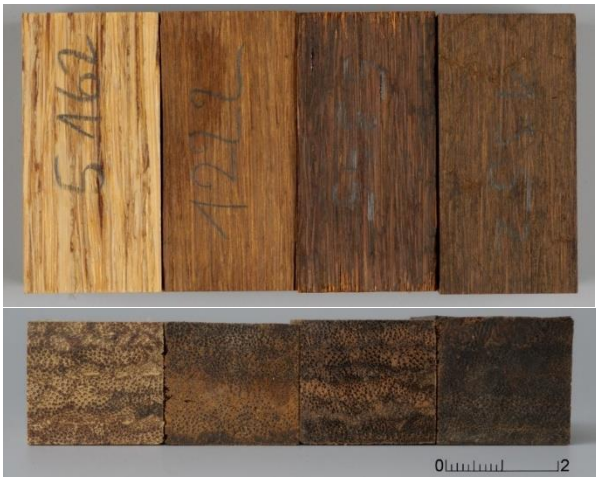

Figure 77: Top view and cross section (left) of specimens tested against basidiomycetes from samples made from heat treated bamboo scrimber (Ctrl, 160, 180, 200 °C) and specimens from surface layer and core layer (right)

5.3.5.4 Durability classification

The DIN EN 350:2016-12 defines five distinct DC displayed in table 32. The derivation of DC against basidiomycetes was done using the median ML per treatment respecting the rules of DIN EN 17009:2019-06. The basidiomycete species causing the highest median ML was taken for DC derivation in accordance with the ML criteria in table 32. The ML values of the very same sample were then used to compute the DC variation among the classes.

For outdoor applications and ground contact, DIN EN 335:2013-06 defines use class 3 and 4 and DIN EN 350:2016-12 sets a test against SR in a soil bed according to DIN CEN/TS 15083-2:2005-10 for preliminary durability classification. Since virulence of fungi is not constant, the mass or MOE loss of a tested sample is divided by the one of a low durability reference timber to yield the x-value needed to classify in accordance to table 32. Pine sapwood is used for the MOE loss calculation and beech for ML.

Table 32: Durability class (DC) derived from mass loss figures for basidiomycetes and x-values computed from mass loss (ML) and stiffness loss for soft rot testing according to DIN EN 350:2016-12 as referred by DIN EN 17009:2019-06

Durability	**Class**	**Basidiomycetes [%]**	**Soft rot [-]**
Very durable	DC1	ML ≤ 5	x < 0.1
Durable	DC2	5 < ML ≤ 10	0.1 < x ≤ 0.2
Moderately durable	DC3	10 < ML ≤ 15	0.2 < x ≤ 0.45
Slightly durable	DC4	15 < ML ≤ 30	0.45 < x ≤ 0.8
Not durable	DC5	30 < ML	x > 0.8

For modified wood, van Acker and Palanti (2017) understand variability as a performance indicator. The DIN EN 350:2016-12 requires to incorporate variability in testing and analysis. The standard further asks for the class distribution of the mass and MOE loss values of the tested material, based on adjusted probability distribution functions, in different durability classes. If a parameter spread to more than 40 %, once each in two DC, the product was declared in a DC range (x – y). In case there was a remarkable variation, the DC had to be marked (v).

5.3.6 Statistical analysis

All results have first been tested for outliers either in a Grubb's test ($n > 10$) or in a Nalimov test ($n \leq 10$). Subsequently, descriptive statistics were produced (median, mean, SD, min, max) and data was checked for normal distribution and equal variance of means. The significance of mean differences was then either checked using (2-w)-Anova, Kruskal-Wallis-Anova (KW-Anova) or a χ^2-test for categorical factors. Dunn's post-hoc test identified the mean differences. Screening results have been checked for plausibility and median values were calculated. No further statistical analysis was applied. All graphs, diagrams and analyses were produced using OriginPro 9.1 (OriginLab Corporation, USA).

5.4 Results and discussion

The technical market requirements as discussed in the introduction were tested empirically and results were sub-divided in four parts. The flexural properties of heat-treated bamboo scrimber are presented for static and bending creep and related to the raw material properties. The second part dealt with the mechanical surface characterization followed by the weathering experiments. The last part presents results regarding fungal attack and discusses the different methodologies and their effect on the durability classification.

5.4.1 Flexural properties

This section presents results and discussion of industrially produced scrimber from heat treated African highland bamboo in static bending before and after cyclic moisture treatments and its flexural creep behavior.

5.4.1.1 Static bending

The MOE and MOR were measured in a three-point bending setup. The three variants (untreated, 160, 180 °C) were tested after a wetting cycle according to DIN EN 321:2001-11. The results for the flexural MOE before and after cyclic treatment are shown in figure 78. The variant treated at 180 °C resulted in the highest MOE with 22.11 kN/mm². The untreated scrimber showed the lowest value being 19.72 kN/mm². This is a well-known effect which at least partly has its cause with the lower EMC in thermally modified bamboo (Doering-Arjes and Schmidt 2018). The results of the one-way ANOVA showed that all flexural MOE means under standard climate conditions differed significantly from each other. Once underwent the moisture cycle, all variants suffered a severe MOE loss. In contrast to the dry conditions, figure 78 shows that the untreated sample lost few while the 160 and 180 °C ones dropped by more than one third.

The flexural MOR before and after cyclic treatment is shown in figure 78 (top left). The untreated BS had significantly higher MOR (132.71 N/mm²) compared to the 160 and 180 °C treated samples with 82.81 and 84.08 N/mm², respectively. The comparison with the commercial product (128.30 N/mm²) showed that the bending MOR of the untreated panel ranked within highest quality range. The bamboo scrims for the commercial product were not thermally modified prior to production. Nevertheless, the commercial panel comprises a higher bulk density and resin content, i.e. the specific MOR of an untreated highland BS was superior to the commercial variant. The SD of all tested variants was within an expected +/-10 %, which was acceptable for a lignocellulosic composite panel.

Scrimber made from untreated bamboo with comparable panel target densities and resin systems, found in Fan and Fu (2017), Xie *et al.* (2016), Kumar *et al.* (2016) and Guan *et al.* (2012), showed flexural MOR of 220.6, 193.0, 132.0 and 203.0 N/mm², respectively. Despite the MOR of the heat-treated samples ranged at the bottom line of the commercial and literature references, the MOE ranks within market compatible values. Additionally, the maximum deflection and the maximum load of the characteristic cross-section were recorded. No single specimen showed $F_{max} \leq 3.3$ kN. Moreover, no mean $F_{max} \leq 3.0$ kN, i.e. standard requirements were completely fulfilled. Values for deflection and maximum load are shown figure 78 (bottom). At their maximum deflection single values of each tested specimen remained $\delta \leq 2.5$

mm and mean deflection was δ < 2.0 mm for all samples. The requirements for both, maximum flexural force and maximum tolerable deflection at 500 N were fulfilled. Both criteria, mean values as well as for single values, were fulfilled according to DIN EN 15534-1:2014-04.

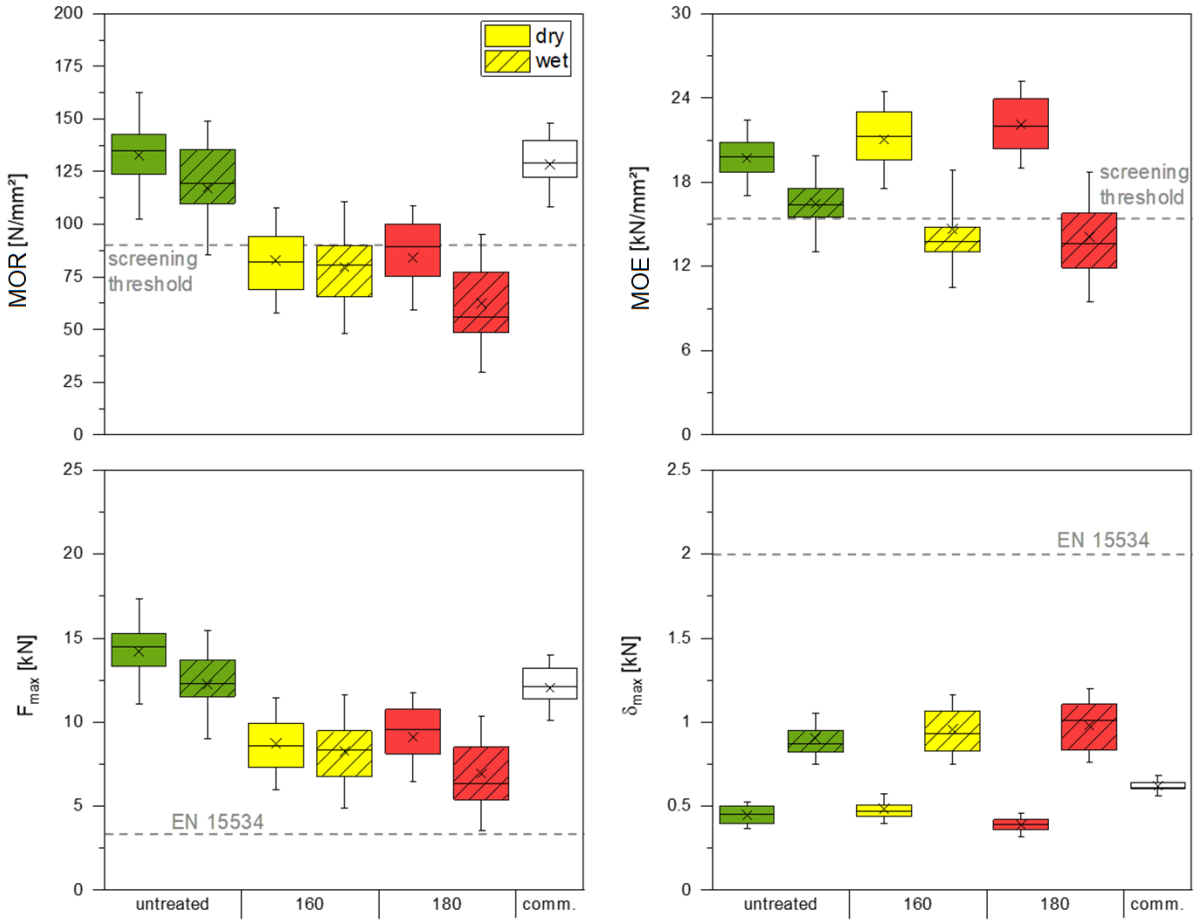

Figure 78: Mean flexural modulus of elasticity (MOE), strength (MOR), maximum load (F) and deflection (δ) of industrial-scale scrimber produced from untreated and heat treated highland bamboo (160, 180 °C) before (dry) and after (wet) a moisture cycle

Figure 79 shows the clustered values of BS flexural MOR against MOE and compares it with values obtained on unprocessed highland bamboo tested in compression, bending and tension. The flexural MOE of raw bamboo ranged between 10 and 25 kN/mm² but bending MOR spread from 100 up to 275 N/mm². At the same time tension MOE values of raw bamboo started below 8 kN/mm² and reached up to 32 kN/mm². The tension MOR comprised values from 50 N/mm² nearly up to 300 N/mm². In contrast to compression, the bending and tension values overlapped along a constant density line. The untreated scrimber (green) showed a slightly increased MOE-to-MOR ratio compared to its raw material but did not outperform the raw bamboo. This applied for both, flexural MOE and MOR. At the same time, the heat treatment at 160 °C (yellow) obviously decreased MOR by more than 50% without notably MOE gains. The values spread along a steeper constant MOE:MOR ratio than the untreated ones did. The treatment at 180 °C (red) did not make the scrimber stiffer than the 160 °C (also see mean values in figure 78), but slightly reduced the MOR.

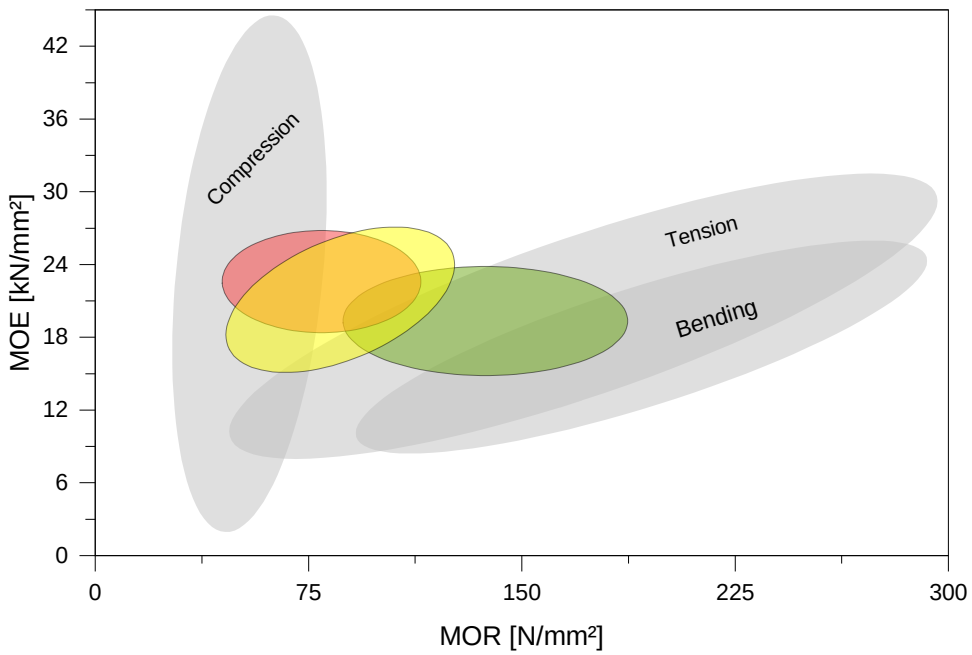

Figure 79: Modulus of elasticity (MOE) against strength (MOR) in bending, tension and compression for raw highland bamboo scrims (grey ellipses) and for industrial-scale scrimber from untreated (green) and heat treated (yellow: 160 °C; red: 180 °C) highland bamboo in bending

5.4.1.2 Creep behavior

The creep MOE was calculated for each treatment as well as for the untreated BS and the commercial BS for comparison. Additionally, the flexural creep strain was recorded under load and the recovery strain after the load had been released from the specimen. The resulting logarithmic curves are shown in figure 80. Their formulae and their regression R^2 are shown in appended table 49. Neither the mean flexural MOR, nor the MOE from the static bending tests revealed significant differences between the 160 and 180 °C treatment. In contrast, the mean creep moduli of the 160 and 180 °C samples differed in 3.22 at the initial stage and 4.34 kN/mm² after 24 h. The differences between the creep moduli of untreated and 160 °C were negligible. The curves started with an initial creep MOE of 11.23 and 12.07 and a final MOE of 8.45 and 8.40 kN/mm² for the untreated and 160 °C sample, respectively. The initial MOE of 21.11 kN/mm² of the commercial scrimber outperformed all other samples. Surprising that after 24 h, the commercial product dropped to 3.98 kN/mm², below all other samples. The results corresponded to the flexural creep strain displayed in figure 80. The commercial product showed the highest strain notably above 1 %.

Four specimens from the untreated sample showed irregular deformations after the 24 h load. Two specimens slightly deformed convexly, which might have underestimated the deflection value. On the other hand, two additional specimens from the same sample showed a light concave deformation, which might have led to an overvalued deflection. When eliminating the values from those samples, the tendencies described before remained the same. The deformations and the subsequent over- and underestimation seem to have compensated the effect on mean creep moduli and mean strain. No other samples showed visible irregularities.

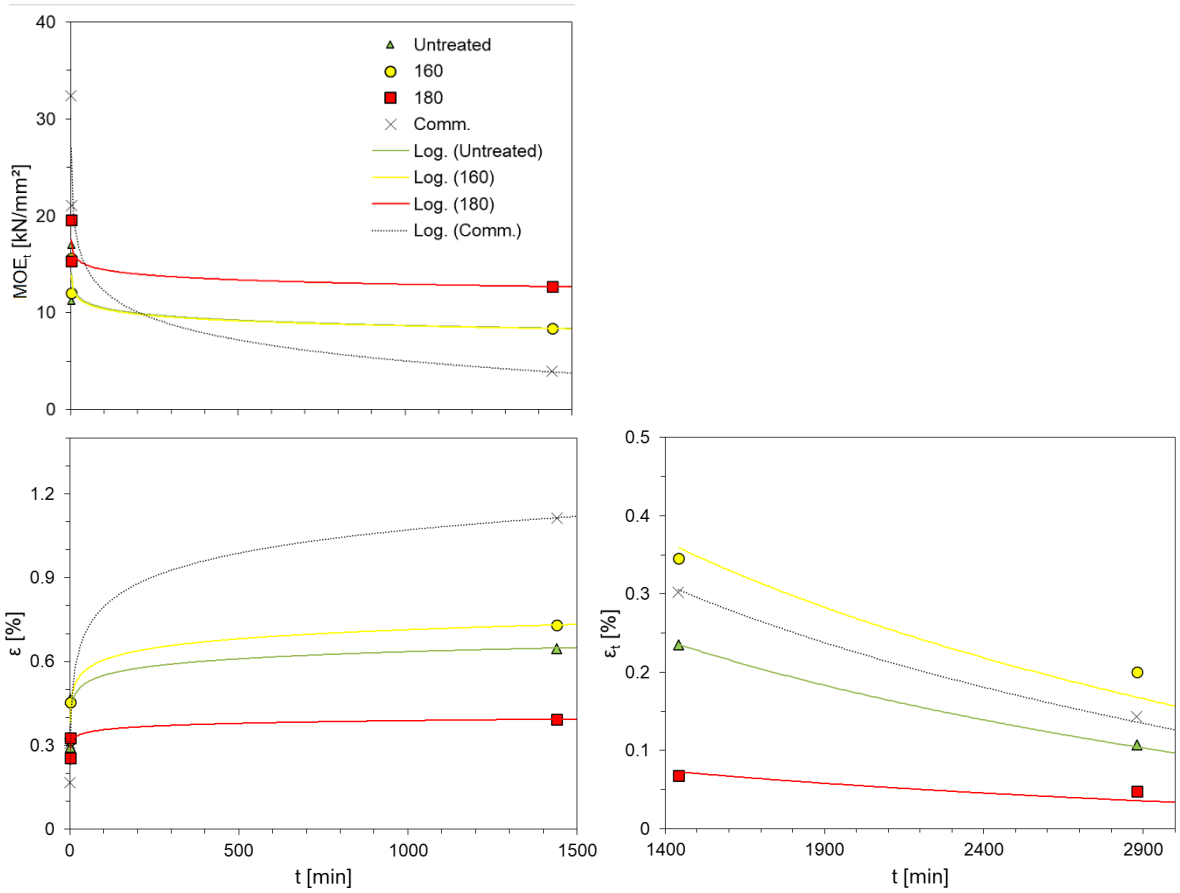

Figure 80: Flexural creep-modulus of elasticity (MOE$_t$) and the corresponding strain (ε) during 24 hours load (left) and the recovery strain (right) of industrial-scale bamboo scrimber (Untreated, 160, 180 °C) and a commercial scrimber product (Comm.)

The requirements defined in DIN EN 15534-1:2014-04 were all fulfilled. The residual MOE after 24 h flexural creep was above 50 % of the initial creep modulus for all variants. Only the commercial product lost more than 80 % of its original stiffness. The creep strain of the commercial product increased with constant load and passed by the 1 % criterion after 12 h whilst the highland BS stayed below 0.8% in all variants. When the load was released, only the 180 °C achieved to return to 0.1 % creep strain. The residual creep strain of all other variants ranged between 0.1 and 0.3 %. The requirements for flexural creep behavior were fulfilled by all highland bamboo treatments except the residual creep strain which was only fulfilled by the 180 °C sample. The commercial variant failed in all tests.

5.4.2 Mechanical surface characterization

In this section, test results for hardness, impact resistance, abrasion, sliding friction and pull through resistance of fasteners were evaluated.

5.4.2.1 Hardness and elastic recovery

The resistance against indentation for heat treated bamboo scrimber, a commercial scrimber and WPC are presented in figure 81. The produced samples showed nearly similar means around 50 N/mm². No significant difference was found between heat treated and untreated

variants and a relatively high variation of 20 % was observed. Nevertheless, the results were considered valid due to the scattering nature of the test. Remarkably, the 160 °C sample showed the lowest hardness (40 N/mm²) and a SD twice as high (40 %). The commercial scrimber product outperformed all other samples with HBS of 121 N/mm². Since the density-dependent relation shown by Schwab and Schlusen (1999) was fulfilled for the untreated highland bamboo scrimber, it was presumably the high resin content of the commercial scrimber responsible for the high hardness. However, surprisingly even the WPC sample showed a higher HBS than the highland bamboo scrimber. Its elastic relaxation (ER) after force release is shown in figure 81. The ER after indentation was lower in samples from heat treated bamboo. The commercial scrimber product, just like the untreated highland bamboo scrimber showed an ER around 85 %, which means they had recovered a major portion of the indentation damage. The heat-treated highland bamboo scrimber recovered only between 60 and 70 % which might be due to a more brittle behavior. The thermoplastic composite showed similar behavior. Adding wax to the scrimber panel recipe did not significantly affect neither hardness nor elastic rebounds.

The highland bamboo scrimber hardly compared with the commercial scrimber which showed HBS more than double as high. Although there was no explicit hardness requirement stated neither in DIN EN 17009:2016-07 nor in DIN EN 15534-1:2014-04, HBS must be further investigated. The SKH regulation demands 10 N/mm² for flooring in UC 1 and 2 (SKH 2014). Hardness of highland bamboo scrimber may be improved by a layered mat structure with higher resin in the face layer and lower in the core layer. A finer strand geometry may improve the absolute value as well as the SD.

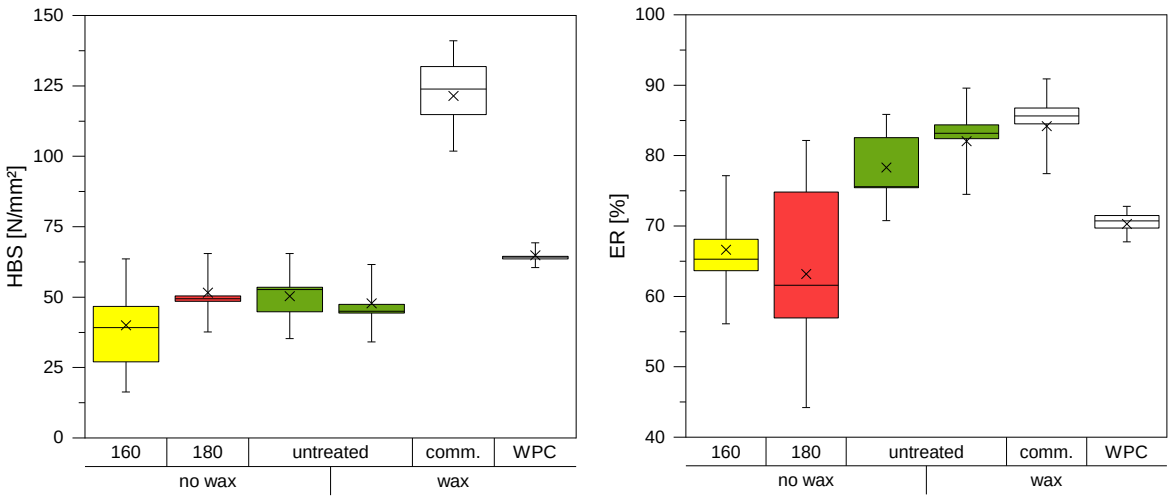

Figure 81: Mean Brinell hardness (HBS) and elastic rebound (ER) of industrial-scale bamboo scrimber (untreated, 160, 180 °C) and a commercial scrimber product (comm.) and a WPC product (WPC)

5.4.2.2 Abrasion resistance

The results of the abrasion test are shown in table 33. Both treatment temperatures led to nearly the same abrasion mass loss of about 58 mg per 50 revolutions of the abrasion wheel. This effect was due since the surface is more brittle than the untreated one. The untreated variant showed a significantly lower mass loss of 37.6 mg. Interestingly, it is on the same level with the rough profile of the commercial scrimber product, although the highland BS was neither sanded nor profiled before testing. The rough profile lost slightly more mass than the

fine one. It is supposed that heat-treated variants would perform like the commercial product once they receive a proper profile milling as well.

Table 33: Mean abrasion mass loss per 50 rounds [mg] after a total of 500 cycles with a S-34 emery paper for n = 3 for industrial-scale highland bamboo scrimber (Untreated, 160, 180 °C) and a commercial product (comm.) with rough (R) and fine (f) profiles

untreated	**160**	**180**	**comm.**	
			R	f
37.6	58.2	58.5	37.0	33.6

A formal requirement was not defined prior to testing. Nevertheless, the untreated highland BS showed very similar values as the commercial product whereas the heat-treated variants suffered approximately 50 % more abrasion mass loss.

5.4.2.3 Impact resistance

A pre-trial showed that the kinetic energy at 700 mm falling height did not achieve workable results with clearly distinguished variants. Since the requirements had been defined with focus on WPC decking, the impact energy was expected to increase for BS. Thus, the actual falling mass height was doubled to 1400 mm. The impact resistance of the thermally treated industrial scale BS variants, the commercial scrimber product and WPC are displayed in figure 82.

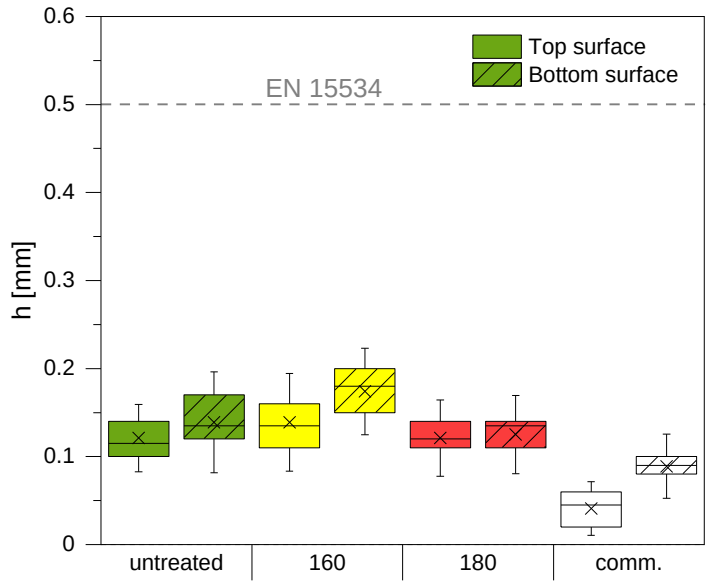

Figure 82: Impact resistance determined by indentation depth (h) of industrial-scale bamboo scrimber (untreated, 160, 180 °C) and a commercial scrimber product (comm.)

Regarding maximum indentation depth all highland bamboo samples fulfilled the requirements. Moreover, no major cracks were observed in the highland BS. However, no significant difference between treatment temperature was found. Interestingly, all top surfaces resulted in lower mean and median values than their bottom surface equivalent. The commercial product suffered cracks already at 700 mm drop height. The test showed that both profiles fulfilled the indentation depth requirement (h < 0.5 mm), but six out of ten specimens failed due to cracks in the surface especially on the smooth profile side.

5.4.2.4 Pull through resistance of fasteners

The means of the maximum load and deflection are shown in figure 83. The highest values were achieved for the untreated BS, followed by the 160 and the 180 °C heat treatment. The heat-treated variants differed significantly from each other. The lower pull-through load after heat treatment is probably a result of the brittle character of the BS. The maximum deflection was not significantly affected by the treatment. The mean value of the untreated variant seemed to be higher than the treated ones, but median and SD indicate that there was no notable effect.

In contrast, Chung and Wang (2018a) stated that a heat treatment would increase the nail withdrawal resistance after testing BS from moso and maki bamboo. They used metal screws which they drilled into a depth of 11.0 mm and then pulled up vertically at 2.0 mm/min. The maximum load was measured and the average of three measurements was taken as the nail withdrawal resistance. Their treatment happened at 120 °C and used saturated steam which might have had a plasticizing effect on the scrims, so the vertical density profile could have been more homogeneous after treatment. Density has not been recorded for those samples, though density variations might have played a notable role in the present work. Lee *et al.* (1996) produced strandboards using a comparable PF resin and moso bamboo. They stated that there is no significant influence of density or resin content on nail withdrawal resistance. However, comparison of the present experiment with other research is not sound due to very different methodologies.

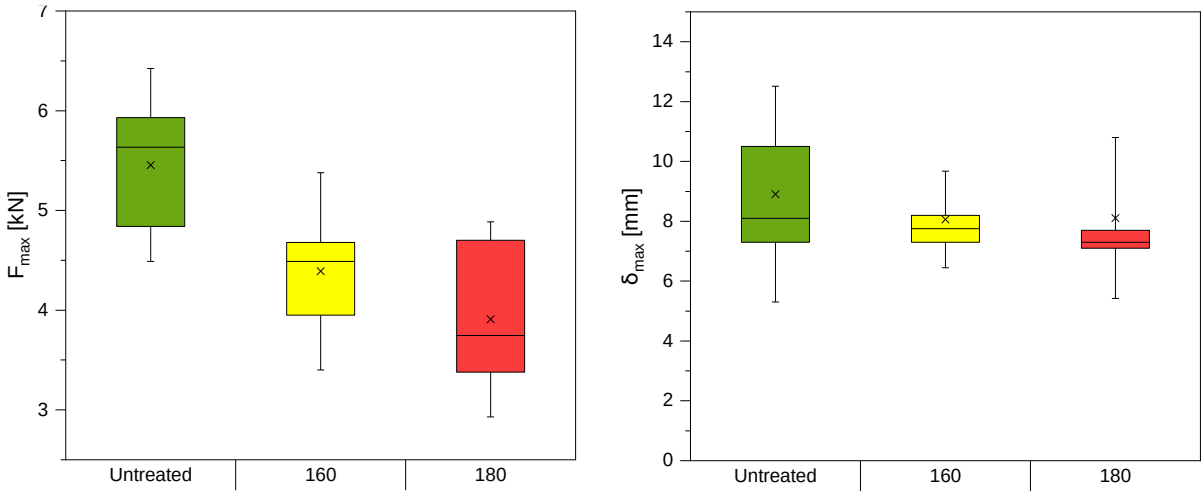

Figure 83: Mean pull-through resistance maximum load (F) and deflection (δ) of a stainless-steel screw with defined torque applied to industrial-scale highland bamboo scrimber (untreated, 160, 180 °C)

5.4.2.5 Sliding friction

The mean sliding friction coefficients are displayed in figure 84. The results showed higher values in lengthwise direction for all samples. In opposite, the commercially available products with surface finish on both sides of the product show significantly higher μ values in perpendicular direction. Nevertheless, the highland BS fulfilled the requirements of DIN CEN/TS 15676:2008-02 defined in DIN EN 15534-1:2014-04, for the lengthwise direction. The critical value for the sliding friction coefficient (μ ≥ 0.36) was achieved with a sanded surface, but without profiling or polishing it. The much higher value for the commercial scrimber was a result of the profiled surface. The friction coefficient for the rough profile was higher than the

fine one while the lengthwise friction was in the range of the highland bamboo scrimber. However, the heat treatment did not show any notable effect on the sliding friction.

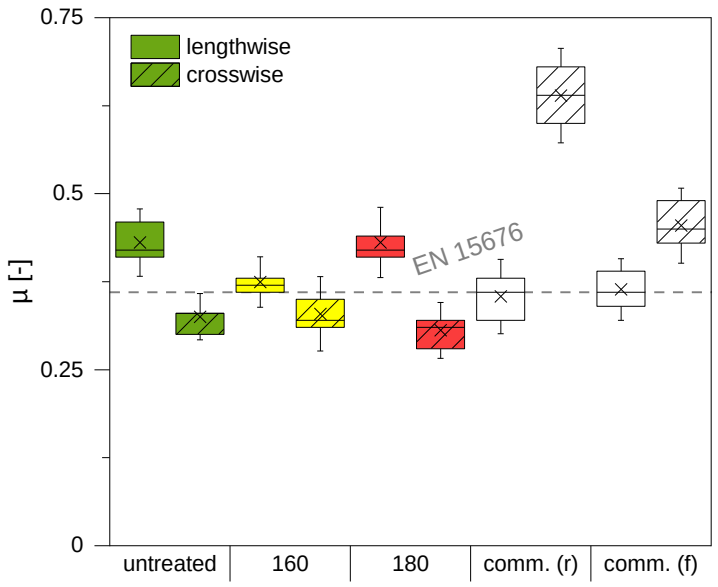

Figure 84: Mean sliding friction coefficient (μ) of industrial-scale bamboo scrimber (Untreated, 160, 180 °C) and a commercial product (comm.) with rough (r) and fine (f) profiles

Further development should include different surface profiles to obtain values for later commercial stage products. Future tests should apply the unpolished slip resistance value, which is used for comparison of wooden parquet flooring and to take the different profiles and finishes into consideration.

5.4.3 Humidity and weathering

The results for humidity-induced swelling and shrinking of heat-treated highland BS are presented. Additionally, the effect of heat treatment on the artificial and natural weathering of the bamboo scrimber surfaces is presented.

5.4.3.1 Dimensional stability

The relative dimensional changes in thickness and length due to change of humidity are shown in figure 85. The results represent the swelling or shrinking as per cent MC change. Generally, the relative dimensional change in thickness was higher for swelling (30 % < 65 % < 85 % RH) than shrinking (85 % < 65 % < 30 % RH). The highest change in thickness was found in untreated BS, followed by the 160 °C treatment, nevertheless the difference was insignificant for swelling and shrinking. In contrast, the 180 °C treatment halved the relative swelling in thickness whereas the lowest value was found in the commercial panel. A similar pattern was found for the shrinking in thickness. Length changes for untreated and treated panels did not notably differ from each other. However, the produced panels showed better values than the commercially available product at least for the swelling behavior.

The width change was not part of the test, since DIN EN 318:2002-06 asks for the dimensional changes in thickness and length. Due to the Poisson effect, large irreversible thickness

swelling may cause a negative change in width which then leads to unbalanced width changes during water absorption (Yu *et al.* 2017). In fact, the application of DIN EN 318:2002-06 was not appropriate, since fiberboards and bamboo scrimber differ in panel morphology. The length change of a fiberboard is a valid measure for both in-plane directions since fiberboards can be seen as isotropic in this dimension. Bamboo scrimber notably differs in the two in-plane directions. There is an axial length change, a width change and thickness change (perpendicular to the fiber). Summarizing, the dimensional change of untreated and 160 °C treated highland BS was higher than in wood-based panels (Popper *et al.* 2004) and only a treatment at 180 °C significantly increased dimensional stability.

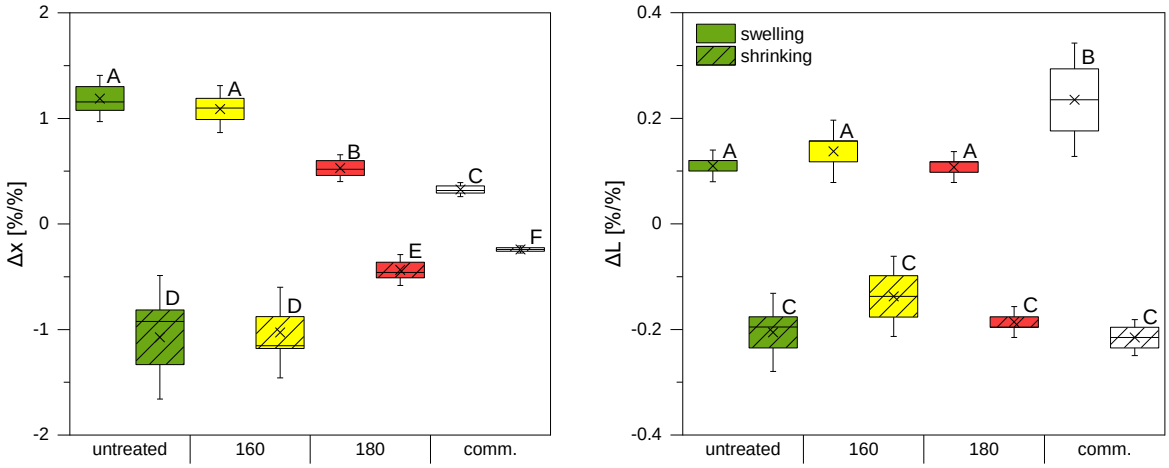

Figure 85: Differential dimensional change in % per % moisture content change in the humidity range 30 < 65 < 85 % (swelling) and 85 < 65 < 30 % (shrinkage) in thickness (left) and length (right) for industrial-scale highland bamboo scrimber (untreated, 160, 180 °C) and a commercial scrimber product (comm.); Means sharing same letters are not significantly different at $p \leq 0.05$

5.4.3.2 Weathering resistance

The results for the artificial and natural weathering are shown in figure 86 and table 34. In figure 87 the commercial product is shown. All tested treatments showed an overall perceived color shift $\Delta E_{ab} \geq 10$ after artificial weathering, except the commercial sample. Even though there are no strict requirements, all panels were considered to have failed the test. The surface of all specimens was destroyed, i.e. not only whitened, but rough, swollen and cracked. Figure 86 and figure 87 document that the treated scrimber variants as well as the commercial product suffered a moisture-induced delamination swelling and fiber bundles peeled off the surface. The latter cause a very rough surface and elevated injury risk. Neither naturally nor artificially weathered samples fulfilled the requirement. The commercial products' superficial damage was notably lower since a UV hardened finishing oil had been applied. The results showed that a surface finish to avoid quick bleaching of exposed surfaces is indispensable.

Table 34 Colorimetric differences ΔE_{ab} for industrial-scale highland bamboo scrimber (untreated, 160, 180, 200 °C) and commercial bamboo scrimber (Comm.) after 300 h exposure to artificial and one year to natural weathering

		Untreated	160	180	200	Comm.
Artificial weathering	ΔL_{ab}	8.3	19.6	23.4	n/a	-0.8
	Δa	-0.3	-2.1	1.4		-1.4
	Δb	-6.0	0.5	4.6		-2.1
	ΔE_{ab}	**10.3**	**19.7**	**24**		**3**
Natural weathering	Gloss change	-1	-1	0	0	0
	Appearance	5	5	5	5	4
	ΔE	**17**	**12**	**13**	**17**	**14**

The harmonized standard for WPC, DIN EN 15534-1:2014-04, does not mention any minimum requirement after weathering. Nevertheless, the determined values for ΔE, ΔL, Δa and Δb must be declared by a manufacturer. In contrast to the European standardization body, the quality assurance certificate "Qualitätszeichen Holzwerkstoffe" of the Qualitätsgemeinschaft Holzwerkstoffe e.V. (2017) requires $\Delta E_{ab} < 10$.

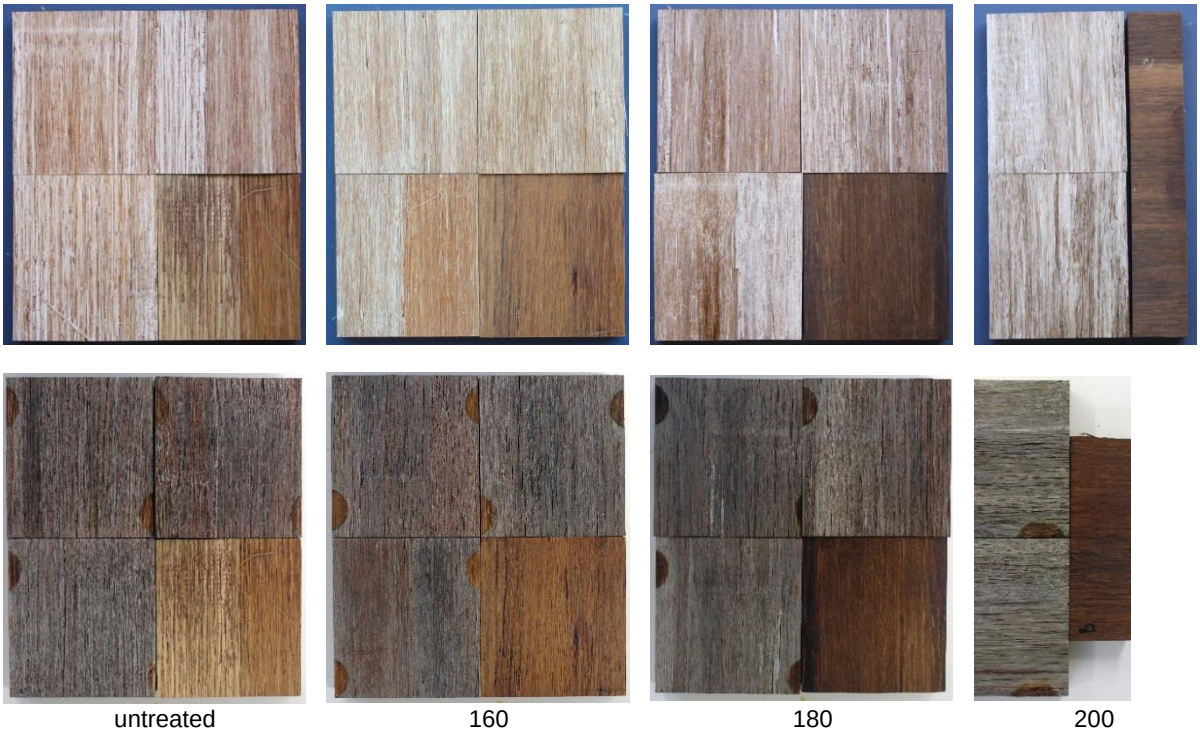

Figure 86: Artificially (top) and naturally (bottom) weathered samples of industrial-scale highland bamboo scrimber (untreated, 160, 180, 200 °C) showing the corresponding reference on the right bottom corner

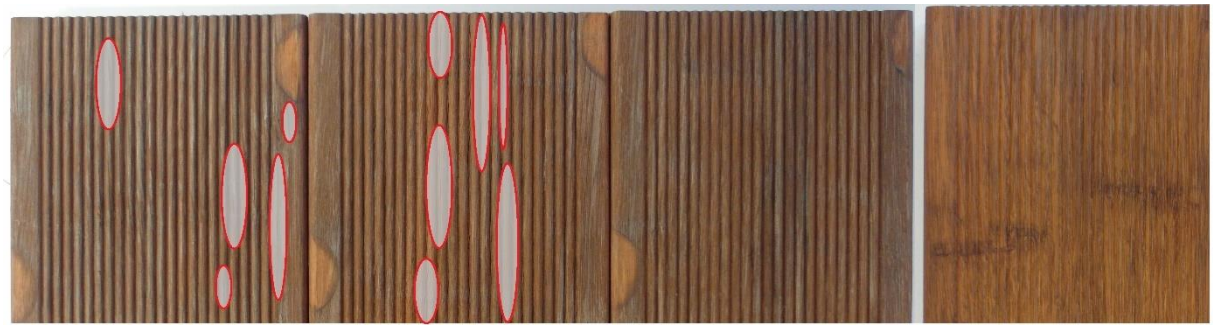

Figure 87: Naturally weathered samples of commercial bamboo scrimber (left) with the reference (right) and severe longitudinal cracks on the surface (red ellipses)

5.4.4 Resistance to fungal attack

The above described defects such as cracks, detached fiber bundles, etc., may lead to higher local moisture content concentrations. Consequently, the risk of cyclic swelling and shrinking occurs and can cause severe damage to the scrimber composite. Such cracks provide potential entrance paths for biodegrading agents, such as soft-, brown-, white rot or mold fungi.

5.4.4.1 Screening

The fungal degradation of heat-treated engineered BS was screened with five basidiomycetes followed by two comprehensive decay tests. Table 35 summarizes the screening results showing median mass losses caused by fungi along with abiotic factors. Brown rot fungi *Tp* and *Gt* did neither achieve notable mass losses on raw bamboo nor on the scrimber. The strongest degradation was however caused by brown rotter *Cp* achieving 12.8 % mass loss on raw bamboo. The same fungus has reached the highest mass loss on BS, namely 6.9 % in the panel core layer. White rot fungi *Cv* and *De* degraded raw bamboo with 10.0 and 8.3 % and BS with 5.3 and 5.2 % in the face layer and 6.1 and 4.8 % mass loss in the core layer, respectively. The sterile sample showed 2.9 % mass loss for raw bamboo and between 3.8 to 4.2 % for scrimber. These notably high abiotic mass losses derogate the prior results on incubated samples. Fungi which caused comparably low mass losses onto scrimber are *De, Tp* and *Gt*.

Table 35: Median mass loss of the sterile control and raw bamboo (raw) and industrial-scale highland bamboo core (CL) and face layer (FL) after 8 weeks incubation with brown rot (BR) and white rot (WR) basidiomycetes; n = 6

[%]		**Raw bamboo**	**Scrimber FL**	**Scrimber CL**	**Reference**
Sterile		2.9	3.8	4.2	
C. puteana	(BR)	12.8	5.1	6.9	32.8
C. versicolor	(WR)	10.0	5.3	6.1	36.0
D. expansa	(WR)	8.3	5.2	4.8	29.2
G. trabeum	(BR)	5.7	5.0	4.4	26.3
T. placenta	(BR)	4.2	4.3	3.7	27.6

The low mass losses for brown rot fungi *Gt* and *Tp* in particular do not notably differ between raw bamboo and scrimber. For brown rotter *Cp*, results are in contrast with the findings from

Leithoff and Peek (2001). Incubated with *Cp* monocultures, they found low 3.7 % mass loss in *Phyllostachys pubescens* bamboo. The same authors report 15 % mass loss for white rotter *Cv* confirming the present screening results.

The FESEM images in figure 88 show the hyphae growth pattern on raw bamboo and after being processed into BS. The cross-section (A) and longitudinal-radial plane (C) of unprocessed bamboo represent a single specimen with a corrected mass loss of 10.2 %. Whereas the same fungus, *C. versicolor,* caused 1.8 % on scrimber (B and D). No mycelium growth was observed (B) in the densified parenchyma tissue. The production process, i.e. hot-pressing, increased the bulk density by plastic compaction of the parenchyma cells (Gao *et al.* 2018). Noteworthy are additional axial cracks in the fiber caps (B) which represent potential voids for hyphae growth. In contrast to Kumar *et al.* (2018) who believe that there is only superficial hyphae growth, figure 88D clearly indicates hyphae penetrating especially along the vessels even in highly densified tissue.

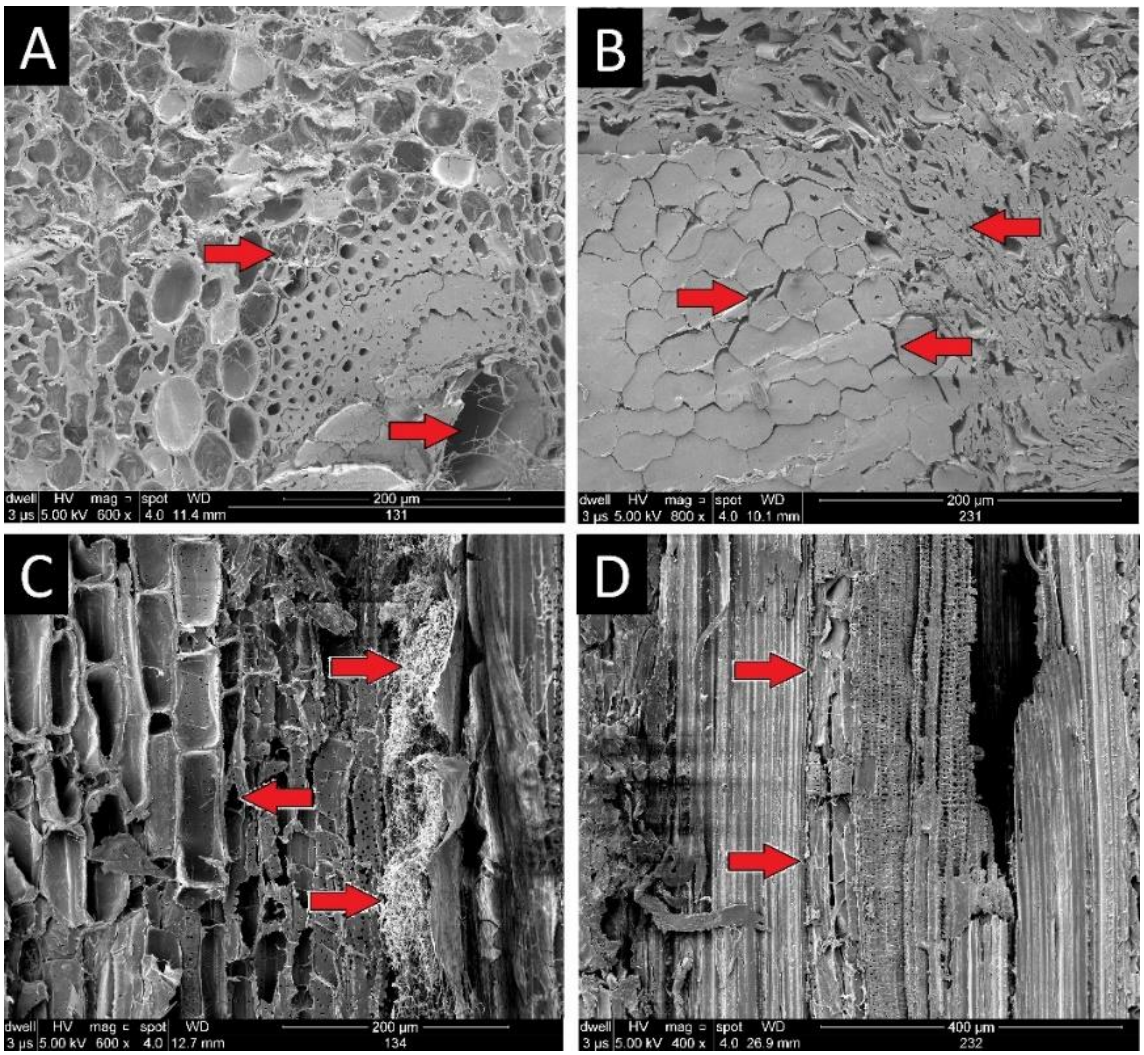

Figure 88: FESEM images after 8 weeks incubation: Cross section (A, B) and longitudinal section (C, D) of raw bamboo (A, C) and face layer bamboo scrimber (B, D) showing mycelium growth (red arrows) in lumen of axial parenchyma and vessel (A, C) as well as ruptures between fiber cells and strongly densified parenchyma tissue (B) with minor mycelium growth in vessel (D)

Figure 89 (left) shows the density of raw bamboo being lower than that of scrimber. Though densification ratio is below 2, densification in the scrimber core layer was poorer than in the face layer. Mass loss in face and core layer slightly differed for brown rot and white rot, namely *Cp* and *Cv*, the same fungi which caused the highest mass losses on raw bamboo. As shown

in figure 89 (right) MC is higher in raw bamboo than in the scrimber CL, higher than in the FL. The lower density of raw bamboo incubated with *Cv* and *Cp* might have led to higher water availability and explains the stronger decay. The same effect is not visible for scrimber. The soil bed test further investigates the results of the screening.

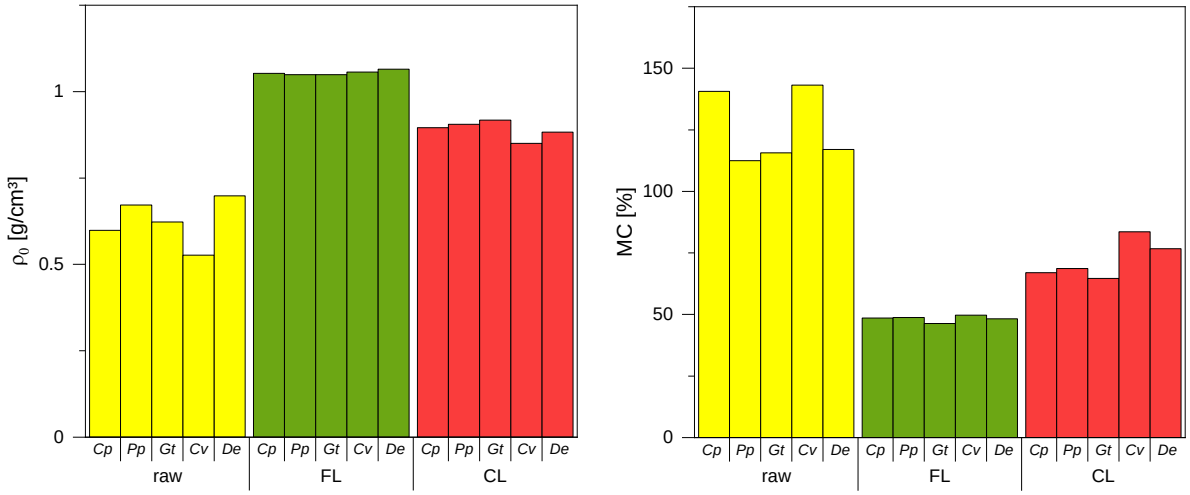

Figure 89: Oven-dry density (ρ_0) and moisture content (MC) of raw bamboo and industrial-scale highland bamboo scrimber core and face layer after 8 weeks screening incubation with five basidiomycetes

5.4.4.2 Basidiomycete monocultures

The efficacy of an industrial scale heat treatment against fungal decay of BS was studied with pure cultures of one BR and three WR fungi as well as in a SR soil bed test. The corrected median mass and MOE losses after 28 weeks are summarized in table 36. The highest ML was found in the untreated control group, whereas the lowest ML was caused by BR to scrimber made from bamboo scrims treated at 200 °C.

The pure basidiomycete cultures caused corrected median ML of less than 5 %. The heat treatment at 160 °C significantly improved the ML caused by *Tp* by one third, whereas against *Cp*, *Gt* and *Cv* effects were negligible. The treatment at 180 °C decreased the ML caused by *Tp* by two thirds. The 180 °C treatment also yielded a notable improvement for *Cp*, *Gt* and *Cv*. The highest treatment temperature of 200 °C led to hardly any ML for *Tp* and two thirds less ML for *Cp*. The same treatment did not show further notable improvement for *Gt* or *Cv.* However, the difference between the 180 and 200 °C treatment was statistically insignificant for all fungi. In fact, significant differences were found only in the control group for the 180 and 200 °C treatment, respectively.

Hamid *et al.* (2012) found 5.3 % ML for *Cv* and 8.9 % for *Cp* after exposing mature *P. pubescens* samples for eight weeks. Kumar *et al.* (2018) made a hydrothermal treatment and toxic compounds responsible for ML below 5 % though no further specifications were made by the authors. High temperature treatments chemically transform the structural polymer constituents of wood and bamboo. Although there are structural alterations in lignin and cellulose after heat treatments, they are comparatively thermally stable. Hemicelluloses are degraded earlier due to their lower decomposition temperature (Windeisen *et al.* 2009). The 200 °C treatment degraded the xylan backbone of *Y. alpina* nearly completely (Starke *et al.* 2016). Hence, lacking hemicelluloses deprived the substrate for *Tp* and other BR. In particular, some authors (Bremer *et al.* 2013, Kamdem *et al.* 2000) believed that treatment temperatures

above 180 °C may yield new compounds inhibiting fungal decay. Hakkou *et al.* (2006) investigated the reasons for increased durability of beech and concluded that the primary reason is lacking substrate instead of fungicidal compounds or low MC. Kumar *et al.* (2018) suspected that leached phenolic compounds might have had inhibited fungal attack.

Nevertheless, the moisture exclusion efficacy (MEE), i.e. a low MC due to changed sorption behavior as a consequence of thermal modification, is one of the main drivers of increased durability (Thybring 2013). The degradation of free hydroxyl groups and the formation of hydrophobic condensation products reduce the hygroscopicity and thus the water absorption. Just like in wood (Joma *et al.* 2016), heat treated bamboo shows a lower EMC (Nguyen *et al.* 2012, Schmidt 2013). The climate conditioning at 20 °C and 65 % relative humidity prior to incubation led to an EMC below 15 %, which increased to 20 % and higher after 16 weeks incubation in the moist container (see figure 91). Jacobs *et al.* (2011) found an EMC of 8.3 % for untreated BS with a bulk density of 1.1 g/cm³. The samples treated at 180 °C reached an EMC of 9.25 % at a target bulk density of 1 g/cm³. The 200 °C samples achieved an initial EMC of 4.84 %, which increased to 26 % at the end of the incubation period. Li and Chen (2010) cited a Chinese bamboo scrimber standard and mentioned an acceptable range between 6 ⩽ MC ⩽ 14 %.

Table 36: Corrected median mass loss (Δm) and stiffness loss (ΔMOE) as percentual share of the original value prior to exposure for industrial-scale bamboo scrimber (untreated, 160, 180, 200 °C) after 16 weeks incubation with basidiomycetes and 28 weeks soft rot soil bed test according to the standards DIN CEN/TS 15083-1:2005-10, DIN CEN/TS 15083-2:2005-10; Median in the same row sharing same letter belong to means which did not significantly at p ≤ 0.05

		untreated	**160 °C**	**180 °C**	**200 °C**	**Reference**
Δm [%]	Sterile	3.3^{A}	3.0^{AB}	1.9^{BC}	1.2^{C}	
	C. puteana	4.4^{A}	3.7^{A}	2.2^{AB}	1.4^{B}	21.3^{C}
	T. placenta	4.8^{A}	3.0^{B}	1.7^{BC}	0.4^{C}	20.8^{D}
	G. trabeum	3.3^{A}	3.0^{B}	1.9^{BC}	1.7^{C}	33.3^{D}
	C. versicolor	4.4^{A}	3.9^{AB}	1.9^{B}	1.9^{B}	39.1^{C}
	Soft rot soil bed	19.9^{A}	14.6^{B}	11.8^{BC}	5.1^{C}	54.3^{D}
ΔMOE [%]		60.9^{A}	52.9^{B}	50.2^{B}	52.5^{B}	80.2^{C}

Fungal decay requires free water for colonizing the substrate (Candelier *et al.* 2017a, Thybring *et al.* 2018). Figure 90 shows the MC of specimens before and after incubation with monoculture basidiomycetes. The MC of the control and the 160 °C treated samples did not differ before or after incubation and go up to 47.8 and 48.9 %, respectively. This is relatively high compared to Kumar *et al.* (2018), who found an increase in MC of 33 to 42 % after 12 weeks incubation, or Jacobs *et al.* (2011) who found 34.8 % for *Cp* and 32.2 % for *Cv.* One explanation for this difference is the higher scrimber density in both studies. These high MCs contribute to the availability of free water and subsequently fungal decay. Thybring *et al.* (2018) stated that a 25 % minimum MC in modified wood is needed for basidiomycetes being able to continuously decompose the substrate. Figure 90 (left) shows that a higher treatment temperature led to lower MC, though the 160 °C and control sample showed no significant difference. The 200 °C treatment was the only one leading to a MC below 25 %. Figure 90 (right) further illustrates the correlation between EMC prior to incubation and fungal ML of all heat treatments, distinguished by species. Table 50 complements the regression analysis. Unlike Paul *et al.* (2007), we found a polynomial function describing the correlation rather than a linear one. For the soil bed test a similar relation can be obtained for ML, but not for MOE loss.

To what extent the lack of hemicelluloses, formation of fungicide compounds or lower EMC caused the differences in ML cannot be concluded from the data. Which modification plays the major role in inhibiting fungal decomposition is subject to ongoing discussions for wood (Candelier *et al.* 2017b, Hakkou *et al.* 2006, Hill 2006) and bamboo, which was not widely studied.

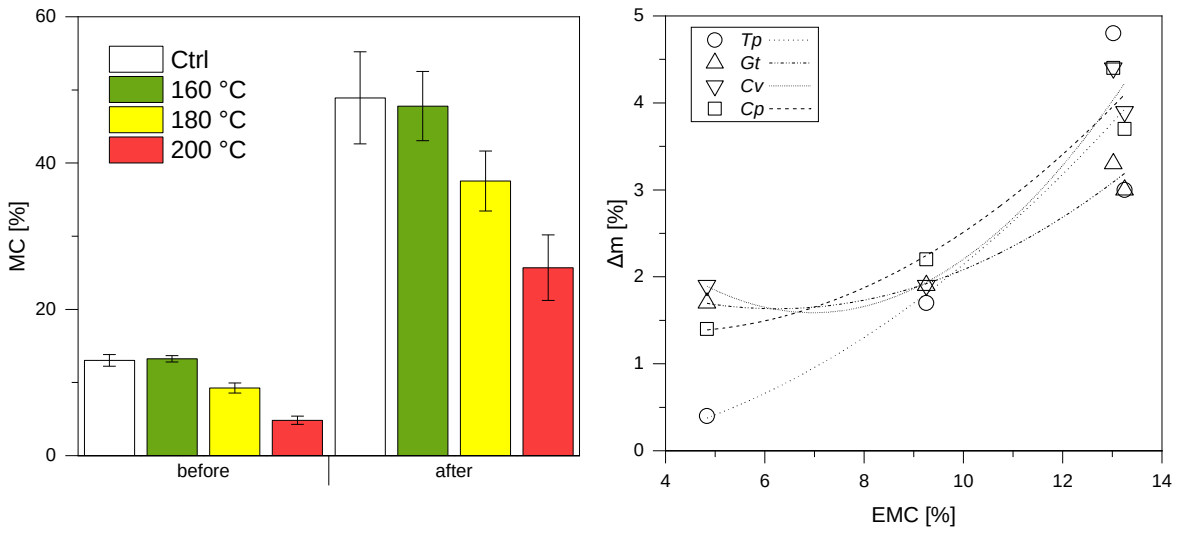

Figure 90: Mean moisture content (MC) of industrial-scale bamboo scrimber (untreated, 160, 180, 200 °C) before and after 16 weeks incubation with basidiomycetes (left) and the correlation between fungal mass loss (Δm) and equilibrium moisture content (EMC)

Table 36 shows that a notably high ML due to abiotic factors was observed in the basidiomycete test. The sterile sample lost 3.3 % mass in the untreated control group. Jacobs *et al.* (2011) reported 6 % ML after a leaching procedure. Liese (1998) explains this with starch reservoirs in bamboo tissue being degraded. Okahisa *et al.* (2006) investigated the influence of seasonal fluctuations of sugar contents on the biodegradation by insects and fungi. Their study showed that higher amounts of free glucose led to stronger degradation by rot fungi, whereas starch did not notably affect the fungal decay. Depending on the harvest season, starch in highland bamboo accounts for up to 4.7 % of the culm dry weight (Schmidt *et al.* 2016a), which might explain the high ML due to abiotic factors. Moreover, the results shown in table 36 indicate that heat treatment leads to successively lower abiotic ML, i.e. the higher the temperature, the stronger the thermal degradation of soluble sugars and their partial removal (volatile part). This effect confirms findings by Leithoff and Peek (2001), who identified agar block tests to cause less abiotic ML than soil bed tests. In contrast to the agar block test, where samples are floating on a metal separator, the physical contact of specimens with the soil container facilitates the transport of degraded substances and leads to faster water uptake of the substrate. The mean ML in table 36 for basidiomycetes decay have been corrected accordingly.

5.4.4.3 Soft rot soil bed test

A leaching procedure prior to SR soil bed incubation removed soluble substances, hence ensured comparability. Table 36 shows the median mass and MOE losses after 28 weeks. The untreated control samples lost nearly 20 % mass, whereas heat treatment at 160 °C significantly decreased ML by one quarter and halved it at 180 °C. The 200 °C samples showed a 5.1 % ML, which corresponds to a three-quarter improvement compared to the

control group. Dunn's post-hoc test revealed that the means of the 160 and 180 °C and the 180 and 200 °C treatments do not differ significantly.

In contrast, the median MOE decreased by 60.9 % in untreated samples. The heat-treated samples lost between 50.2 and 52.9 % of their MOE, but no significant difference was found between treatment temperatures at the end of the 28 weeks incubation time. Figure 91 shows the MOE loss progression and the moisture uptake over the entire test period. The initial MOE of the pine reference has been 7.35 kN and then decreased to 2.67 kN after only 16 weeks. In accordance to DIN CEN/TS 15083-2:2005-10, this remarkable MOE loss of 64 % meets the criterion (> 40 %) to stop the experiment after 16 weeks instead of 28. However, we continued the experiment to measure the losses and derive the durability over a longer period. The losses after 16 weeks are higher than the ML from the pure culture test but do show a similar pattern when it comes to treatment temperature. In the course of the experiment, however, all treated samples aligned with each other and achieved MOE losses of about 50 %. During a soil block test, not only SR causing micro-fungi but also basidiomycetes attack the substrate (Schmidt *et al.* 2013). The heat treatments locally delayed water uptake and distinguished levels of degradation occurred after 16 weeks. The slower growth pattern of SR fungi detained degradation up to 24 weeks when the substrate was fully saturated and MOE loss in all treatments was seen (Hamid *et al.* 2012, Sulaiman and Murphy 1993,1995). Although, the 200 °C treatment led to significantly lower MC over the whole test period, figure 91 shows that the MOE loss did not differ at the end. Interestingly, the ML of the 200 °C samples shown in figure 92 did not follow this trend. From studies on pine it is known that strength loss without significant ML is caused by fungal damage to galactan and arabinan (Curling *et al.* 2002). The degradation of mannan and xylan led to notable ML. MOE losses were thus attributed to glucan degradation and major ML. This phenomenon needs research, since composition and structure of hemicelluloses differ for bamboo.

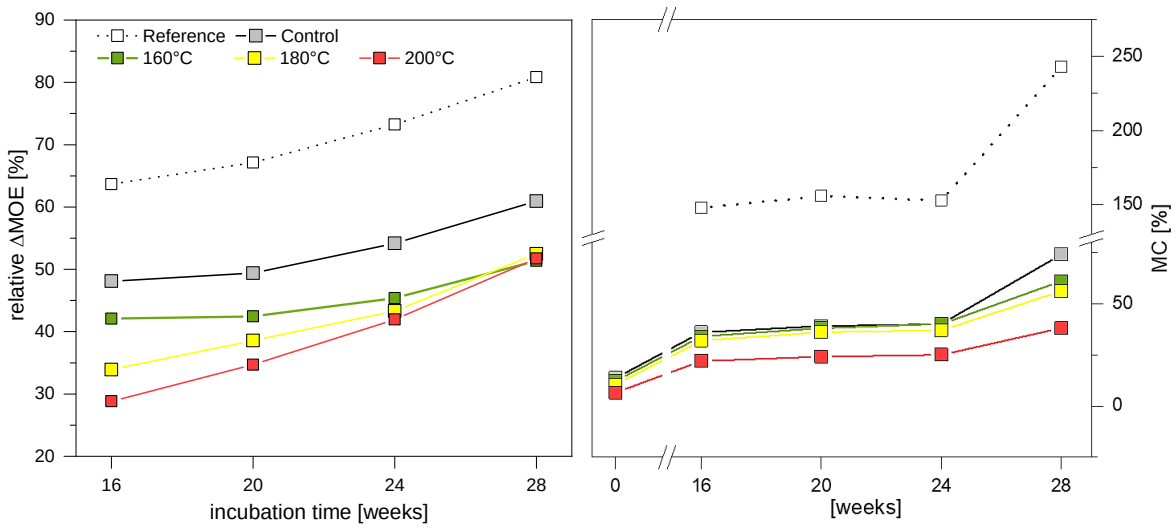

Figure 91: Mean stiffness loss (ΔMOE) as percentual share of the original value and corresponding moisture content (MC) of industrial-scale bamboo scrimber (untreated, 160, 180, 200 °C) prior to exposure and during incubation in a soft rot soil bed test

BS core and face layer dry density before incubation were 1.04 and 0.97 g/cm³, respectively. Figure 92 shows the difference in oven-dry density (left) and ML after incubation in the SR test (right). Anova shows that mean density significantly differed in core and face layer, but not between the heat treatments. The screening results on poorer densification in the core layer were confirmed. The ML in the core layer seems to be slightly higher following the pattern of

the densification, though statistically not significant. Nevertheless, the heat treatment did not have an interacting effect with layer density onto fungal degradation. A stronger moisture-induced set recovery in the core layer, due to a thermal modification effect within the surface layers (pressing plates), cannot be confirmed. This effect is known from studies on hardness recovery of thermally modified and densified wood (Laine *et al.* 2016).

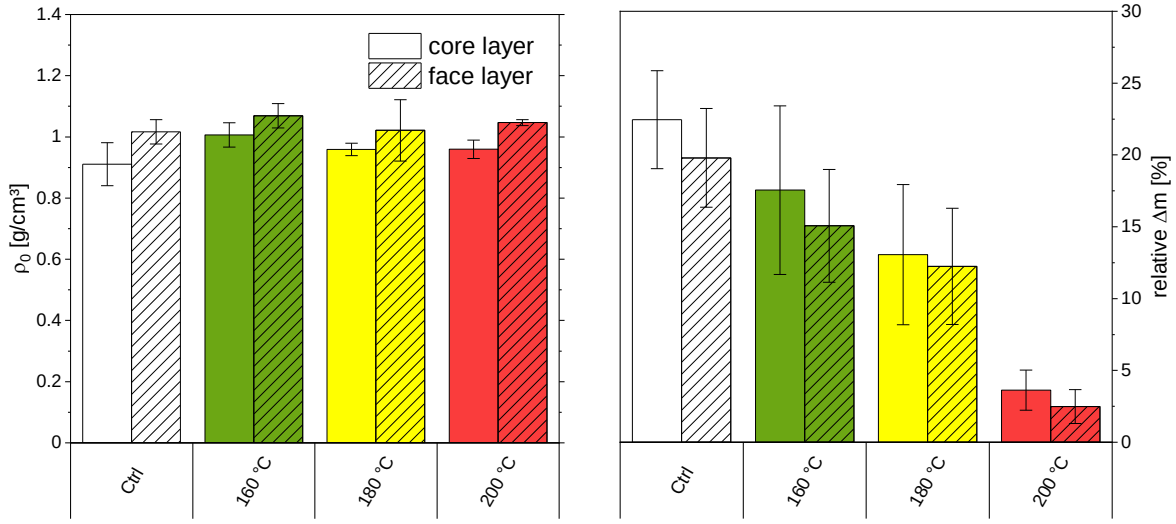

Figure 92: Mean oven-dry density (ρ_0) and relative mass loss (Δm) of industrial-scale bamboo scrimber (untreated, 160, 180, 200 °C) core and face layer after 28 weeks incubation in the soft rot soil bed test

Yu *et al.* (2017) showed that increasing the resin contents improves water repellency more than densification does. A better protection of engineered BS against fungal degradation using more phenolic formaldehyde resin calls for economic and ecological attention. Moreover, white-rot fungi (Gusse *et al.* 2006) and microbes (Krastanov *et al.* 2013) are known to be able also to degrade phenolic resins to a certain extent. Similar to timber, smart strategies avoiding water in the substrate, such as constructional wood preservation (Huckfeldt 2017), regio-selective modification with nano-materials (Ginoble Pandoli *et al.* 2019) or in-situ polymerization with olefins (Gurr *et al.* 2018) do offer alternative protection methods while keeping the anatomical structure of scrimber intact. The steam injection scrim lumber technology enabling *in situ* impregnation in the hot-press (Kitchens *et al.* 2016) offers a novel approach to increase durability.

5.4.4.4 Durability classification

The durability rating is based on the value that is most likely to be sampled, i.e. the durability class is set by where the probability distribution takes its maximum value. The logics of DC derivation in table 37 goes top-down so that the resulting DCs are shown in the last row. Table 37 further shows the highest median ML for all specimens exposed to each of the test fungi. The maximum median then identified the fungal species with highest ML, which was taken into account for DC classification. Each treatment was considered as a distinct timber species. The control, as well as the heat-treated samples achieved DC 1 against basidiomycetes with one exception: The *Cp* reference sample did not meet the ML minimum of 30 %. Following the standard, the result produced with the BR causing fungi *Cp* was therefore formally invalid and excluded from further durability classification. The maximum median mass loss slightly reduced with increasing heat treatment intensity. This is also reflected by the lower variation

in the distribution among the DCs. Where about 25 % of the untreated and 160 °C samples spread into DC 2, the samples treated at 180 and 200 °C were entirely classified as DC 1.

Furthermore, the soil bed test in accordance with DIN CEN/TS 15083-2:2005-10 requires a proof of SR fungi being present in the substrate. Figure 93 shows light microscopy images of pine sapwood and scrimber samples. The typical spiral cavities in the tracheid cell wall (Nilsson 1976) and typical hyphae in the lumen proved the presence of SR causing fungi in all examined samples and validated the experiment.

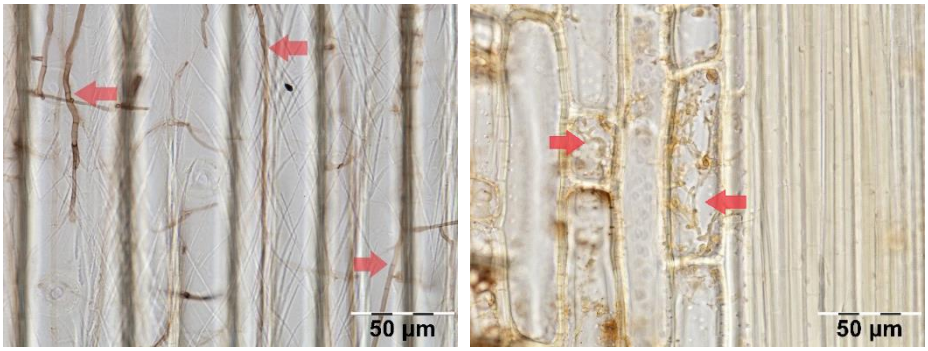

Figure 93: Transmitted light microscopy (100x) of the longitudinal-radial section of degraded pine tracheid cells (left) and axial bamboo parenchyma and fiber cells (right), red arrows indicating soft rot hyphae in lumina and spiral cavities in the cell wall

The SR testing standard distinguishes between using ML for hardwoods and MOE loss for softwoods to determine the x-value. Figure 94 visualizes the different ratios of mean relative ML and MOE losses. When using ML, the x-value of the untreated variant was 0.4 and heat treatment lowered it down to 0.28, 0.22 and 0.11 with 160, 180 and 200 °C, respectively and DC ranged from 1 to 3. The MOE related test delivered DC 4 for all treatments and x-values did not show notable differences between treatment temperatures. Only the 200 °C treatment and the ML derived x-value achieved DC 1. Jacobs *et al.* (2011) found DC 2 for SR, but did not consider MOE losses.

Table 37: Relevant basidiomycete species, x-value and maximum median, median probability distribution among the classes (DC1-5) and the resulting durability class for industrial-scale bamboo scrimber (untreated, 160, 180, 200 °C) after 16 weeks incubation with basidiomycetes and 28 weeks soft rot soil bed test

Treatment	**Ctrl.**			**160 °C**			**180 °C**			**200 °C**		
Fungus	*Tp*	SR		*Cv*	SR		*Cv*	SR		*Gt*	SR	
Parameter	Δm		ΔMOE	Δm		ΔMOE	Δm		ΔMOE	Δm		ΔMOE
x-value (SR)		0.40	0.76		0.28	0.66		0.22	0.63		0.11	0.66
max. Median (BR/WR)	4.82			3.22			1.93			1.88		
DC1	**73.3**			**75**			**100**	13.33		**100**	**71.43**	
DC2	26.7	13.33		25	**75.86**			**76.67**			28.57	
DC3		**86.67**	2.38		24.14	4.17		10	3.45			
DC4			**66.67**			**91.67**			**86.21**			**91.67**
DC5			30.95			4.17			10.34			8.33
Resulting DC	**1**	**3**	**4**	**1**	**2**	**4**	**1**	**2**	**4**	**1**	**1**	**4**

In conclusion the DC depends not only on the treatment temperature, but notably on the applied DC derivation method. Additionally, Plaschkies *et al.* (2010) reported that modified timber products apparently perform better in laboratory than outdoor tests. The performance assessment of wood and wood products through the DC concept is under discussion (van Acker *et al.* 2003) The increased use of lesser known species, non-woody lignocellulosic products and diverse modification techniques consequently leads to difficulties when comparing test results and an integrated service life prediction approach was favored (Jones and Brischke 2017, van Acker *et al.* 2003, Winandy *et al.* 2000, Windt *et al.* 2013). The service life prediction approach takes the exposure dosage, but also inherent natural durability, moisture dynamics, biological agents into account (van Acker and Palanti 2017). In contrast to optimistic recommendations by Kumar *et al.* (2018), service life prediction on the base of standard experiments is not legitimate. Generally, long-term experiments are needed to accompany laboratory results for engineered BS and prior heat treatments.

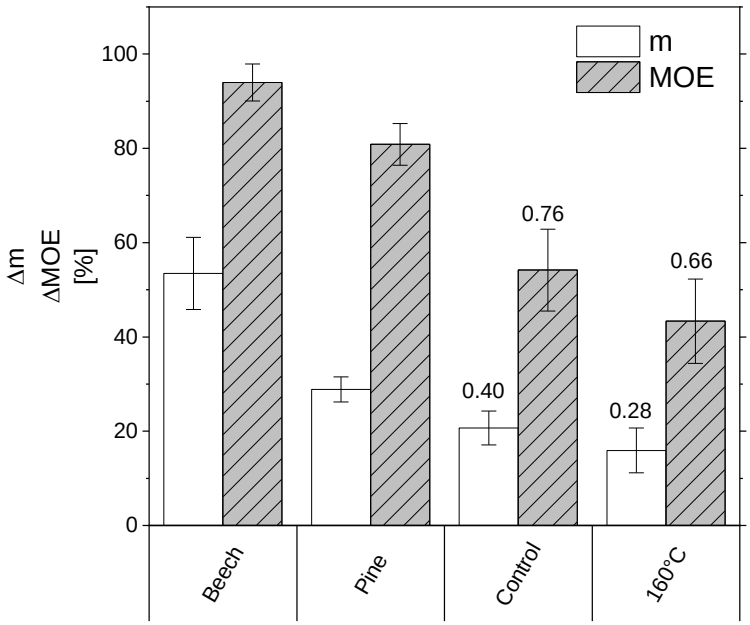

Figure 94: Mean mass (Δm) and modulus of elasticity loss (ΔMOE) as percentual share of the original value prior to exposure for and the calculated x-value for industrial-scale bamboo scrimber (untreated, 160 °C) and references after 28 weeks incubation in a soft rot soil bed

5.5 Intermediate conclusion

A scrimber product for flooring and decking purposes was made on industrial scale from heat treated highland bamboo. A completely new testing scheme was worked out based on legal standards and informal regulations. The industrial bamboo scrimber was then assessed in four main aspects of product quality. The results were categorized into flexural properties, mechanical surface characterization, humidity and weathering as well as resistance against fungal attack. The color-coded matrix in table 38 shows whether a treatment fulfilled the requirements (green), failed the test (red), or ranged within tolerable limits (yellow).

The necessary threshold values were all fulfilled for static flexural MOR, maximum deflection, force and MOE. Except for the tested commercial product, all samples showed satisfactory flexural creep performance. The requirements were set with the aim of using bamboo scrimber as outdoor decking material. In terms of flexural MOR and MOE, highland bamboo scrimber performed excellent, however a general application in load-bearing structures will need additional proof of suitability ("*bauaufsichtliche Zulassung*"). Moisture cycles notably decreased MOR and MOE. This moisture related loss in flexural properties increased with increasing heat treatment temperature. In turn this means that heat treatment was no sufficient protection measure against seasonal moisture fluctuation. Terrace decking without finishing oils, heat treated or not, must not be exposed to precipitation when used outdoors.

Mechanically the bamboo scrimber surface performed excellent against impact, sliding and fastener pull through. However, tests revealed weak points especially in surface hardness and abrasion. The mean Brinell hardness reached a third of a commercial scrimber product only and rather compared a thermoplastic based decking product. The untreated highland bamboo scrimber had marginal advantages due to the better elastic rebound after indentation. The heat treatment did not notably interact with surface resistance against mechanical factors, though rather weakening it than improving. Moreover, the heat treatment severely lowered bamboo scrimber resistance against weathering. Without the marking of the panels prior to artificial weathering, the individual specimens would not have been identified anymore by their color difference. Although standards do not mention specific resistance values, none of the variants was considered to fulfill the weathering product requirement. Additionally, the dimensional change in thickness and length was higher than comparable wood-based panels and only the 180 °C treatment halved the swelling and shrinking maxima. Since bamboo scrimber decking is exposed to sunlight and relative humidity changes it is indispensable to use UV resistant coatings.

The highland bamboo scrimber was further tested for its resistance against fungal degradation and resulted in durability class 1 for basidiomycetes, whereas soft rot led to a durability range from class 1 to 4. Bamboo scrimber lost less than 5 % of its mass due to fungal degradation in standard basidiomycetes monocultures and a similar loss due to abiotic factors was observed. Scrimber from heat treated bamboo showed slightly improved resistance against basidiomycetes, especially with 180 °C and beyond. A simulated outdoor test in a soil bed showed nearly 20 % ML for untreated bamboo scrimber and lost 61 % of its MOE. The heat treatment reduced the mass loss with increasing temperature, showing 5 % for the 200 °C variant, whereas MOE loss was reduced to 50 to 53 % for heat treated variants. The temperature did not significantly impact the MOE loss, nor was the DC affected. Using MOE as a parameter resulted in DC 4, whereas ML resulted in DC 1 for treatment at 200, DC 2 for 180 and 160 °C and DC 3 for the untreated control, respectively. Nevertheless, development of MC in the substrate indicated that fungal growth was delayed by heat treatment

but not stopped. The minimum target treatment temperature to achieve notable improvements in mass loss was 180 °C, which was in line with expected chemical transformations known from other studies. However, the results are limited to the specific industrial setting, the used treatment kilns, its low heating rates and the relatively long treatment durations.

Generally, heat treatment is not recommended as only protection measure for highland bamboo scrimber in use class 3 and 4 (outdoor conditions). With the present product parameters (resin, density, treatment) the use should be restricted to use classes 1 and 2. Future projects should investigate the interdependent effects of densification, phenolic resin and thermal treatment on bamboo scrimber resistance to fungal decay, hardness and weathering resistance. Additional outdoor tests seem indispensable for and alternative protection measures should be considered.

Table 38: Matrix overview on results for industrial-scale bamboo scrimber (untreated, 160, 180 °C) and a commercial product (Comm.) and the regarding test program with color code indicating the failed (red), tolerable (yellow) and passed (green) samples

	Ctrl.	**160**	**180**	**Comm.**
Flexural properties				
Static strength				
Static stiffness				
Static deflection				
Creep stiffness				
Creep strain				
Mechanical surface characterization				
Hardness				
Abrasion				
Impact				
Fasteners				
Sliding friction				
Humidity and weathering				
Natural weathering				
Artificial weathering				
Dimensional stability				
Resistance against fungal attack				
Use class 1 + 2				
Use class 3 + 4 (mass loss)				
Use class 3 + 4 (stiffness loss)				

6 | Final remarks

A building material for an industrial scale production was developed from African highland bamboo aiming at three technology and two market related goals. **Firstly, the Ethiopian construction sector was analyzed for renewable building materials and a potential bamboo-based industrial panel product was defined.** The installment of typical large-scale wood-based panel factories in the country seemed to be less feasible and did not match the existing economic profile. The combination of a value-web analysis with the product space theory identified bamboo scrimber as a promising product development opportunity. Different to traditional wood-based industries where economy of scale effects are of high priority, bamboo scrimber offers the advantages of a relatively low investment, robust process technology and a potential exportability to markets with high purchase power. **Secondly, raw material characteristics and their suitability for the industrial processing were investigated.** The raw material investigation revealed a favorable morphology in the two upper thirds of the bamboo culm with comparably constant culm wall thickness and diameter. The woody volume could be estimated by form factor, breast height diameter and height which enables to calculate the industrially usable volumes even for small plots. The scrimber panel composes of crushed fiber bundles (scrims) which show densities between 0.66 and 0.75 g/cm³ and fiber bundle share of 29.8 to 38.3 %. The bending and tensile MOR of a scrim without nodes was four times higher (> 200 N/mm²) than in compression load. Nodes harm the integrity of the scrimber panel because scrim strands containing a node loose half of their flexural and tension MOR. The difference in tension explains with lacking fiber alignment and anatomical features. Nodal fiber cells are not as slender as internodal fiber though their length (1.4 mm) is the same. Nodes also contained more silica (1.5 %) but less than in other woody species and lowered after washing. Overall, Ethiopian highland bamboo showed to be technically well suited for scrimber. **In the third step, the technical feasibility was shown by combining existing technologies, developing the process parameters and scaling it up to industry size.** Adding wax to the resin solution and heat treatment at moderate temperatures (160 – 180 °C) reduced the panel thickness swelling by more than a third. Higher treatment temperatures (200 – 220 °C) showed similar effect but notably weakened bending MOR. At this stage, the full factorial exploratory screening experiment yielded ambiguous results and thus parameters were approximated with data clusters. Hereafter, adhesive distribution and scrim form were investigated with larger sample groups overcoming the prior statistical problems. The influence of the culm height portion (top, middle, bottom) on panel properties was found negligible so that scrims had to be further modified by crushing them finer. Those showed slightly better compaction behavior, but the low resin content (5 %) and a higher specific surface let them swell extraordinarily. Increased resin content in the panel core layer lowered swelling and increased internal bond. In the industrially upscaled hot-press (no cooling), 10 % resin caused high vapor pressure (blowout) or extensive (> 2 h) batch time. To overcome these problems, the industrial heat treatment at 180 °C with stacks of 40 mm led to a proper moisture content (5 %). **Lastly, the technical export market entrance hurdles were analyzed and product quality tested.** The inadequately regulated market situation led to the development of an own test scheme. The heat-treated decking boards fulfilled bending and surface requirements, improved dimensional stability at 180 °C treatment temperature but failed in weathering tests. When attacked by wood-destroying fungi, the heat-treated bamboo scrimber showed to be slightly to very durable, depending on the use class and test method. However, the densification and surface finishing must be further improved to be able to compete in the very demanding outdoor building product market.

6.1 Economic context

The Costs of Goods Manufactured (COGM) was worked out and the competitive landscape was analyzed. This information is needed for price estimates on export markets. The COGM represents the industrial value chain[18] where the Cost of Goods Sold (COGS) includes all expenses related to the production and provision of the bamboo scrimber[19], while excluding the costs for distribution and sale effort. The model used here included the whole value chain from industrial production up to an European warehouse (CIF Hamburg). The complete breakdown and operational assumptions can be found in the digital appendix to this work. The COGM model considered a production system with two hot-press lines for separate product configurations (e.g. indoor and outdoor product). The maximum capacity of both lines would be 223,534 and 277,200 m²/yr, i.e. roughly 500,000 m²/yr with prior production parameters. The progressively changing cost structure during the first ten years of operation was broken down in figure 95. The total COGS grow steeply during the first four years due to rising direct and indirect material costs with increasing production capacity. The first year of operation assumed a production capacity of only 2 % followed by 60, 88 and 95 % in the second, third and fourth year, respectively. In the fifth year the cost model reached total capacity and from here on costs are driven by general price indices and exchange rates. The direct material costs composed of the bamboo raw material costs (17 %), resin (29 %), additive (2 %) and finishing oil (9 %). Together with the direct labor cost (5 %) they are the direct production costs and under current assumptions stand for 62 % of the total COGS. The remaining indirect costs account for tooling and maintenance (8 %), packaging (3 %), utilities (2 %) such as water and electricity, consolidated costs for national transport (2 %), overseas shipping, handling and logistics (20 %). The detailed breakdown of costs item by item can be found in the digital appendix.

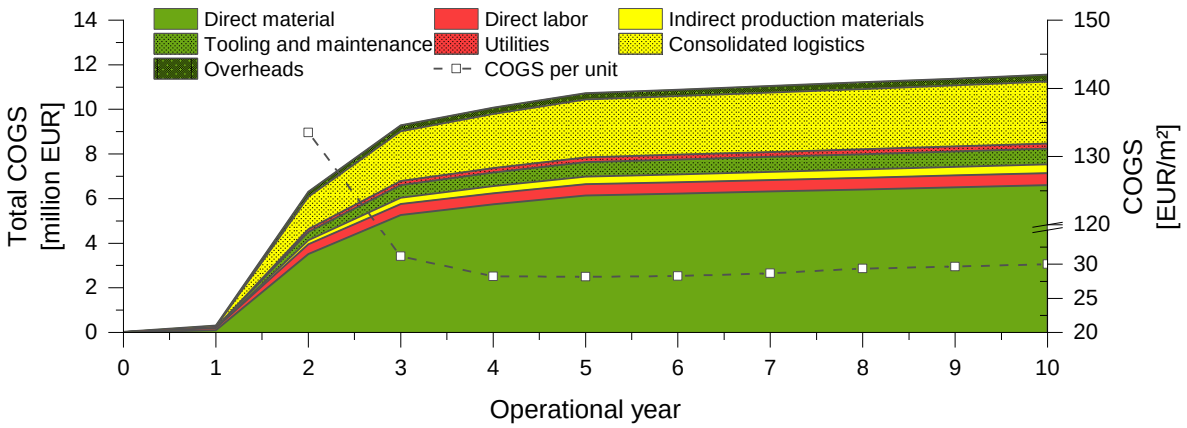

Figure 95: Modelled costs of goods sold (COGS) in total and per unit and its composition during the first 10 operational years

The modeled COGS per unit would fall accordingly from 133.50 EUR/m² in the second production year, to 31.19 EUR/m² in the third year and then arrive at the level of 28.20 EUR/m². No margins have been included with the COGM and the COGS yet. That means the comparison with B2B and B2C prices in table 39 is factually incorrect but gives an orientation. Thus, exemplarily a standard buyer price at FOB Rotterdam of 39.80 EUR/m² was defined

[18] "*Fertigungskosten*"

[19] "*Beschaffungskosten der verkauften Waren*"

based on the COGS[20]. The prices in the current competitive landscape of the European decking market is shown in table 39. The Chinese producers offer bamboo scrimber prices between 27.63 and 38.15 EUR/m²; most of them are offered at FOB Shanghai or other international Asian ports. Substitutional products such as WPC were found more affordable, but insurance and freight cost are the same due to the bulky format of the product. Selected tropical hardwoods and European thermally modified wood go beyond 40 EUR/m², some available at FOB South America, others being locally available at the destination market. It can be noted that the COGS based pricing of the Ethiopian BS decking ranged at the upper part of the market segment.

Table 39 Competitive landscape analysis based on unpublished survey data from 2018 with bamboo scrimber (BS), wood-plastic-composite (WPC) hardwood (HW) and softwood (SW) in different product lines (HT heat treated, LT carbonized, TG tongue and groove joint, M machined profile)

			Dimension [cm]			**Price**	
	Company	Product	L	W	T	€/m²	Incoterm
BS	Producer PRC (1)	HT, TG, M	183	13.7	4.0	33.50	-
	Producer PRC (2)	LT, M	185	10.0	2.0	33.76	FOB
		HT, TG, M	185	14.0	2.0	34.64	FOB
		LT, TG	185	14.0	2.0	33.76	FOB
		HT, TG, M	185	10.0	2.2	38.15	FOB
	Producer PRC (3)	LT, TG, M	185	14.0	2.0	33.46	FOB
		LT, tile, M	30	30.0	2.5	34.13	FOB
	Producer PRC (4)	LT, TG, M	187	13.9	1.8	27.63	FOB
		LT, TG, M	187	13.9	2.0	28.94	FOB
	Exporter PRC	-	96	9.6	15.0	35.00	-
WPC	Producer PRC	hollow		-		14.73	FOB
	Exporter PRC	co-extruded	100	14.0	2.5	26.31	-
HW	Exporter IDN	Bangkirai, TG, M	-	14.5	2.5	28.94	FOB
	Exporter BR	Cumarú	183	14.0	2.5	28.50	FOB
		Ipê	183	8.9	2.5	39.47	FOB
		Teak (plantation)	183	8.9	2.5	19.73	FOB
	Retailer GER	Ash, HT, TG, M	240	13.5	2.1	53.50	B2C-VAT
		Garapa	240	14.5	2.1	53.60	B2C-VAT
SW		Douglas fir	360	13.8	2.6	17.82	B2C-VAT
		Larch	300	14.0	3.0	25.94	B2C-VAT
		Pine, HT, TG, M	300	13.7	2.5	42.10	B2C-VAT

The decreasing exchange rate of the national Ethiopian currency *Birr* favored on the one hand the export, on the other hand made it difficult to purchase import production materials, such as additives and resin. However, even with this enormous and long term currency inflation, the lower labor cost and a relatively cheap bamboo raw material, the competition with established producers on cost base did not seem to be wise. Pricing is probably the most important marketing instrument and price elasticity on demand in this market segment is relatively high. This in turn means that customers are willing to pay a higher amount since there is a strong believe that high prices are indicators of better quality. A popular and exposed project such as

[20] Typically, a tiered sale system would set a price range (wholesale goods partner 75 % of standard price; contractual sale 90 % of standard price)

happened with the façade cladding in Madrid airport would be the key to gain consumer trust in high purchase power markets. Other marketing aspects, for example labelling (certification) and the creation of a genuine brand must be focused. This new brand imaging shall take advantage of the export success stories of adjacent agro-processing industries in Ethiopia. A coordinated cross-branding strategy with coffee, floriculture, textile or leather products may arouse delight associations with the potential customer.

The prospective production capacity of 500,000 m² annually (corresponding to 11,500 m³) and the suggested pricing policy resulted in a calculated 6 to 41 % gross margin. With a theoretical full export ratio the revenue potentially attained EUR 16.3 million, or USD 19 million, in the fifth production year. Although the model considered production rejects and other losses, this figure is obviously only valid with once the whole annual production was sold. However, it showed that a fully operating BS factory significantly contributed to the Ethiopian trade balance in wood products. Figure 5 illustrated that the past Ethiopian export of wood and wood products accounted to only USD 3.15 million (0.15 %) while import accounted to USD 104 million (0.58 %) lately. This ratio may notably shift with a successfully exported bamboo scrimber product. In addition, substitution effects in the import market for coniferous sawn wood (USD 40.5 million in 2016) are imaginable.

6.2 Outlook

The range of building products that potentially can be made from scrimber is wide: beams, columns, flanges, façade cladding, parquet flooring and others. The terrace decking application demands a highly resistant material and might not be the first choice when developing a new market for highland bamboo. In the short term, a diversification of products to indoor products may stimulate the bamboo supply chain and at the same time mitigate the needed investment sum at the beginning. A scrimber factory for outdoor products shall potentially stand at the end of such a development, as many uncertainties require practical experience and were not solved by the present research.

Crucial weak points of highland bamboo scrimber in exposed outdoor environment are hardness, susceptibility to weathering and biodegradation. The identified risks for the surface might be solved with coatings on a later commercialization stage. Weathering experiments with oiled surfaces had been planned by the project partners but did not form part of this work anymore. Further refinement of the scrim making (crusher) and a better understanding of the densification process in the hot press are crucial. A systematic multivariate analysis shall prospectively elaborate the interdependence of panel target density, resin content and scrim strand geometry. The latter was not investigated systematically in the present work and must not be neglected in future studies. The densification of the surface layer in particular and the forming of a homogeneous vertical density profile will help make a panel of consistent quality.

A major drawback from economic as well as environmental perspective is the excessive use of phenolic formaldehyde resins. Despite this work made efforts to reduce the resin content below common industry standards, the amounts are still notably higher than in plywood or wooden strand boards. Alternatives such as lignin-based PF resins, acrylate or isocyanate adhesives shall be studied with bamboo scrimber. They bear the potential to reduce environmental impact and the latter may even avoid process problems due to the condensation reaction in the hot press. A soy-protein based resin has been successfully used within the development project at Fraunhofer WKI and fulfilled given emission (VOC) standards for usage as indoor flooring product.

The needed raw material supply with consistent bamboo culms is a complex logistical challenge which must be worked in parallel. The potential benefit for rural bamboo producers is impressive and motivates to practically implement such an operation in Ethiopia and elsewhere in East Africa. The average monthly family income of a small farm in ranges between a 1000 to 1890 ETB (24 to 45 EUR), with only two thirds coming from crop sales. The projected bamboo scrimber industry at full capacity consumes 2,050,027 culms annually which will be provided by subsistence farmers at a price of roughly 15 ETB per culm (0.6 EUR). The forestry advisors and private partner in Ethiopia involve about 2,500 farmers in the supply chain project. The vast amount of semi-processed bamboo culms needed for a bamboo scrimber factory has the potential to double the farm income. The industrial demand may encourage rural communities to manage their bamboo stock, increase productivity and diversify their crop income.

List of figures

Figure 1: Total gross domestic product (GDP) and the cumulated shares of agriculture, industrial and manufacturing sector in the Ethiopian economy from 1993 to 2017, adopted from World Bank (2018) data 19

Figure 2: Structure of this work 23

Figure 3: Structure of the state of the art chapter 24

Figure 4: Import share by origin country with import volumes higher than USD 100 million in 2016 (UNcomtrade 2018) 25

Figure 5: Normalized value share of Ethiopian wood products import of the five largest categories (left axis) and the total value of the imported wood products (right axis) using HS92 codes from 2000 to 2016 (UNcomtrade 2018) 28

Figure 6: Landsat imagery bamboo mapping using data from 2016 extracted from Zhao *et al.* (2018) and the occurrence of the two native bamboo species in Ethiopia by federal districts (Desalegn and Tadesse 2014) 30

Figure 7: The actual and potential Ethiopian bamboo-based value web illustrating 1. Existing (black arrows) and potential supply relations (grey arrows), 2. Processing depth (red: highly intense; yellow: medium; green: low), 3. Economic impact (line thickness) and 4. Product spaces (grey domains) 33

Figure 8: Traditional Sidamo dome house made from woven bamboo strips (left) and mechanically extracted technical bamboo fiber (right) 34

Figure 9: View on infrastructure utility tunnel made from a bamboo-based winding composite (XZBBC 2016) 35

Figure 10: Classification of engineered composite panels from bamboo by their intermediate raw materials from large to small element size 37

Figure 11: RM pulp produced with atmospheric pressure from Ethiopian highland bamboo (Kickhöfen 2019) 39

Figure 12: Hammer mill produced particles from Ethiopian highland bamboo (Stute 2018) ..40

Figure 13: Bamboo strands produced with a Pallmann universal knife ring flaker including nodes (A) and without nodes (B) on a Yung Lifa strander, adopted from Grossenbacher (2012) 41

Figure 14: The scrims after being released from the crusher line (Hemmings 2019) 43

Figure 15: Apparatus described by Harvey Jr (1972) using three pairs of crusher rollers (a), four pairs of press rollers (b) and a scrubber device for strand separation (c) 43

Figure 16: The two basic log disintegration principles in the Eastern German “Quetschholz” technology (Götze and Luthardt 1974 cited in Joscak *et al.* 2006) 44

Figure 17: The two roll press splitters in the Japanese SST process disintegrating the log into slabs with a coarse disc profile (1) and a fine disc profile for transforming the slabs into scrims (2), modified sketch from Miyatake (2004) cited in Ceccotti and van Kuilen (2004) 45

Figure 18: Device for the production of macro-fibers from wood trunks (Graeter *et al.* 2012)46

Figure 19: Scrimber billets made from pitch pine produced with the TimTek® technology (A), European beech produced in Fraunhofer laboratories (B), guadua bamboo produced with the GrassBuilt® process (C) and moso bamboo scrimber from a commercial batch from China (D) 48

Figure 20: The two most common bamboo veneer production methods (left): Rotary slicing of a culm (A) and fineline block-slicing (B), adopted from Hidalgo López (2003) and a Fineline veneer industrial plant in Hangzhou, Zhejiang (right), adopted from Fu (2008) 49

Figure 21: Planed moso slats (1) for Chinese glue laminated bamboo lumber (2) and Colombian ply boards made from raw guadua strips (3) and a hand woven highland bamboo mat produced for Ethiopian vernacular construction (4)) 51

Figure 22: The hot press and cold molding process scheme in Chinese bamboo scrimber productions (Yu *et al.* 2015b) 53

Figure 23: Highland bamboo scrims leaving the machine (1) and cross section of planer (A-A) and profiled rollers (B-B)) in the scrim crusher machine used in this study 54

Figure 24: Bamboo scrim produced in a 4th generation fluffing machine comprising the epidermal green part of moso (Yu *et al.* 2014a) 55

Figure 25: Chemical composition of highland bamboo after heat treatment at four temperature levels and two holding times, mass percentage related to the final oven-dry mass, modified from Starke *et al.* (2016) 57

Figure 26: Fluorescence microscopy photograph of a cross section of a commercial bamboo scrimber decking product and a magnified section (red box) showing the distinct fiber bundle layers (A, B, C, D) 59

Figure 27: Vertical density profiles of aleatorily laid bamboo scrim mat (a, b) and a systemically layered scrim mat (c, d) as shown in Zhou *et al.* (2019) 60

Figure 28: Illustration of the process scheme starting at the splitter and crusher, and then weaving or knitting single bamboo fiber bundles into a veneer like mat with a cotton lining, as shown in Zhou *et al.* (2019) 61

Figure 29: Flooring products from bamboo scrimber in three market typical sortiments: Bleached with tongue and groove, carbonized click parquet and a three layered product with MDF base layer and poplar counter veneer 65

Figure 30: Structure of the raw material study 66

Figure 31: Isometric view on FESEM pictures of culm tissue with vascular bundles embedded in a parenchymatic matrix in African lowland bamboo *Oxythenantera abyssinica* (A) and highland bamboo *Yushania alpina* (B) 70

Figure 32: Light microscopy (200x) of the cortex, epidermis and hypodermis of *Bambusa polymorpha* (Liese 1998) 72

Figure 33: The macroscopic and microscopic anatomical structure of a node (A) and internode (B) of African highland bamboo showing a cross-section (10x) and a modified schematic draft based on Liese (1998) 73

Figure 34: Crossectional FESEM picture of a 4 years old internode indicating parenchymatic cells filled with starch granulate in African highland bamboo *Yushania alpina* 74

Figure 35: Edited map section of the harvest region in Southern Ethiopia (Earthstar Geographics 2018) 78

Figure 36: Microscopic image and processed binary image of a compression sample cross section 80

Figure 37: Stress-strain curves for bamboo internode (green) and node (red) samples in tension measured with mechanical lever gauge sensor (A) and a contact free method via video monitoring (B) 81

Figure 38: Strain measurement on a compression sample prepared with a speckle pattern (A) through makroXtens extensometer and videoXtens, showing the strain heat map before load was applied (B) and when the sample reached 0.2 x F_{max} (C) 82

Figure 39: Internode length (L_{IN}) and the regarding outer diameter (D), inner diameter (d) and culm wall thickness (wt) represented by the bubble size (left) and its normalized height curves (right) 84

Figure 40: Wall thickness (green), inner (red) and outer diameter (yellow) at culm breast height against its total culm height....86

Figure 41: Cross-sectional area of annulus defined by wall thickness with inner diameter (green/red circles) and with outer diameter (yellow/green circles) against apparent cross-sectional area computed through outer diameter D and their respective linear relationship 87

Figure 42: Reflected-light microscopy images (50x) from the outer (left), middle and inner (right) portion of the cross section of an internode of highland bamboo 90

Figure 43: Transmitted light microscopy image (500x) of a fiber bundle cross section of *Y. alpina* for cell wall and diameter measurement 91

Figure 44: Transmitted light microscopy (25x) of macerated fiber cells from the node (left) and internode (right) of *Y. alpina* for fiber length measurement....92

Figure 45: Mass percentage of ash and silica content of nodes (NO) and internodes (IN) in thin-walled and thick-walled bamboo culm before and after a washing step 93

Figure 46: FESEM image (100x) of the terminal cortex cell layer containing silica crystals...94

Figure 47: Axial tension strength (MOR) and modulus of elasticity (MOE) against density for highland bamboo scrims containing an internode (triangles) and node (circles)....95

Figure 48: Interlaminar shear and fiber pullout in a tension loaded bamboo internode sample with a high FBD indicating the initial location of failure occurred at the specimen clamping edge 96

Figure 49: Stress-strain curves for tension loaded bamboo internode and node samples with a high (A), moderate (B) and low (C) fiber share (FBD) 97

Figure 50: Compression strength (MOR) and modulus of elasticity (MOE) against density for highland bamboo scrims containing an internode (triangles) and node (circles) and transition zone (pentagrams)....98

Figure 51: Mean strength (MOR) and modulus of elasticity (MOE) of highland bamboo internode (red), node (green), transition (yellow) loaded axially and normalized to flexural means....99

Figure 52: Structure of the process engineering research 102

Figure 53: Workflow scheme for the African highland bamboo scrimber process development 103

Figure 54: Meaning of symbols in box plots throughout the study....107

Figure 55: Broad, medium and narrow (f.l.t.r.) width classes of scrim strands used during the screening of production parameters....110

Figure 56: The lab-scale kiln chamber (left) and treated strands after 3 h / 160 °C (right)...111

Figure 57: Resin spray application on lab-scale scrims (left) and the press-ready mat with a temperature probe in the core layer (right) at Fraunhofer WKI laboratory 113

Figure 58: Mat formation with narrow scrims in the core, medium strands in the center and broad strands in the face layer (left) using a softboard template (right) 113

Figure 59: Press-ready fiber bundle mat with a temperature probe in the core layer (left) and conditioning in a warm veneer press forming a hot stack for curing (right) 114

Figure 60: Resin application by liquid extrusion gluing pushing the glue paste through several fine nozzles composing a pseudo-curtain (left) and the bottom side of the circular jet gun station atomizing the resin solution with pressurized air (right) 116

Figure 61: Thickness swelling (TS) and internal bond (IB) of scrimber panels against density produced with four different phenolic systems (PF1-4) shown as cluster for all heat-treated samples (V1) 121

Figure 62: Surface photography of lab-scale scrimber produced of heat-treated highland bamboo (160, 180, 200, 220 °C).....124

Figure 63: Thickness swelling (TS) and water absorption (WA) of highland bamboo scrimber with three different resin gradients and concentrations tested after 2 and 24 h 128

Figure 64: Internal bond (IB) of highland bamboo scrimber with three different resin gradients and concentrations tested in standard climate (20 °C/65 %), oven-dry and after 2 or 5 h water storage 129

Figure 65: Internal bond (IB) of highland bamboo scrimber with three different resin gradients and concentrations tested after 5 h water storage; Means sharing same letters are not significantly different at $p \leqslant 0.05$ 130

Figure 66: Cross section layers under fluorescence microscopy showing different resin concentration in the surface (SL) and core layer (CL) with 12-12-12 (A); 14-14-14 (B); 16-16-16 (C); 16-12-16 (D); 14-12-14 (E) in %.....131

Figure 67: Surface, transversal and longitudinal section of laboratory scale highland bamboo scrimber with red boxes indicating superficial flaws, arrows pointing from the left to the right indicating low density and from right to left high compaction regions 132

Figure 68: Scrim strands from the top portion (left) and fine crushed scrims from the same top portion (right) 133

Figure 69: Thickness swelling (TS) for scrimber made from scrims coming from the bottom (B), middle (M), top (T) portion of the culm and a finer crushed (F) variant (left) and F and T means against sample density class (right) 135

Figure 70: Internal bond (IB) for scrimber made from scrims coming from the bottom (B), middle (M), top (T) portion of the culm and a finer crushed (F) variant (left) and F and T mean against sample density class (right); Means sharing same letters are not significantly different at $p \leqslant 0.05$.....136

Figure 71: Thickness swelling (TS) and internal bond (IB) for scrimber made from heat treated (180 °C) highland bamboo produced with different resin concentrations and a sample of finely (F) crushed scrims.....137

Figure 72: Manual fiber bundle layup (A), hot press compression (B), finished bamboo scrimber panel (C) and blow-out in the cross section from the industrial scale pilot production 139

Figure 73: Resin impregnated highland bamboo scrims (A) in close-up (B) applied with industrial curtaining and spraying and the resulting hot-pressed panels as seen in cross-section (C), lateral (D), top (E) and bottom (F) 141

Figure 74: A chamber-ready batch of manually stacked scrim strands with 20 mm spacing and 20 mm layer thickness separated by aluminum spacers 143

Figure 75: Structure of the export market requirements chapter 147

Figure 76: Bamboo scrimber classification with regards to the testing standard GB/T 30364:2013-11 149

Figure 77: Top view and cross section (left) of specimens tested against basidiomycetes from samples made from heat treated bamboo scrimber (Ctrl, 160, 180, 200 °C) and specimens from surface layer and core layer (right) 162

Figure 78: Mean flexural modulus of elasticity (MOE), strength (MOR), maximum load (F) and deflection (δ) of industrial-scale scrimber produced from untreated and heat treated highland bamboo (160, 180 °C) before (dry) and after (wet) a moisture cycle 165

Figure 79: Modulus of elasticity (MOE) against strength (MOR) in bending, tension and compression for raw highland bamboo scrims (grey ellipses) and for industrial-scale scrimber from untreated (green) and heat treated (yellow: 160 °C; red: 180 °C) highland bamboo in bending.....166

Figure 80: Flexural creep-modulus of elasticity (MOE_t) and the corresponding strain (ε) during 24 hours load (left) and the recovery strain (right) of industrial-scale bamboo scrimber (Untreated, 160, 180 °C) and a commercial scrimber product (Comm.) 167

Figure 81: Mean Brinell hardness (HBS) and elastic rebound (ER) of industrial-scale bamboo scrimber (untreated, 160, 180 °C) and a commercial scrimber product (comm.) and a WPC product (WPC).....168

Figure 82: Impact resistance determined by indentation depth (h) of industrial-scale bamboo scrimber (untreated, 160, 180 °C) and a commercial scrimber product (comm.).....169

Figure 83: Mean pull-through resistance maximum load (F) and deflection (δ) of a stainless-steel screw with defined torque applied to industrial-scale highland bamboo scrimber (untreated, 160, 180 °C).....170

Figure 84: Mean sliding friction coefficient (μ) of industrial-scale bamboo scrimber (Untreated, 160, 180 °C) and a commercial product (comm.) with rough (r) and fine (f) profiles 171

Figure 85: Differential dimensional change in % per % moisture content change in the humidity range 30 < 65 < 85 % (swelling) and 85 < 65 < 30 % (shrinkage) in thickness (left) and length (right) for industrial-scale highland bamboo scrimber (untreated, 160, 180 °C) and a commercial scrimber product (comm.); Means sharing same letters are not significantly different at $p \leqslant 0.05$ 172

Figure 86: Artificially (top) and naturally (bottom) weathered samples of industrial-scale highland bamboo scrimber (untreated, 160, 180, 200 °C) showing the corresponding reference on the right bottom corner.....173

Figure 87: Naturally weathered samples of commercial bamboo scrimber (left) with the reference (right) and severe longitudinal cracks on the surface (red ellipses) 174

Figure 88: FESEM images after 8 weeks incubation: Cross section (A, B) and longitudinal section (C, D) of raw bamboo (A, C) and face layer bamboo scrimber (B, D) showing mycelium growth (red arrows) in lumen of axial parenchyma and vessel (A, C) as well as ruptures between fiber cells and strongly densified parenchyma tissue (B) with minor mycelium growth in vessel (D) 175

Figure 89: Oven-dry density (ρ_0) and moisture content (MC) of raw bamboo and industrial-scale highland bamboo scrimber core and face layer after 8 weeks screening incubation with five basidiomycetes.....176

Figure 90: Mean moisture content (MC) of industrial-scale bamboo scrimber (untreated, 160, 180, 200 °C) before and after 16 weeks incubation with basidiomycetes (left) and the correlation between fungal mass loss (Δm) and equilibrium moisture content (EMC) 178

Figure 91: Mean stiffness loss (ΔMOE) as percentual share of the original value and corresponding moisture content (MC) of industrial-scale bamboo scrimber (untreated, 160, 180, 200 °C) prior to exposure and during incubation in a soft rot soil bed test.....179

Figure 92: Mean oven-dry density (ρ_0) and relative mass loss (Δm) of industrial-scale bamboo scrimber (untreated, 160, 180, 200 °C) core and face layer after 28 weeks incubation in the soft rot soil bed test.....180

Figure 93: Transmitted light microscopy (100x) of the longitudinal-radial section of degraded pine tracheid cells (left) and axial bamboo parenchyma and fiber cells (right), red arrows indicating soft rot hyphae in lumina and spiral cavities in the cell wall 181

Figure 94: Mean mass (Δm) and modulus of elasticity loss (ΔMOE) as percentual share of the original value prior to exposure for and the calculated x-value for industrial-scale bamboo scrimber (untreated, 160 °C) and references after 28 weeks incubation in a soft rot soil bed 182

Figure 95: Modelled costs of goods sold (COGS) in total and per unit and its composition during the first 10 operational years.....186

Figure 96: Transformation paths of a culm to engineered bamboo (World Bamboo Organization 2018) 218

Figure 97: Probability distribution density functions of culm wall thickness, outer diameter, internodal length and their respective 25,75 quartile boundaries.....219

Figure 98: Flexural strength (MOR) and modulus of elasticity (MOE) for scrims from highland bamboo internode (red) and node (green) 222

Figure 99: Flexural modulus of elasticity (MOE) for bottom (B), middle (M), top (T) as well as fine (F) scrims against sample density.....228

Figure 100: Flexural strength (MOR) for bottom (B), middle (M), top (T) as well as fine (F) scrims against sample density 228

Figure 101: Internal bond (IB) and a linear regression and confidence interval against the actual specimen density of panels made from bottom (squares), middle (crosses), top (x) and fine (triangles) strands.....229

Figure 102: Cross section of scrimber specimens made from crushed scrims coming from bottom (B), middle (M), top (T) portion of the culm and a finer crushed (F) variant 230

Figure 103: Progression of actual stack temperature (H.T. temp 1-4), chamber temperature (Temp, Temp 2) and relative humidity (Rel-Hum 2) at a nominal target temperature of 180 °C (above) and 160 °C (below) and 3 h holding time in the industrial scale treatment 231

Figure 104: Characteristic press diagrams for untreated bamboo scrimber in a laboratory trial (top) and an industrial hot press (bottom) 232

Figure 105: Market requirements for bamboo scrimber in flooring and decking products, developed from customer demands, formal and informal standards 233

Figure 106: Sample cutting scheme showing the original plank and the position of specimens, 1-6 being assigned to test against basidiomycetes, 7 for the three panel layers testing against soft rot, 8 for density and moisture content determination and 9 reserved for termite or borer testing.....234

List of tables

Table 1 Extent of bamboo forest cover in SSA by country (top 5) and the world total according to Lobovikov *et al.* (2007) and FAO (2006) for 1990 to 2005 and Zhao *et al.* (2018) for 2017 29

Table 2: Bending strength (MOR) and elasticity (MOE), internal bond (IB) and thickness swelling after 24 h water immersion (TS) of oriented strand board from steam-treated Ethiopian highland bamboo produced with different resin contents (Fraunhofer 2014) 42

Table 3 Descriptive statistics of highland bamboo wall thickness in three height portions according to Schmidt (2013) 68

Table 4 Mean fiber lengths of some major commercial bamboo species selected from Liese (1998)[A], Liese and Grosser (1972)[B] and Osorio *et al.* (2018)[C] 71

Table 5 Descriptive statistics of culm form parameters culm height (h), outer and inner diameter at breast height (D_{bh}, d_{bh}), wall thickness (wt), breast height (h_b).....83

Table 6 Descriptive statistics of artificial form factor f with reference to breast height (bh) for the outer (D) and inner (d) shape and the height dependent form factor (λ) at two relative heights (i, j) 88

Table 7 Apparent volume V(D), actual woody volume calculated by the substitutional method V(D,d) and the reduction factor V(r) method for the sectional approach ($\sum V_i$), the form factor approach (V_f) and the two-way equation approach (V_λ) 89

Table 8: Number of vascular bundles, fiber fraction and morphology (cell wall, diameter, length) in internode (IN) and node (NO) as a mean across the whole culm wall thickness.....91

Table 9: Mean moisture content (MC), density (ρ) and fiber volume fraction (FBD) and their regarding standard deviation (in brackets) for node (NO), internode (IN) and transition (INNO) samples in three mechanical tests with n = 20 each 94

Table 10: Flexural, tensile and compression strength (MOR) and modulus of elasticity (MOE) parallel to grain for highland bamboo scrim strands containing node (NO), internode (IN) and transition zone (INNO) and their descriptive statistics 96

Table 11: Process control variables and estimated process impact on the final product quality and/or the following process step intermediate product (+ low impact, ++ medium impact, +++ strong impact).....105

Table 12: Full factorial experimental matrix for the screening of production parameters 109

Table 13: Hot-press phases configuration at laboratory scale.....114

Table 14: Full factorial experimental matrix for the screening of press temperature.....115

Table 15: Test and measurement standards as well as total plan number of specimens during the screening phase 116

Table 16: Mean and standard deviation (in brackets) of moisture content (MC) and density for all specimens tested coming from panels for the production parameter and press temperature investigation.....117

Table 17: Mean thickness swelling (TS), water absorption (WA), internal bond (IB), bending strength (MOR) and modulus of elasticity (MOE) for scrimber panels hot pressed with three target temperatures (120, 130, 140 °C) using two resin concentrations by tank dipping untreated bamboo scrim strands.....118

Table 18: Mean and standard deviation (in brackets) of moisture content (MC) and density (ρ) for panels produced with three hot-press target temperatures 118

Table 19: Mean thickness swelling (TS), water absorption (WA), internal bond (IB), bending strength (MOR) and modulus of elasticity (MOE) for scrimber panels hot-pressed with three target temperatures using two resin concentrations, untreated (Ctrl.) and heat treated (HT) scrims 119

Table 20: Descriptive statistics of the effect of four different phenolic systems (PF1-4) on thickness swelling (TS), water absorption (WA) and internal bond (IB) of scrimber panels produced from all heat treated V1(T; t) bamboo scrims grouped in one cluster with means in the same column sharing same letters are not significantly different at $p \leqslant 0.05$ 120

Table 21: Descriptive statistics of the effect of four different phenolic systems (PF1-4) on thickness swelling (TS), water absorption (WA), internal bond (IB), flexural strength (MOR) and modulus of elasticity (MOE) for scrimber panels produced from untreated (V0) as well as heat treated (V1) bamboo scrims grouped in differently sized cluster.....122

Table 22: Descriptive statistics of mean thickness swelling (TS), water absorption (WA) and internal bond (IB) of scrimber panels produced from scrim strands priorly treated at low temperatures 160, 180 °C (LT) and high temperatures 200, 220 °C (HT) for the cluster comprising V2, V3 and V4; Means in the same column sharing same letters are not significantly different at $p \leqslant 0.05$ 125

Table 23: Descriptive statistics of clustered mean thickness swelling (TS), water absorption (WA) and internal bond (IB) of scrimber panels produced with and without wax for all variants V0, V1, V2 and V3 126

Table 24: Moisture content (MC) and density (ρ) for panels produced with different resin concentrations in core (CL) and face layer (FL) 127

Table 25: Sample size, mean and standard deviation (in brackets) of moisture content (MC) and density (ρ) for bamboo scrimber panels produced with different fiber bundle classes and a lowered target density (0.9 g/cm³) and resin concentration (c = 5 %).....133

Table 26: Flexural modulus of elasticity (MOE) and strength (MOR) for panels from bottom (B), middle (M), top (T) and fine (F) scrims; Means sharing same letters are not significantly different at $p \leqslant 0.05$ 134

Table 27: Internal bond (IB) and press observations of industrial bamboo scrimber panels with different opening times (t) and opening temperatures (T) in the panel core 139

Table 28: Weight of scrim and resin and the resulting resin concentration using two industrial application methods: circular jet gun spraying (CJG) and liquid extrusion glue curtaining (LEG).....140

Table 29: Calculated mass difference (Δm) and equilibrium moisture content (EMC) at standard climate (20 °C/65 %) of highland bamboo fiber bundle batches before and after heat treatment in an industrial scale chamber using different layer thickness (LY) and spacing distance (SP) between the layers for temperatures of 160 and 180 °C and 3 h holding time 142

Table 30: Potential test program for bamboo scrimber products in outdoor decking purposes, modified from Schmidt *et al.* (2016a) 151

Table 31: Screened fungi, strain origin, white rot or brown rot (WR/BR) and obligatory use according DIN EN 17009:2016-07 161

Table 32: Durability class (DC) derived from mass loss figures for basidiomycetes and x-values computed from mass loss (ML) and stiffness loss for soft rot testing according to DIN EN 350:2016-12 as referred by DIN EN 17009:2019-06 162

Table 33: Mean abrasion mass loss per 50 rounds [mg] after a total of 500 cycles with a S-34 emery paper for n = 3 for industrial-scale highland bamboo scrimber (Untreated, 160, 180 °C) and a commercial product (comm.) with rough (R) and fine (f) profiles 169

Table 34 Colorimetric differences ΔEab for industrial-scale highland bamboo scrimber (untreated, 160, 180, 200 °C) and commercial bamboo scrimber (Comm.) after 300 h exposure to artificial and one year to natural weathering 173

Table 35: Median mass loss of the sterile control and raw bamboo (raw) and industrial-scale highland bamboo core (CL) and face layer (FL) after 8 weeks incubation with brown rot (BR) and white rot (WR) basidiomycetes; n = 6.....174

Table 36: Corrected median mass loss (Δm) and stiffness loss (ΔMOE) as percentual share of the original value prior to exposure for industrial-scale bamboo scrimber (untreated, 160, 180, 200 °C) after 16 weeks incubation with basidiomycetes and 28 weeks soft rot soil bed test according to the standards DIN CEN/TS 15083-1:2005-10, DIN CEN/TS 15083-2:2005-10; Median in the same row sharing same letter belong to means which did not significantly at $p \leqslant 0.05$.....177

Table 37: Relevant basidiomycete species, x-value and maximum median, median probability distribution among the classes (DC1-5) and the resulting durability class for industrial-scale bamboo scrimber (untreated, 160, 180, 200 °C) after 16 weeks incubation with basidiomycetes and 28 weeks soft rot soil bed test.....181

Table 38: Matrix overview on results for industrial-scale bamboo scrimber (untreated, 160, 180 °C) and a commercial product (Comm.) and the regarding test program with color code indicating the failed (red), tolerable (yellow) and passed (green) samples 184

Table 39 Competitive landscape analysis based on unpublished survey data from 2018 with bamboo scrimber (BS), wood-plastic-composite (WPC) hardwood (HW) and softwood (SW) in different product lines (HT heat treated, LT carbonized, TG tongue and groove joint, M machined profile) 187

Table 40 Regression parameter of outer and inner diameter at breast height (D_{bh}, d_{bh}) and wall thickness (wt) against culm height (h).....219

Table 41: Ash and silica content for raw and washed bamboo with thin and thick culm walls measured in the node and internode 220

Table 42: Quantitative analysis of monomeric carbohydrates shares [%] in *Y. alpina* by site, age and culm height section (< 0.1 was below LoD) 221

Table 43: Linear regression analysis of the correlation between stress and strain calculated in the function interval defined by four different boundaries, namely downer limit F_1 and upper limit F_2 222

Table 44: Panel recipe calculation for the screening trials experiments 223

Table 45: Resin gradient experimental matrix.....224

Table 46: Mean thickness swelling (TS), water adsorption (WA), internal bond (IB), flexural strength (MOR), modulus of elasticity (MOE) for press temperatures (T) and resin type (c); 225

Table 47: Density (R), thickness swelling (TS), water adsorption (WA), internal bond (IB), flexural strength (MOR), elasticity (MOE) for one panel pressed from heat treated V1(160 °C, 5 h) highland bamboo scrimber and PF1 resin.....227

Table 48: Regression ($y = a + b*\rho$) parameter comparison of IB against the actual specimen density and the theoretical critical density ρ_{crit} at IB = 0, for panels made from bottom, middle, top and fine scrims (B, M, T, F).....230

Table 49: Regression formulae for flexural creep strain and creep modulus of highland bamboo scrimber.....233

Table 50: Linear and polynomial regression analysis of the correlation between equilibrium moisture content (x) and fungal mean mass loss (y) for four different basidiomycetes shown in figure 90.....234

Literature

Journal articles

Abdalla A M and Sekino N. 2005. Veneer strand flanged I-beam with MDF or particleboard as web material III: effect of strand density and preparation method on the basic properties. *J Wood Sci* **51**, 492–497.

Abdul Khalil H, Bhat I, Jawaid M, Zaidon A, Hermawan D and Hadi Y S. 2012. Bamboo fibre reinforced biocomposites. A review. *Materials & Design* **42**, 353–368.

Ahmad M and Kamke F A. 2011. Properties of parallel strand lumber from Calcutta bamboo (*Dendrocalamus strictus*). *Wood Sci Technol* **45**, 63–72.

Akrami A and Laleicke P F. 2018. Densification, screw holding strength, and Brinell hardness of European beech and poplar oriented strand boards. *Wood Material Science & Engineering* **13**, 236–240.

Amada S, Ichikawa Y, Munekata T, Nagase Y and Shimizu H. 1997. Fiber texture and mechanical graded structure of bamboo. *Composites Part B: Engineering* **28**, 13–20.

Amada S, Munekata T, Nagase Y, Ichikawa Y, Kirigai A and Zhifei Y. 1996. The Mechanical Structures of Bamboos in Viewpoint of Functionally Gradient and Composite Materials. *Journal of Composite Materials* **30**, 800–819.

Amada S and Untao S. 2001. Fracture properties of bamboo. *Composites Part B: Engineering* **32**, 451–459.

André J-P. 1998. A Study of the Vascular Organization of Bamboos (Poaceae-Bambuseae) Using a Microcasting Method. *IAWA J* **19**, 265–278.

Anokye R, Bakar E S, Ratnasingam J, Yong A C C and Bakar N N. 2016. The effects of nodes and resin on the mechanical properties of laminated bamboo timber produced from *Gigantochloa scortechinii*. *Construction and Building Materials* **105**, 285–290.

Archila-Santos H F, Ansell M P and Walker P. 2014. Elastic Properties of Thermo-Hydro-Mechanically Modified Bamboo (*Guadua angustifolia* Kunth) Measured in Tension. *Key Engineering Materials* **600**, 111–120.

Ayana D E. 2014. Study on Fruit Production and Fruit Characteristics of *Oxytenanthera abyssinica* (A. Richard Munro) in Benishangul Gumuz Regional State, Northwestern Ethiopia. *International Journal of Life Sciences* **3**.

Bahar D, Hausmann R and Hidalgo C A. 2014. Neighbors and the evolution of the comparative advantage of nations: Evidence of international knowledge diffusion? Evidence of International Knowledge Diffusion? *Journal of International Economics* **92**, 111–123.

Bao M, Li N, Huang C, Chen Y, Yu W and Yu Y. 2019. Fabrication, physical–mechanical properties and morphological characterizations of novel scrimber composite. *Eur. J. Wood Prod.* **7**, 2948.

Barnes H M, Aro M D and Rowlen A. 2018. Thermally Modified Engineered Wood Products Durability. *Forest Products Journal* **68**, 99–104.

Beech E, Rivers M, Oldfield S and Smith P P. 2017. GlobalTreeSearch: The first complete global database of tree species and country distributions. *Journal of Sustainable Forestry* **36**, 454–489.

Bliem P, Frömel-Frybort S, van Herwijnen H W G, Pinkl S, Krenke T, Mauritz R and Konnerth J. 2019. Engineering of material properties by adhesive selection at the example of a novel structural wood material. *The Journal of Adhesion* **51**, 1–21.

Böck F. 2014a. Green gold of Africa – Can growing native bamboo in Ethiopia become a commercially viable business? *The Forestry Chronicle* **90**, 628–635.

Böck F. 2014b. Review: Bambus als Rohstoff - Potenziale prozesstechnischer Umsetzung; Prozesstechnische Vielfalt im Holzwerkstoffbereich mit Bambus als Rohstoff. *Holztechnologie* **55**, 47–52.

Bowden J. 2007. The great "scrimber" mystery. *Inwood*, 20.

Brandner R, Flatscher G, Ringhofer A, Schickhofer G and Thiel A. 2016. Cross laminated timber (CLT): overview and development. *Eur. J. Wood Prod.* **74**, 331–351.

Bremer M, Fischer S, Nguyen T C, Wagenführ A, Phuong L X and and Dai V H. 2013. Effects of thermal modification on the properties of two Vietnamese bamboo species. Part II: Effects on chemical composition. *BioResources* **8**, 981–993.

Brischke C and Hanske M. 2016. Durability of untreated and thermally modified reed (*Phragmites australis*) against brown, white and soft rot causing fungi. *Industrial Crops and Products* **91**, 49–55.

Buckingham K, Jepson P, Wu L, Rao I V R, Jiang S and Liese W *et al.* 2011. The potential of bamboo is constrained by outmoded policy frames. *Ambio* **40**, 544–548.

Buckingham K, Wu L and Lou Y. 2014. Can't see the (bamboo) forest for the trees: examining bamboo's fit within international forestry institutions. *Ambio* **43**, 770–778.

Candelier K, Pignolet L, Lotte S, Guyot A, Bousseau B, Cuny E and Thevenon M-F. 2017a. Decay resistance variability of european wood species thermally modified by industrial process. *PROLIGNO* **13**, 10–20.

Candelier K, Thevenon M-F, Petrissans A, Dumarcay S, Gerardin P and Petrissans M. 2016. Control of wood thermal treatment and its effects on decay resistance: a review. *Annals of Forest Science* **73**, 571–583.

Chaowana P. 2013. Bamboo. An Alternative Raw Material for Wood and Wood-Based Composites. *JMSR* **2**.

Cheng D, Jiang S and Zhang Q. 2013. Mould resistance of Moso bamboo treated by two step heat treatment with different aqueous solutions. *Eur. J. Wood Prod.* **71**, 143–145.

Cheng R and Zhang Q. 2011. A Study on the Bonding Technology in Sliced Bamboo Veneer Manufacturing. *Journal of Adhesion Science and Technology* **25**, 1619–1628.

Chung M J and Wang S Y. 2018a. Effects of peeling and steam-heating treatment on mechanical properties and dimensional stability of oriented *Phyllostachys makinoi* and *Phyllostachys pubescens* scrimber boards. *J Wood Sci* **21**, 625–634.

Chung M-J and Wang S-Y. 2018b. Mechanical properties of oriented bamboo scrimber boards made of *Phyllostachys pubescens* (moso bamboo) from Taiwan and China as a function of density. *Holzforschung* **72**, 151–158.

Colla W A, Beraldo A L and Brito J O. 2011. Effects of thermal treatment on the physicochemical characteristics of giant bamboo. *CERNE* **17**, 361–367.

Cui Z, Xu M, Chen Z and Xiang J. 2018. Experimental study on thermal performance of bamboo scrimber at elevated temperatures. *Construction and Building Materials* **182**, 178–187.

Curling S F, Clausen C A and Winandy J E. 2002. Relationships between mechanical properties, weight loss and chemical composition of wood during incipient brown-rot decay. *Forest Products Journal* **52**, 34–39.

Cutini A, Chianucci F and Manetti Maria C. 2013. Allometric relationships for volume and biomass for stone pine (*Pinus pinea* L.) in Italian coastal stands. *iForest* **6**, 331–335.

Deng J, Chen F, Wang G and Zhang W. 2016. Variation of Parallel-to-Grain Compression and Shearing Properties in Moso Bamboo Culm (*Phyllostachys pubescens*). *BioResources* **11**, 1784–1795.

Deng J, Li H, Wang G, Chen F and Zhang W. 2015. Effect of removing extent of bamboo green on physical and mechanical properties of laminated bamboo-bundle veneer lumber (BLVL). *Eur J Wood Prod* **73**, 499–506.

Deng J, Li H, Zhang D, Chen F, Wang G and Cheng H. 2014. The Effect of Joint Form and Parameter Values on Mechanical Properties of Bamboo-Bundle Laminated Veneer Lumber (BLVL). *BioResources* **9**, 6765–6777.

Depuydt D E, Billington L, Fuentes C, Sweygers N, Dupont C and Appels L *et al.* 2019. European bamboo fibres for composites applications, study on the seasonal influence. *Industrial Crops and Products* **133**, 304–316.

Desalegn G and Tadesse W. 2014. Resource potential of bamboo, challenges and future directions towards sustainable management and utilization in Ethiopia. *Forest Systems* **23**, 294–299.

Doering-Arjes P and Schmidt G. 2018. Some Myths of Bamboo Rodmaking and Beyond. Dedicated to the Making of Fine Bamboo Fly Rods. *Power Fibers Online Magazine* **58**, 1-49.

Dongsheng H, Aiping Z and Yuling B. 2013. Experimental and analytical study on the nonlinear bending of parallel strand bamboo beams. *Construction and Building Materials* **44**, 585–592.

Dosdall R, Jülich W-D and Schauer F. 2015. Impact of heat treatment of the water reed *Phragmites communis* Trin. used for thatching on its stability, elasticity and resistance to fungal decomposition. *International Biodeterioration & Biodegradation* **103**, 85–90.

Du C, Yao X, Hua Y and Huang Q. 2018. Preparation and Characterization of Combed Sawmill Slab Residues from Chinese Fir and its Scrimber. *BioResources* **13**, 8477–8487.

Duan A, Zhang S, Zhang X and Zhang J. 2016. Development of a stem taper equation and modelling the effect of stand density on taper for Chinese fir plantations in Southern China. *PeerJ* **4**, e1929.

Düking R, Gielis J and Liese W. 2011. Carbon Flux and Carbon Stock in a Bamboo Stand and their Relevance for Mitigating Climate Change. Bamboo Science and Culture. *The Journal of the American Bamboo Society* **24**, 1–6.

Eerikäinen K P, Mabvurira D and Saramäki J. 1999. Alternative Taper Curve Estimation Methods for *Eucalyptus cloeziana* (F. Muell.). *The Southern African Forestry Journal* **184**, 12–24.

Elias E. 2004. The Tarapoto Process: establishing criteria and indicators for the sustainable management of Amazon forests. *Unasylva* **55**.

Embaye K. 2000. The Indigenous Bamboo Forests of Ethiopia. An Overview. *AMBIO: A Journal of the Human Environment* **29**, 518–521.

Embaye K, Weih M, Ledin S and Christersson L. 2005. Biomass and nutrient distribution in a highland bamboo forest in southwest Ethiopia. Implications for management. *Forest Ecology and Management* **204**, 159–169.

Endalamaw T, Lindner A and Pretzsch J. 2013. Indicators and Determinants of Small-Scale Bamboo Commercialization in Ethiopia. *Forests* **4**, 710–729.

Esteves B M and Pereira H M. 2009. Wood modification by heat treatment: A review. *BioResources* **4**, 370–404.

Fan H, Zhang J, Bao J-H, Yuan S-F, Wang H-Y and Li Q. 2017. 建筑结构用重组竹材重要性能研究现状及发展趋势/. Current Situation and Trend of Researches on Properties of Bamboo Scrimber for Architectural Structure. (In Chinese). *J Zhejang Sci Tech* **37**.

Fan M, Yu, Yang, Zhu, Rong, Zhang Y and Yu W. 2011. Effect of Resin Impregnation Rate on Physical and Mechanical Properties of Laminated Bamboo Fibrillated-Veneer Lumber. (In Chinese). *China Wood Industry* **2**.

Fatrawana A, Maulana S, Nawawi D S, Sari R K, Hidayat W and Park S H *et al.* 2019. Changes in chemical components of steam-treated betung bamboo strands and their effects on the physical and mechanical properties of bamboo-oriented strand boards. *Eur. J. Wood Prod.* **77**, 731–739.

Febrianto F, Jang J-H, Lee S-H, Santosa I A, Hidayat W, Kwon J-H and Kim N-H. 2015. Effect of Bamboo Species and Resin Content on Properties of Oriented Strand Board Prepared from Steam-treated Bamboo Strands. *BioResources* **10**, 2642–2655.

Febrianto F, Sahroni, Hidayat W, Bakar E S, Kwon G-J and Kwon J-H *et al.* 2012. Properties of oriented strand board made from Betung bamboo (*Dendrocalamus asper* (Schultes.f) Backer ex Heyne). *Wood Sci Technol* **46**, 53–62.

Fu J. 2019. 埃塞俄比亚竹产业现状与发展机遇. Current Status and Development Opportunities of Bamboo Industry in Ethiopia. (In Chinese). *世界竹藤通讯* **16**, 1–5.

Fujii T and Miyatake A. 1993. Manufacturing and properties of SST (Super strand Timber) I. SST manufacturing from small-diameter logs. (in Japanese). *43rd annual meeting of the Japan Wood Research Society* **552**.

Fujii T and Miyatake A. 2003. SEM-EDXA study on the interface between wood and cement in Cement Strand Slab. *Bulletin of the Forestry and Forest Products Research Institute* **2**, 93–109.

Gao L, Guo W and Luo S. 2018. Investigation of changes in compressed moso bamboo (*Phyllostachys pubescens*) after hot-press molding. *J Wood Sci* **74**, 633.

Gauss C, Araujo V D, Gava M, Cortez-Barbosa J and Savastano Junior H. 2019. Bamboo particleboards: recent developments. *Pesqui. Agropecu. Trop.* **49**, 49.

Ghavami K, Allameh S M, Sánchez M L and Soboyejo W O. 2003. Multiscale study of bamboo *Phyllostachys edulis*. IAC-NOCMAT.

Gibson L J. 2012. The hierarchical structure and mechanics of plant materials. *Journal of the Royal Society, Interface* **9**, 2749–2766.

Ginoble Pandoli O, Martins R S, Toni K L G de, Paciornik S, Maurício M H P and Lima R M C *et al.* 2019. A regioselective coating onto microarray channels of bamboo with chitosan-based silver nanoparticles. *J Coat Technol Res* **3**, 1.

Götze H, Lehmann G, Luthardt H and Schultze-Dewitz. 1980. Holzwerkstoffforschung für die Zielgerechtete Substitution von Schnittholz. *Beiträge f. d. Forstwirtschaft* **3-4**.

Grosser D and Liese W. 1971. On the anatomy of Asian bamboos, with special reference to their vascular bundles. *Wood Science and Technology* **5**, 290–312.

Grosser D and Liese W. 1974. Verteilung der Leitbündel und Zellarten in Sproßachsen verschiedener Bambusarten. *Holz als Roh-und Werkstoff* **32**, 473–482.

Gu L, Zhou Y, Mei T, Zhou G and Xu L. 2019. Carbon Footprint Analysis of Bamboo Scrimber Flooring—Implications for Carbon Sequestration of Bamboo Forests and Its Products. *Forests* **10**, 51.

Guan M, Yong C, Wang L and Zhang Q. 2012. Selected Properties Of Bamboo Scrimber Flooring Made Of India *Melocanna Baccifera*. *Proceedings of the 55th International Convention of Society of Wood Science and Technology. August 27-31, 2012 - Beijing, China*.

Gurr J, Luinstra, G.A. and Krause A. 2018. Katalytisch angeregte in-situ-Polymerisation von Polyethylen in hierarchisch porösen Holzstrukturen. *Holztechnologie* **60**, 19–23.

Gusse A C, Miller P D and Volk T J. 2006. White-rot fungi demonstrate first biodegradation of phenolic resin. *Environmental science & technology* **40**, 4196–4199.

Hakkou M, Pétrissans M, Gérardin P and Zoulalian A. 2006. Investigations of the reasons for fungal durability of heat-treated beech wood. *Polymer Degradation and Stability* **91**, 393–397.

Hamid N H, Sulaiman O, Mohammad A and Ahmad Ludin N. 2012. The Decay Resistance and Hyphae Penetration of Bamboo *Gigantochloa scortechinii* Decayed by White and Brown Rot Fungi. *International Journal of Forestry Research* **2012**, 1–5.

Harries K A, Bumstead J, Richard M and Trujillo D. 2017. Geometric and material effects on bamboo buckling behaviour. *Proceedings of the Institution of Civil Engineers - Structures and Buildings* **170**, 236–249.

Harries K A, Sharma B and Richard M. 2012. Structural Use of Full Culm Bamboo. The Path to Standardization. *IJAEC* **1**, 66–75.

He G and Riedl B. 2004. Curing kinetics of phenol formaldehyde resin and wood-resin interactions in the presence of wood substrates. *Wood Science and Technology* **38**, 69–81.

He M-J, Zhang J, Li Z and Li M-L. 2016. Production and mechanical performance of scrimber composite manufactured from poplar wood for structural applications. *J Wood Sci* **62**, 429–440.

He S, Xu J, Wu Z, Yu H, Chen Y and Song J. 2018. Effect of bamboo bundle knitting on enhancing properties of bamboo scrimber. *Eur J Wood Prod* **76**, 1071–1078.

Helander M, Jia R, Huitu O, Sieber T N, Jia J, Niemelä P and Saikkonen K. 2013. Endophytic fungi and silica content of different bamboo species in giant panda diet. *Symbiosis* **61**, 13–22.

Hidalgo C. 2011. Discovering Southern and East Africa's industrial opportunities. *Economic policy paper series* **1101**.

Hidalgo C A, Klinger B, Barabási A-L and Hausmann R. 2007. The product space conditions the development of nations. *Science* **317**, 482–487.

Hu M, Wang C, Lu C, Anuar N I S, Yousfani S H S and Jing M *et al.* 2019. Investigation on the Classified Extraction of the Bamboo Fiber and Its Properties. *Journal of Natural Fibers* **30**, 1–11.

Hu Y, He M, Hu X, Song W, Chen Z and Yu Y *et al.* 2018. Bonding Technology for Bamboo-based Fiber Reinforced Composites with *Phyllostachys bambusoides* f. shouzhu Yi. *BioResources* **13**, 6047–6061.

Huang P, Chang W-S, Ansell M P, Chew Y J and Shea A. 2015. Density distribution profile for internodes and nodes of Phyllostachys edulis (Moso bamboo) by computer tomography scanning. *Construction and Building Materials* **93**, 197–204.

Huang X, Xie J, Qi J, Hoop C F de, Xiao H, Chen Y and Li F. 2018. Differences in physical–mechanical properties of bamboo scrimbers with response to bamboo maturing process. *Eur. J. Wood Prod.* **76**, 1137–1143.

Huang Y, Ji Y and Yu W. 2019a. Development of bamboo scrimber: a literature review. *J Wood Sci* **65**, 68.

Huang Y, Qi Y, Zhang Y and Yu W. 2019b. Progress of Bamboo Recombination Technology in China. *Advances in Polymer Technology* **2019**, 1–10.

Huang Z, Sun Y and Musso F. 2017. Assessment of bamboo application in building envelope by comparison with reference timber. *Con Build Mat* **156**, 844–860.

Huckfeldt T. 2017. Fäulepilze und baulicher Holzschutz. Teil 1. *Neue Quadriga - Holzbau* **1**, 21–26.

Huckfeldt T and Melcher E. 2008. Moderfäulepilze. *Europäischer Sanierungskalender*, 233–250.

Inoue A, Sakamoto S, Suga H and Kitahara F. 2011. Estimation of culm volume for bamboo, *Phyllostachys bambusoides*, by two-way volume equation. *Biomass and Bioenergy* **35**, 2666–2673.

Inoue A, Sakamoto S, Suga H, Kitazato H and Sakuta K. 2013. Construction of one-way volume table for the three major useful bamboos in Japan. *Journal of Forest Research* **18**, 323–334.

Inoue A and Suga H. 2009. Relationships of culm surface area to other culm dimensions for bamboo, Phyllostachys pubescens. *Journal of Forest Research* **14**, 236–239.

Iwakiri S, Trianoski R, Cunha A B d, Castro V G de, Braz R L and Villas-Bôas B T *et al.* 2014. Evaluation of the quality of particleboard panels manufactured with wood from *Sequoia sempervirens* and *Pinus taeda*. *CERNE* **20**, 209–216.

Jacobs K, Weiß B and Schmitt G S. 2011. Hohe Pilzresistenz von Bambuskompositen; Hohe Dauerhaftigkeit gegen holzzerstörende Basidiomyceten und Moderfäulepilze im Laborversuch erwiesen. *Nummer 50. Holz-Zentralblatt*, 1267.

Jin W. 2001. Comparison and analysis of the main technological factors of influencing mechanical properties of scrimber and PSL. *Journal of Forestry Research* **12**, 266–268.

Joffroy T. 2016. Learning from Local Building Cultures to Improve Housing Project Sustainability. *UN Chronicle* **LIII**. https://unchronicle.un.org/article/learning-local-building-cultures-improve-housing-project-sustainability.

Joma E, Schmidt G, Cremonez V G, Venson I and Simetti R. 2016. The Effect of Heat Treatment on Wood Water Relationship and Mechanical Properties of Commercial Uruguayan Plantation Timber *Eucalyptus Grandis*. *Austral J Bas Appl Sci* **10**, 704–708.

Joscak T, Mueller U, Mauritz R and Teischinger A. 2006. Production and material performance of long-strand wood composites - Review. *Wood Research* **51**, 37–50.

Kadivar M, Gauss C, Mármol G, Sá A D de, Fioroni C, Ghavami K and Savastano H. 2019. The influence of the initial moisture content on densification process of D. asper bamboo: Physical-chemical and bending characterization. *Construction and Building Materials* **229**, 116896.

Kamdem D P, Pizzi A and Jermannaud A. 2002. Durability of heat-treated wood. *Holz als Roh-und Werkstoff* **60**, 1–6.

Kamdem D P, Pizzi A and Triboulot M C. 2000. Heat-treated timber: potentially toxic byproducts presence and extent of wood cell wall degradation. *Holz als Roh- und Werkstoff* **58**, 253–257.

Katumbi N M, Kinyanjui M J, JM K and Mware M J. 2017. Biomass Energy Resource of the Highland Bamboo (*Yushania alpina*) and Its Potential for Sustainable Exploitation in Southern Aberdares Forest. *J of Sustainable Bioenergy Systems* **07**, 85–97.

Kaur V, Chattopadhyay D P and Kaur S. 2013. Study on Extraction of Bamboo Fibres from Raw Bamboo Fibres Bundles Using Different Retting Techniques. *Textiles and Light Industrial Science and Technology* **2**.

Kebede Y, Tadesse Z, Getahun A and Mulatu Y. 2017. Vegetative Propagation Techniques of Highland Bamboo (*Yushania alpina*) in Amhara Region, North-Western Ethiopia. *World Scientific News* **61**, 122–136.

Kelemwork S. 2009. Effects of some anatomical characteristics of Ethiopian lowland bamboo (*Oxytenanthera abyssinica*) on physical and mechanical properties. *Journal of Bamboo and Rattan* **8**, 161–174.

Kelemwork S, Tahir P M, Ding W E and Sudin R. 2008. The effects of selected anatomical characteristics on physical properties of Ethiopian Highland Bamboo *Arundinaria Alpina* K. Schum. (Poaceae). *Ethiopian Journal of Biological Sciences* **7**.

Kikata Y, Nagasaka H and Machiyashiki T. 1989. Zephyr wood, a network of continuous fibres. II. Production of low-density zephyr wood. *Mokuzai Gakkaishi = Journal of the Japan Wood Research Society* **35**, 918–923.

Kim Y-J, Okuma M and Yokota T. 1998. Study on sheet material made from zephyr strands V: Properties of zephyr strand board and zephyr strand lumber using the veneer of fast-growing species such as poplar. *J Wood Sci*, 438–443.

Kitchens S C, Amburgey T L, Barnes H M and Seale R D. 2016. Mechanical and Durability Properties of Steam-Pressed Scrim Lumber. *BioResources* **11**, 5343–5357.

Kleinn C and Morales-Hidalgo D. 2006. An inventory of Guadua (*Guadua angustifolia*) bamboo in the Coffee Region of Colombia. *Eur J Forest Res* **125**, 361–368.

Kozak A, Munro D and Smith J. 1969. Taper functions and their application in forest inventory. *The Forestry Chronicle* **45**, 278–283.

Krastanov A, Alexieva Z and Yemendzhiev H. 2013. Microbial degradation of phenol and phenolic derivatives. *Eng Life Sci* **13**, 76–87.

Kryzanowski T. 2009. Engineering new revenues with Scrimtec. An engineered wood product called Scrimtec—developed in Australia and now being produced in the U.S. South—could help B.C. forest companies further utilize beetle killed wood, and other sawmills utilize small diameter logs. *Logging and Sawmilling Journal* **12**.

Kumar A, Ryparovà P, Kasal B, Adamopoulos S and Hajek P. 2018. Resistance of bamboo scrimber against white-rot and brown-rot fungi. *Wood Mat Sci & Eng* **3**, 1–7.

Kumar A, Vlach T, Laiblova L, Hrouda M, Kasal B, Tywoniak J and Hajek P. 2016. Engineered bamboo scrimber. Influence of density on the mechanical and water absorption properties. *Construction and Building Materials* **127**, 815–827.

Laine K, Segerholm K, Wålinder M, Rautkari L and Hughes M. 2016. Wood densification and thermal modification. Hardness, set-recovery and micromorphology. *Wood Sci Technol* **50**, 883–894.

Lee A, Bai X and Peralta P N. 1996. Physical and mechanical properties of strandboard made from Moso bamboo. *Forest Products Journal* **46**, 84–88.

Lee C-H, Chung M-J, Lin C-H and Yang T-H. 2012. Effects of layered structure on the physical and mechanical properties of laminated moso bamboo (*Phyllosachys edulis*) flooring. *Construction and Building Materials* **28**, 31–35.

Lee S H, Lum W C, Zaidon A, Fatin-Ruzanna J, Tan L P, Mariusz M and Chin K L. 2017. Effect of post-thermal treatment on the density profile of rubberwood particleboard and its relation to mechanical properties. *Journal of Tropical Forest Science* **29**, 93–104.

Li H and Chen T. 2010. 高性能重组竹制造技术研究. A Study of Manufacturing Technique of High Performance Re-constituted Bamboo. (In Chinese). *World Bamboo and Rattan* **8**.

Li H, Wang J, Wei P and Wang L. 2019. Cross-laminated Timber (CLT) in China: A State-of-the-Art. *Journal of Bioresources and Bioproducts* **4**, 22–30.

Li J, Chen Y, Xu J, Ren D, Yu H, Guo F and Wu Z. 2018. The Influence of Media Treatments on Color Changes, Dimensional Stability, and Cracking Behavior of Bamboo Scrimber. *International Journal of Polymer Science* **2018**, 1–7.

Li Q, Xi Q and Qi L. 2001. 重组竹发展前景展望. Prospects for the development of reorganized bamboo. (in Chinese). *J Bamboo Research* **20**.

Li Q, Yu W and Yu Y. 2012a. Research on Properties of Reconstituted Bamboo Lumber Made by Thermo-Treated Bamboo Bundle Curtains. *Forest Products Journal* **62**, 545–550.

Li Y, Hu Y, Zhang L, Yao J and Yuan J. 2013. The Optimized Design of Manufacturing Process of Shrub Scrimber. *Advanced Materials Research* **715**, 597–600.

Li Y, Huang C, Wang L, Wang S and Wang X. 2017. The effects of thermal treatment on the nanomechanical behavior of bamboo (*Phyllostachys pubescens* Mazel ex H. de Lehaie) cell walls observed by nanoindentation, XRD, and wet chemistry. *Holzforschung* **71**, 197.

Li Y, Shen H, Shan W and Han T. 2012b. Flexural behavior of lightweight bamboo–steel composite slabs. *Thin-Walled Structures* **53**, 83–90.

Li Y, Shen Y, Wang S, Du C, Wu Y and Hu G. 2012c. A Dry–Wet Process to Manufacture Sliced Bamboo Veneer. *Forest Products Journal* **62**, 395–399.

Liese W. 2005. The two bamboos of Ethiopia. *Australian Bamboo Bulletin* **7**, 18–19.

Liese W. 2009. Bamboo as carbon sink - fact or fiction? Professor Ueda Koichiro Memorial lecture at the VIII World Bamboo Congress, Bangkok, Thailand. *Journal of Bamboo and Rattan* **8**, 103–114.

Liese W and Grosser D. 1972. Untersuchungen zur Variabilität der Faserlänge bei Bambus. *Holzforschung* **26**, 202–211.

Liese W and Weiner G. 1996. Ageing of bamboo culms. A review. *Wood Science and Technology* **30**, 77–89.

Lin J, Gupta S, Loos T and Birner R. 2019. Opportunities and Challenges in the Ethiopian Bamboo Sector: A Market Analysis of the Bamboo-Based Value Web. *Sustainability* **11**, 1644.

Lin Q, Huang Y, Li X and Yu W. 2020. Effects of shape, location and quantity of the joint on bending properties of laminated bamboo lumber. *Construction and Building Materials* **230**, 117023.

Linton J M, Barnes H M and Seale R D. 2008. Effect of Species-type on Properties of Steam Pressed Scrim Lumber (SPSL). *Proceedings of the 51st International Convention of Society of Wood Science and Technology November 10-12, 2008 Concepción, CHILE* **51**.

Liu H, Jiang Z, Fei B, Hse C and Sun Z. 2015a. Tensile behaviour and fracture mechanism of moso bamboo (*Phyllostachys pubescens*). *Holzforschung* **69**.

Liu J, Zhang H, Chrusciel L, Na B and Lu X. 2013. Study on a bamboo stressed flattening process. *Eur. J. Wood Prod.* **71**, 291–296.

Liu X, Smith G D, Jiang Z, Bock M C D, Boeck F and Frith O *et al.* 2015b. Nomenclature for Engineered Bamboo. *BioResources* **11**, 1141–1161.

Liu Y and Lee A. 2003. Selected Properties of Parallel Strand Lumber Made from Southern Pine and Yellow-Poplar. *Holzforschung* **57**, 70.

Lopes J, Oliveira R and Abreu M I. 2017. The Sustainability of the Construction Industry in Sub-saharan Africa: Some New Evidence from Recent Data. *Procedia Engineering* **172**, 657–664.

Ma T P, Jai S Y and Tsou C T. 1976. Experiment on the manufacture of bamboo glu-lam. *Bulletin Taiwan Forestry Research Institut* **285**.

Mabvurira D and Eerikäinen K. 2002. Taper and volume functions for *Eucalyptus grandis* in Zimbabwe. *Journal of Tropical Forest Science* **14**, 441–455.

Magel E, Kruse S, Lütje G and Liese W. 2005. Soluble carbohydrates and acid invertases involved in the rapid growth of developing culms in *Sasa palmata* (Bean) Camus. *Bamboo Science and Culture* **19**, 23–29.

Mahdavi M, Clouston P L and Arwade S R. 2011. Development of Laminated Bamboo Lumber. Review of Processing, Performance, and Economical Considerations. *J. Materials in Civ. Eng.* **23**, 1036–1042.

Mahdavi M, Clouston P L and Arwade S R. 2012. A low-technology approach toward fabrication of Laminated Bamboo Lumber. *Construction and Building Materials* **29**, 257–262.

Malanit P, Barbu M and Frühwald A. 2011. Physical and mechanical properties of oriented strand lumber made from an Asian bamboo (*Dendrocalamus asper* Backer). *Eur. J. Wood Prod.* **69**, 27–36.

Mekonnen Z, Worku A, Yohannes T, Alebachew M, Teketay D and Kassa H. 2014. Bamboo Resources in Ethiopia. Their value chain and contribution to livelihoods. *Ethnobot. Res. App.* **12**, 511.

Meng F, Liu R, Zhang Y, Huang Y, Yu Y and Yu W. 2017. Improvement of the water repellency, dimensional stability, and biological resistance of bamboo-based fiber reinforced composites. *Polym Compos* **107**, 26.

Miyatake A. 2002. Manufacture of Wood Strand-Cement Composite for Structural Use. *Wood-cement composites in the Asia-Pacific region* **2002**, 148–152.

Muchiri M N and Muga M O. 2013. A preliminary yield model for natural *Yushania alpina* bamboo in Kenya. *Journal of Natural Sciences Research* **3**, 77–84.

Mulatu Y and Feng D. 2014. Propagation Techniques for Highland Bamboo (*Arundinaria alpina*) in the Choke Mountain, Northwestern Ethiopia. *Ethiop. J. Agric. Sci.*, 23–36.

Mulatu Y and Fetene M. 2013. Stand structure, growth and biomass of Arundinaria alpina (highland bamboo) along topographic gradient in the Choke Mountain, northwestern Ethiopia. *Ethiopian Journal of Biological Sciences* **12**, 1–23.

Mulatu Y and Kindu M. 2010. Review of status of Bamboo resources and research in Ethiopia. *Ethiopian Journal of Natural Resources* **1**, 19–98.

Müller C, Deetz R, Schwarz U and Thole V. 2012. Agricultural residues in panel production – Impact of silica particle content and morphology on tool wear. *Wood Material Science & Engineering* **7**, 217–224.

Müller U, Gindl W and Teischinger A. 2005. Berührungslose Dehnungsmessung in Holz- und Holzwerkstoffen mittels Elektronischer Laser Speckle Interferometrie. *Holztechnologie* **46**, 48–49.

Munis R A, Camargo D A, Almeida A C D, Araujo V A D, Junior, Mauri Pedroso de Lima and Morales E A M *et al.* 2018. Parallel Compression to Grain and Stiffness of Cross Laminated Timber Panels with Bamboo Reinforcement. *BioResources* **13**, 3809–3816.

Nayak L and Mishra S P. 2016. Prospect of bamboo as a renewable textile fiber, historical overview, labeling, controversies and regulation. *Fash Text* **3**, 844.

Nguyen C T, Wagenführ A, Phuong L X, Dai V H, Bremer M and Fischer S. 2012. The effects of thermal modification on the properties of two Vietnamese bamboo species, Part I: Effects on physical properties. *BioResources* **7**, 5355–5366.

Niemz P. 2014. Eigenschaften von Werkstoffen auf Vollholzbasis. Forestry and Wood Technology. *Annals of Warsaw University of Life Sciences* **88**, 304–321.

Niklas K J. 2005. Modelling below- and above-ground biomass for non-woody and woody plants. *Annals of botany* **95**, 315–321.

Nilsson T. 1976. Soft-Rot Fungi - Decay Patterns and Enzyme Production. *Beihefte zu Material und Organismen, Nr. 3*, 103–112.

Nogata F and Takahashi H. 1995. Intelligent functionally graded material: Bamboo. *Composites Engineering* **5**, 743–751.

Nugroho N and Ando N. 2001. Development of structural composite products made from bamboo II: fundamental properties of laminated bamboo lumber. *Journal of Wood Science* **47**, 237–242.

Okahisa Y, Yoshimura T and Imamura Y. 2006. Seasonal and height-dependent fluctuation of starch and free glucose contents in moso bamboo (*Phyllostachys pubescens*) and its relation to attack by termites and decay fungi. *Journal of Wood Science* **52**, 445–451.

Osorio L, Trujillo E, Lens F, Ivens J, Verpoest I and van Vuure A W. 2018. In-depth study of the microstructure of bamboo fibres and their relation to the mechanical properties. *Journal of Reinforced Plastics and Composites* **37**, 1099–1113.

Parkkeeree T, Matan N and Kyokong B. 2015. Mechanisms of bamboo flattening in hot linseed oil. *Eur. J. Wood Prod.* **73**, 209–217.

Paton R. 1997. Modelling stress transfer in a wood composite. *Proceedings of ICCM* **11**, 813–824.

Paul W, Ohlmeyer M and Leithoff H. 2007. Thermal modification of OSB-strands by a one-step heat pre-treatment – Influence of temperature on weight loss, hygroscopicity and improved fungal resistance. *Holz Roh Werkst* **65**, 57–63.

Paul W, Ohlmeyer M, Leithoff H, Boonstra M J and Pizzi A. 2006. Optimising the properties of OSB by a one-step heat pre-treatment process. *Holz Roh Werkst* **64**, 227–234.

Pelaez-Samaniego M R, Yadama V, Lowell E and Espinoza-Herrera R. 2013. A review of wood thermal pretreatments to improve wood composite properties. *Wood Sci Technol* **47**, 1285–1319.

Peng G, Jiang Z, Liu X, Fei B, Yang S and Qin D *et al.* 2014. Detection of complex vascular system in bamboo node by X-ray µCT imaging technique. *Holzforschung* **68**, 223–227.

Perremans D, Trujillo E, Ivens J and van Vuure A W. 2018. Effect of discontinuities in bamboo fibre reinforced epoxy composites. *Composites Science and Technology* **155**, 50–57.

Plaschkies K, Scheiding W, Weiß B and Jacobs K. 2010. Dauerhaftigkeit verwendungsbezogen ermitteln. Biologische Dauerhaftigkeit von thermisch modifizierten Hölzern – Ergebnisse aus Labor- und Freilandprüfungen. *Holz-Zentralblatt* **136**, 524–525.

Platts M J. 2013. Wind energy turns to bamboo. *Energy Materials Materials Science and Engineering for Energy System* **1**, 84–87.

Platts M J. 2014. Strength, Fatigue Strength and Stiffness of High-Tech Bamboo/Epoxy Composites. *AS* **05**, 1281–1290.

Popper R, Niemz P and Eberle G. 2004. Untersuchungen zur Gleichgewichtsfeuchte und Quellung von Massivholzplatten. *Holz als Roh- und Werkstoff* **62**, 209–217.

Qi J, Xie J, Yu W and Chen S. 2015. Effects of characteristic inhomogeneity of bamboo culm nodes on mechanical properties of bamboo fiber reinforced composite. *Journal of Forestry Research* **26**, 1057–1060.

Qi J Q, Xie J L, Huang X Y, Yu W J and Chen S M. 2014. Influence of characteristic inhomogeneity of bamboo culm on mechanical properties of bamboo plywood. Effect of culm height. *J Wood Sci* **60**, 396–402.

Qin G, Cheng B and Zeng Y. 2015. Analysis of the Impact of Chinese Wood Product Manufacturers' Exports. *Forest Products Journal* **65**, 387–394.

Richard M J and Harries K A. 2015. On inherent bending in tension tests of bamboo. *Wood Sci Technol* **49**, 99–119.

Ringman R, Pilgård A, Kölle M, Brischke C and Richter K. 2016. Effects of thermal modification on Postia placenta wood degradation dynamics: measurements of mass loss, structural integrity and gene expression. *Wood Science and Technology* **50**, 385–397.

Roh J-K. 2007. Manufacture of Wood Veneer-Bamboo Zephyr Composite Board II. Effect of Manufacturing Conditions on Properties of Composite Board. *Mokchae Konhak* **35**, 108–117.

Roh J-K and Ra J-B. 2009. Effect of moisture content and density on the mechanical properties of veneer-bamboo zephyr composites. *Forest Products Journal* **59**, 75.

Sanquetta C R, Inoue M N, Corte A P, Netto S P, Mognon F, Wojciechowski J and Rodrigues A L. 2015. Modeling the apparent volume of bamboo culms from Brazilian plantation. *Afr. J. Agric. Res.* **10**, 3977–3986.

Sato M, Inoue A and Shima H. 2017. Bamboo-inspired optimal design for functionally graded hollow cylinders. *PloS one* **12**.

Schindelin J, Arganda-Carreras I, Frise E, Kaynig V, Longair M and Pietzsch T *et al.* 2012. Fiji. An open-source platform for biological-image analysis. *Nature methods* **9**, 676–682.

Schmidt O, Sheng Wei D, Liese W and Wollenberg E. 2011. Fungal degradation of bamboo samples. *Holzforschung* **65**, 310.

Schmidt O, Wei D, Bahmani M, Tang T K and Liese W. 2015. Pilzbefall und Schutz von Bambushalmen und Palmenholz - Eine Übersicht. *Zeitschrift für Mykologie* **1**, 57–80.

Schmidt O, Wei D S, Tang T K and Liese W. 2013. Bamboo and fungi. *J Bamboo Rattan* **12**, 1–14.

Schumacher F and Hall F. 1933. Logarithmic expression of timber-tree volume. *Journal of Agricultural Research* **47**.

Schwab E and Schlusen K. 1999. Eigenschaften von Bambus-Parkett-Elementen. *Holz als Roh- u. Werkstoff* **57**, 63–68.

Scolforo H F, McTague J P, Raimundo M R, Weiskittel A, Carrero O and Scolforo J R S. 2018. Comparison of taper functions applied to eucalypts of varying genetics in Brazil. Application and evaluation of the penalized mixed spline approach. *Can. J. For. Res.* **48**, 568–580.

Semple K E, Zhang P K and Smith G D. 2015. Stranding Moso and Guadua Bamboo. Part I: Strand Production and Size Classification **10**.

Seyoum G, Lemma T and Yigardu M. 2018. Indigenous knowledge on highland bamboo (*Yushania alpina*) management and utilization practices in Kokosa Woreda, South East Ethiopia. *Sci. Res. Essays* **13**, 111–122.

Shang X, Ma Y, Zhang J and Zhang N. 1998. 国内外重组木研究近况及发展前景. Research Status and Development Prospects of Reconstituted Wood at Home and Abroad. (In Chinese). *World forestry research*.

Shangguan W, Gong Y, Zhao R and Ren H. 2016. Effects of heat treatment on the properties of bamboo scrimber. *J Wood Sci* **62**, 383–391.

Shao Z-P, Fang C-H, Huang S-X and Tian G-L. 2010. Tensile properties of Moso bamboo (Phyllostachys pubescens) and its components with respect to its fiber-reinforced composite structure. *Wood Sci Technol* **44**, 655–666.

Shao Z-P, Fang C-H and Tian G-L. 2009. Mode I interlaminar fracture property of moso bamboo (Phyllostachys pubescens). *Wood Sci Technol* **43**, 527–536.

Shimels H and Woldesenbet E. 2014. Particleboard from Ethiopian Lowland Bamboo *Oxytenanthera abyssinica*. *International Journal of Research in Mechanical Engineering* **2**.

Shukla K S and Negi A. 1996. Reconstituted wood from Eucalyptus hybrid. *Journal of the Timber Development Association of India* **42**, 5–8.

Shukla K S and Prasad J. 1988. Reconstituted wood from bamboo for structural uses. *J Ind Acad Wood Sci* **19**, 19–27.

Siba E and Gebreeyesus M. 2016. Learning to export and learning from exporting. The case of Ethiopian manufacturing. *J Afr Econ* **26**, 1–23.

Socha J and Kulej M. 2008. Variation of the tree form factor and taper in European larch of Polish provenances tested under conditions of the Beskid Sądecki mountain range (southern Poland). *J. For. Sci.* **53**, 538–547.

Sommerhuber P F, Wenker J L, Rüter S and Krause A. 2017. Life cycle assessment of wood-plastic composites. Analysing alternative materials and identifying an environmental sound end-of-life option. *Resources, Conservation and Recycling* **117**, 235–248.

Starke R, Rosenthal M, Bues C-T, Bremer M and Fischer S. 2016. Thermal modification of African alpine bamboo. *Eur J Wood Prod* **74**, 901–903.

Stienen T, Schmidt O and Huckfeldt T. 2014. Wood decay by indoor basidiomycetes at different moisture and temperature. *Holzforschung* **68**, 9–15.

Suga H, Inoue A and Kitahara F. 2011. Derivation of two-way volume equation for bamboo, Phyllostachys pubescens. *Journal of Forest Research* **16**, 261–267.

Sulaiman O and Murphy R J. 1993. Soft rot decay in bamboo. *Material und Organismen* **28**, 167–195.

Sulaiman O and Murphy R J. 1995. Ultrastructue of soft rot decay in bamboo cell walls. *Material und Organismen* **29**, 241–253.

Sumardi I, Suzuki S and Ono K. 2006. Some important properties of Strandboard manufactured from bamboo. *Forest Products Journal* **56**, 59–63.

Sumardi I, Suzuki S and Rahmawati N. 2015. Effect of Board Type on Some Properties of Bamboo Strandboard. *Journal of Mathematical and Fundamental Sciences* **47**, 51–59.

Sun Y, Jiang Z, Liu H, Sun Z and Fang C. 2019. The bending properties of bamboo strand board I-beams. *J Wood Sci* **65**, 1–10.

Suzuki S and Miyagawa H. 2003. Effect of element type on the internal bond quality of wood-based panels determined by three methods. *Journal of Wood Science* **49**, 513–518.

Tafirenyika M. 2016. Why has Africa failed to industrialize? Experts call for bold and creative policies. *United Nations Africa Renewal* **08**.

Tambe S, Patnaik S, Upadhyay A P, Edgaonkar A, Singhal R and Bisaria J *et al.* 2020. Research Trends: Evidence-based policy for bamboo development in India: From “supply push” to “demand pull”. *Forest Policy and Economics* **116**, 102187. http://www.sciencedirect.com/science/article/pii/S1389934120300435.

Tan T, Rahbar N, Allameh S M, Kwofie S, Dissmore D, Ghavami K and Soboyejo W O. 2011. Mechanical properties of functionally graded hierarchical bamboo structures. *Acta biomaterialia* **7**, 3796–3803.

Tang H, Schmidt O and Liese W. 2009. Environment-friendly short-term protection of bamboo against molding. *J Timber Dev Assoc of India* **1**, 8–17.

Tang X, Pérez-Cruzado C, Fehrmann L, Álvarez-González J G, Lu Y and Kleinn C. 2016. Development of a Compatible Taper Function and Stand-Level Merchantable Volume Model for Chinese Fir Plantations. *PloS one* **11**.

Tarmeze W, Khairul A and Zairul-Amin R. 2016. Scrimber from sustainable Malaysian bio-resources. *Timber Technology Bulletin*.

Taylor D, Kinane B, Sweeney C, Sweetnam D, O'Reilly P and Duan K. 2015. The biomechanics of bamboo. Investigating the role of the nodes. *Wood Sci Technol* **49**, 345–357.

Teshale F T. 2015. The Contribution of Highland Bamboo (*Yushania alpina*) to Rural Livelihoods and Status of its Domestication at Bule District, Gedeo Zone, SNNPR. *Commons Amidst Complexity and Change, the Fifteenth Biennial Conference of the International Association for the Study of the Commons, May 25-29, 2015. Edmonton, Alberta.*

Teshale T, Woldeamanuel T, Bekele T, Alemu A and Pretzsch J. 2017. Market Channels for Highland Bamboo Poles Originated from Hula District, Sidama Zone Southern Ethiopia. *Small-scale Forestry* **16**, 469–485.

Thybring E E. 2013. The decay resistance of modified wood influenced by moisture exclusion and swelling reduction. *International Biodeterioration & Biodegradation* **82**, 87–95.

Thybring E E, Kymäläinen M and Rautkari L. 2018. Moisture in modified wood and its relevance for fungal decay. *iForest* **11**, 418–422.

Trung Cong N, Pfriem A and Wagenführ A. 2006. Alternatives Verfahren zur Zerfaserung von Einjahrespflanzen für Klein- und mittelständische Unternehmen. Teil 1. *Holztechnologie* **47**.

Ueda K. 1980. Mechanical Properties of Moso Bamboo (*Phyllostachys pubescens* MAZEL). Distribution of Modulus of Elasticity across the Culm Wall. *Hokkaido University Collection of Scholarly and Academic Papers* **37**, 817–836.

van Acker J, Stevens M, Carey J, Sierra-Alvarez R, Militz H and Le Bayon I *et al.* 2003. Biological durability of wood in relation to end-use. *Eur. J. Wood Prod.* **61**, 35–45.

Virchow D, Beuchelt T D, Denich M, Loos T K, Hoppe M and Kuhn A. 2014. The value web approach – so that the South can also benefit from the bioeconomy. *Rural 21* **03**, 16–18.

Wang F and Hu Y. 2007. Effect of resin pH on creep behaviour of cured phenol formaldehyde resins. *Journal of Central South University of Technology* **14**, 306–309.

Wang F, Shao Z, Wu Y and Wu D. 2014a. The toughness contribution of bamboo node to the Mode I interlaminar fracture toughness of bamboo. *Wood Sci Technol* **48**, 1257–1268.

Wang S. 2017. Bamboo sheath-A modified branch based on the anatomical observations. *Scientific reports* **7**, 16132.

Wang X, Keplinger T, Gierlinger N and Burgert I. 2014b. Plant material features responsible for bamboo's excellent mechanical performance: a comparison of tensile properties of bamboo and spruce at the tissue, fibre and cell wall levels. *Annals of botany* **114**, 1627–1635.

Wang Z, Gong M and Chui Y-H. 2015. Mechanical properties of laminated strand lumber and hybrid cross-laminated timber. *Construction and Building Materials* **101**, 622–627.

Wardani L. 2014. Performance of Zephyr Board Made From Various Rolling Crush Number and Palm Oil Petiole Parts. *AFF* **3**, 71.

WBPI. 2012. Aiming for domination. *Wood Based Panels International* **June**.

WBPI. 2018. Siempelkamp in India. *Wood Based Panels International* **May**.

Wegst U G K. 2011. Bending efficiency through property gradients in bamboo, palm, and wood-based composites. *Journal of the mechanical behavior of biomedical materials* **4**, 744–755.

Wei D, Schmidt O and Liese W. 2013. Durability test of bamboo against fungi according to EN standards. *Eur J Wood Prod* **71**, 551–556.

Wei J, Lin Q, Zhang Y, Yu W, Hse C-Y and Shupe T. 2019a. Surface Properties of Pine Scrimber Panels with Varying Density. *Coatings* **9**, 397.

Wei J, Rao F, Huang Y, Zhang Y, Qi Y, Yu W and Hse C-Y. 2019b. Structure, Mechanical Performance, and Dimensional Stability of Radiata Pine (*Pinus radiata* D. Don) Scrimbers. *Advances in Polymer Technology*, 1–8.

Wei P, Wang B J, Wang L, Wang Y, Yang G and Liu J. 2019c. An Exploratory Study of Composite Cross-Laminated Timber (CCLT) Made from Bamboo and Hemlock-fir Mix. *BioResources* **14**, 2160–2170.

Winandy J E, Clausen C E and Curling S F. 2000. Predicting the Effects of Decay on Wood Properties and Modeling Residual Service-Life. *Proceedings of the 2nd Annual Conference on Durability and Disaster Mitigation in Wood-Frame Housing, November 6-8, 2000, Madison, Wisconsin*.

Windeisen E, Bächle H, Zimmer B and Wegener G. 2009. Relations between chemical changes and mechanical properties of thermally treated wood. *Holzforschung* **63**, 221.

Windt I de, van den Bulcke J, Brischke C, Welzbacher C R, Gellerich A, Bollmus S and Humar M. 2013. Statistical analysis of durability tests - Part 1: Principles of distribution fitting and application on laboratory tests. *The International Research Group on Wood Protection* **IRG/WP/13-20504**.

Xie J, Qi J, Hu T, Hoop C F de, Hse C Y and Shupe T F. 2016. Effect of fabricated density and bamboo species on physical–mechanical properties of bamboo fiber bundle reinforced composites. *Journal of Materials Science* **51**, 7480–7490.

Xu M, Cui Z, Chen Z and Xiang J. 2018. The charring rate and charring depth of bamboo scrimber exposed to a standard fire. *Fire and Materials* **151**, 732.

Xu Y and Teng F. 2015. 我国高性能重组竹研究进展及其研发建议. Research Progress on High-performance Reconstituted Bamboo Lumber in China and Its Development Suggestions. (In Chinese). *World Bamboo and Rattan* **13**.

Yan W, Zhou J, Zhang B, Fu W and Chen Z. 2017. Development design and mechanical properties of arc bamboo. *Wood Research* **62**, 365–372.

Yang T-C and Lee T-Y. 2018. Effects of density and heat treatment on the physico-mechanical properties of unidirectional round bamboo stick boards (UBSBs) made of Makino bamboo (*Phyllostachys makinoi*). *Construction and Building Materials* **187**, 406–413.

Yen T-M and Lee J-S. 2011. Comparing aboveground carbon sequestration between moso bamboo (*Phyllostachys heterocycla*) and China fir (*Cunninghamia lanceolata*) forests based on the allometric model. *Forest Ecology and Management* **261**, 995–1002.

Youssefian S and Rahbar N. 2015. Molecular Origin of Strength and Stiffness in Bamboo Fibrils. *Scientific reports* **5**, 11116.

Yu H X, Fang C R, Xu M P, Guo F Y and Yu W J. 2015a. Effects of density and resin content on the physical and mechanical properties of scrimber manufactured from mulberry branches. *J Wood Sci* **61**, 159–164.

Yu Y, Huang X and Yu W-J. 2014a. A novel process to improve yield and mechanical performance of bamboo fiber reinforced composite via mechanical treatments. https://doi.org/10.1016/j.compositesb.2013.08.007.

Yu Y, Huang Y, Zhang Y, Liu R, Meng F and Yu W. 2018. The reinforcing mechanism of mechanical properties of bamboo fiber bundle-reinforced composites. *Polym. Compos.* **76**, 83.

Yu Y, Liu R, Huang Y, Meng F and Yu W. 2017. Preparation, physical, mechanical, and interfacial morphological properties of engineered bamboo scrimber. *Construction and Building Materials* **157**, 1032–1039.

Yu Y, Zhu R, Wu B, Hu Y and Yu W. 2015b. Fabrication, material properties, and application of bamboo scrimber. *Wood Sci Technol* **49**, 83–98.

Yu Y-L, Huang X-A and Yu W-J. 2014b. High performance of bamboo-based fiber composites from long bamboo fiber bundles and phenolic resins. *J. Appl. Polym. Sci.* **131**, n/a-n/a.

Yuan Z, Kapu N S, Beatson R, Chang X F and Martinez D M. 2016. Effect of alkaline pre-extraction of hemicelluloses and silica on kraft pulping of bamboo (*Neosinocalamus affinis* Keng). *Industrial Crops and Products* **91**, 66–75.

Zhang H, Pizzi A, Lu X and Zhou X. 2014. Optimization of Tensile Shear Strength of Linear Mechanically Welded Outer-to-Inner Flattened Moso Bamboo (Phyllostachys pubescens). *BioResources* **9**.

Zhang J, Lei Y, Shi M and Song X. 2016. Influence of Fiber Bundle Morphology on the Mechanical and Bonding Properties of Cotton Stalk and Mulberry Branch Reconstituted Square Lumber. *BioResources* **11**.

Zhang Y, Huang X, Zhang Y, Yu Y and Yu W. 2018a. Scrimber board (SB) manufacturing by a new method and characterization of SB's mechanical properties and dimensional stability. *Holzforschung* **72**, 283–289.

Zhang Y, Huang Y, Qi Y and Yu W. 2018b. Novel engineered scrimber with outstanding dimensional stability from finely fluffed poplar veneers. *Measurement* **124**, 318–321.

Zhang Y, Qi Y, Huang Y, Yu Y, Liang Y and Yu W. 2018c. Influence of veneer thickness, mat formation and resin content on some properties of novel poplar scrimbers. *Holzforschung* **72**, 673–680.

Zhang Y M, Yu Y L and Yu W J. 2013. Effect of thermal treatment on the physical and mechanical properties of *Phyllostachys pubescens* bamboo. *Eur J Wood Prod* **71**, 61–67.

Zhao Y, Feng D, Jayaraman D, Belay D, Sebrala H and Ngugi J *et al.* 2018. Bamboo mapping of Ethiopia, Kenya and Uganda for the year 2016 using multi-temporal Landsat imagery. *International Journal of Applied Earth Observation and Geoinformation* **66**, 116–125.

Zhong Y, Wu G, Ren H and Jiang Z. 2017. Bending properties evaluation of newly designed reinforced bamboo scrimber composite beams. *Construction and Building Materials* **143**, 61–70.

Zhou A, Huang D, Li H and Su Y. 2012. Hybrid approach to determine the mechanical parameters of fibers and matrixes of bamboo. *Construction and Building Materials* **35**, 191–196.

Zhou H, Wei X, Smith L M, Wang G and Chen F. 2019. Evaluation of Uniformity of Bamboo Bundle Veneer and Bamboo Bundle Laminated Veneer Lumber (BLVL). *Forests* **10**, 921.

Standards

ASTM E562-01:2001. Test Method for Determining Volume Fraction by Systematic Manual Point Count. E04 Committee-ASTM International, West Conshohocken, PA.

BS EN 477:2018-08. Unplasticized polyvinylchloride (PVC-U) profiles for the fabrication of windows and doors - Determination of the resistance to impact of main profiles by falling mass; English version EN 477:2018.

DIN 899-2:2015-06. Plastics - Determination of creep behaviour - Part 2: Flexural creep by three-point loading; German version EN ISO 899-2:2003 + A1:2015.

DIN CEN/TS 15083-1:2005-10. Durability of wood and wood-based products - Determination of the natural durability of solid wood against wood-destroying fungi, test methods - Part 1: Basidiomycetes; German version CEN/TS 15083-1:2005.

DIN CEN/TS 15083-2:2005-10. Durability of wood and wood-based products - Determination of the natural durability of solid wood against wood-destroying fungi, test methods - Part 2: Soft rotting micro-fungi; German version CEN/TS 15083-2:2005.

DIN CEN/TS 15676:2008-02. Wood flooring - Slip resistance - Pendulum test; German version CEN/TS 15676:2007.

DIN EN 317:1993-08. Particleboards and fibreboards; determination of swelling in thickness after immersion in water; German version EN 317:1993.

DIN EN 319:1993-08. Particleboards and fibreboards; determination of tensile strength perpendicular to the plane of the board; German version EN 319:1993.

DIN EN 323:1993-08. Wood-based panels; determination of density; German version EN 323:1993.

DIN EN 310:1993-08. Wood-based panels; determination of modulus of elasticity in bending and of bending strength; German version EN 310:1993.

DIN EN 322:1993-08. Wood-based panels; determination of moisture content; German version EN 322:1993.

DIN EN 326-1:1994-08. Wood-based panels - Sampling, cutting and inspection - Part 1: Sampling and cutting of test pieces and expression of test results; German version EN 326-1:1994.

DIN EN 350-2:1994-10. Durability of wood and wood based products - Natural durability of solid wood - Part 2: Guide to the natural durability and treatability of selected wood species of importance in Europe; German version EN 350-2:1994.

DIN EN 350-1:1994-10. Durability of wood and wood-based products - Natural durability of solid wood - Part 1: Guide to the principles of testing and classification of the natural durability of wood; German version EN 350-1:1994.

DIN EN 1087-1:1995-04. Particleboards - Determination of moisture resistance - Part 1: Boil test; German version EN 1087-1:1995.

DIN EN 84:1997-05. Wood preservatives - Accelerated ageing of treated wood prior to biological testing - Leaching procedure; German version EN 84:1997.

DIN EN 321:2001-11. Wood-based panels - Determination of moisture resistance under cyclic test conditions; German version EN 321:2001.

DIN EN 318:2002-06. Wood-based panels - Determination of dimensional changes associated with changes in relative humidity; German version EN 318:2002.

DIN EN 300:2006-09. Oriented Strand Boards (OSB) - Definitions, classification and specifications; German version EN 300:2006.

DIN EN 1534:2011-01. Wood flooring - Determination of resistance to indentation - Test method; German version EN 1534:2010.

DIN EN 15185:2011-07. Furniture - Assessment of the surface resistance to abrasion; German version EN 15185:2011.

DIN EN 117:2013-01. Wood preservatives - Determination of toxic values against Reticulitermes species (European termites) (Laboratory method); German version EN 117:2012.

DIN EN 335:2013-06. Durability of wood and wood-based products - Use classes: definitions, application to solid wood and wood-based products; German version EN 335:2013.

DIN EN 14342:2013-09. Wood flooring - Characteristics, evaluation of conformity and marking; German version EN 14342:2013.

DIN EN 1156:2013-10. Wood-based panels - Determination of duration of load and creep factors; German version EN 1156:2013.

DIN EN 15534-1:2014-04. Composites made from cellulose-based materials and thermoplastics (usually called wood-polymer composites (WPC) or natural fibre composites (NFC)) - Part 1: Test methods for characterisation of compounds and products; German version EN 15534-1:2014.

DIN EN 15458:2014-11. Paints and varnishes - Laboratory method for testing the efficacy of film preservatives in a coating against algae; German version EN 15458:2014.

DIN EN 13986:2015-06. Wood-based panels for use in construction - Characteristics, evaluation of conformity and marking; German version EN 13986:2004+A1:2015.

DIN EN 17009:2016-07. Flooring of lignified materials other than wood – Characteristics, evaluation of conformity and marking; German and English version prEN 17009:2016.

DIN EN 1383:2016-07. Timber structures - Test methods - Pull through resistance of timber fasteners; German version EN 1383:2016.

DIN EN 350:2016-12. Durability of wood and wood-based products - Testing and classification of the durability to biological agents of wood and wood-based materials; German version EN 350:2016.

DIN EN 15534-1:2018-02. Composites made from cellulose-based materials and thermoplastics (usually called wood-polymer composites (WPC) or natural fibre composites (NFC)) - Part 1: Test methods for characterisation of compounds and products; German version EN 15534-1:2014+A1:2017.

DIN EN 17009:2019-06. Flooring of lignified materials other than wood - Characteristics, assessment and verification of constancy of performance and marking; German version EN 17009:2019.

DIN EN ISO 877-2:2011-03. Plastics - Methods of exposure to solar radiation - Part 2: Direct weathering and exposure behind window glass; German version EN ISO 877-2:2010.

DIN EN ISO 4892-2:2013-06. Methods of exposure to laboratory light sources – Part 2: Xenon-arc lamps; German version EN ISO 4892-2:2013.

DIN EN ISO 2813:2015-02. Paints and varnishes - Determination of gloss value at 20°, 60° and 85°; German version EN ISO 2813:2014.

DIN ISO 16000-3:2013-01. Indoor air - Part 3: Determination of formaldehyde and other carbonyl compounds in indoor air and test chamber air - Active sampling method.

DIN V ENV 12038:2002-07. Durability of wood and wood-based products - Wood-based panels - Method of test for determining the resistance against wood-destroying basidiomycetes; German version ENV 12038:2002.

EN 113:1996-11. Wood preservatives - Method of test for determining the protective effectiveness against wood destroying basidiomycetes - Determination of the toxic values;

EN ISO 178:2006-04. Determination of flexural properties (ISO:2001 + Amd. 1:2004); German version EN 178:2003 + A1:2005.

GB/T 17657:2013-11. 人造板及饰面人造板理化性能试验方法. National Standards of People's Republic of China.

GB/T 30364:2013-11. 重组竹地板.

ISO 3340:1976-04. Fibre building boards; Determination of sand content.

ISO 4582:2007-08. Plastics - Determination of changes in colour and variations in properties after exposure to daylight under glass, natural weathering or laboratory light sources.

ISO 16869:06-2008. Plastics - Assessment of the effectiveness of fungistatic compounds in plastics formulations.

ISO 22157:2019-01. Bamboo structures - Determination of physical and mechanical properties of bamboo culms - Test methods.

Patents

Coleman J. 1980. Reconsolidated wood product. Patent no. US4232067.

Coleman J. 2002. Manufacture of reconstituted wood products. Patent no. US6344165.

Coleman J. 2011. Manufacture of reconstituted wood products. Patent no. EP0973633B1.

Fliedner E, Cornick M and van Herwijnen H. 2011. Stable aqueous novolac dispersion. Patent no. US7994243B2.

Fujii T and Miyatake A. 1998. Wood piled with split and disrupted pieces and its manufacturing method and manufacturing apparatus. Patent no. EP0666155A1/B1.

Graeter P, Frybort S, Müller U and Mauritz R. 2012. Device for the production of macro-fibres from wood trunks and method for the production of a wood composite material by means of macro-fibres. Patent no. WO2012/042028AI.

Harvey Jr H C. 1972. Green-wood fibrating means and method. Patent no. US3674219.

Jarck W. 2009. System and methods for the production of steam-pressed long fiber reconsolidated wood products. Patent no. US007537669B2.

Miller R B, Creighton S M and Raczuk T W. 1969. Sugarcane processing. Patent no. US003464877.

柃 叶刚 朱钟坚瑜陈文强. 2010. Bamboo fiber winding composite pipe. Patent no. CN201434160Y.

Other references

African Development Bank. 2018. Industrialize Africa: Brochure Industrialiser L'Afrique, Abijan, Côte d'Ivoire, 24 p.

Ansell M P. 2015. Wood Composites. Woodhead Publishing, Cambridge, 444 p.

Aping J. 2015. Herstellung und Biegeprüfung eines laminierten Werkstoffs aus *Guadua angustifolia*. B.Sc., Hamburg.

Bansal A K, Balwani G and Sheokand S. 2019. Chapter 12 - Critical Material Attributes in Wet Granulation. In *Handbook of pharmaceutical wet granulation*: *Theory and practice in a quality by design paradigm / edited by*

Ajit S. Narang, Sherif I.F. Badawy. A.S. Narang and S.I.F. Badawy (eds). Academic Press is an imprint of Elsevier, pp. 421–453.

Batterbury S and Ndi F. 2016. Land-grabbing in Africa. In *The Routledge Handbook of African Development.* L.K. Binns J.A. and E. Nel (eds). Routledge, pp. 573–582.

Benthien J. 2020. Schlussbericht: Entwicklung eines Verfahrens zur Bestimmung der Durchtrittbeständigkeit von Pferdebox-Ausfachungsbohlen sowie Entwicklung von Alternativen zu derzeit verwendeten Ausfachungsmaterialien für den Bau von Pferdeboxen“. *Thünen Report,* Braunschweig, 97 p.

Benthien J, Engehausen N, Gäckler S and Ohlmeyer M. 2019. Schlagzähigkeit von Stallbohlen für Pferdeboxen: Einflussgrößen auf die Bruchschlagarbeit. *Thünen Working Paper,* Braunschweig, 45 p.

Benthien J, Höpken M, Melcher E, Gäckler S and Ohlmeyer M. 2018. Zur Dauerhaftigkeit von Stallbohlen für die Pferdehaltung. *Thünen Working Paper,* Braunschweig, 45 p.

Berhe A. 2019. Visit with the BioHome team; Talk on actual and prospective product portfolio. Personal conversation.

Beronov B, Böcher C, Bretzinger L, Hartmann P, Kores M, Kübler S and Ederer P. 2015. Making the Case for Local Rotor Blade Manufacturing in Kenya, 23 p.

Berthold D. 2013. Schlussbericht zum Vorhaben: Verbundvorhaben: Eschentriebsterben - Forst- und holzwirtschaftliche Strategien zum Umgang mit dem neuartigen Eschentriebsterben; Teilvorhaben 3: Innovative Holzverwendung (Scrimber-Wood), 15 p.

Best J. 2017. Colour Design: Theories and Applications. Elsevier Science, 704 p.

Bodig J and Jayne B A. 1993. Mechanics of wood and wood composities. Krieger Pub, Malabar, Florida, 712 p.

Brittell J, Rondoni P and Xie J. 2013. Timber Industry & Corruption: Sub-Saharan Africa. The Elliott School of International Affairs, 39 p.

Candelier K, Thévenon M-F, Collet R, Gerardin P and Dumarçay S. 2017b. Do extractive compounds of thermally modified woods play an important role in the decay and termites resistances of these modified materials? A preliminary study. In *Proceedings of the 3rd COST Action FP1407 International Conference*: *Wood modification research & applications*. G. Tondi, M. Posavcevic, A. Kutnar and R. Wimmer (eds). Salzburg University of Applied Sciences, pp. 122–123.

Ceccotti, A. and van Kuilen, J.W.G. de (eds). 2004. Proceedings of the International Symposium on Advanced Timber and Timber-composite Elements for Buildings: Design, construction, manufacturing & fire safety : COST E29. IVALSA.

Cherenet Z and Helawi S. 2015. Building Ethiopia. 1st edn. EiABC, Addis Ababa, 294 p.

Dalbiso A D and Addissie D. 2019. Ethiopian vernacular bamboo architecture and its potentials for adaptation in modern urban housing. A case study. In *Sustainable Construction Materials and Technologies*. Peter Claisse, Esmaiel Ganjian and Tarun Naik. (ed). International Committee of the SCMT conferences.

Deressa T, Hassan R M and Ringler C. 2008. Measuring Ethiopian Farmers' Vulnerability to Climate Change Across Regional States. *IFPRI Discussion Paper*, 33 p.

Dujesiefken D and Liese W. 2008. Das CODIT-Prinzip: Von den Bäumen lernen für eine fachgerechte Baumpflege. Haymarket Media, Braunschweig, 159 p.

Dynea. 2004. Data and safety sheet Prefere 4976, Lillestrøm, 5 p.

Dynea. 2010. Data and safety sheet EXP 3G, Guangdong, 8 p.

Earthstar Geographics. 2018. World Map. powered by ESRI. Satellites Pro.

Economist. 2011. The sun shines bright. *Briefing section,* London.

European Panel Federation. 2018. Annual report 2017-2018: Special topic: EPF for Africa, Brussels, 6 p.

European Parliament. 2011. Regulation (EU) No 305/2011 of the European Parliament and of the council of 9 March 2011 laying down harmonised conditions for the marketing of construction products and repealing Council Directive 89/106/EEC. *Official Journal of the European Union*.

Fan, M. and Fu, F. (eds). 2017. Advanced high strength natural fibre composites in construction. Woodhead Publishing, 342 p.

FAO. 2006. Global forest resources assessment update 2005 Ethiopia: Country report on bamboo resources. *Working Paper.* Food and Agriculture Organization of the United Nations, Addis Ababa, 20 p.

FAO. 2015. Global forest resources assessment 2015. Food and Agriculture Organization of the United Nations, Rome, 253 p.

Fey A. 2017. Entwicklung eines Prüfungsverfahrens für die Bewertung der Wirksamkeit einer thermischen Behandlung von Bambus gegenüber *Reticulitermes* spp. B.Sc., Hamburg.

Fordaq. 2018. Patentstreit: MOSO widerspricht Darstellung von Dasso – Dasso reagiert prompt. https://holz.fordaq.com/fordaq/news/MOSO_Dasso_Terrassendielen_60950.html (accessed on 02 February, 2019).

Fraunhofer. 2014. Results OSB from highland bamboo 6.2: Internal report Frank Froning, Braunschweig, Germany.

Fu J. 2008. Bamboo veneer for car interior decoration of BMW and Mercedes Benz. Interview via LinkedIn.

Ganapathy P M, Huan-Ming Z, Zoolagud S S, Turcke D and Espiloy Z B. 1999. Bamboo panel boards: A State-of-the-Art Review. *INBAR technical report,* Beijing, China.

Gatzweiler, F.W. and Braun, J.v. (eds). 2016. Technological and Institutional Innovations for Marginalized Smallholders in Agricultural Development. Springer International Publishing, 435 p.

Gebreyouhanes E. 2016. Discussion of the influence of Chinese construction enterprises on the Ethiopian (local) concrete sector. Personal conversation.

Gebru M. 2013. Industrial lowland bamboo supply in Benishangul Gumuz region. Personal conversation.

Götze H and Luthardt H. 1974. Die Verwertung von Quetschholzpartikeln aus Dünnholz der Forstwirtschaft zur Herstellung von Verbundelementen und Profilen in Kombination mit Plasten/Elasten für die Fensterproduktion. *Interner Bericht,* Eberswalde.

Grossenbacher M. 2012. Herstellung von Bambus OSB Containerböden: Key note speech. *2. Bieler Holzwerkstoff-Workshop,* Biel, Switzerland, 31 p.

Haag V. 2020. Anatomisch-strukturelle und topochemische Untersuchungen zur Charakterisierung der Holzeigenschaften neu eingeführter Handelshölzer (lesser known species). Doctoral, Hamburg, 145 p.

Hannula E-L. 2012. Going green: A handbook of sustainable housing practices in developing countries. UN-HABITAT, Nairobi, 124 p.

Hemmings S. 2017. GRASSBuilt Flooring Options: Flooring TriFold GB3, Meridian, Mississipi, 2 p.

Hemmings S. 2019. These Bamboo fibers get transformed into ultra-strong, fire-resistant, ultra-sustainable building & construction billet in record-breaking time!: Talk about a #glowup! #bamboo #rapidlyrenewable #ecobuilding #ecoconstruction #MadeinUSA #MississippiMade @genmississippi. https://twitter.com/GRASS_Built/status/1095434268505985025 (accessed on 12 February, 2019).

Heske F. 1966. Erkenntnisse und Erfahrungen zur forstlichen Bodenbenutzung der Entwicklungsländer am Beispiel von Äthiopien. *Forschungsberichte des Landes Nordrhein-Westfalen.* VS Verlag für Sozialwissenschaften, Wiesbaden, 201 p.

Hess S and Aidoo R. 2015. Charting the roots of anti-Chinese populism in Africa. *The political economy of the Asia Pacific.* Springer, Cham, 154 p.

Hidalgo López O. 2003. Bamboo: The gift of the gods. 1st edn., Bogotá Colombia, 553 p.

Hill C A S. 2006. Wood modification: Chemical, thermal and other processes. *Wiley series in renewable resources.* John Wiley & Sons, Chichester, England, Hoboken, NJ, 239 p.

Hocking M B. 2005. 21 - Commercial Polycondensation (Step-Growth) Polymers. In *Handbook of chemical technology and pollution control*. M.B. Hocking (ed). Academic, pp. 689–712.

Hoffmann J. 2018. Investigation on the application of an engineered bamboo board in cross laminated timber. B.Sc., Rosenheim.

Huang Z. 2019. Application of bamboo in building envelope. *Green energy and technology.* Springer, Cham.

INBAR. 2001. Transfer of technology model: Bamboo mat board: Indian Plywood Industries Research and Training Institute, Beijing, China, 39 p.

INBAR. 2018. Press release: New China-Africa centre in Addis Ababa promotes bamboo for sustainable development. https://www.inbar.int/pressrelease_chinaafricacentre/ (accessed on 13 December, 2018).

Janssen J J A. 2000. Designing and building with bamboo. *INBAR technical report*, 211 p.

Jarck W. 2017. Meeting in Meridian. Interview.

Jarck W and Seale R D. 2011. TimTek at College of Forest Resources. http://www.cfr.msstate.edu/timtek/ (accessed on 22 September, 2018).

Jawaid M, Tahir P M and Saba N. 2017. Lignocellulosic Fibre and Biomass-Based Composite Materials: Processing, Properties and Applications. Elsevier Science.

Jones, D. and Brischke, C. (eds). 2017. Performance of bio-based building materials. Woodhead Publishing.

Kedir F, Pullen T, Hall D, Boyd R and Da Silva J. 2020. A Sustainable Transition to Industrialized Housing Construction in Developing Economies. ETH Zurich, Switzerland, 35 p.

Kelemwork S, Tahir P M, Ding W E and Ashaari Z. 2005. Effects of Particle Size and Orientation on Properties of Particleboard Made From Ethiopian Highland Bamboo (*Yushania Alpina*). In *Using Wood Composites as a Tool for Sustainable Forestry*: *Forests in the Balance*. Proceedings of Scientific Session 90. J.E. Winandy, R.W. Wellwood and S. Hiziroglu (eds).

Kickhöfen. 2019. Effect of lubrication on mechanical properties, rheology and fibre degradation of wood plastic composites (WPC), 82 p.

Kigomo B. 2007. Guidelines for growing bamboo. *KEFRI Guideline Series,* Nairobi Kenya, 65 p.

Kröckel K. 2017. Einfluss der Rohstoffsortierung auf das vertikale Dichteprofil von Bambus Scrimber. B.Sc., Hamburg.

Lammert M. 2017. Untersuchung zu einem modularen low-tech Doppel-T-Träger aus Bambuswerkstoffen und möglichen Längsverbindungen. M.Sc., Hamburg.

Leithoff H and Peek R D. 2001. Heat treatment of bamboo. IRG/WP 01-40216. In *International Research Group on Wood Preservation*. IRG/WP 01-40216 (ed). IRG Secretariat, pp. 2–11.

Liese W. 1998. The Anatomy of Bamboo Culms. *INBAR technical report.* International Network for Bamboo and Rattan, Beijing, 199 p.

Liese W and Kumar S. 2003. Bamboo preservation compendium. *INBAR technical report.* Centre for Indian Bamboo Resource and Technology, New Delhi, 231 p.

Liese W and Tang T K H. 2015. Preservation and Drying of Bamboo. In *Bamboo*. W. Liese and M. Köhl (eds). Springer International Publishing, pp. 257–297.

Liese, W. and Köhl, M. (eds). 2015. Bamboo: The plant and its uses. Springer, 362 p.

Lobovikov M, Paudel S, Piazza M, Ren H and Wu J. 2007. World bamboo resources: A thematic study prepared in the framework of the Global Forest Resources Assessment 2005, 80 p.

LUSO consult. 1997. Study on sustainable bamboo management: Technical cooperation Ethiopia-Germany. Final Report. *GTZ report,* Hamburg, 85 p.

Marra A A. 1992. Technology of wood bonding: Principles in practice, New York.

Matthies F. 2015. Untersuchungen zu Bambus als Baumaterial für Türme von Windkraftanlagen. B.Eng., Rosenheim.

McKinsey. 2017. MGI-Reinventing-construction-A-route-to-higher-productivity-Full-report, 168 p.

Michanickl A. 2013. Vorlesung Holzwerkstofftechnik: Verbrauch und Produktion von elektrischer und thermischer Energie in der Holzwerkstoffproduktion. Bachelor Holztechnik, HS Rosenheim.

Ministry of Environment, Forest and Climate Change. 2017. Ethiopia Forest Sector Review: Focus on commercial forestry and industrialization. Technical Report, Addis Ababa, 52 p.

Miyatake A. 2004. SST: Superior Strength Timber. A new material for buildings. In *Proceedings of the International Symposium on Advanced Timber and Timber-composite Elements for Buildings*: *Design, construction, manufacturing & fire safety : COST E29*. A. Ceccotti and J.W.G. de van Kuilen (eds). IVALSA.

MOSO. 2017. Press release. CE-Kennzeichnung für Bambus Bodenbeläge: Zwei neue Standards sorgen für Rechtssicherheit (11.05.2017), Zwaag, Netherlands, 3 p.

Muche F A and Degu Y M. 2019. Test and Characterization of Tensile Strength of *Oxytenanthera Abyssinica* and *Yushania Alpina* Bamboos. In *Advances of science and technology*: *6th EAI International Conference, ICAST 2018, Bahir Dar, Ethiopia, October 5-7, 2018, Proceedings / Fasikaw Atanaw Zimale, Temesgen Enku Nigussie, Solomon Workneh Fanta (eds.)*. F.A. Zimale, T. Enku Nigussie and S.W. Fanta (eds). Springer, pp. 160–169.

Mulatu Y. 2012. Growth, Morphology and Biomass of *Arundinaria alpina* (Highland Bamboo) (Poaceae) as Affected by Landrace, Environment and Silvicultural Management in the Choke Mountain, Northwestern Ethiopia. Doctoral, 196 p.

Mulatu Y, Alemayehu A and Tadesse Z. 2016a. Bamboo species introduced in Ethiopia: Biological, ecological and management aspects. Ethiopian Environment and Forest Research Institute, Addis Ababa, 75 p.

Mulatu Y, Alemayehu A and Tadesse Z. 2016b. Biology and Management of Indigenous Bamboo Species of Ethiopia: Based on Research and Practical Field Experience. Ethiopian Environment and Forest Research Institute, Addis Ababa, 67 p.

Müssig J. 2001. Untersuchung der Eignung heimischer Pflanzenfasern für die Herstellung von naturfaserverstärkten Duroplasten - vom Anbau zum Verbundwerkstoff. *Fortschritt-Berichte VDI Reihe 5, Grund- und Werkstoffe, Kunststoffe.* VDI-Verlag, Düsseldorf, 200 p.

National Planning Commission. 2016. Federal Democratic Republic of Ethiopia: Growth and Transformation Plan II (GTP II) (2015/16-2019/20): GTPII. World Bank, 236 p.

Negash L. 2010. A selection of Ethiopia's indigenous trees: Biology, uses, and propagation techniques. Addis Ababa University Press, Addis Ababa Ethiopia, xviii, 386 pages.

Nguyen A. 2018. Upcycling disposable post-consumer bamboo into a value-added product. B.Sc., Hamburg.

nova-institute. 2010. Lenzing expands product range with bamboo stem fibers - Bio-based News -. http://news.bio-based.eu/lenzing-expands-product-range-with-bamboo-stem-fibers/ (accessed on 10 July, 2019).

Pardo, R. (ed). 1987. Small-scale forest enterprises: They call it scrimber. 157th edn. FAO, 1 p.

Paulitsch M and Barbu M C. 2015. Holzwerkstoffe der Moderne. 1st edn. DRW-Verlag, Leinfelden-Echterdingen, 524 p.

Pilato L. 2010. Phenolic Resins: A Century of Progress. Springer Berlin Heidelberg, Berlin, Heidelberg, 543 p.

Prunier G and Ficquet É. 2015. Understanding contemporary Ethiopia. Hurst & Company, London, xv, 521.

Puettmann M, Kaestner D and Taylor A. 2016. Corrim Report – Module D2: Life Cycle Assessment of Softwood Plywood Production in the US Southeast, Tennessee, 55 p.

Qualitätsgemeinschaft Holzwerkstoffe e.V. 2017. Qualitäts- und Prüfbestimmungen zur Produktionskontrolle von Terrassendecks aus Holz-Polymer-Werkstoffen: QGHWS, 27 p.

Rabik A. 2016. Talks on the quality of heat treate fiber bundles and their influence to the bamboo scrimber quality. Personal conversation.

Reuters. 2016. Ethiopian protesters attack factories in Africa's rising economic star. https://www.reuters.com/article/us-ethiopia-unrest/ethiopian-protesters-attack-factories-in-africas-rising-economic-star-idUSKCN1270MX (accessed on 08 October, 2016).

Rowell R M. 2005. Handbook of wood chemistry and wood composites. CRC Press, Boca Raton Fla., 485 p.

Sampath P and Oyelaran-Oyeyinka B. 2016. Sustainable industrialization in Africa. Palgrave Macmillan, New York.

Sasol. 2013. Datasheet HydroWax Pro A18, Hamburg, 2 p.

Schlegelmilch M. 2015. Vergleichende Untersuchung von Konstruktionsvarianten aus Holz, Bambus und Holzwerkstoffen für den Holzbau in Ostafrika. B.Eng., Rosenheim.

Schmidt G. 2013. Ethiopian highland bamboo (*Yushania alpina* K. Schum. W.C. Lin.) as raw material for industrial panel production: Investigations on basic properties and raw material preparation. M.Sc., Hamburg.

Schmidt G, Belda M, Berthold D, Girma K and Ressel J B. 2016a. Technical feasibility report: Bamboo scrimber Ethiopia: Phase I+II. 3rd edn., Hamburg.

Schmidt G, Berthold D and Belda M. 2016b. Establishment of the bamboo panel industry sector in East Africa. Development of a scrimber panel based on Ethiopian highland bamboo. In *European Wood Based Panel Symposium*. EWBP (ed).

Schmidt G, Sommerhuber P and Krause A. 2017. BioHome: Building materials made from bio-based & recycling resources. Unpublished, Hamburg.

Schmidt O. 2010. Wood and tree fungi: Biology, damage, protection, and use. Springer, Cham, 334 p.

Scurlock J. 2000. Bamboo: an overlooked biomass resource?: Prepared for the USDE, US, 34 p.

Semple K E. 2014. Optimising the Stranding of Moso Bamboo (*Phyllostachys Pubescens* Mazel) Culms Using a CAE 6/36 Disk Flaker. In *57th International Convention of Society of Wood Science and Technology*. H. Michael Barnes and Victoria L. Herian (ed).

Sheriff D W. 1998. Productivity and economic assessment of hardwood species for scrimber production : a report for the Rural Industries Research and Development Corporation: A report. *RIRDC research paper series,* Barton, ACT, 2 p.

Shiferaw A. 2017. Productive Capacity and Economic Growth in Ethiopia. *CDP Background Paper*, 24 p.

Shu J and Wang H. 2015. Pests and Diseases of Bamboos. In *Bamboo*: *The plant and its uses*. W. Liese and M. Köhl (eds). Springer, pp. 175–192.

SKH. 2014. Basis of Assessment (BoA)-005: Semi-manufactured bamboo for exterior and interior applications, Wageningen, 41 p.

Stamm J. 2019. Mechanical fiber extraction from *Guadua* spp. Interview.

Stute T. 2018. Investigations on bamboo cement composites: The influence of bamboo particles on cement hydration as an approach towards green cement for the Ethiopian construction sector. M.Sc., Hamburg.

Suzuki S. 2005. Using Cedar Plantation Materials for Wood-Based Composites in Japan. In *Using Wood Composites as a Tool for Sustainable Forestry*: *Forests in the Balance*. Proceedings of Scientific Session 90. J.E. Winandy, R.W. Wellwood and S. Hiziroglu (eds), pp. 17–33.

Thoemen, H., Irle, M. and Šernek, M. (eds). 2010. Wood-based panels: An introduction for specialists. Brunel University press, 283 p.

Trujillo E. 2014. Polymer composite materials based on bamboo. Doctoral, Belgium, 244 p.

UNcomtrade. 2018. United Nations Department of Economic and Social Affairs Statistic Division. https://comtrade.un.org/ (accessed on 30 April, 2018).

UNIDO. 2008. Bamboo mat weaving techniques and applications: Cottage industry manuals. United Nations Industrial Development Organization, Vienna, Austria, 35 p.

UNIDO. 2009a. Bamboo cultivation manual: Guidelines for cultivating Ethiopian highland bamboo. United Nations Industrial Development Organization, Vienna, Austria, 65 p.

UNIDO. 2009b. Report Testing of Two Ethiopian Bamboo Species for Value-added Products, Addis Ababa, 25 p.

UNIDO. 2016. Industrialization in Africa and Least Developed Countries: Boosting growth, creating jobs, promoting inclusiveness and sustainability. A report to the G20 development working group by UNIDO, Vienna, Austria, 61 p.

Ushakov I A. 2012. Probabilistic reliability models. Wiley, San Diego, CA, 1 online resource.

van Acker J and Palanti S. 2017. 5.3 Durability. In *Performance of bio-based building materials*. D. Jones and C. Brischke (eds). Woodhead Publishing, pp. 249–333.

van der Lugt P and Otten G. 2006. Bamboo Product Commercialization in the European Union: An Analysis of Bottlenecks and Opportunities. *INBAR technical report*, 100 p.

Virchow D, Beuchelt T D, Kuhn A and Denich M. 2016. Biomass-Based Value Webs: A Novel Perspective for Emerging Bioeconomies in Sub-Saharan Africa. In *Technological and Institutional Innovations for Marginalized*

Smallholders in Agricultural Development. F.W. Gatzweiler and J.v. Braun (eds). Springer International Publishing, pp. 225–238.

Wagenführ, A. and Scholz, F. (eds). 2008. Taschenbuch der Holztechnik: Mit 84 Tabellen. Fachbuchverl. Leipzig im Hanser-Verl., 568 p.

West P W. 2015. Tree and Forest Measurement. Springer International Publishing, Cham, 218 p.

World Bamboo Organization. 2018. World Bamboo Congress 2018: 14.-18.08.2018. 11th edn., Xalapa, Mexico, 228 p.

World Bank. 2018. Ethiopia | Data. https://data.worldbank.org/country/ethiopia (accessed on 06 November, 2018).

Xiao C. 2013. ZCZK190 Crushing machine: User's manual. Anji Yukang and Luan Wobam, 31 p.

Xiao Y, Shan B, Yang R Z, Li Z and Chen J. 2014. Glue Laminated Bamboo (GluBam) for Structural Applications. In *Materials and Joints in Timber Structures*. S. Aicher, H.-W. Reinhardt and H. Garrecht (eds). Springer Netherlands, pp. 589–601.

Xiao, Y., Inoue, M. and Paudel, S.K. (eds). 2008. Modern bamboo structures: Proceedings of First International Conference on Modern Bamboo Structures (ICBS-2007), Changsha, China, 28-30 October 2007. CRC Press, 314 p.

XZBBC. 2016. Zhejiang Xinzhou Bamboo-based Composites Technology Co. Ltd. http://www.xzbbc.com/ (accessed on 01 March, 2018).

Zhang Q, Jiang S and Tang Y. 2002. Industrial utilization on bamboo. *INBAR technical report.* International Network for Bamboo and Rattan, New Delhi, 206 p.

Zhiyong L and Junqi W. 2017. 100 heroes of China's bamboo industry. 外文出版社, Beijing, China, 303 p.

Zhu Z and Jin W. 2018. Sustainable bamboo development. CABI, Boston MA, 243 p.

Author’s peer-reviewed publications

Da Silva, E.J., Schmidt, G., Mantau, U. 2020. Wood resource balance for plantation forests in Brazil: Resources, consumption and cascading use. *Cerne* **26**(2), 247–255.

Schmidt, G., Stute, T., Lenz, M.T., Melcher, E. and Ressel, J.B. 2020. Fungal deterioration of a novel scrimber composite made from industrially heat treated African highland bamboo. *Industrial Crops and Products* **147**, 1–10.

Jorch, V, Fock, H.O., González-Mellado, A., Schmidt, G. 2020. Sharing knowledge – to the benefit of all: Scientific training and education in Thünen Institute’s cooperation with Africa. *Rural 21 The International Journal for Rural Development* **54**(2):50-51.

Acosta, R., Montoya, J.A. and Schmidt, G. 2020. Influence of a Thermal Treatment on the Tensile Strength and Equilibrium Moisture Content of Bamboo (*Guadua angustifolia* Kunth). *BioResources* **15**, 3103–3111.

Da Silva, E.J., Schmidt, G., Cremonez, V.G., Venson, I. and Simetti, R. 2016. The Effect of Heat Treatment on Wood Water Relationship and Mechanical Properties of Commercial Uruguayan Plantation Timber *Eucalyptus grandis*. *Australian journal of basic and applied sciences* **10**, 704–708.

Author’s conference contributions

Schmidt, G. and Krause, A. 2019 Life Cycle Assessment of Recycled Wood Plastic Composites, Keynote speech. H2020 project URBANREC closing conference. September 2019. Izmir, Turkey.

Schmidt, G. 2019. Thermisch behandelter Bambus Scrimber und der Abbau durch Moderfäule und holzzerstörende Pilze. At Deutsche Holzschutztagung. 30th edn. H. Militz and S. Tobisch (eds). IHD. April 2019, Dresden, Germany.

Mertens, O., Nopens, M., Gurr, J. and Schmidt, G. (eds). 2017. Proceedings of the "Think outside of the wooden box!" PhD workshop Hamburg within COST Action FP1407 STSM. Universität Hamburg. July 2017, Hamburg, Germany.

Schmidt, G. 2016. Ethiopian bamboo as “sustainable supreme flooring product” in the international market: Product development, Quality characters, Market assets. GD Holz Branchentag, March 2016. Cologne, Germany.

Schmidt, G. 2017a. Does thermal treatment matter? Resistance of bamboo scrimber to biodegradation IUFRO Div. 5 Conference, June 2017. Vancouver, Canada.

Schmidt, G., Berthold, D. and Belda, M. 2016a. Establishment of the bamboo panel industry sector in East Africa: Development of a scrimber panel based on Ethiopian highland bamboo. EWBP Symp., Hamburg, October 2016.

Schmidt, G., Gurr, J., Mertens, O. and Nopens, M. Think outside of the wooden box! PhD Workshop Hamburg – COST Action FP1407. September 2018. Kuchl, Austria.

Sommerhuber, P., Schmidt, G. and Krause, A. 2017. Environmental parameters of value-added products made of secondary wood and non-wood materials. Poster session. IUFRO Div. 5 Conference, June 2017. Vancouver, Canada.

Others

Radio broadcast. SWR2 Matinee 2020. “Tolles Rohr: Bambus“. Im Gespräch mit Jörg Biesler. EA 12.4.2020 9:03 Uhr. Südwestrundfunk. Stuttgart. Köln.

Television broadcast. Galileo Pro7. 2019. “Alternative zu Plastik: wie gut sind Produkte aus Bambus?“. Episode 225. EA 21.08.2019. 19:05. München.

Gauss, C. and Schmidt, G. 2018 BRALECOMP: 1st Brazilian-German Workshop on Composite Products from Alternative Lignocellulosic Resources - Workshop report. Universität Hamburg.

Doering-Arjes P and Schmidt G. 2018. Some Myths of Bamboo Rodmaking and Beyond. Dedicated to the Making of Fine Bamboo Fly Rods. *Power Fibers Online Magazine* **58**, 1-49.

Gurr, J., Schmidt, G., Nopens, M. and Krause, A. 2016. Wood Drive. In Das Lehrlabor: Förderung von Lehrinnovationen in der Studieneingangsphase – eine Bilanz. Universitätskolleg-Schriften. C. Gaigl, M. Kenter and K. Siemonsen (eds). Universität Hamburg, Universitätskolleg.

Schmidt, G., Belda, M., Berthold, D., Girma, K. and Ressel, J.B. 2016b Technical feasibility report – Bamboo scrimber Ethiopia: Phase I+II. 42.

Schmidt, G., Robert, R., Da Silva, E.J. and Magel, E. 2016c The joint-venture expedition project "IX. Brasil Norte-Sul" - Concept.

Schmidt, G., Da Silva, E.J. and Robert, R. 2015 Deutschland Nord-Süd 2015 DAAD Studienpraktikum Academic internship Project Report.

Schmidt, G. 2014. Expedition „Brasil Norte-Sul“ – Tropische Forstwirtschaft in Brasilien und Peru. *BDH-Mitteilungen* **1**, 25–28.

Schmidt, G. 2013 Ethiopian highland bamboo (*Yushania alpina* K. Schum. W.C. Lin.) as raw material for industrial panel production: Investigations on basic properties and raw material preparation. M.Sc. Universität Hamburg.

Schmidt, G. 2011 Untersuchungen zur enzymatischen Modifikation von Lignin. B.Sc. Universität Hamburg.

Student supervision

Nine bachelor and master theses were developed during my doctoral studies. Not only did the students help building scientific and technical expertise, but they offered a great opportunity to switch the perspective from being supervised to supervising. Thank you for your passion for the topic, your patience with me and wish you all good luck on your future missions: **Jakob Aping** (2015) produced a laminated bamboo veneer lumber and tested the reinforcement effect of raw material sorting in flexural bending. Mr. Aping was my first student and most probable the most challenging one. **Friederike Matthies** (2015) investigated the question of how engineered bamboo CLT can be theoretically used in wind energy towers together with the pioneer company TimberTower in Hamburg and Hannover, Germany. Friederike joined our team as a guest from FH Rosenheim first and later became an integral team member who successfully finished a very challenging master thesis on dynamic-mechanical analysis in our working group. The utilization of I-joists containing bamboo composites in modular housing for the exploding East African construction sector was the focus of **Moritz Schlegelmilch**’s (2015) bachelor thesis. Moritz joined us as a guest student from FH Rosenheim too and worked a couple of months in the context of the Tanzania branch office of Bavarian timber pioneers Livable Home GmbH. The modular I-joist concept was then further developed by **Maren Lammert** (2017). With her master thesis she solved static calculations and conducted flexural experiments on a lengthwise joist connection system. These joists are made from highland bamboo scrimber flanges and OSB in the web. Maren now works in a timber construction company near Cologne, Germany. **Arne Fey** (2017) tried to find a suitable examination method for BS resistance against termite attack in his bachelor thesis together with the Federal Material Testing agency BAM in Berlin. The bachelor thesis of **Konstantin Kröckel** (2017) helped in understanding the density-related difficulties when producing BS with homogenous technological characteristics. As a former boat craftsman, he is now in Liberia, promoting the wood-working vocational education for UNIDO. Inspired by ChopValue, a successful startup business from Vancouver, **Anh Nguyen 2018** (2018) investigated the upcycling of post-consumer bamboo disposables in her bachelor thesis. The reinforcement potential of industrial BS in hybrid cross laminated timber was shown by **Jannik Hoffmann** (2018), another FH Rosenheim student. A very different approach of using bamboo in the construction sector was worked out in the master thesis project by **Thomas Stute** (2018). He analyzed the influence of bamboo particles on cement hydration and found that small amounts of bamboo sugar even improve setting. Thomas works as technical engineer at Fagus GreCon today.

Appendix

A2. State of the art

A3. Raw material study

A4. Process engineering

A5. Market entrance

A5. Export market requirements

D5. Digital appendix (COGS model)

A2. State of the art

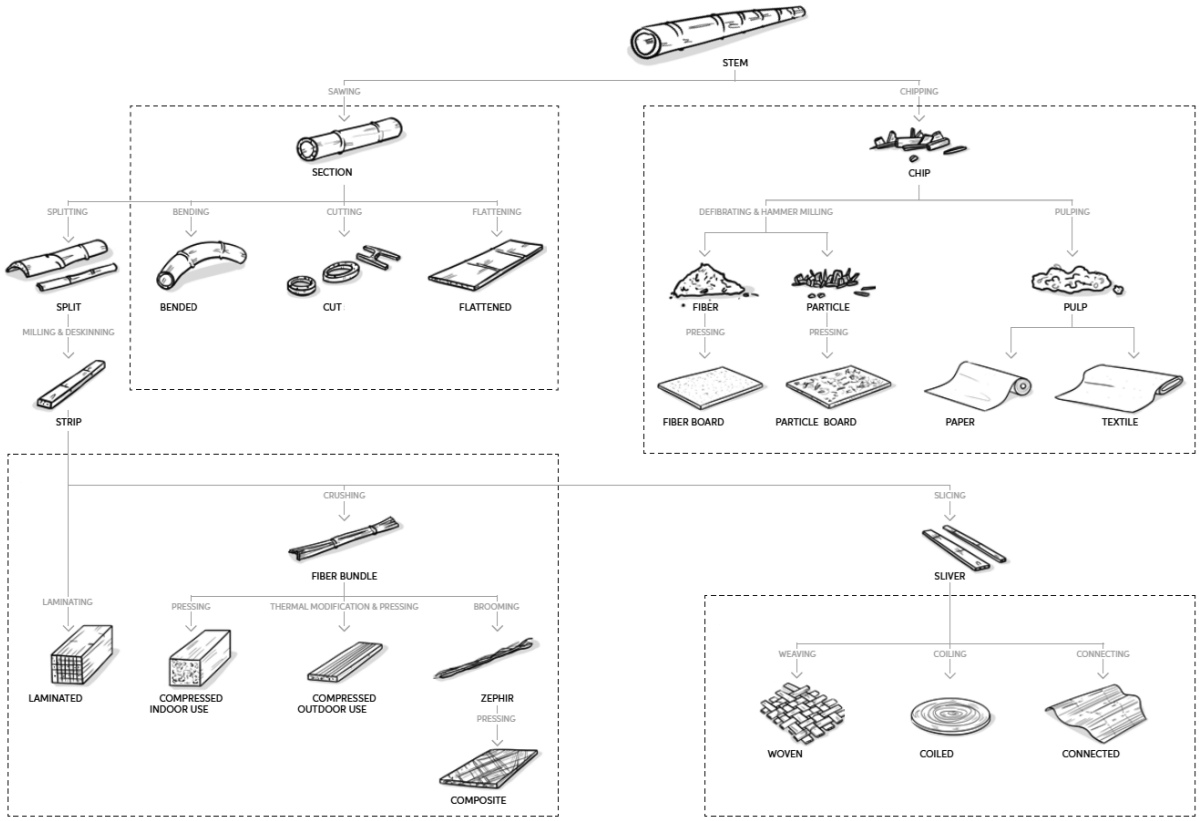

Figure 96: Transformation paths of a culm to engineered bamboo (World Bamboo Organization 2018)

A3. Raw material study

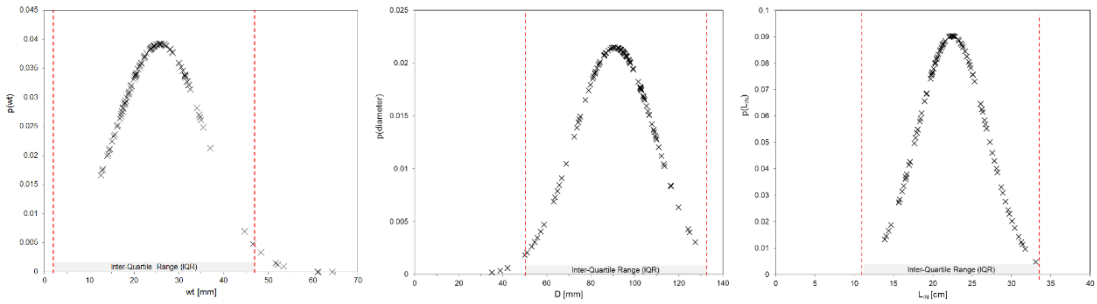

Figure 97: Probability distribution density functions of culm wall thickness, outer diameter, internodal length and their respective 25,75 quartile boundaries

Table 40 Regression parameter of outer and inner diameter at breast height (D_{bh}, d_{bh}) and wall thickness (wt) against culm height (h)

	wt	**d**	**D**
	y = B1*exp(-x/B2)+y0	y = y0+B1*x^1+B2*x^2+B3*x^3+B4*x^4	y = y0+B1*x^1+B2*x^2
y0	0.15 ± 0.02	0.61 ± 0.04	0.77 ± 0.03
B1	0.47 ± 0.02	1.38 ± 0.62	-0.04 ± 0.14
B2	0.23 ± 0.03	-2.83 ± 2.89	-0.63 ± 0.15
B3		0.59 ± 4.75	
B4		0.44 ± 2.53	
R^2	0.76	0.56	0.68
Adj. R^2	0.76	0.55	0.67

Table 41: Ash and silica content for raw and washed bamboo with thin and thick culm walls measured in the node and internode

			sample	**Ash**	**Silica**
				[m%]	
Raw	Thin wall	Nodes	1	2.62	1.49
			2	2.57	1.55
			3	2.58	1.57
			mean	**2.59**	**1.54**
		Internodes	1	1.85	0.92
			2	1.80	0.92
			3	1.88	0.96
			mean	**1.84**	**0.93**
	Thick wall	Nodes	1	1.77	0.57
			2	1.76	0.50
			3	1.88	0.60
			mean	**1.80**	**0.56**
		Internodes	1	1.75	0.10
			2	1.86	0.20
			3	1.82	0.21
			mean	**1.81**	**0.17**
Washed	Thin wall	Nodes	1	1.64	0.75
			2	1.38	0.47
			3	1.73	0.71
			mean	**1.58**	**0.64**
		Internodes	1	1.18	0.38
			2	1.17	0.28
			3	1.26	0.29
			mean	**1.20**	**0.32**
	Thick wall	Nodes	1	1.76	0.67
			2	1.59	0.54
			3	1.54	0.53
			mean	**1.63**	**0.58**
		Internodes	1	1.70	0.02
			2	1.64	0.02
			3	1.72	0.02
			mean	**1.69**	**0.02**

Table 42: Quantitative analysis of monomeric carbohydrates shares [%] in *Y. alpina* by site, age and culm height section (< 0.1 was below LoD)

Site	Age	Section	Glu	Ara	Gal	Xyl	Man	Rha	Hydrolysis residue
A	4	B	41.7	1.9	0.7	19.5	<0.1	<0.1	25.6
		M	46.1	1.5	0.6	19.8	<0.1	<0.1	23.6
		T	46.3	1.3	0.5	18.7	<0.1	<0.1	24.8
	5	B	41.6	1.6	0.6	19.1	<0.1	<0.1	26.9
		M	45.2	1.6	0.7	19.5	0.1	<0.1	27.1
		T	46	1.3	0.4	18.5	<0.1	<0.1	25.7
B	4	B	40.5	1.7	0.7	19.1	<0.1	<0.1	28.1
		M	39.6	2.5	1.4	12.4	0.3	<0.1	29.7
		T	43.6	1.5	0.5	18.6	0.1	<0.1	28.1
	5	B	37.3	2	1.1	11.4	0.4	<0.1	31.6
		M	39.8	1.5	0.7	9.8	0.4	<0.1	27.9
		T	44.5	1.5	0.7	10.2	0.5	<0.1	28.6

Table 43: Linear regression analysis of the correlation between stress and strain calculated in the function interval defined by four different boundaries, namely downer limit F_1 and upper limit F_2

F_1 **F_2**	**$0.2*F_{max}$** **$0.4*F_{max}$**	**150N** **$0.5*F_{max}$**	**$0.3*F_{max}$** **$0.5*F_{max}$**	**$0.2*F_{max}$** **$0.5*F_{max}$**
a	-9919.21 ± 9144.3	-16076.19 ± 10841.93	13934.46 ± 7181.51	40784.96 ± 30245.2
b	44810.88 ± 13778.25	58265.67 ± 16426.15	3277.7 ± 10835.48	-29427.1 ± 44116.46
RSS	8.1E9	1.04E10	5.68E9	2.38E11
Pearson's r	0.37	0.4	0.04	-0.07
R^2	0.13	0.16	0.01	0
Slope sign. different from 0	yes	yes	no	no

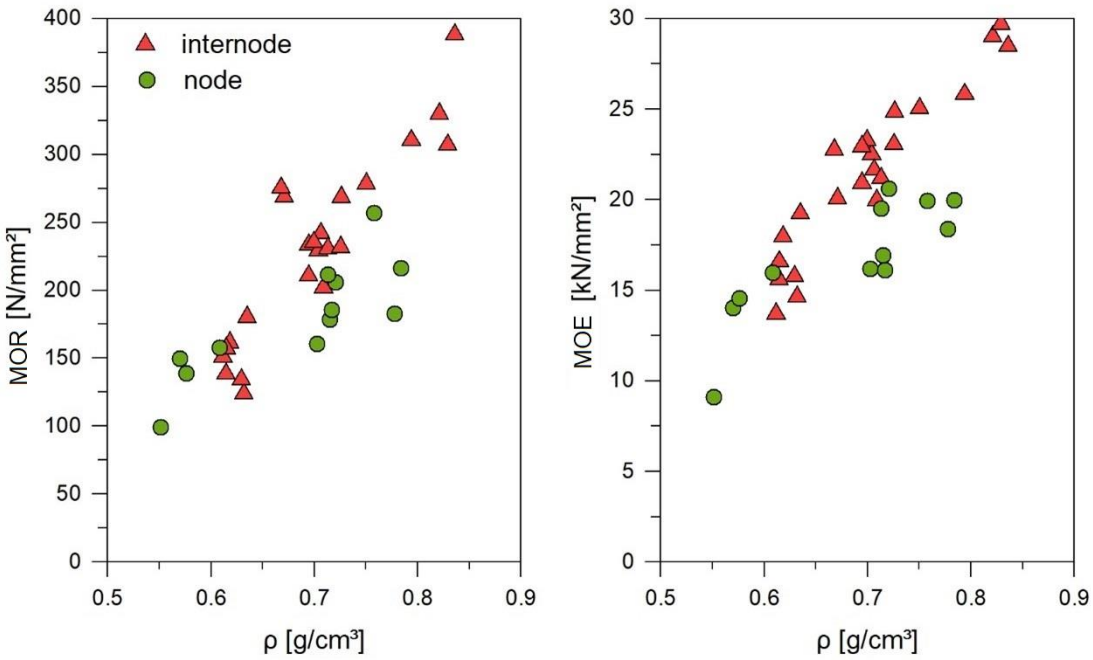

Figure 98: Flexural strength (MOR) and modulus of elasticity (MOE) for scrims from highland bamboo internode (red) and node (green)

A4. Process engineering

Table 44: Panel recipe calculation for the screening trials experiments

Width:	500 mm	Bulk density dry:	934.58 kg/m^3
Length:	500 mm	Bulk density moist:	1000 kg/m^3
Thickness:	21 mm	Target EMC:	7 %
Volume:	0.00525 m^3		
Resin type:	PF		
Designation:	Dynea 4976		
Solids content:	50 %		
Solids, in atro particles:	10 %		
Additive type:	Sasol Wax		
Designation:	Pro A 18		
Solids content, additive:	50 %		
Solids, additive, in atro particles:	2 %		
Mass calculation without mixing supplements			
Board mass at equilibrium moisture:	5240 g	(Volume*bulk density moist)*1000	
Board mass atro:	4907 g	(Volume*bulk density atro)*1000	
	Solids	Water	Solids + water
Particle mass for the board:	4303.98 g	129.12 g	4433.10g
Resin mass:	516.48 g	260.18 g	776.66 g
Hydrophobization:	86.08 g	86.08 g	172.16 g
Mat mass:			5381.92 g
Mixing proportions and spread mass with mixing supplement			
Mixing supplement:	15 %		
Mixing quantity, particle:	5035.66 g	151.07 g	5186.73 g
Mixing quantity, adhesive:	604.28 g	304.41 g	908.69 g
Mixing quantity, hydrophobization:	100.71 g	100.71 g	201.43 g

Table 45: Resin gradient experimental matrix

Board No.	Date of production	Pre-Treatment		Board Parameter			Binder					Hydrophobic Agent			Pressing Parameter		
		Condition of treatment thermally modification)	dried in kiln to moisture content of ca. 3%	Description	dimension (mm)	density (kg/m³)	application	Dynea 4976	glue on dry particle (%)			type	wax on dry particle (%)		pressing temperature (°C)	pressing time (s/mm)	pressing procedere
									Uper surface	Middle surface	lower surface		ohne	2%			
39401	27.06.2017	Treated at 180°C for 3h	X	Outdoor Boards	500x500x23	1000	spraying	X	12	12	12	Sasol Wax Pro A18		X	130	ca. 30	heating up to 110°C core temperature than cooling down to 95° C
39402	27.06.2017							X	12	12	12			X			
39403	28.06.2017							X	12	12	12			X			
39404	28.06.2017							X	12	12	12			X			
39405	28.06.2017							X	12	12	12			X			
39406	28.06.2017							X	12	12	12			X			
39407	26.06.2017							X	14	14	14			X			
39408	26.06.2017							X	14	14	14			X			
39409	26.06.2017							X	14	14	14			X			
39410	26.06.2017							X	14	14	14			X			
39411	27.06.2017							X	14	14	14			X			
39412	27.06.2017							X	14	14	14			X			
39413	16.06.2017							X	16	16	16			X			
39414	16.06.2017							X	16	16	16			X			
39415	15.06.2017							X	16	16	16			X			
39416	15.06.2017							X	16	16	16			X			
39417	15.06.2017							X	16	16	16			X			
39418	15.06.2017							X	16	16	16			X			
39419	12.06.2017							X	14	12	14			X			
39420	12.06.2017							X	14	12	14			X			
39421	12.06.2017							X	14	12	14			X			
39422	12.06.2017							X	14	12	14			X			
39423	13.06.2017							X	14	12	14			X			
39424	13.06.2017							X	14	12	14			X			
39425	13.06.2017							X	16	12	16			X			
39426	13.06.2017							X	16	12	16			X			
39427	14.06.2017							X	16	12	16			X			
39428	14.06.2017							X	16	12	16			X			
39429	14.06.2017							X	16	12	16			X			
39430	14.06.2017							X	16	12	16			X			

Table 46: Mean thickness swelling (TS), water adsorption (WA), internal bond (IB), flexural strength (MOR), modulus of elasticity (MOE) for press temperatures (T) and resin type (c);

Pre-Treatment (V0; V1)						Resin parameter (V2; V3)					Wax (V4)								
T [°C]				t [h]		Applic.	Resin type				m [%]		TS [%]		WA [%]		IB [N/mm²]	MOR [N/mm²]	MOE [kN/mm²]
160	180	200	220	3	5		PF1	PF2	PF3	PF4	0	2	2 h	24 h	2 h	24 h			
						Spraying	X				X		2.08	5.83	6.27	16.72	0.06	109.3	24.4
												X	1.19	4.15	5.09	15.07	0.69	127.93	22
								X			X		1.73	4.3	6.18	13.83	0.31	87.25	18.36
												X	1.03	2.78	4.43	11.18	0.26	57.84	14.92
X				X															
						Powdering			X		X		4.69	9.47	8.31	19.86	0.6	142.8	24.06
												X	1.08	5.16	3.02	11.25	0.49	124.06	23.26
										X	X		1.35	4.45	5.57	14.09	0.74	126.59	23.16
												X	0.73	3.29	3.08	10.53	0.19	91.93	19.83
						Spraying	X				X		1.38	4.62	5.36	15.09	1.04	171.69	26.05
												X	1.28	4.94	3.78	12.78	0.7	131.48	24.65
								X			X		0.44	2.15	3.32	9.8	1.27	135.97	21.91
												X	0.32	1.78	2.67	8.41	1.05	109.76	20.06
X					X														
						Powdering			X		X		3.64	8.01	2.67	8.41	0.14	95.43	20.97
												X	0.76	4.02	2.96	11.27	0.61	116.13	22.39
										X	X		0.69	3.59	3.74	12.03	0.85	150.43	25.53
												X	0.34	1.46	1.79	6.59	0.86	116.97	21.79
						Spraying	X				X		0.79	3.18	4.34	12.12	1.03	146.54	23.6
												X	0.63	3.1	3.61	11.91	0.8	124.16	23.41
								X			X		2.74	6.44	8.28	18.63	0.17	119.74	26.57
												X	0.67	2.59	3.76	12.06	0.67	116.38	24.17
	X			X															
						Powdering			X		X		1.23	5.66	6.01	17.53	0.63	127.27	23.25
												X	0.45	2.78	2.4	8.57	0.62	114.54	21.89
										X	X		0.64	2.44	5.21	13.35	0.71	123.81	22.56
												X	0.18	1.63	2.05	7.6	0.91	149.83	23.03
						Spraying	X				X		0.94	2.76	5.19	12.72	0.59	104.72	23.1
												X	0.96	3.37	4.12	11.62	0.67	118.7	23.97
								X			X		0.4	1.98	3.66	10.71	0.73	130.57	24.32
												X	0.31	1.33	2.57	8.24	0.62	119.81	24.22
	X				X														
						Powdering			X		X		1.46	4.92	7.8	18.08	0.31	90.04	23.1
												X	0.22	1.37	2.04	6.92	0.46	74.63	20.94
										X	X		0.67	3.52	5.37	15	0.51	96.43	23.87
												X	0.48	1.83	2.78	8.73	0.59	92.12	23.09
						Spraying	X				X		2.59	6.01	8.33	18.54	0.45	87.33	26.25
		X		X								X	0.41	2.35	2.92	10.19	0.44	101.65	25.08
								X			X		0.99	3.56	5.23	14.61	0.77	114.95	26.46

												X	0.53	2.97	2.59	9.57	0.52	99.55	26.73
											X		1.69	4.58	7.06	17.37	0.26	84.83	24.75
										X									
												X	0.76	4.31	2.87	11.66	0.21	62.66	23.51
											X		0.87	3.62	4.9	15.07	0.55	98.91	24.86
										X									
												X	0.19	1.6	1.76	6.86	0.42	95.73	25.02
											X		0.73	2.88	3.85	11.72	0.6	97.31	22.05
									X										
												X	0.37	1.79	2.85	9.98	0.41	89.55	23.04
											X		1.14	4.3	4.04	12.59	0.95	131	25.58
										X									
												X	0.6	1.88	2.43	8.45	0.85	130.3	23.96
X											X		0.94	3.21	4.59	13.71	0.5	85.94	21.96
										X									
												X	0.17	1.54	1.54	6.88	0.27	72.27	21.75
											X		0.8	3.08	5.11	14.49	0.27	82.75	22.84
										X									
												X	0.2	1.11	1.83	7.04	0.49	92.04	24.53
											X		0.77	3.23	3.8	11.98	0.47	72.03	21.81
									X										
												X	0.77	3.19	4.32	13.69	0.38	73.44	21.45
											X								
										X									
												X	0.81	3.04	4.02	12.88	0.22	58.69	19.56
										X									
											X		0.54	2	3.23	10.7	0.19	62.7	20.28
											X		0.41	1.81	3.9	11.07	0.77	126.1	19.28
									X										
												X	0.58	2.28	4.26	11.68	0.5	117.6	19.44
											X		1.53	5.81	6.45	17.89	0.97	195.52	26.49
										X									
												X	0.76	3.12	4.43	12.99	1.31	213.25	25.29
											X		1.57	5.55	8.68	22.5	0.75	128.44	22.85
										X									
												X	0.77	4.09	4.61	13.96	0.84	149.69	24.69
											X		0.92	3	5.22	13.57	0.49	132.65	18.92
										X									
												X	0.48	2.45	3.99	11.63	0.9	163.68	23

Table 47: Density (ρ), thickness swelling (TS), water adsorption (WA), internal bond (IB), flexural strength (MOR), elasticity (MOE) for one panel pressed from heat treated V1(160 °C, 5 h) highland bamboo scrimber and PF1 resin

		n	Mean	SD	Min	Median	Max
ρ [g/cm³]	160	8	1.049	0.031	0.978	1.059	1.073
	180	8	1.055	0.037	0.986	1.062	1.114
	200	9	1.070	0.049	0.985	1.074	1.136
	Control	8	1.039	0.045	0.971	1.027	1.100
TS [%]	160	8	4.62	2.26	2.39	3.69	8.31
	180	8	2.76	1.59	1.3	2.34	6.05
	200	9	3.53	2.22	1.83	2.69	8.73
	Control	8	1.81	0.62	1.11	1.91	2.89
WA [%]	160	8	15.09	4.75	10.58	13.6	24.25
	180	8	12.72	4.04	7.73	12.49	19.61
	200	9	12.91	4.77	8.17	10.94	22.46
	Control	8	11.07	2.24	8.1	11.69	13.94
IB [N/mm²]	160	8	1.04	0.18	0.76	1.1	1.24
	180	8	0.59	0.18	0.23	0.58	0.85
	200	9	0.58	0.15	0.44	0.51	0.88
	Control	8	0.77	0.4	0.25	0.78	1.22
MOR [N/mm²]	160	4	17.2	0.7	16.50	17.24	1.79E-04
	180	4	10.5	1.9	7.56	11.40	1.15E-04
	200	5	9.49	0.9	8.53	9.50	1.10E-04
	Control	4	12.6	2.5	9.98	12.74	1.51E-04
MOE [kN/mm²]	160	4	26.05	1.3	24.39	26.35	27.1
	180	4	23.1	1.72	20.71	23.52	24.65
	200	5	22.89	2.43	20.17	22.07	26.22
	Control	4	19.28	2.7	15.84	19.58	22.12

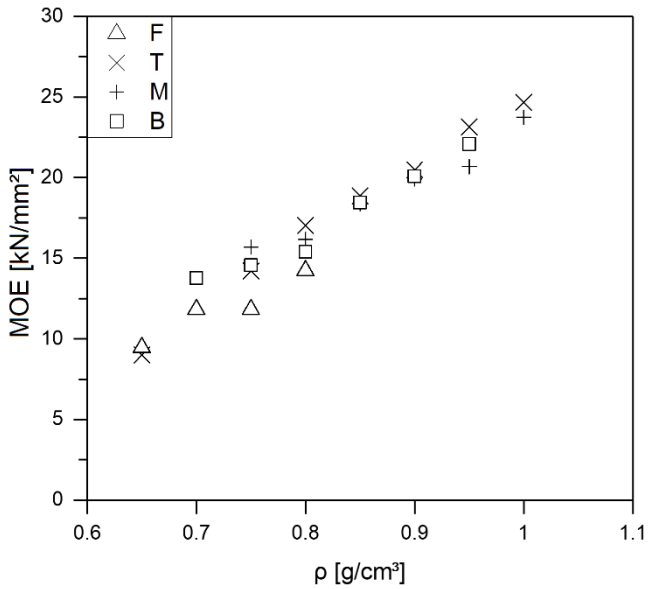

Figure 99: Flexural modulus of elasticity (MOE) for bottom (B), middle (M), top (T) as well as fine (F) scrims against sample density

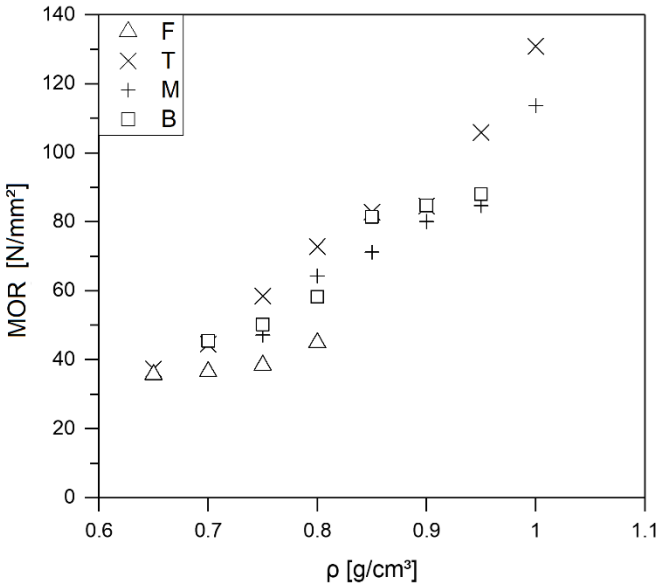

Figure 100: Flexural strength (MOR) for bottom (B), middle (M), top (T) as well as fine (F) scrims against sample density

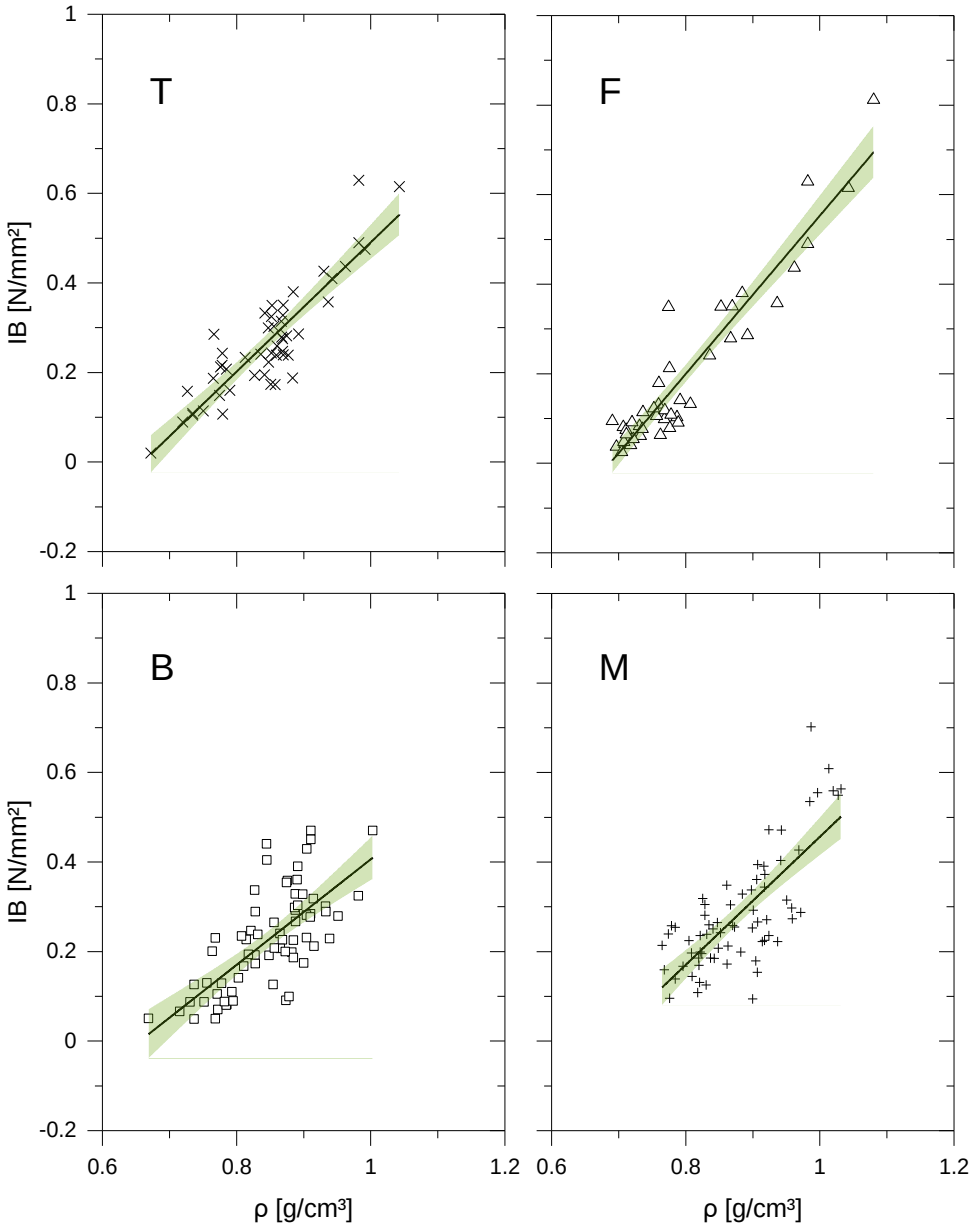

Figure 101: Internal bond (IB) and a linear regression and confidence interval against the actual specimen density of panels made from bottom (squares), middle (crosses), top (x) and fine (triangles) strands

Figure 102: Cross section of scrimber specimens made from crushed scrims coming from bottom (B), middle (M), top (T) portion of the culm and a finer crushed (F) variant

Table 48: Regression (y = a + b*ρ) parameter comparison of IB against the actual specimen density and the theoretical critical density ρ_{crit} at IB = 0, for panels made from bottom, middle, top and fine scrims (B, M, T, F)

Strand class	**Intercept [N/mm²]**	**Slope [N/mm²]**	**Pearson's r**	**R^2**	**ρ_{crit} (IB = 0) [g/cm³]**
F	-1.22 (0.08)	1.77 (0.09)	0.95	0.89	0.69
T	-0.95 (0.09)	1.44 (0.11)	0.89	0.78	0.66
M	-0.97 (0.13)	1.43 (0.15)	0.75	0.57	0.68
B	-0.77 (0.12)	1.18 (0.14)	0.71	0.49	0.65

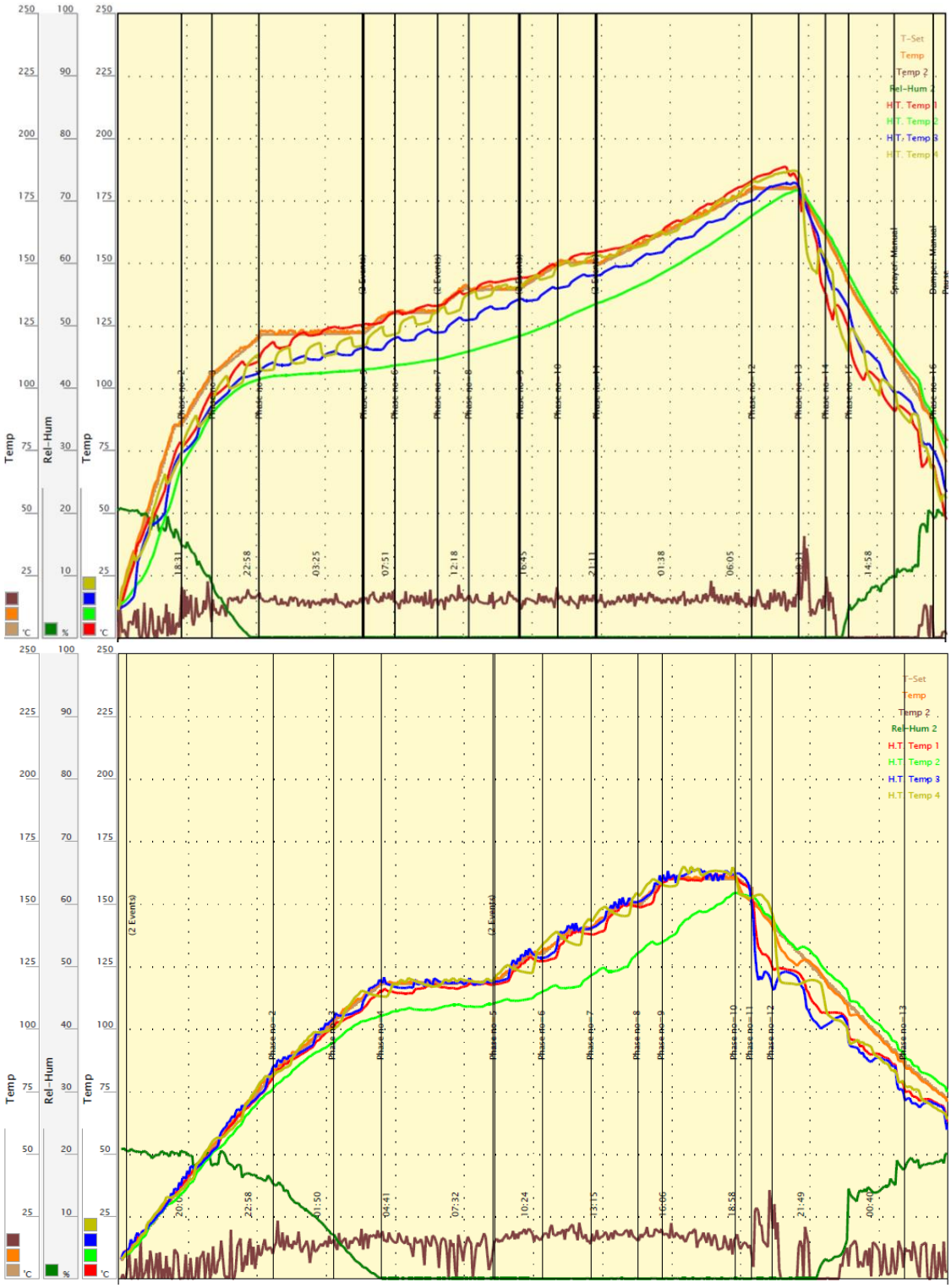

Figure 103: Progression of actual stack temperature (H.T. temp 1-4), chamber temperature (Temp, Temp 2) and relative humidity (Rel-Hum 2) at a nominal target temperature of 180 °C (above) and 160 °C (below) and 3 h holding time in the industrial scale treatment

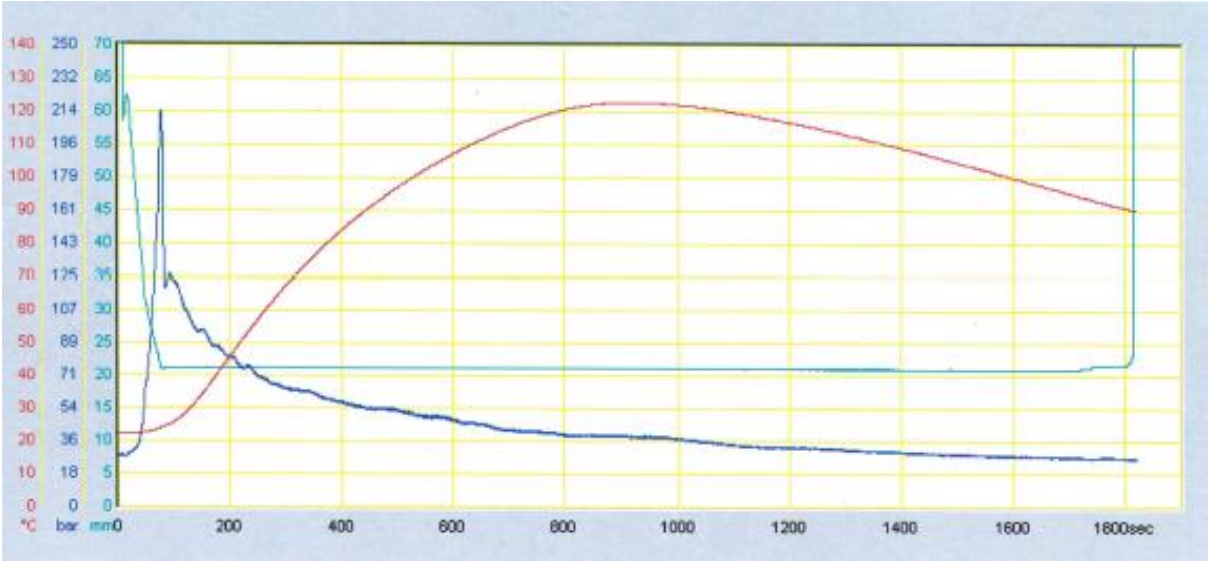

Figure 104: Characteristic press diagrams for untreated bamboo scrimber in a laboratory trial (top) with distance (turquoise), pressure (blue) and temperature (red) and in an industrial hot press (bottom) with distance (red), pressure (green) and temperature (brown, pink)

A5. Export market requirements

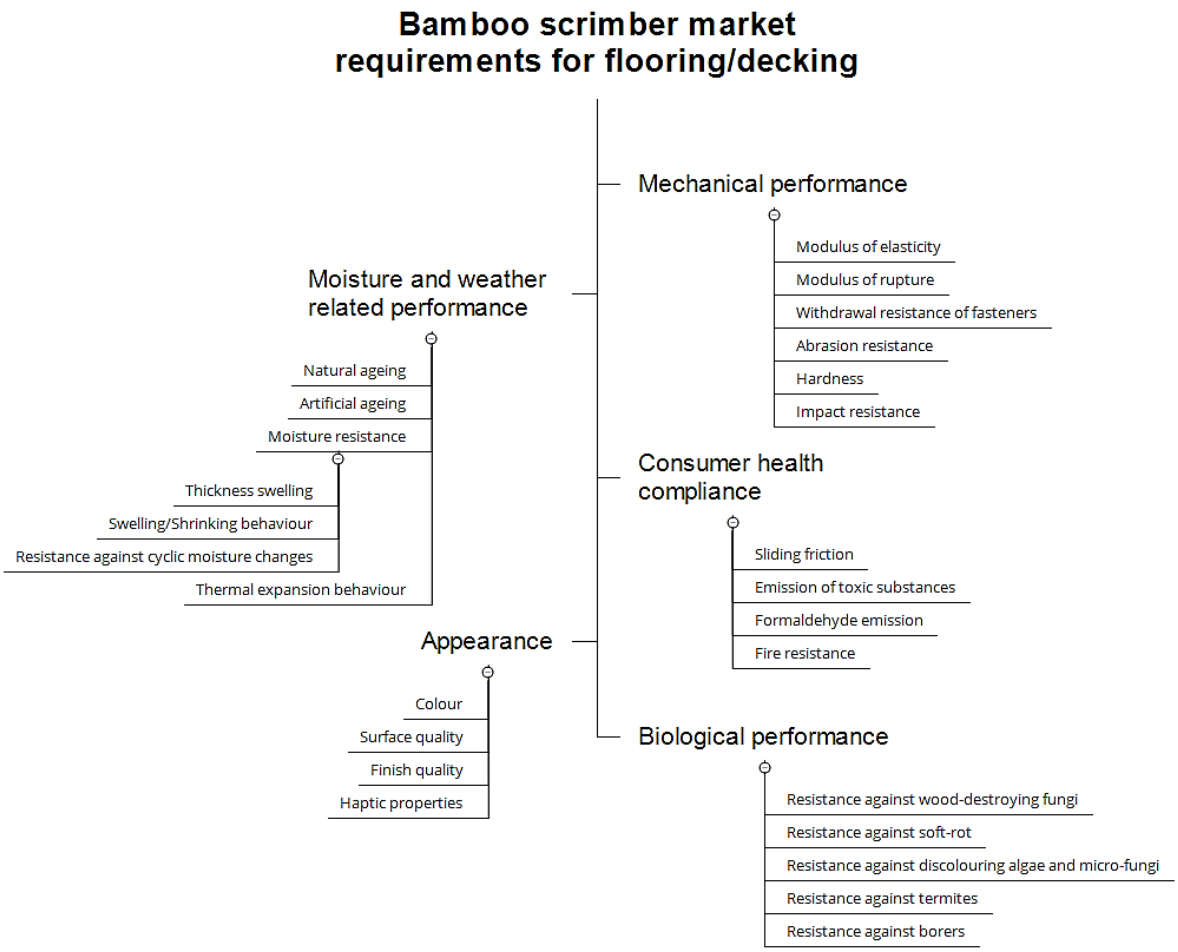

Figure 105: Market requirements for bamboo scrimber in flooring and decking products, developed from customer demands, formal and informal standards

Table 49: Regression formulae for flexural creep strain and creep modulus of highland bamboo scrimber

	Untreated	160	180	Comm.
ε [-]				
Load	y = 0.037ln(x) + 0.38 R^2 = 0.7786	y = 0.0471ln(x) + 0.3888 R^2 = 0.9039	y = 0.0142ln(x) + 0.2906 R^2 = 0.7451	y = 0.1198ln(x) + 0.2437 R^2 = 0.9844
Release	y = -0.19ln(x) + 1.6148 R^2 = 0.9997	y = -0.276ln(x) + 2.3698 R^2 = 0.9746	y = -0.053ln(x) + 0.4605 R^2 = 0.9087	y = -0.244ln(x) + 2.0807 R^2 = 0.9986
MOE [kN/mm²]				
	y = -0.78ln(x) + 14.084 R^2 = 0.5754	y = -0.747ln(x) + 13.807 R^2 = 0.7714	y = -0.649ln(x) + 17.426 R^2 = 0.6277	y = -3.123ln(x) + 26.613 R^2 = 0.8537

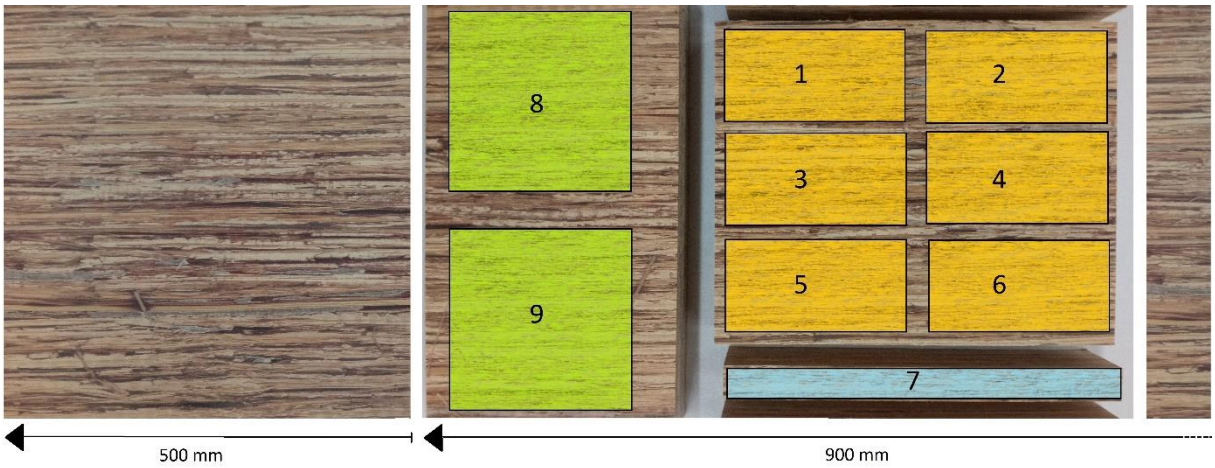

Figure 106: Sample cutting scheme showing the original plank and the position of specimens, 1-6 being assigned to test against basidiomycetes, 7 for the three panel layers testing against soft rot, 8 for density and moisture content determination and 9 reserved for termite or borer testing

Table 50: Linear and polynomial regression analysis of the correlation between equilibrium moisture content (x) and fungal mean mass loss (y) for four different basidiomycetes shown in figure 90

Fungus	***Cp***	***Tp***	***Gt***	***Cv***
	y = a + b*x			
a	-0.39 ± 0.83	-1.84 ± 1.57	0.62 ± 0.6	0.09 ± 1.21
b	0.33 ± 0.08	0.43 ± 0.15	0.18 ± 0.06	0.29 ± 0.11
RSS	0.57	2.03	0.3	1.21
R^2	0.9	0.81	0.84	0.77
	$y = a + b*x + c*x^2$			
a	1.89 ± 2.99	-0.09 ± 6.96	2.86 ± 1.43	4.84 ± 2.47
b	-0.26 ± 0.74	-0.02 ± 1.72	-0.39 ± 0.35	-0.93 ± 0.61
c	0.03 ± 0.04	0.02 ± 0.09	0.03 ± 0.02	0.07 ± 0.03
RSS	0.35	1.9	0.08	0.24
R^2	0.94	0.82	0.96	0.95

Statutory declaration

I herewith declare that I have completed the present thesis independently making use only of the specified literature and auxiliary sources. Identification of references about the statement and scope of the work is quoted. The thesis in this form or in any other form has not been submitted to an examination body and has not been published so far. The print version is a complete replication of the digital one.

Hamburg, 2020-08-21

Goran Schmidt